



UNIVERSITY OF
BIRMINGHAM

Synthesis of Medium-Ring Nitrogen Heterocycles and their Application to Diverse Scaffold Assembly

Russell Jason Hardy Wood

A thesis submitted to the
University of Birmingham
for the degree of
Doctor of Philosophy

School of Chemistry

College of Engineering and Physical Sciences

University of Birmingham

September 2020

UNIVERSITY OF
BIRMINGHAM

University of Birmingham Research Archive

e-theses repository

This unpublished thesis/dissertation is copyright of the author and/or third parties. The intellectual property rights of the author or third parties in respect of this work are as defined by The Copyright Designs and Patents Act 1988 or as modified by any successor legislation.

Any use made of information contained in this thesis/dissertation must be in accordance with that legislation and must be properly acknowledged. Further distribution or reproduction in any format is prohibited without the permission of the copyright holder.

Abstract

Medium ring-containing scaffolds have been shown to display a broad range of biological activity and yet are under-represented within approved pharmaceuticals. Diversity-oriented synthesis (DOS) is a methodology by which multiple compounds can be efficiently synthesised in a diversity-driven approach.

Combining both DOS and medium-ring methodology, a 10-membered ring containing an alkene, an amine and a ketone, was identified as a key intermediate for the synthesis of a library of scaffolds. The synthesis of the 10-membered ring in which the amine is protected as a tosylsulfonamide is described. The synthesis was accomplished in 34% overall yield over seven steps, utilising a key Cope-type rearrangement to enable synthesis of the ring. Conformational analysis and the crystal structure demonstrated that the ring sat preferentially in a chair-chair-chair conformation, although other conformations were accessible at room temperature. External nucleophilic addition into the ketone proved challenging, with only reduction successfully providing an alcohol product. A decalol scaffold was generated *via* an intramolecular Prins or ene type cyclisation. Epoxidation of the alkene, followed by treatment with a Lewis acid generated a diketone, which could be further transformed into a range of 5,7-fused rings, albeit with poor diastereoselectivity. Treatment of the epoxide with a Brønsted acid gave an enol ether embedded within a rare [5,3,1]-bicyclic framework, which could be reversibly transformed into the methyl acetal by further treatment with a Brønsted acid and methanol. Treatment of the methyl acetal with an acid and a nucleophile generated a variety of different bicyclic ether scaffolds.

Deprotection of the tosylsulfonamide functionality was unsuccessful. Use of the alloc protecting group proved more successful and optimisation of the alloc removal step is described. All of the previous scaffolds were accessed using this alternative amine protecting group. Cheminformatic analysis guided the identification of three key scaffolds which were decorated *in silico* with a selection of 45 compounds identified for synthesis. A library of 15 decalol derivatives and eight bicyclic ether derivatives was synthesised. A Paternò-Büchi reaction on the free amine produced an oxetane scaffold albeit in low yield, which was successfully derivatised. Overall, 30 compounds representing 26 different Murcko scaffolds have been synthesised and submitted to an in-house compound library – future investigations of further scaffold development are discussed.

Acknowledgements

As I sit here, having finished writing up, I must admit there were a few moments I didn't think I would make it through. However, thanks to the help of my wonderful friends and colleagues, here I am, four years later, putting the finishing touches to my thesis.

First and foremost, I must thank Liam, without whom none of this would have been possible. He has been incredibly kind and helpful throughout my time at Birmingham. I could not have wished for a better supervisor, although he may have wished for a better student... I would not be the chemist I am today without his guidance.

The analytical staff were always on hand to help, but special thanks must be paid to Chris and Cecilé, who went out of their way to help everyone.

There have been so many people that have helped me through my time at Birmingham, whether they know it or not and in some small way they have all contributed to this piece of work. I would like to thank Nick, Ed, Matt and Sajni for making settling in so much easier; they made a strange city feel like home. The breakfast club; Izzy, Nick, Matt and Glenn, was always something to look forward to and I have missed the tradition since. There was never a bad day in office 408 and that comes down to the lovely people that occupied it. Especially the goldfish.

My lab companions, Ian and Connor, made days fly by in the lab and there was never a dull moment. I miss working with them both every day.

I must also thank my lunch buddies Charlotte, Orla and Lizzie, who were always there to listen and lend a shoulder if I was having a bad day. I never would have made it without you guys.

Outside of work, I couldn't have done this without the help of my friends and family. Without the support of my parents, none of this would have been possible, even if they did abandon me for seven months...

Finally, I need to thank my fiancée Chloe, who has patiently stood by me throughout this, even when the circumstances have been incredibly difficult. I never could have done it without your unwavering support.

Table of Contents

CHAPTER ONE: INTRODUCTION	1
1.1 History of Drug Discovery	2
1.1.1 Early Modern Era	2
1.1.2 Target-Oriented Synthesis	4
1.1.3 High-Throughput Screening	7
1.1.4 Combinatorial Chemistry	7
1.1.5 Diversity-Oriented Synthesis.....	12
1.2 Molecular Diversity	13
1.2.1 Chemical Space	14
1.2.2 Molecular Diversity	16
1.2.3 Lead-likeness.....	18
1.3 Synthetic Strategies within DOS	21
1.3.1 Substrate-based approach.....	21
1.3.2 Reagent-based approach.....	24
1.3.3 Build/Couple/Pair Strategy	29
1.3.4 Advanced Build/Couple/Pair Strategy	34
1.4 Medium-sized Rings	37
1.5 Aims and Objectives	41
CHAPTER TWO: DESIGN AND SYNTHESIS OF A LIBRARY OF SCAFFOLDS	42
2.1 Introduction	43
2.2 Synthesis of ten-membered ketone 69	44
2.2.1 Choice of Protecting Group.....	44
2.2.2 Synthesis of the linear precursor amino alcohol 75.....	44
2.2.3 Synthesis of piperidinone 81.....	45
2.2.4 Formation of alcohol 85	49
2.2.5 Formation of ten-membered ring ketone 96.....	52
2.2.6 Properties of the ten-membered ring.....	59

2.3	Design and Synthesis of a Library of Scaffolds	68
2.3.1	Scaffold Definition.....	68
2.3.2	Carbonyl Transformations	70
2.3.3	Double Bond Transformations.....	75
2.3.4	Intramolecular Reactions.....	80
2.4	Summary and conclusions.....	96
 CHAPTER THREE: SYNTHESIS OF A SCREENING LIBRARY		97
3.1	Introduction	98
3.2	Synthesis of Amine 69	99
3.2.1	Attempted tosyl removal.....	99
3.2.2	Alternative protecting groups.....	101
3.2.3	Alloc cleavage	108
3.3	Chemoinformatic analysis of a potential library of scaffolds	110
3.4	Synthesis of a screening library	117
3.4.1	Synthesis of a compound library based on decalol scaffold 181	117
3.4.2	Synthesis of a compound library based on alcohol scaffold 185	121
3.4.3	Synthesis of a compound library based on oxetane scaffold 216.....	127
3.4.4	Synthesis of a compound library based on ether scaffold 188.....	130
3.5	Summary and Conclusions.....	137
 CHAPTER FOUR: SUMMARY AND FUTURE WORK.....		141
4.1	Summary.....	142
4.2	Future Work.....	142
 CHAPTER FIVE: EXPERIMENTAL		144
5.1	General Experimental Details.....	145
5.2	Synthetic Procedures.....	147

CHAPTER SIX: APPENDIX	234
6.1 Crystallographic Data.....	235
6.2 Conformational analysis settings	251
CHAPTER SEVEN: REFERENCES	252
7.1 Bibliography.....	253

Abbreviations

A ³ reaction	Aldehyde-Amine-Alkyne coupling
AIBN	azobisisobutyronitrile
AllocCl	allyl chloroformate
AlogP	atomic partition coefficient
API	Active Pharmaceutical Ingredient
BCC	Boat-Chair-Chair
BCB	Boat-Chair-Boat
BCP	Build/Couple/Pair
Boc	<i>tert</i> -butyloxycarbonyl
BOP-Cl	<i>bis</i> (2-oxo-3-oxazolidinyl)phosphinic chloride
Cbz	carboxybenzyl
CCC	Chair-Chair-Chair
CDI	1,1'-carbonyldiimidazole
COSY	homonuclear correlation spectroscopy
DBU	1,8-diazabicyclo[5.4.0]undec-7-ene
DCC	<i>N,N'</i> -Dicyclohexycarbodiimide
DCE	1,2-dichloroethane
DDQ	2,3-dichloro-5,6-dicyano-1,4-benzoquinone
DEAD	diethyl azodicarboxylate
DHEA	dehydroepiandrosterone
DIAD	diisopropyl azodicarboxylate
DIBALH	diisobutylaluminium hydride
DIPCI	chlorodiisopinocampheylborane
DIPEA	<i>N,N</i> -Diisopropylethylamine
DMAD	dimethyl acetylenedicarboxylate
DMAP	4-dimethylaminopyridine
DMF	dimethyl formamide
DMP	Dess-Martin Periodinane
DMSO	dimethyl sulfoxide
DNP	Dictionary of Natural Products
DOS	Diversity-Oriented Synthesis

DPPA	diphenylphosphoryl azide
dppb	1,4-bis(diphenylphosphino)butane
d.r.	diastereomeric ratio
DTS	Diverted Total Synthesis
EDC	1-ethyl-3-(3-dimethylaminopropyl)carbodiimide
EDTA	ethylenediaminetetraacetic acid
Fmoc	fluorenylmethyloxycarbonyl
Fsp ³	fraction of sp ³ carbons
HSAB	Hard-Soft Acid-Base
HTS	High-Throughput Screening
IBX	2-iodoxybenzoic acid
IC ₅₀	inhibitory concentration required to inhibit the growth of 50% of organisms
LDA	lithium diisopropylamide
LiHMDS	lithium <i>bis</i> (trimethylsilyl)amide
LLAMA	Lead-Likeness And Molecular Analysis
LLP	Lead-Likeness Penalty
<i>m</i> CPBA	<i>meta</i> -chloroperoxybenzoic acid
MCR	Multi-Component Reaction
MIC ₉₀	minimum inhibitory concentration required to inhibit the growth of 90% of organisms
NBS	<i>N</i> -bromosuccinimide
NHS	<i>N</i> -hydroxysuccinimide
NIS	<i>N</i> -iodosuccinimide
NMM	<i>N</i> -methylmorpholine
NMO	<i>N</i> -methylmorpholine- <i>N</i> -oxide
NMR	Nuclear Magnetic Resonance
nOe	nuclear Overhauser effect
NOESY	Nuclear Overhauser Effect Spectroscopy
Ns/nosyl	4-nitobenzenesulfonyl
PAINS	pan assay interference compounds
PCC	pyridinium chlorochromate
PMI	Principle Moment of Inertia

r.t.	room temperature
RCM	Ring Closing Metathesis
SAR	Structure Activity Relationship
SSH	Sonic HedgeHog signalling protein
STAB	sodium triacetoxyborohydride
TBAF	tetra- <i>N</i> -butylammonium fluoride
TBSCl	<i>tert</i> -butyldimethylsilyl chloride
TBTU	2-(1 <i>H</i> -benzotriazole-1-yl)-1,1,3,3-tetramethylammonium tetrafluoroborate
TFA	trifluoroacetic acid
TfOH	triflic acid
THF	tetrahydrofuran
Ts/tosyl	<i>para</i> -toluenesulfonyl

Chapter One: Introduction

1.1 History of Drug Discovery

1.1.1 Early Modern Era

It can be argued that modern drug discovery began in 1805, when Friedrich Sertürner isolated morphine **1** from the opium poppy *Papaver somniferum*.^{1,2} From here began an era of drug discovery wherein Active Pharmaceutical Ingredients (APIs) were purified from natural sources and administered in precise doses. Subsequently isolated from the opium poppy were codeine **2** in 1830 and papaverine **3** in 1848.³

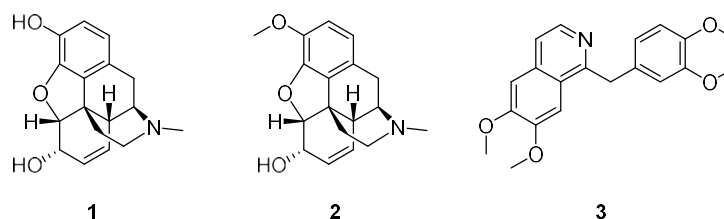


Figure 1 – Examples of APIs isolated in the 19th Century.

Alongside the isolation of alkaloids in the 19th Century, drug discovery also benefited from developments in the fields of analytical and synthetic organic chemistry. One of the early pioneers was Justus von Liebig, who synthesised chloroform and chloral hydrate in the early 1830s, both of which went on to be used as anaesthetics.^{1,4} In 1864, barbituric acid was synthesised by Adolf von Baeyer.⁵ Barbituric acid itself is pharmacologically inactive due to the low pK_a (4.1) of the CH_2 unit, causing ionisation within the gastrointestinal tract, which in turn leads to poor absorption in the gut. Further developments by Joseph von Mering and Emil Fischer for Bayer in the early 20th Century, yielded bis-alkylated derivatives. The removal of the CH_2 unit increased the pK_a of the molecule and consequently improved absorption, in turn creating an entire class of sedatives that were used for a century (Figure 2).^{6,7}

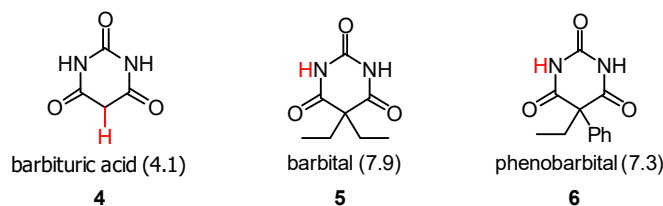


Figure 2 – Barbituric acid and selected derivatives. The proton with the lowest pK_a is highlighted in red, with the value given in brackets.⁷

In addition to barbiturates, Bayer also worked on developing analgesics. Willow bark extracts had been used since ancient times to treat fevers, aches and pains, amongst other conditions.⁸ The natural product salicin **7** was present in these extracts and is metabolised within the body into salicylic acid **8**, which is the API responsible for the pain-relieving effects of willow bark.⁸ In 1874, Hermann Kolbe, alongside Fredrich von Heyden, developed an industrial synthesis of salicylic acid **8**, removing the need to extract it from its natural source. Neat salicylic acid can cause stomach irritation, which led pharmaceutical companies to seek alternatives. Felix Hoffmann, a chemist at Bayer, synthesised acetylsalicylic acid **9** which would become known as aspirin (Figure 3). First marketed in 1899, aspirin is the first and quintessential example of a drug discovered from a natural product lead, a route of discovery which is still used today.^{1,9}

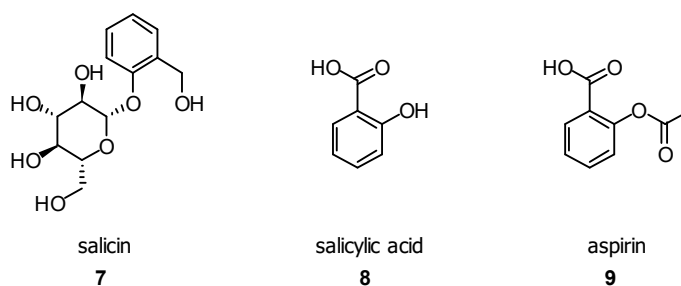


Figure 3 – The natural product **7** responsible for the pain-relieving properties of willow bark and drugs derived from its structure.

In the early to mid-20th Century, one focus of drug research was the isolation and industrial synthesis of antibiotics after the discovery of penicillin by Alexander Fleming in 1929.¹⁰ Large microorganism culture libraries were cultivated in the hope of discovering new antibiotics. Referred to as the “Golden Age of Antibiotics”, twelve different classes of antibiotics were isolated or derived from natural products between 1935 and 1968 (Figure 4), covering a broad range of structures and mechanisms of action.^{11–13} The success of many of these compounds, along with advances in both synthetic and analytical chemistry, once again drove drug discovery towards using nature as an inspiration for future drugs.¹⁴

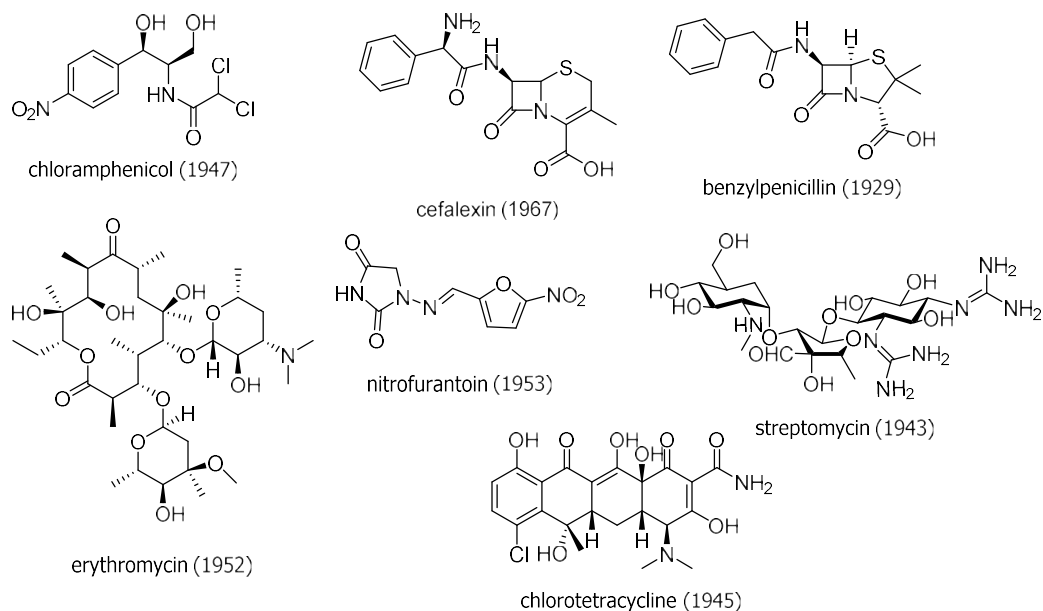


Figure 4 – Examples of antibiotics isolated between 1929 – 1967.

1.1.2 Target-Oriented Synthesis

Synthetic theory and techniques available to organic chemists advanced dramatically throughout the 20th Century.^{9,14,15} One of the key landmarks was the development of retrosynthetic analysis by E.J. Corey in the 1960s, which encouraged and facilitated the rational design of synthetic routes for increasingly complex molecules.¹⁶ A diagrammatic version of this analysis can be seen in Figure 5; the complex target molecule is broken into two halves, which can each be further simplified to basic starting materials enabling the elucidation of a forward synthesis.

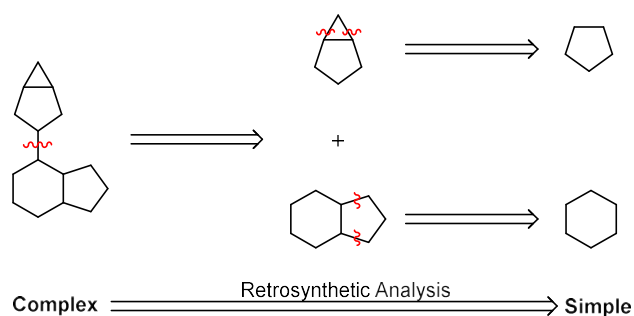


Figure 5 – A conceptual retrosynthetic pathway going from a complex target molecule on the left to simple starting materials on the right.

By opening new pathways to natural products, retrosynthetic analysis allowed the synthesis of natural products that were either hard to isolate in analytically pure form or could only be isolated in very small quantities from their natural sources. Improved access to natural products in useful quantities connected total synthesis to biological investigations in a way never seen before. By 1990, 80% of all approved drugs were either natural products or analogues of natural products, the highest percentage that the category would ever reach.¹⁷

If the natural product itself was not an ideal drug candidate, then analogues could now be synthesised and tested, probing the Structure Activity Relationship (SAR) of the compounds. Statins are an early example of how drugs have been developed from a natural product using this strategy.¹⁸ Statins are inhibitors of HMG-CoA reductase, an enzyme involved in cholesterol biosynthesis. The first statin to be isolated from two species of fungi was mevastatin **10**ⁱ in 1976.^{19,20} Mevastatin turned out to be unsuitable as a drug owing to its high toxicity in animals, but another, closely related natural product, lovastatin **11**, did enter the market. A synthetic analogue of lovastatin, simvastatin **12**, was also brought to market in 1992. The efficiency of these drugs and their widespread use led to the introduction of entirely synthetic analogues, with a similar pharmacophore (Figure 6). Brought to market in 1996, atorvastatin **13** (Lipitor[®]) became one of the most successful drugs ever made.

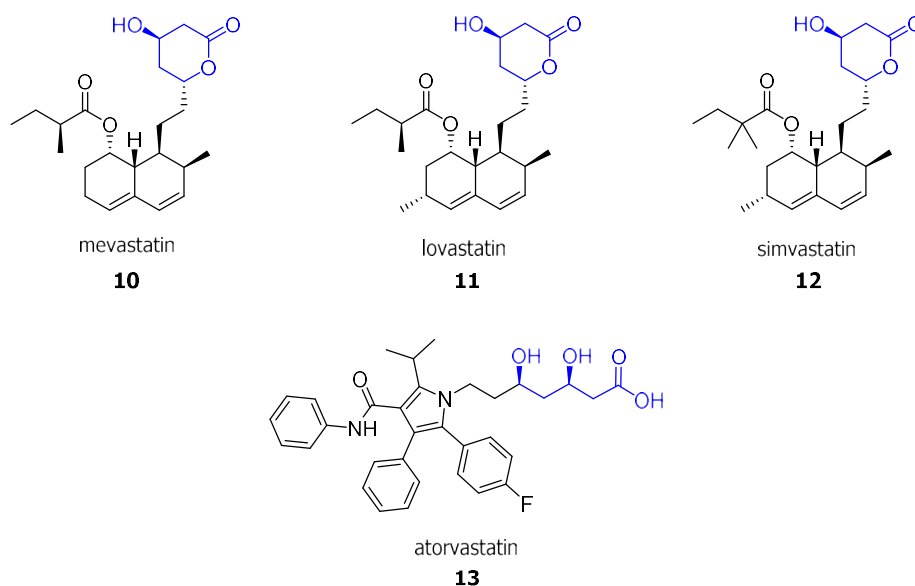


Figure 6 – Structures of statin compounds. The common pharmacophore is highlighted in blue.

ⁱ For ease of reading, all statins are referred to as “__statin”, rather than their brand or natural product name.

relatively low resource input. As these “low-hanging fruits” were picked, it became increasingly difficult to discover a more efficient drug, and more resource-intensive to discover a new target. This problem has been more thoroughly reviewed elsewhere.^{9,11,15,17,23–25}

1.1.3 High-Throughput Screening

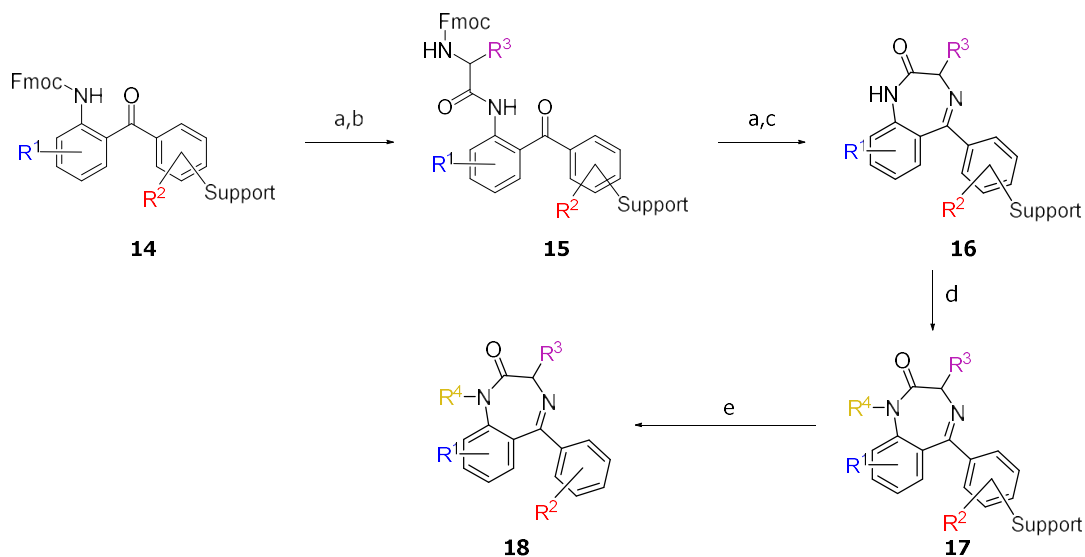
In the mid-1980s, companies were screening 20–50 compounds per week using individual test tubes and assay volumes of around 1 mL. New types of therapeutic targets, such as those revealed using recombinant DNA, highlighted the inadequacy of “modern” drug-discovery techniques. Driven by a need to screen more compounds and get results more quickly, High-Throughput Screening (HTS) was developed.²⁶ HTS is the use of automated equipment, in conjunction with a researcher, to test samples rapidly for biological activity.

Pfizer found that by switching from test tubes to 96-well plates, reducing the assay volume to 50–100 μL and using DMSO solutions of synthetic compounds, they were able to assess 800 compounds a week. By 1990, optimisation of the processes had increased the capacity of their assays to 7200 compounds.²⁶ With this increased capacity came a need for larger libraries of novel compounds to test. Libraries made up entirely of natural products were unrealistic due to their high cost and limited availability;²⁷ instead, chemists turned to a new technique known as combinatorial chemistry.²⁵

1.1.4 Combinatorial Chemistry

Compound libraries generated by combinatorial chemistry fall into two main categories, namely focused libraries, where analogues of a compound with known biological activity are used to probe SAR, and prospecting libraries, which contain a variety of “random” structures.²⁸ Focused libraries are used for optimisation of a drug candidate (*i.e.* hit to lead optimisation), with a specific target in mind. Prospecting libraries on the other hand, are synthesised with the intention of maximising the number of novel compounds and diversity, and typically used for hit identification and new target discovery.

The first time that combinatorial chemistry was used can be attributed to Robert Merrifield, who in 1963, used a solid-phase support to synthesise tetrapeptides.²⁹ The potential of solid-phase synthesis to drug discovery was finally realised in 1992, when Ellman and Bunin published the synthesis of ten different benzodiazepines using solid-phase synthesis (Scheme 2).³⁰



Scheme 2 – The first synthesis of a prospecting library of benzodiazepines using solid-phase synthesis. The substrate is linked to a polystyrene solid support by a linker. Reagents and conditions: (a) 20% piperidine in DMF; (b) *N*-Fmoc-amino acid fluoride, 4-methyl-2,6-di-*tert*-butylpyridine, CH₂Cl₂; (c) 5% acetic acid, DMF, 60 °C; (d) lithiated 5-(phenylmethyl)-2-oxazolidinone, THF, –78 °C, followed by alkylating agent, DMF; (e) TFA, H₂O, Me₂S (85:5:10).

Ellman and Bunin began by coupling 2-aminobenzophenone derivative **14** to a solid support through a carboxylic acid or hydroxyl functionality. The choice of benzophenone allowed them to vary both R¹ and R². After Fmoc deprotection, the choice of amino acid fluoride in the subsequent coupling step allowed for further analogues to be made with variation of R³. Fmoc deprotection of **15**, and exposure of the resulting free amine to acid provided benzodiazepine **16**. Further analogues could be synthesised by incorporation of an alkylation step, introducing a fourth point of diversity. Finally, treatment with trifluoroacetic acid (TFA) cleaved the benzodiazepine **18** from the resin. All of the resulting compounds were synthesised in excellent yield (85–100%).

Throughout the 1990s, as HTS became more efficient and the demand for larger libraries increased, combinatorial chemistry began to make use of the split-pool technique.^{31,32} The concept is summarised in Figure 7. Substrates, bound to solid beads, are first split and then derivatised (Step I). Once complete, all of the beads are pooled to randomise the beads (Step II). Next, the beads are split again and a second functionalisation carried out (Step III). By a sequence of continual pooling and splitting of the beads, an exponential number of compounds can be generated using this technique.

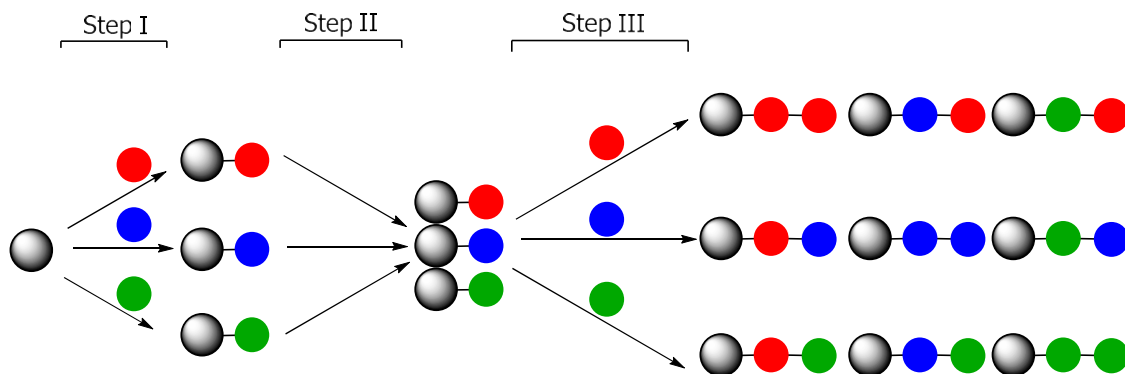
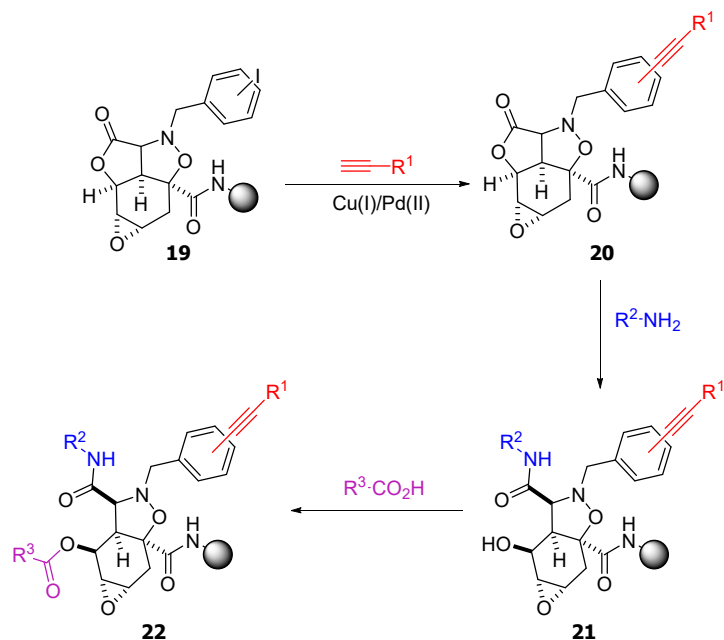


Figure 7 – A cartoon example of split-pool combinatorial synthesis. Each of the coloured balls represents a different functional group that has been added to the molecule.

An example of a combinatorial synthesis pathway using the split-pool technique is summarised in Scheme 3.³³ The parent tricycles were chosen by Tan *et al.* due to their dense functionality, allowing for the introduction of a variety of functional groups without the need for protecting groups. Tricycle **19** was first attached to a solid support and the resulting functionalised beads then split. Subsequent reaction with thirty different alkynes in a Sonogashira coupling produced compounds **20**. These compounds were pooled and then split, maximising the R groups present in each subsequent reaction. Compounds **20** were then treated with a primary amine to effect lactone aminolysis, giving compounds **21**. Finally, the revealed alcohol underwent acylation to yield the final compounds **22**. Using this split-pool synthesis technique a library of 2.18 million novel compounds were generated.



Scheme 3 - The shaded sphere represents the solid support to which each structure was linked. Single enantiomers and *ortho*-, *meta*- and *para*- derivatives were used. Employing 30 alkynes, 62 amines and 62 carboxylic acids in the combinatorial synthesis generated over two million compounds.

Despite being able to generate millions of compounds relatively quickly, combinatorial chemistry has major downsides that have prevented it from becoming the premier tool in drug discovery. First, while generation of the compounds is relatively easy, purification and isolation of individual compounds is difficult unless using a one compound–one bead approach, which itself is cumbersome and expensive.³⁴ Combinatorial chemistry is also limited in the types of reactions that can be widely used and high-yielding, predominantly nucleophilic substitution, cross coupling, reductive amination and acylation reactions.³⁵ These limitations have led to libraries with low diversity, which make them inefficient for HTS. Another outcome of the small number of reaction types is that many compound libraries are comprised of “flat” molecules, molecules with a low fraction of sp^3 carbons (F_{sp^3}), which confer poor physicochemical properties and therefore make the compounds much more likely to fail due to a lack of efficacy, leading to high rates of attrition.³⁶

The importance of structural diversity in compound screening libraries was highlighted in 1998, in a study by Dixon and Villar.³⁷ The study demonstrated that multiple, diverse structures bound to human serum albumin with good (nM) affinity in a competitive binding assay. However, when structurally similar analogues of inhibitor **23** were subjected to the same assay conditions, they found that the inhibition was weak (>2.5 mM) (Figure 8). These results

suggested that if a potential prospecting library only contains structurally similar analogues, the probability of one of the molecules being a good inhibitor is small whilst screening a structurally diverse library improves the chance of finding a strong inhibitor.

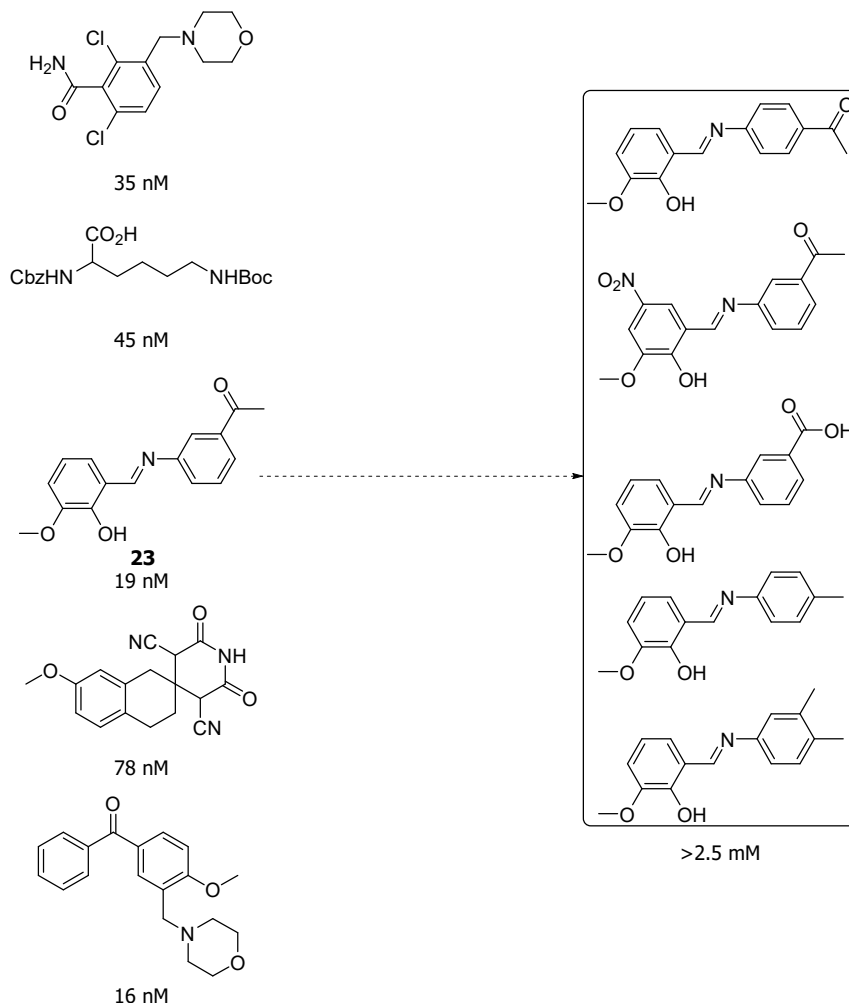


Figure 8 – Demonstration of how structural diversity can be more important for finding a good inhibitor than structural analogues. Binding affinities are the IC_{50} values for human serum albumin in a competitive binding assay.

Between 1981 and 2019, 1881 new drugs were approved for use worldwide, only three of which were developed purely using combinatorial synthesis (Figure 9).³⁸ The low success rate of utilising combinatorial chemistry as a starting point for drug discovery has caused it to be seen as a failure; however, once an active compound has been identified, the ability of combinatorial chemistry to enable structural optimisation is without parallel.^{39,40} Therefore new methods are needed for generating large libraries of skeletally diverse compounds to identify more and better starting points for drug discovery. In 2000, Stuart Schreiber codified a new

school of thought known as Diversity-Oriented Synthesis (DOS) that aimed to address this problem.⁴¹

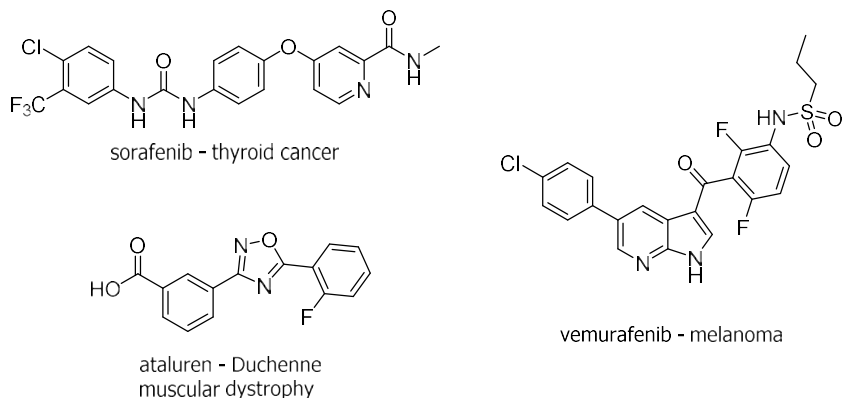


Figure 9 – Three drugs molecules and the conditions they are used to treat that have been discovered using combinatorial synthesis between 1980-2019.⁴²⁻⁴⁴

1.1.5 Diversity-Oriented Synthesis

Diversity-Oriented Synthesis can be defined as *"the deliberate, simultaneous and efficient synthesis of more than one target compound in a diversity-driven approach to answer a complex problem."*⁴⁵ Target-oriented synthesis works by taking a complex structure (the target) and breaking it down into more simple components using retrosynthetic analysis, before constructing a forward pathway to the target molecule. In DOS, there isn't a single target compound; instead, a small number of simple compounds are transformed into diverse structures (Figure 10). In this approach, the synthesis is planned in a forward, rather than a backward direction.^{41,45} Substrate selection must now be considered carefully as the substrates must be able to be diversified easily. DOS, by avoidance of a singular target, provides an advantage in the synthesis of a prospecting library over TOS. To fully understand the subsequent advances that DOS has brought in, some key concepts first need to be defined.

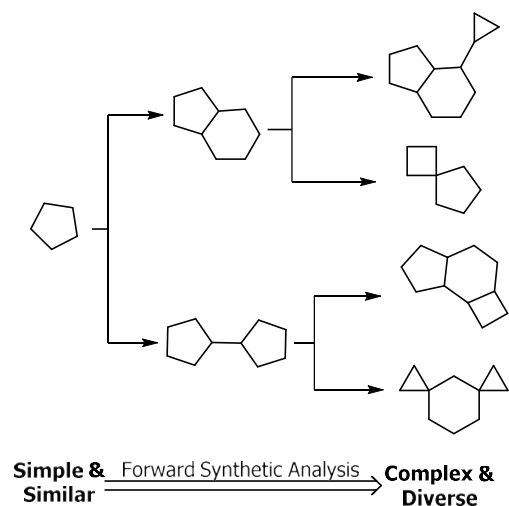


Figure 10 - A DOS pathway starts from a simple starting material and progresses to diverse, complex products.

1.2 Molecular Diversity

DOS generates both structurally complex and structurally diverse molecules, which intertwines two concepts that are important in drug discovery: chemical space and molecular diversity. Chemical space, otherwise known as multi-dimensional descriptor space, is a region confined by a set of descriptors.⁴⁶ At its largest, it encompasses all of the carbon-based small molecules that could be created; however, most people working in drug discovery limit the compounds they consider to those occupying “biologically relevant” chemical space by restricting what descriptors they look at.⁴⁶ Intertwined with the concept of chemical space is the concept of molecular diversity. By creating a library with a greater number of diverse molecules, a larger amount of chemical space can be probed at once, which means that a selective hit is more likely to be found. Four main types of molecular diversity are considered in the literature and using each of these different types of diversity, different areas of chemical space can be explored (see Section 1.2.2).^{45,47}

1.2.1 Chemical Space

Every compound possible occupies a single point in chemical space, with "similar" compounds grouped together and "dissimilar" compounds further apart. In this context, similar compounds are those which, with reference to a set of descriptors, are close together in space. By maximising the number of "dissimilar" compounds within a library, a wider amount of chemical space can be covered by a single library. The descriptors most commonly used for drug discovery are molecular weight, polarisability, F_{sp^3} (fraction of carbons which are sp^3 -hybridised), log P (a measure of lipophilicity) and topological features.^{46,48} Once descriptors have been chosen, algorithms can be used to generate a chemical space within the limits of

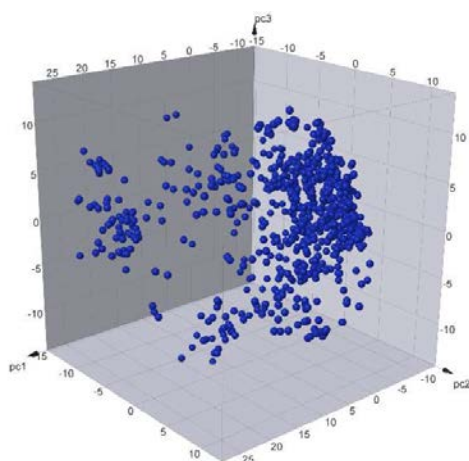


Figure 11 – A 3D chemical space containing 1000 small molecules, generated in DataWarrior using the Haworth Chemically-Enabled Compound Collection by Dr Holly Adcock.

these descriptors. Principal component analysis can then be used to condense all of this information into a two- or three-dimensional scatter plot, an example of which is shown in Figure 11. These plots provide an easy way of visualising the chemical space coverage of a particular compound library. However, due to potential differences in the descriptors chosen or how the analysis is carried out, the diversity of compound libraries cannot always be directly compared unless the same analysis is applied to multiple compound libraries.⁴⁹

The classical tool chosen for comparison of different libraries is normalised principal moment of inertia (PMI) analysis.⁵⁰ Developed in 2003 by Sauer and Schwartz, it takes the lowest energy conformation of a molecule and generates the three principal moments of inertia (I_{xx} , I_{yy} , I_{zz}), which can then be plotted on a triangular graph, with vertices at (0,1), (0.5, 0.5) and (1,1) (Figure 12). Each apex represents a perfect rod, disc or sphere. The shape of the molecule in 3D space determines where it is plotted on the graph, with planar, aromatic compounds appearing on the rod-disc axis and natural products typically appearing more towards the centre. The overall coverage of a PMI plot is a good approximation for how much 3D chemical space a library interrogates.

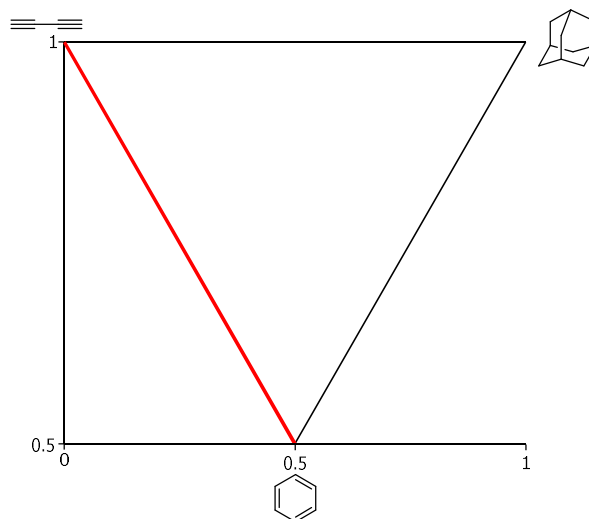


Figure 12 – A blank PMI plot. Most current drug molecules are found on – or close to – the rod-disc axis highlighted in red.

Although the overall size of chemical space is infinite, the size of drug-like chemical space, bound by compounds following Lipinski's rules, has been estimated to be between 10^{23} and 10^{60} compounds.⁵¹ It has been estimated that the total number of stable organic compounds under 500 Da is 10^{63} molecules, which rises to 10^{180} molecules for compounds under 1000 Da.⁵² The current estimate for the number of synthesised compounds is 100 million (10^8).^{52,53} A comparison of the two estimates shows that only $10^{-15}\%$ of all possible "drug-like" compounds have been synthesised.

Despite the relatively small number of synthesised molecules, many compound libraries restrict themselves to traits that have already been found in drug-like molecules, further reducing the amount of chemical space that is explored and the chance of discovering a unique biologically active molecule.⁴⁷ One of the root causes of the under-exploration of chemical space is the development of a number of constraints, such as the aforementioned Lipinski's rule of 5, the rule of 3, the GSK 4/400 rule, the golden triangle and the rapid elimination of swill and pan assay interference compounds (PAINS).^{54–60}

The development of DOS provided a tool to rapidly expand the amount of chemical space that is explored by a library with the aim of identifying small molecules that could treat otherwise "classically" untreatable conditions by exploring outside the confines of "classical" drug-like chemical space.⁶¹ Since DOS is conducted without a target in mind, the aforementioned constraints can be ignored, enabling synthesis that maximises chemical space coverage. Figure

13 is representation of the respective chemical space coverage of a TOS library, a combinatorial chemistry library and a DOS library.

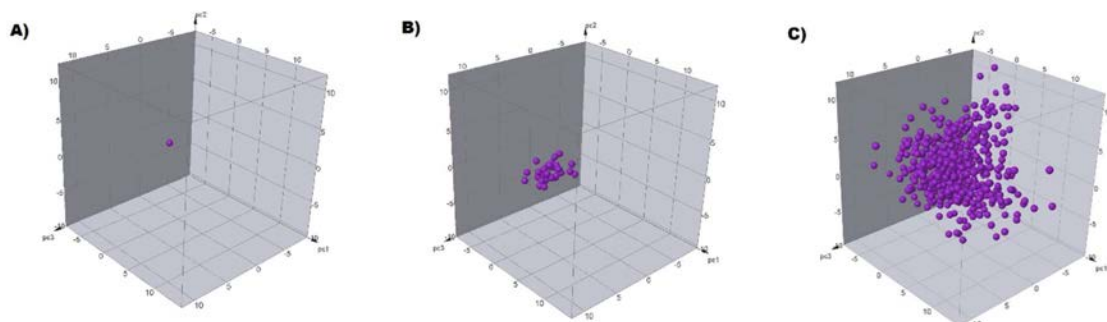


Figure 13 – A comparison of the chemical space explored by TOS (A), combinatorial chemistry (B) and DOS (C). TOS aims towards a single target so only explores a single point within chemical space; combinatorial chemistry utilises a common skeletal structure, so explores a confined area of chemical space; DOS creates a number of different scaffolds, increasing the diversity of the library and therefore exploring the greatest amount of chemical space.⁴⁷

1.2.2 Molecular Diversity

Molecular diversity, although not an absolute quantity that can be measured, can be imagined as a spectrum, with the largest amount of molecular diversity coming from libraries which are derived from DOS (Figure 14), for the reasons discussed in Section 1.2.1. There are four main types of molecular diversity that are commonly considered when assessing the diversity of a particular library, namely building block, functional group, stereochemical and skeletal diversity, each of which will be considered in turn below.^{45,47}

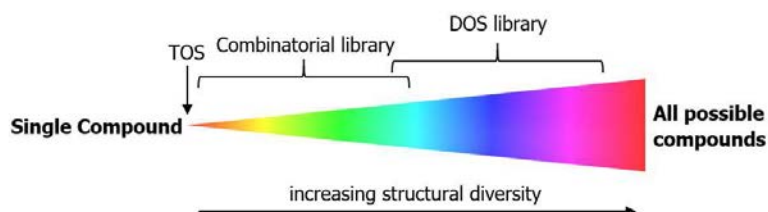


Figure 14 – A molecular diversity spectrum comparing the relative amount of diversity achieved by TOS, combinatorial synthesis and DOS. Adapted from ref.⁶²

- 1) *Building block diversity*: The choice of starting materials allows for variation of structural moieties around a single skeleton. This type of diversity is what occurs within combinatorial libraries and is generally viewed as the least important of the four types of diversity due to the small amount of chemical space it probes (Figure 15).

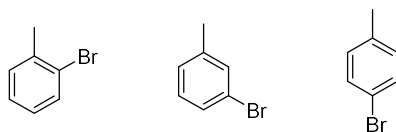


Figure 15 – Example of compounds which can be used to introduce building block diversity.

- 2) *Functional group diversity* is similar to building block diversity but instead refers to variation of functional groups around the molecule, as well as specific points within the molecule. Variation of these groups tunes the molecule to potentially interact with polar, apolar or charged residues present in a biological target. Variation of functional groups around a single skeleton has a negligible effect on the 3D shape of the molecule and therefore is also ranked low in the four types of molecular diversity (Figure 16).

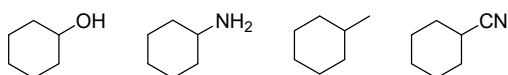


Figure 16 – Example of variation of a functional group on the same scaffold. Each scaffold adopts the same conformation in solution.

- 3) *Stereochemical diversity* describes the variation of the functional group orientations within a molecule as well as any potential macromolecule-interacting elements. This type of molecular diversity is important for a number of reasons. First, often the greater the number of stereocentres, the more complex the molecule.⁶³ Complexity can be equated to selectivity, increasing the chance that screening a library may discover a selective hit. Second, there is a need for branching pathways to be able to develop many compounds from one. By introducing elements of chirality, each stereocentre can be controlled to add another branch to the pathway, increasing the diversity within the compound library. Third, molecules involved in biological processes are chiral, so there is a greater chance of a strong interaction with a target if the compounds used in a screen are also chiral (Figure 17).

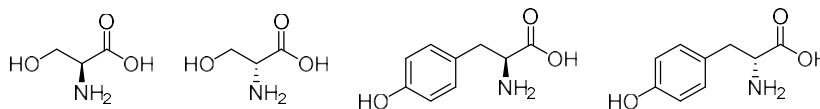


Figure 17 – Examples of chiral starting materials which allow for incorporation of stereochemical diversity.

4) *Skeletal diversity*: Also known as scaffold diversity, this is considered to be the most important of the four types of diversity as it has the greatest impact on how much chemical space is interrogated by a library.⁵⁰ Typically, skeletal diversity is defined as the variation in the overall molecular framework, such as the ring structures or other rigidifying elements, which results in compounds with different molecular shapes. Since the molecular skeleton determines the overall shape of the molecule, it is the most important and explains why libraries with a wide range of distinct molecular skeletons are so desirable (Figure 18).

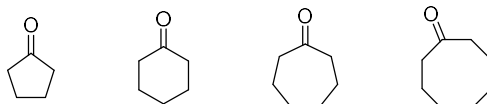


Figure 18 – Variation of ring size quickly changes the skeletal diversity of a library.

1.2.3 Lead-likeness

The uneven exploration of chemical space stemming from the problems discussed above has led to screening campaigns which have tried to explore chemical space in a random fashion. Unfortunately, these campaigns have not proved more successful than rules-based screens.^{64–66} Simple, random exploration generates many compounds with unfavourable traits such as high lipophilicity or a large molecular weight. It has been shown that as a compound progresses from hit to drug, lipophilicity and molecular weight increase, so a hit being near the boundary typically makes it unsuitable for further exploration. As these problems became clear, the idea of “lead-likeness” was formulated and developed in the 2000s and 2010s.^{56,67–69}

Concurrently, to assist synthetic chemists in the better design of libraries and exploration of unknown but useful chemical space, cheminformatics tools were developed.^{64,70} One such tool was PMI (Section 1.2.1), which can assess the 3D character of compounds in the library. Another tool, developed in 2009 by Wetzels and co-workers, is Scaffold Hunter, which can break down molecular frameworks to show similarities between different frameworks, enabling the replacement of one scaffold with a structural simile to avoid undesired issues, such as toxicity.⁷¹ It can also be used to assess the uniqueness of the scaffolds present in a library by comparison to the Dictionary of Natural Products (DNP) (Figure 19).

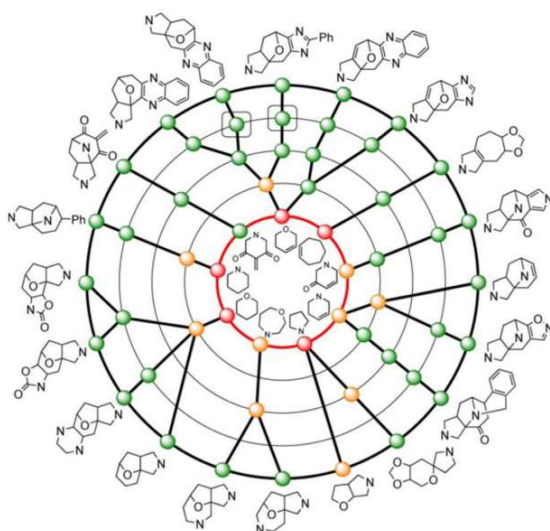


Figure 19 – Hierarchical scaffold tree of 26 molecular scaffolds. Each node represents the occurrence of a framework in the DNP database. Green: never found, orange: found in <1%, red: found in >1%. Reproduced with permission from ref.⁷²

To assist with exploring “lead-like” chemical space, *in silico* tools have been developed, which enable analysis of libraries before synthesis has even begun, reducing the time and cost of developing an effective library. One such program is Lead-Likeness And Molecular Analysis (LLAMA), which can virtually decorate submitted scaffolds with pharmaceutically relevant capping agents (e.g. sulfonyl chlorides, ketones, aryl bromides) using traditional medicinal chemistry reactions (sulfonamide formation, reductive amination, amide arylation etc). Each compound within the generated library is given a “Lead-Likeness” Penalty (LLP) depending on whether it contains features that are deemed non-lead-like such as too many aromatic rings (≥ 4) or undesirable functionalities (eg. acyl chloride, isocyanate) (Figure 20).⁷³

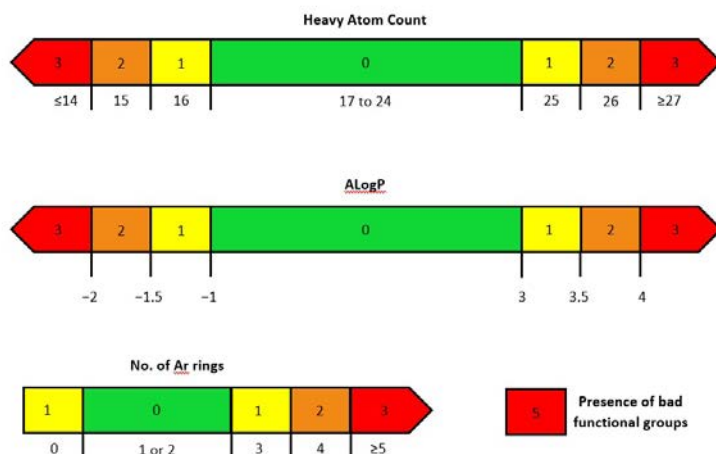


Figure 20 – Graphical representation of the LLP values assigned to each physicochemical property. Bad functional groups are defined as PAINS.⁶⁰ Adapted from ref.⁷³

DOS was initially envisaged to be conducted using two distinct strategies. Subsequently, these strategies have evolved, and new ones have been designed, such as Build/Couple/Pair, enriching the available strategies for the synthesis of a library containing a diverse array of scaffolds. The evolution of these strategies is covered in detail in Section 1.3.

1.3 Synthetic Strategies within DOS

Efficient syntheses that create molecular diversity have been an incredible challenge since the conception of DOS in 2000. Initially, two distinct strategies emerged, both pioneered by Schreiber.⁴⁷ The first is a reagent-based approach, which takes a single molecule and applies a range of different reagents and reaction conditions to create distinct, diverse compounds. The second approach is substrate-based, where multiple starting materials are “pre-encoded” with skeletal information (called σ elements) and transformed into distinct molecular skeletons using a set of common reagents and reaction conditions (Figure 21).⁷⁴

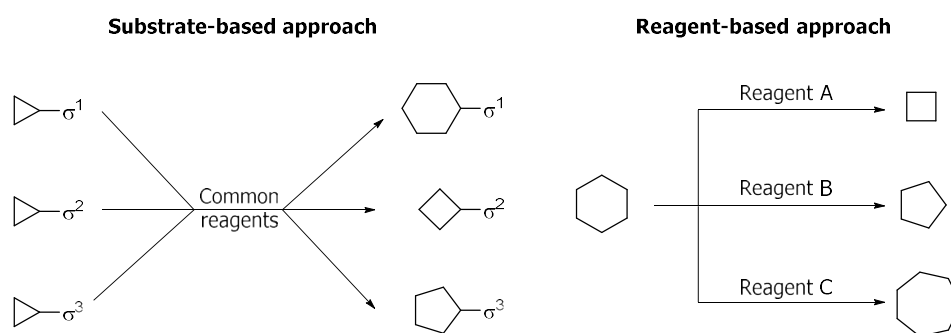
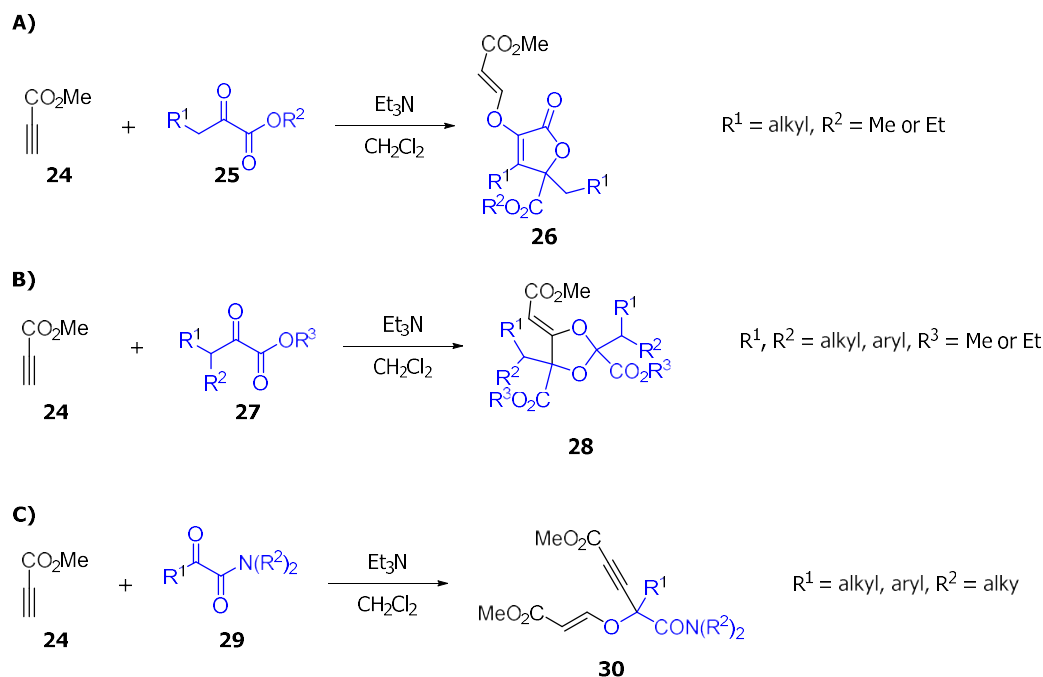


Figure 21 – Cartoon representation of a reagent- and substrate-based approach to DOS.

1.3.1 Substrate-based approach

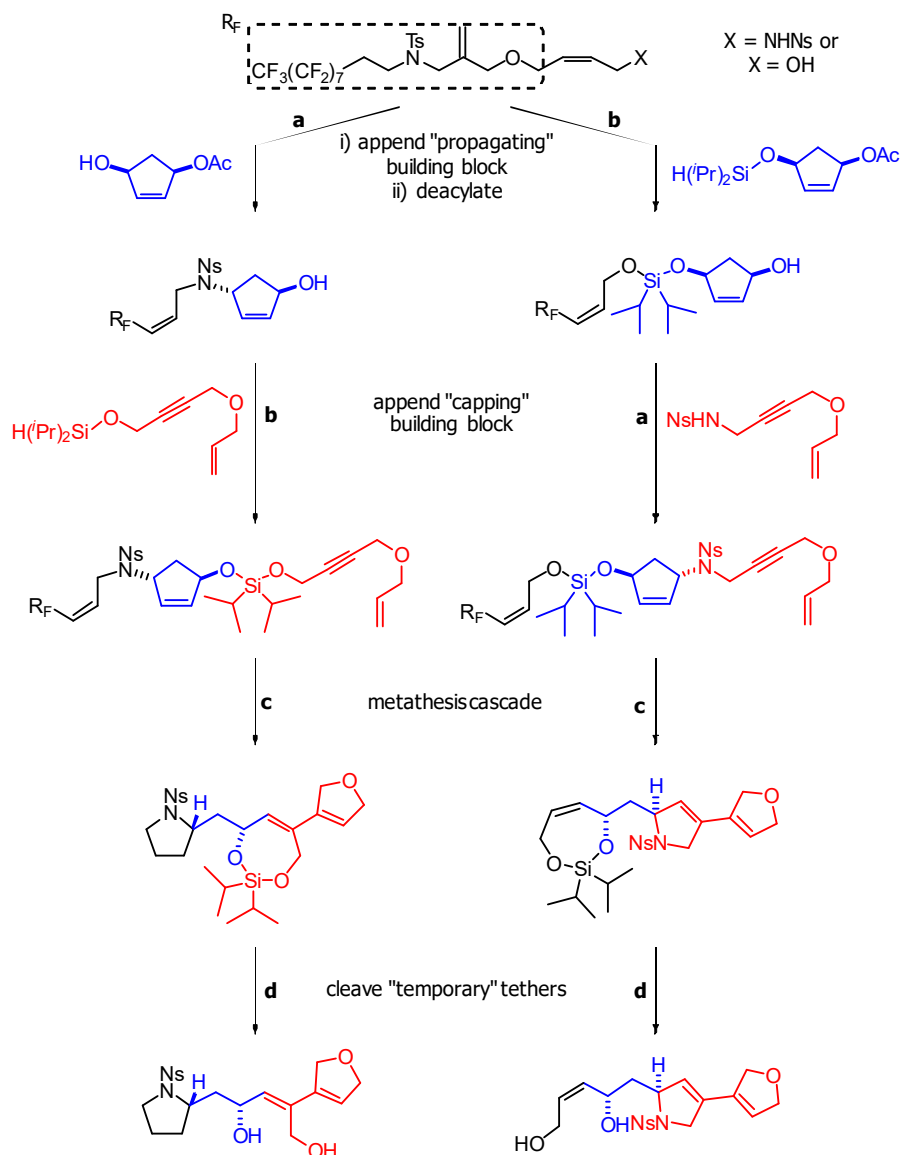
In 2007, Tejedor *et al.* reported a substrate-based approach to generate three different molecular topologies from simple starting materials in one step (Scheme 4).⁷⁵ The group utilised a multi-component reaction (MCR), specifically a chemodifferentiating organocatalysed ABB' three-component reaction, where A is methyl propiolate **24** and B and B' are α -dicarbonyl compounds.⁷⁶ The dicarbonyl compound acts as the skeletal encoding element, σ , as the judicious choice of R group can increase the reactivity of one of the carbonyls preferentially. Pathway A shows the reaction of simple alkyl α -ketoesters **25** with methyl propiolate to generate γ -lactones **26**. Pathway B utilises β,β -disubstituted α -ketoesters **27**, which generates 1,3-dioxolanes **28** instead. β,β -Disubstituted α -ketoesters are less acidic than the α -ketoesters used in pathway A, which accounts for the difference in reaction outcome; ketoester **25** reacts as an enolate while ketoester **27** reacts as an activated ketone.



Scheme 4 – Substrate-based DOS where variation of the functional groups of the α -dicarbonyl substrate (highlighted in blue) pre-encodes the skeletal outcomes.

Changing from an α -ketoester to an α -ketoamide (Pathway C) further reduces the acidity of the compound, as well as decreasing its reactivity,⁷⁷ and as a consequence, no cyclisation occurs; instead, two molecules of methyl propiolate are incorporated in the resulting γ,γ -disubstituted propargylic enol ethers **30**. Overall, three different molecular topologies were generated, all of which contained a β -alkoxyacrylate which could be used for further diversification.

A quintessential example of the substrate-based approach was demonstrated by Morton *et al.* in 2009.⁷⁸ Their approach utilised a fluorine-tagged linker, R_F (Scheme 5), which enabled fluorine-phase separation, providing a rapid method for product isolation. Careful design of the linker meant that only fully cyclised products would be released, enabling easy removal of side-products from the final metathesis cascade.⁷⁹



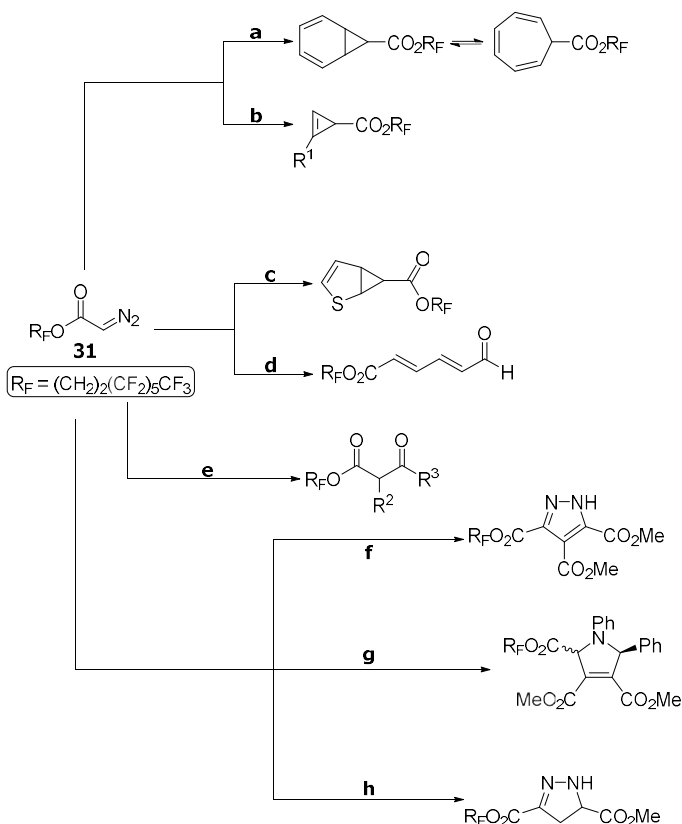
Scheme 5 – Two examples of the synthetic approach taken by Morton *et al.* Overall, 96 compounds comprising 84 different scaffolds were synthesised. Reagents and conditions: (a) (i) DEAD, PPh_3 , (ii) NH_3 , MeOH; (b) (i) NBS, (ii) DMAP, Et_3N , (iii) NH_3 , MeOH; (c) (i) Grubbs I, (ii) NEt_3 , $\text{P}(\text{CH}_2\text{OH})_3$; (d) $\text{HF}\cdot\text{pyridine}$, Me_3SiOMe .

Two sets of building blocks were utilised in the synthetic route, "propagating" blocks and "capping" blocks. While Scheme 5 only shows two examples of each, twelve propagating blocks and eighteen capping blocks were used in the synthesis of the library. Together, the propagating and capping blocks act as the σ elements, which pre-encode the skeletal information. The metathesis cascade was expected to begin at the terminal alkene of the "capping element", which would ensure that only cyclised products were released from the linker.⁸⁰ Finally, any temporary tethers could be cleaved to reveal the final scaffolds. The

overall library consisted of 96 compounds derived from 84 unique scaffolds. These reactions show the power of pre-encoded substrates, and how a small change in the capping or propagating group can lead rapidly to a large variety of scaffolds.

1.3.2 Reagent-based approach

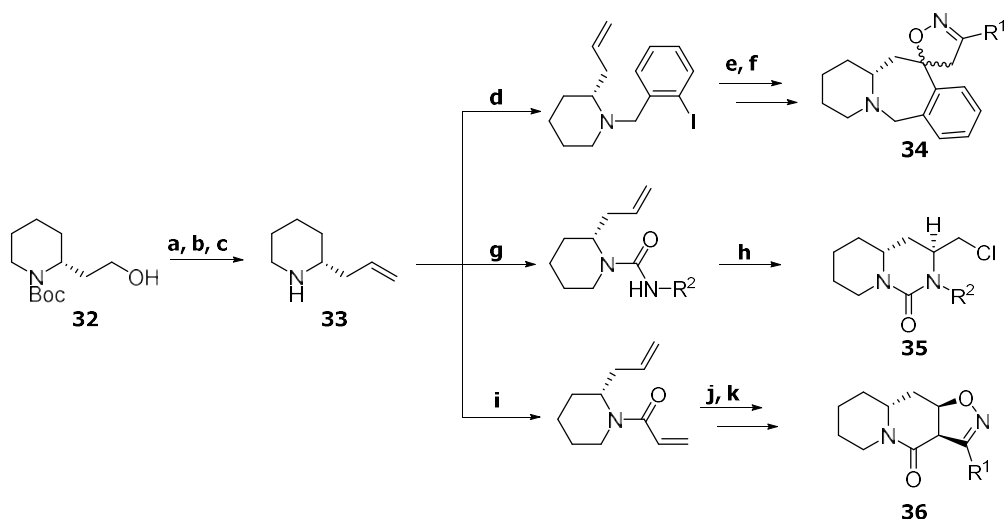
An alternative to the substrate-based approach is the reagent-based approach, which uses a common starting material and transforms it into a diverse library, ideally in a small number of steps. Scheme 6 shows one of the libraries generated by Wyatt *et al.* using this approach.⁸¹ The starting material is a fluorinated diazoacetate **31**, which was selected due to the pluripotent nature of the molecule, with the diazo group able to act as a nucleophile or an electrophile depending on the reacting partner and reaction conditions. Only the products from the first step are shown in Scheme 6; however, overall Wyatt *et al.* generated a library of 223 small molecules with 30 distinct skeletons in two to four steps.



Scheme 6 – Reagent-based DOS starting from compound **7**. First step of each reaction is shown. Reagents and conditions: (a) C₆H₆, Rh₂(OCOCF₃)₄; (b) R¹CCH, Rh₂(OAc)₄, CH₂Cl₂; (c) thiophene, Rh₂(OAc)₄; (d) furan, Rh₂(OAc)₄ then I₂; (e) LDA, -78 °C then R²COR³, THF then Rh₂(OAc)₄, CH₂Cl₂; (f) DMAD; (g) PhCHO, PhNH₂ then DMAD, Rh₂(OAc)₄ or PhMe [Cu(OTf)]₂, CH₂Cl₂; (h) methyl acrylate.

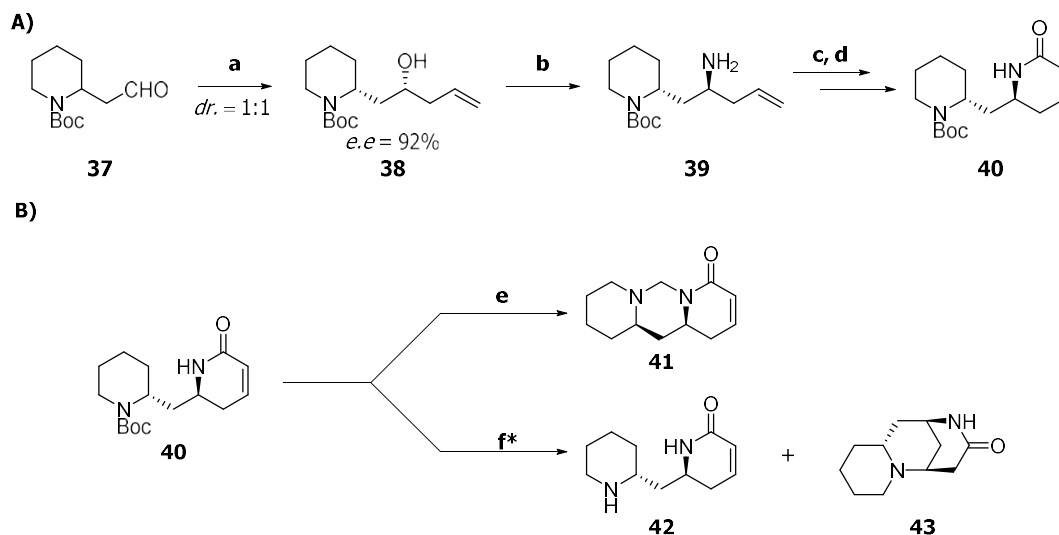
In a series of papers, the Passarella group utilised 2-piperidine ethanol as a versatile building block to generate natural products, natural product hybrids and DOS libraries.^{82–85} 2-Piperidine ethanol contains both hydroxyl and amine functionalities, which can be utilised within scaffold synthesis, widening the scope of available scaffolds. Its chirality influences the stereochemical outcome of the subsequent scaffold-forming reactions, increasing the stereochemical diversity of the library.

The synthetic route used by Passarella to synthesise their first library is summarised in Scheme 7. All three scaffolds started with the transformation of 2-piperidine ethanol into 2-allylpiperidine **33** by a sequential oxidation and Wittig reaction. Spirocyclic scaffold **34** was accessed in three steps by alkylation of the free amine with 2-iodobenzylbromide, followed by an intramolecular Heck reaction, which selectively formed the seven-membered ring with an exocyclic double bond. Finally, a 1,3-dipolar cycloaddition afforded spirocycles **34** as a diastereomeric mixture. Cyclic urea **35** was obtained in two steps; first, reacting the free amine with an isocyanate to form the intermediate urea, then cyclising via an intramolecular oxidative Pd(II)-catalysed chloroamination reaction. The chloro substituent, while not desirable in a library for drug discovery, can act as a handle for further diversification of the scaffold via reactions such as alkylation, hydrolysis *etc.* Tricycle **36** was synthesised by an amide formation with acryloyl chloride, which was followed by ring-closing metathesis (RCM) and in this instance, a completely diastereoselective 1,3-dipolar cycloaddition.



Scheme 7 – Reagent-based DOS starting from compound **32**. Stereochemistry is absolute. R¹ and R² are aryl substituents. Reagents and conditions: (a) DMSO, (COCl₂)₂, NEt₃, CH₂Cl₂; (b) PPh₃⁺CH₃I⁻, BuLi; (c) TFA; (d) 2-iodobenzylbromide, K₂CO₃; (e) Pd(PPh₃)₄, NEt₃; (f) R¹CNO; (g) R²NCO; (h) Pd(MeCN)₂Cl₂, CuCl₂; (i) acryloyl chloride, NEt₃; (j) Grubbs II; (k) R¹CNO.

The second library synthesised is summarised in Scheme 8. The Passarella group exploited the pluripotency of the aldehyde group, utilising a Brown allylation to furnish homoallylic alcohol **38** as a 1:1 mixture of diastereomers. A single diastereomer of alcohol **38** was converted into the corresponding amine **39** *via* a Mitsunobu reaction and Staudinger reduction of the intermediate azide. Acylation and RCM gave bicycle **40**, which was used as the common intermediate for the synthesis of scaffolds **41–43** (Scheme 8A).

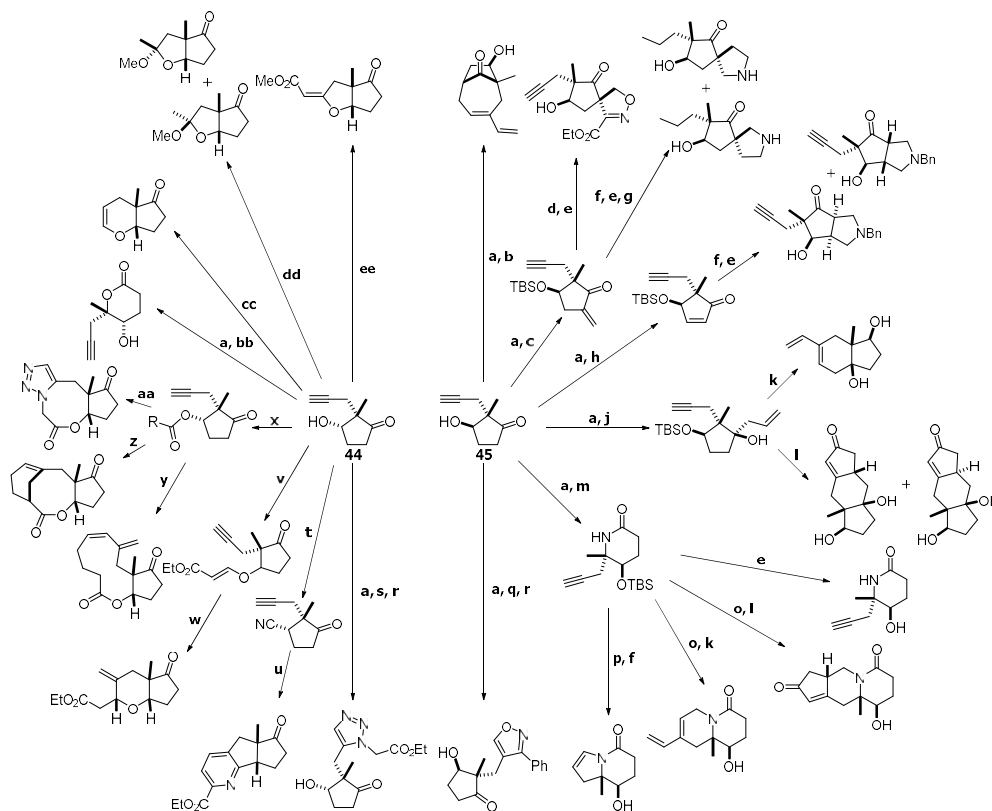


Scheme 8 – Reagent-based DOS starting from compound **37**. Stereochemistry is absolute. Reagents and conditions: (a) (+)-DIP-Cl, allylmagnesium bromide, -78 °C to r.t.; (b) PPh_3 , DIAD, DPPA then PPh_3 , THF/ H_2O ; (c) acryloyl chloride, NEt_3 ; (d) M73 SIMes; (e) HCHO, HCO_2H ; (f) TFA. *Bicycles with *syn*-stereochemistry just deprotect, bicycles with *anti*-stereochemistry form the Michael adduct.

Three scaffolds were obtained from lactam **40** in one step. Tricyclic lactam **41** was obtained *via* an Eschweiler–Clarke reaction for all stereoisomers in good to moderate yield. Treatment of lactam **40** with TFA led to two different products dependent on the relative stereochemistry of the starting material. If the relationship was *syn*, then carbamate deprotection afforded free amine **42**. In contrast, substrates with an *anti*-relationship underwent an intramolecular aza-Michael addition to form tricycle **43**. Overall, six different skeletons were synthesised using 2-piperidine ethanol, with all stereoisomers available, providing a library with wide chemical space coverage.

Utilising a pluripotent, chiral, small molecule to create a diverse library has also been demonstrated by the Spring group.⁸⁶ Starting from cyclopentanone, the group synthesised diastereomeric cyclopentanones **44** and **45**, which contains three different functional groups,

enabling a wide variety of chemistry. Twenty unique frameworksⁱⁱ were synthesised in a maximum of five steps (Scheme 9). The library has a high natural-product likeness, with 92% of the scaffolds outside of “flatland”ⁱⁱⁱ and an average of 2.5 stereogenic centres, demonstrating the range of both stereochemical and skeletal diversity that was achieved.³⁶



Scheme 9 – Reagent-based DOS starting from compounds **44** and **45**. All stereochemistry is relative. Reagents and conditions: (a) TBSCl, imidazole, DMF; (b) (i) LiHMDS, allyl bromide, THF, (ii) Hoveyda–Grubbs II, ethylene, PhMe, (iii) TBAF, THF; (c) CH₂Br₂, Et₃NH, CH₂Cl₂; (d) 1-ethyl oxalyl chloride 2-oxime, Et₃N, CH₂Cl₂; (e) TBAF, THF; (f) *N*-(methoxymethyl)-*N'*-(trimethylsilylmethyl)benzylamine, TFA, CH₂Cl₂; (g) 10% Pd/C, H₂; (h) IBX, PhF/DMSO (2 : 1); (j) allylmagnesium bromide, THF; (k) Grubbs II, ethylene, PhMe; (l) (i) Co₂(CO)₈, CH₂Cl₂, then NMO, (ii) TBAF, THF; (m) *O*-(mesitylenesulfonyl)hydroxylamine, CH₂Cl₂, then BF₃·Et₂O; (o) NaH, DMF, then allyl bromide; (p) (i) InCl₃, DIBALH, Et₃B, I₂, THF; (ii) Cs₂CO₃, CuI, *N,N'*-dimethylethyl-1,2-diamine, PhMe; (q) Cp*Ru(COD)Cl, α -chlorobenzaldehyde, Et₃N, DCE; (r) TBAF, AcOH, THF; (s) ethyl azidoacetate, [Cp*RuCl]₄, PhMe; (t) (i) MsCl, pyridine, (ii) KCN, DMSO; (u) CpCo(CO)₂, ethyl propiolate, PhMe; (v) ethyl propiolate, NMM, CH₂Cl₂; (w) (i) Bu₃SnH, AIBN, PhMe, (ii) *p*-TsOH, CH₂Cl₂; (x) RCO₂H, DCC, DMAP, CH₂Cl₂; R = (CH₂)₃CHCH₂, R = CHCH₂, R = CH₂N₃, R = (CH₂)₃N₃; (y) R = (CH₂)₃CHCH₂, Grubbs II, ethylene, PhMe; (z) R = CHCH₂, Hoveyda–Grubbs II, ethylene, PhMe; (aa) R = CH₂N₃ or R = (CH₂)₃N₃, Cp*RuCl(cod), PhMe; (bb) (i) KHCO₃, *m*CPBA, CH₂Cl₂ (ii) TBAF, THF; (cc) NHS, Bu₄NPF₆, NaHCO₃, PPh₃, CpRu(PPh₃)₂Cl, DMF; (dd) [Ir(cod)Cl]₂, MeOH; (ee) Pd(CH₃CN)₂Cl₂, *p*-benzoquinone, CO, CH₂Cl₂.

ⁱⁱ Frameworks within this review are defined using the Murcko definition: “The framework is defined as the union of ring systems and linkers in a molecule”.¹⁸² For a more thorough discussion of what constitutes a unique framework, see Section 2.3.1.

ⁱⁱⁱ Flatland is defined as $npr1 + npr2 \leq 1.1$, where *npr1* and *npr2* are the co-ordinates of the molecule on a PMI plot.

Troelsen *et al.* used six CF₃-containing building blocks and a range of different cycloaddition reactions to synthesise a library containing 115 molecules, with 67 unique frameworks (Figure 22).⁸⁷ The library had an average Fsp³ value of 0.7, with 95% of the synthesised scaffolds outside of “flatland”, demonstrating the complexity that can be achieved starting from simple starting materials. The CF₃ group provided a useful diagnostic tool for biological analysis of the compound library as each CF₃ group appears as a singlet in the ¹⁹F NMR spectrum, with a wide range of chemical shifts exhibited by the library (–56 to –78 ppm). Therefore, rather than individually screening each compound, ~20 compounds were combined into chemical cocktails based on chemical shift dispersion and then screened against biological targets. Suppression of a resonance in the ¹⁹F NMR spectrum meant that binding had occurred, and further testing could be carried out.

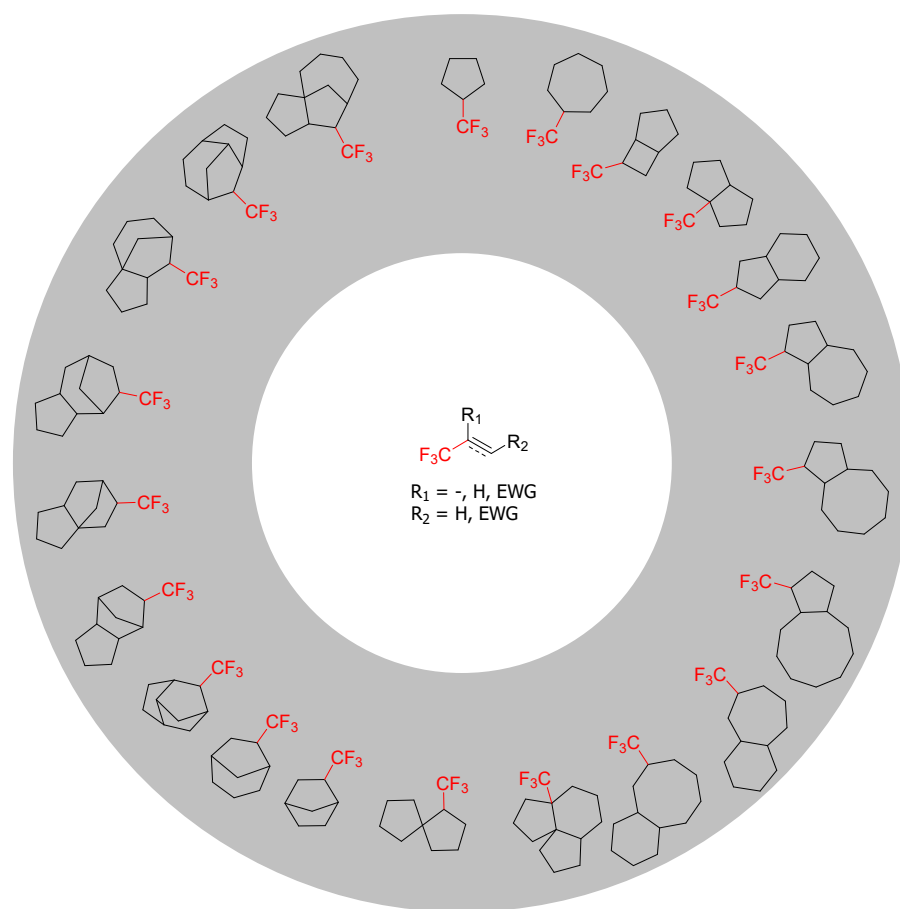


Figure 22 – A representation of some of the scaffolds synthesised by Troelsen *et al.* EWG = Electron-withdrawing group.

Although both reagent-based and substrate-based approaches are useful by themselves, these strategies are not mutually exclusive and can be used in tandem with each other. The reagent-based approach can be used at any stage of DOS to create diverse functionality or transform pre-functionalised molecules into distinct molecules. The use of pluripotent functionality, a functional group which can be transformed into many different functionalities, is a key component of this approach.⁸⁸ The substrate-based approach pre-encodes skeletal information by placing functional groups at strategic points on a molecule. These groups can be placed early in a synthesis and then used at the end to make the pre-encoded molecular skeletons.

1.3.3 Build/Couple/Pair Strategy

The ideas described in the previous sections were developed further into multiple, advanced strategies. One such strategy is build/couple/pair (BCP).⁸⁹ In the build stage, chiral molecules are either synthesised or obtained and used as the starting materials for the library synthesis. These molecules are then reacted together to create densely functionalised products in a couple phase. Ideally, these intermolecular coupling reactions can produce all of the possible stereoisomers. The pair phase then involves the intramolecular reaction of the previously coupled groups to create diverse molecular skeletons. The pair phase can be done either via reagent-based or substrate-based synthesis, depending on the relative positions of the functional groups. In this strategy, it is in these first two steps that the maximal amount of stereochemical diversity is generated from the available starting fragments. The final step, pair, usually closes a ring and is responsible for the skeletal diversity generated. A cartoon representation of each of the stages can be seen in Figure 23. Since its inception, BCP has been widely adopted by groups working on DOS.^{90,91}

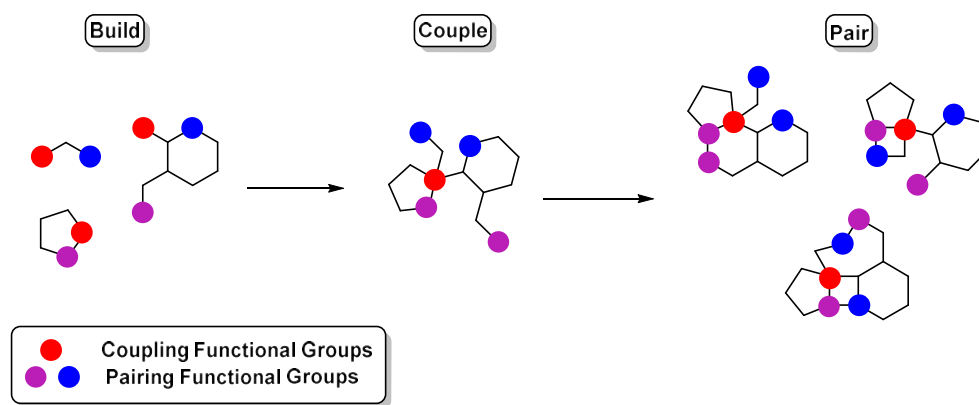
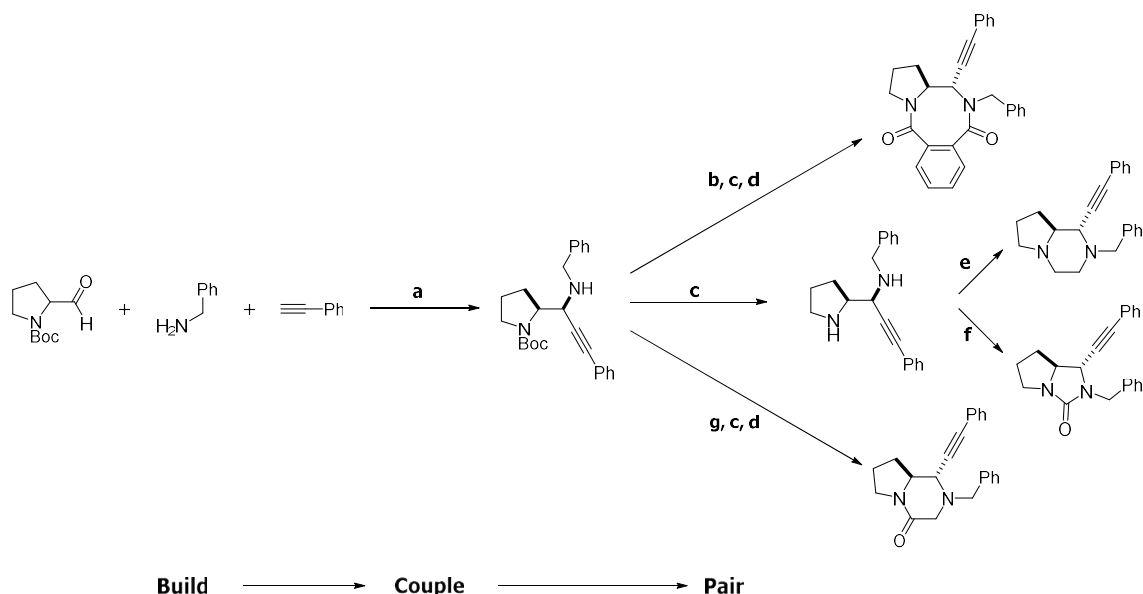


Figure 23 – A cartoon representation of how BCP works.⁹²

To date, BCP has become one of the most prominent synthetic approaches used within DOS, due to its modular and concise nature, which allows for small changes that can alter the generated libraries dramatically. Once a hit has been discovered from libraries generated by BCP, it is relatively easy to incorporate further appendage diversity into the molecule to see if the activity can be enhanced. BCP has evolved significantly since its inception, with a number of groups using different strategies within the broad framework of BCP.^{89,93–96}

BCP is currently mainly used for synthesising a diverse library of macrocycles as it has been superseded by other methods in the arena of small molecules.^{65,66,69,97,98} Nevertheless, some small-molecule libraries have been synthesised utilising BCP methodology. Innocenti *et al.* used commercially available building blocks with an Aldehyde-Amine-Alkyne coupling (A³ reaction) reaction to form linear intermediates, which then underwent intramolecular pairing reactions to generate four different scaffolds in just three steps (Scheme 10).⁹⁹ The library was shown to cover a wide range of chemical space (as defined by PMI analysis), with the bi- and tricyclic systems more disc-like than their pre-cyclised analogues.



Scheme 10 – BCP DOS from an A³ reaction. All stereochemistry is relative. Reagents and conditions: (a) CuI, DCE, μ W; (b) phthalic anhydride, CH₂Cl₂; (c) TFA; (d) TBTU, DIPEA, CH₂Cl₂; (e) 1,2-dibromoethane, K₂CO₃, DMF; (f) CDI, DIPEA, CH₂Cl₂; (g) BrCH₂CO₂tBu, DIPEA, DMF.

In silico design has also been applied to BCP library synthesis. Zhang *et al.* generated a virtual library of 66,800 compounds from 63 scaffolds with multiple points of diversity, which were

then virtually decorated to generate the library.¹⁰⁰ Application of a series of filters, such as only allowing compounds with an AlogP of -1 to 3 , limited the virtual library to $8,500$ compounds, of which 20 were chosen for synthesis, with maximal shape diversity used as the main criteria for the selected scaffolds.¹⁰¹ The initial scaffolds used in the virtual library were based upon previous work in the group that had generated diverse scaffolds, with four main approaches foreseen: 1) Ir-catalysed allylic amination and cyclisation; 2) cyclisation of α -allyl α -amino ester derivatives; 3) cyclic sulfamidate ring-opening and intramolecular Mitsunobu reaction; 4) cyclic sulfamidate ring-opening, Au-catalysed reaction and Ugi reaction.^{102–105} Ultimately only two of the routes were successfully realised in the laboratory, as both the Ir-catalysed route and Mitsunobu reaction proved either low-yielding or poorly regioselective, depending on the substrate. Some of the successfully synthesised scaffolds can be seen in Figure 24, demonstrating the range of frameworks that can be generated using just two reactions.

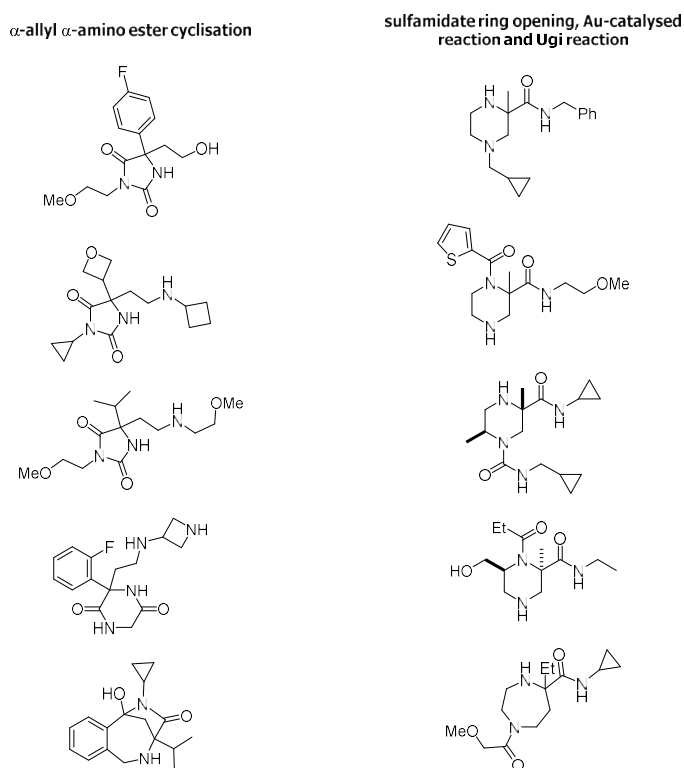
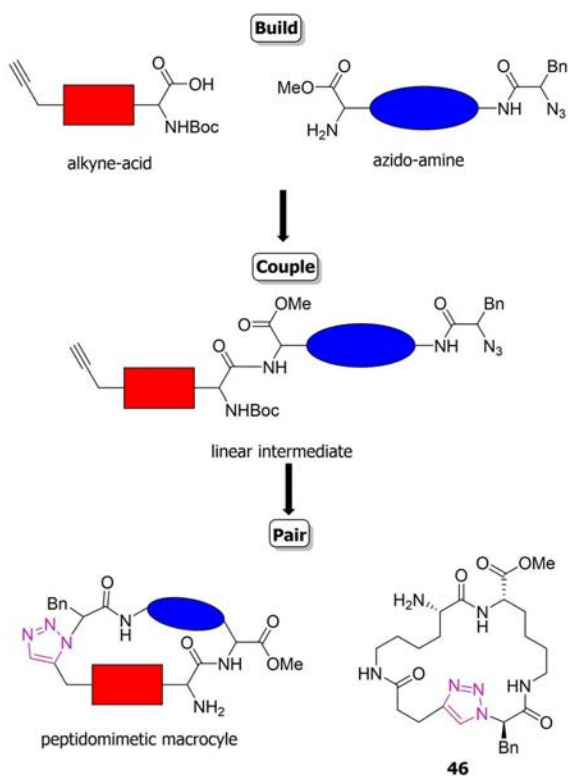


Figure 24 – Ten of the compounds synthesised using a BCP method.

Over the last 15 years, construction of small-molecule libraries using BCP has proven to be the exception rather than the rule.¹⁰⁶ An early example of using BCP to generate a library of macrocycles was reported by the Spring group,⁹³ who used peptidomimetic scaffolds to couple chiral molecules before the final pairing reaction. The structures were synthesised *via* use of

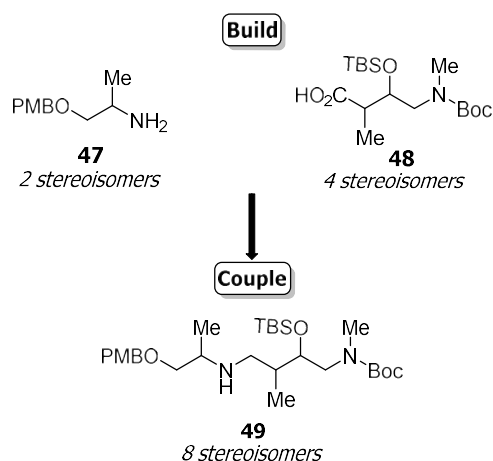
amino acid-derived reactants, which contained functionality useful for both the couple and pair stages of the BCP strategy. By using orthogonal functional groups, a linear precursor could be built in the couple phase using amide chemistry, before the creation of a macrocycle using click chemistry in the pair phase (Scheme 11). The choice of click chemistry allowed for stereochemical selection of either the 1,4- or 1,5-disubstitution of the triazole ring (highlighted in purple, Scheme 11) without compromising the stereogenic centres present within the molecule. The coloured shapes within Scheme 11 represent alkyl chains of varying length that are omitted for simplicity.



Compound **46** is representative of the macrocycles synthesised for this library. Compound **46** was synthesised in nine steps. First, the alkyne-acid and azido-amine were synthesised, followed by an amide coupling to generate the linear intermediate. The final step involved a click reaction, which in this case was carried out via the “copper route” (CuI, DIPEA, THF) to generate 1,4-triazole **46**. The BCP approach shown in Scheme 11 was originally used as a proof of concept, with only fourteen macrocycles synthesised, but has since been used to generate libraries containing a wide range of molecular skeletons.^{107,108}

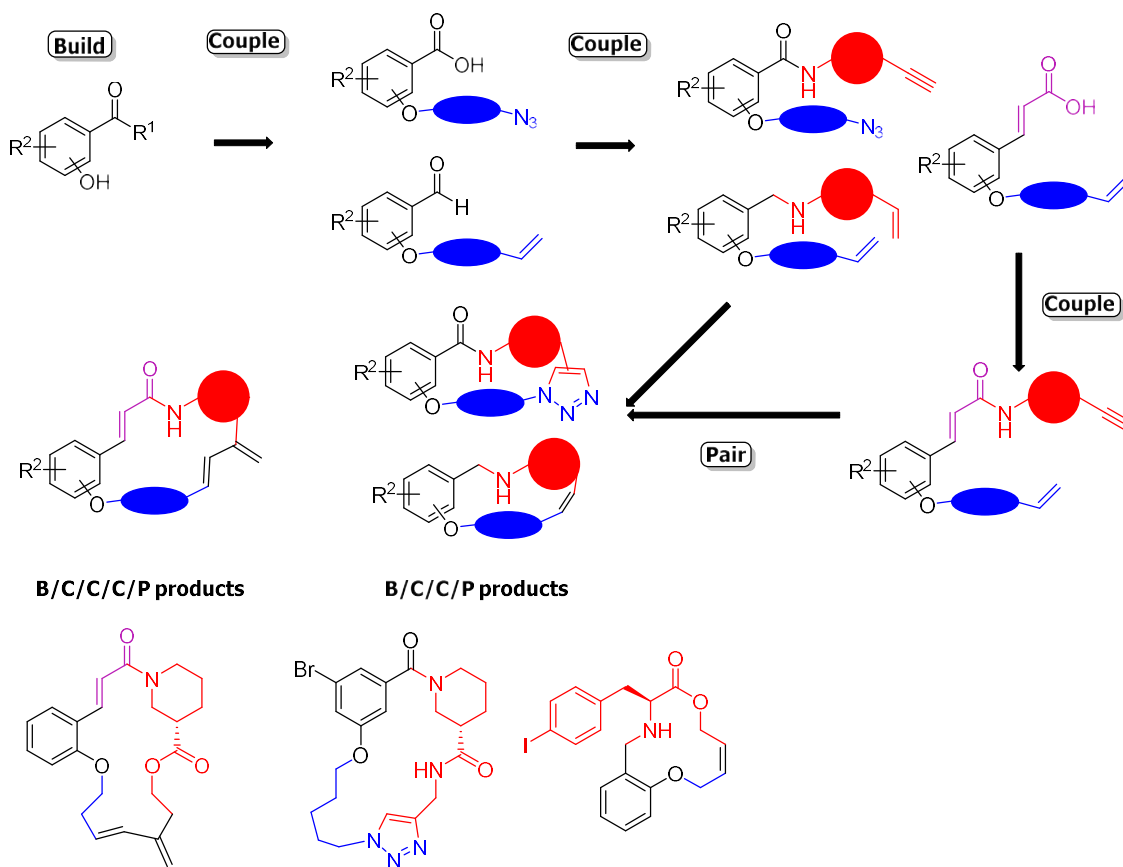
Scheme 11 – Representation of the BCP strategy used to create peptidomimetic macrocycles. Compound **46** is one of the macrocycles synthesised for the library.

Peptidomimetic macrocycles are not the only type of macrocycles that have been synthesised via the BCP method. The Marcaurelle group has developed a BCP strategy in which 12-membered macrolactams can be accessed by utilising a head-to-tail cyclisation to close the ring.⁹⁴ Their methodology is particularly impressive as they are able to access all possible stereoisomers of their scaffolds, maximising the stereochemical diversity potential of their library. Initially, all stereoisomers of amine **47** and acid **48** were synthesised, followed by an amide coupling and reduction to generate **49** (Scheme 12).



Scheme 12 – Generation of the linear intermediate before head-to-tail cyclisation

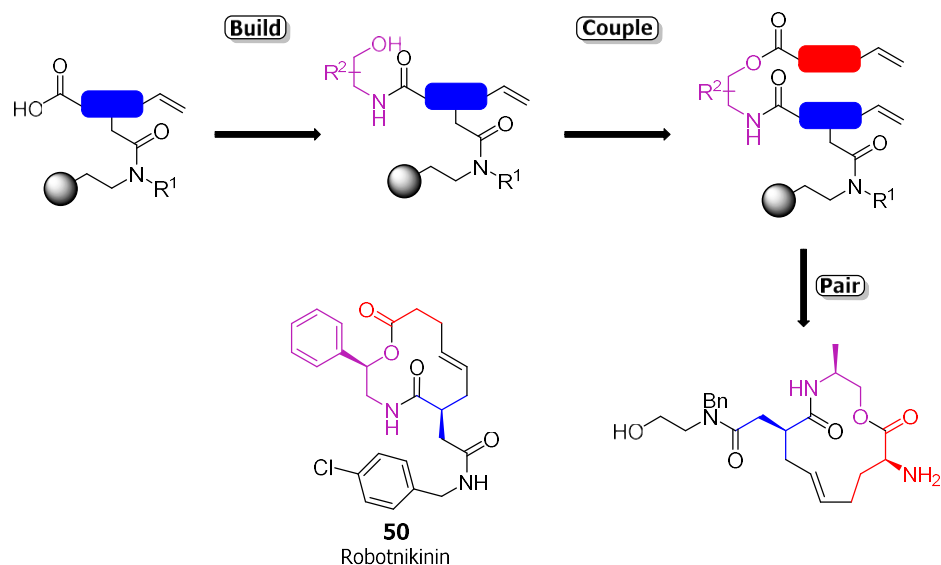
A multi-step process was then carried out to introduce carboxylic acid and amine functionalities at the opposite ends of the chain, where they could then be used in a macrolactamisation reaction to form the macrocycle (Scheme 13). By utilising all eight different stereoisomers of **49** and selectively placing the nitro group at either the 3- or 4- position, 16 different scaffolds were synthesised. Once the skeletal cores had been synthesised, the nitro group was reduced to an amine and then capped using acyl chlorides or isocyanates to provide functional group diversity to the library giving an overall size of 7,936 macrocycles.



Representative examples of macrocycles synthesised for inclusion within the library

Scheme 14 – Representation of the original BCCP route used to synthesise a macrocyclic DOS library. Examples of macrocycles synthesised are also shown.

Building off previous work done within the group,¹¹⁰ Peng *et al.* used BCP methodology with the linear precursor attached to polystyrene macrobeads, which allowed for the rapid generation of a library of 12-, 13- and 14-membered macrocycles (Scheme 15).¹¹¹ Subsequent small-molecule microarray-based screening of the library discovered multiple compounds within the library that bound to the Sonic Hedgehog signalling protein (SHH). SHH has been implicated in the development basal cell carcinoma, pancreatic cancer and prostate cancer.¹¹² Analogue development of the most active compounds led to the discovery of robotnikinin **50**, a highly active compound with $K_d = 3.1 \mu\text{M}$.¹¹³



Scheme 15 – BCP route used which led to the discovery of robotnikinin

Over the last 20 years, DOS has enabled the construction of hundreds of libraries with unprecedented molecular, shape and scaffold diversity, and led to the discovery of new therapeutics with the potential to be licensed.^{113–115} Despite these successes, criticisms of the current approach have also been made by the medicinal chemistry community.^{69,116} Libraries created using BCP and related methodologies often have undesirable physicochemical properties for orally administered compounds (high LogP, high MW), making them undesired for most screening campaigns. Additionally, macrocycles have a high molecular complexity, diminishing the chance of a hit and increasing the difficulty of optimisation. However, BCP and related methodologies have found applications within chemical biology as chemical probes, due to the large binding interfaces of the macromolecule, which can be used to disrupt protein-protein interactions, or to bind other small-molecule modulators of protein function.^{117,118}

1.4 Medium-sized Rings

In the development of natural products and pharmaceutically active agents, diversifiable medium-sized (8- to 12-membered) rings are particularly attractive synthetic targets.^{119,120} In particular, medium-ring nitrogen- and oxygen-containing heterocycles have been shown to have a broad range of biological activity, examples of which can be seen in Figure 25.^{115,121–125} This makes medium-ring heterocycles absence from approved pharmaceuticals even more surprising.¹²⁶ Therefore, the development of a synthetic strategy which enables quick access to heteroatom-containing medium-ring frameworks, would be of great interest to drug discovery today.

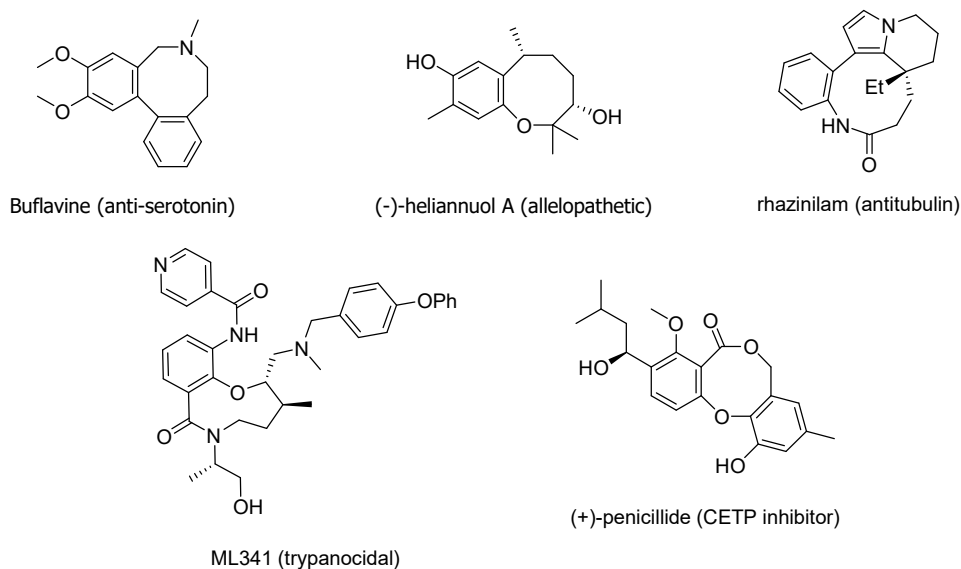
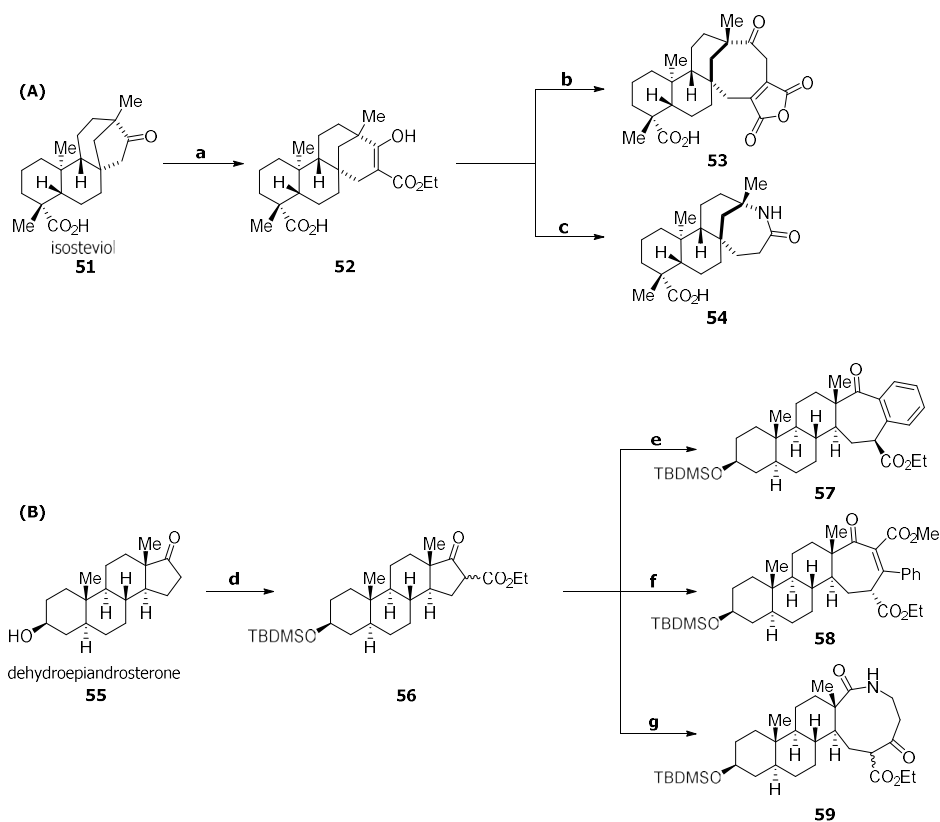


Figure 25 – Medium-ring heterocycles which demonstrate biological activity. The biological activity is given in brackets.

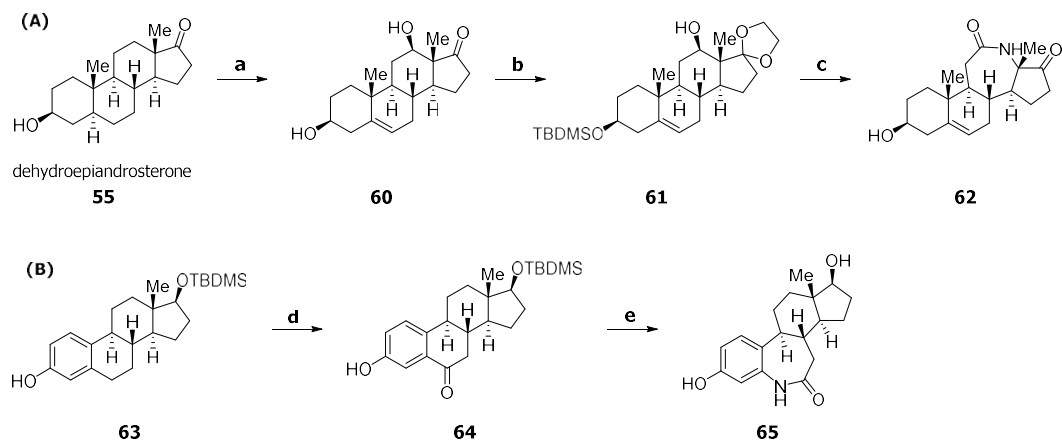
Natural products, many of which include a small, heteroatom containing ring as part of their molecular structure, are the source of inspiration for many of the drugs currently in the clinic (see Section 1.1). However, much of the synthetic exploration of chemical space around each natural product relies on specific functional groups that are already present in the molecule. Zhao *et al.* envisaged using C–H functionalisation, which could be generalised across all classes of natural products, to enable a much more thorough exploration of chemical space around natural products. The group synthesised a library of 123 medium ring-containing molecules, with 27 unique scaffolds either via ring expansion utilising existing C–O bonds or via site-selective oxidation of C–H bonds, followed by ring expansion (Scheme 16, Scheme 17).¹²⁷

A wide variety of chemistry was used to effect the desired transformations. As can be seen in Scheme 16, Zhao *et al.* expanded the bridged five-membered ring of isosteviol **51** to the β -keto ester **52** by treatment with $\text{BF}_3 \cdot \text{OEt}_2$ and ethyl diazoacetate. A Beckmann rearrangement led to lactam **54**, while a formal [2 + 2] cycloaddition with dimethyl acetylenedicarboxylate, followed by ring fragmentation and treatment with acid, led to fused anhydride **53**. Dehydroepiandrosterone (DHEA) **55** was readily acylated after protection of the alcohol to give intermediate **56**. The six-membered ring in **56** could also be readily converted into a medium-sized ring by a two-carbon ring expansion to generate scaffold **58**. Tandem ring expansion and aryne insertion led to scaffold **57**. Finally, an acylation/ring-expansion sequence furnished seven-membered ring **59** bearing a β -keto ester motif.

Scheme 17 shows C–H activation of DHEA and a derivative of estrone. In both cases, Cu-catalysed C–H oxidation was followed by oxidation to the ketone. A Beckmann rearrangement then led to lactams **62** and **65**.

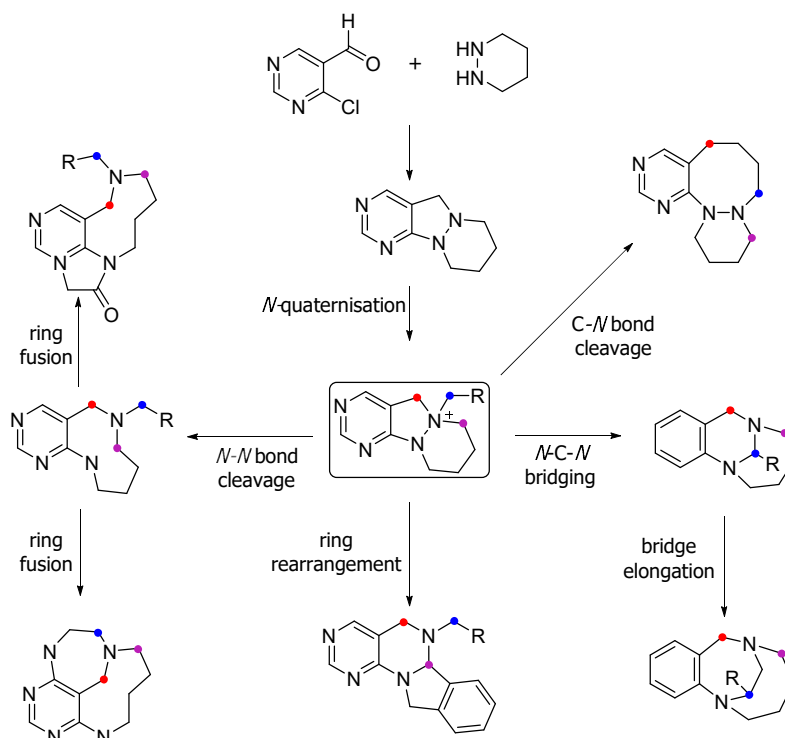


Scheme 16 – Ring expansion of steroids based on native C–O bonds.¹²⁷ Reagents and conditions: (a) i) Me_2SO_4 , LiOH, THF, 65 °C, ii) ethyl diazoacetate, $\text{BF}_3 \cdot \text{Et}_2\text{O}$, $\text{Et}_2\text{O} / \text{CH}_2\text{Cl}_2$, rt; (b) NaH, toluene, then DMAD, rt; (c) i) LiCl, DMSO, H_2O , 120 °C, ii) $\text{NH}_2\text{OH} \cdot \text{HCl}$, KOAc, 70 °C, (c) $p\text{TsCl}$, DMAP, Pyr, 60 °C; (d) i) TBSCl, imidazole, CH_2Cl_2 , rt, ii) LDA, THF, then CNCO_2Et , –78 °C; (e) 2-(trimethylsilyl)phenyl trifluoromethanesulfonate, CsF, MeCN, 80 °C; (f) i) NaH, THF, methyl phenylpropionate, 65 °C, ii) $p\text{TsOH}$, THF, rt; (g) i) MgCl_2 , Py, $\text{NHCbz}(\text{CH}_2)_2\text{COCl}$, CH_2Cl_2 , ii) Pd/C, H_2 , EtOAc, rt.



Scheme 17 - Ring expansion of steroids by sequential C–H oxidation and ring expansion.¹²⁷ Reagents and conditions: (a) i) $p\text{TsOH}$, toluene, (4-methylpyridin-2-yl)methanamine, 120 °C, ii) $[\text{Cu}(\text{MeCN})_4\text{PF}_6]$, O_2 , (+)-sodium-(L)-ascorbate, acetone/ MeOH, 50 °C, 6 h, then, Na_4EDTA , rt; (b) i) glycol, toluene, $p\text{TsOH}$, 120 °C, ii) TBSCl, imidazole, CH_2Cl_2 , rt; (c) i) $(\text{COCl})_2$, DMSO, Et_3N , CH_2Cl_2 , –78 °C, ii) $\text{NH}_2\text{OH} \cdot \text{HCl}$, KOAc, 70 °C, iii) $p\text{TsCl}$, DMAP, Pyr, 60 °C, iv) TsOH, THF / H_2O , rt; (d) $\text{Cr}(\text{CO})_6$, tBuOOH, MeCN, 70 °C; (e) i) $\text{NH}_2\text{OH} \cdot \text{HCl}$, KOAc, EtOH, (b) TsCl, DMAP, Pyr, (c) TFA.

An alternative method of ring expansion, selective bond cleavage to reveal a medium-sized ring, has also been studied.^{128–130} Recently, Choi *et al.* applied this concept to the synthesis of azacycles, synthesising 14 different scaffolds via an *N*-quaternisation strategy (Scheme 18).¹³¹ The synthesised library contained a wide variety of different rings, with eight- to ten-membered rings, bridged structures and fused rings all represented. PMI calculations showed a good coverage of chemical space, with most of the scaffolds lying outside of “flatland”.



Scheme 18 – Divergent synthetic pathway for synthesis of medium-ring azacycles. For full conditions, see ref.¹³¹

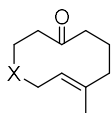
Other routes to medium-sized rings have been reported, including the use of RCM,¹³² migratory ring expansion,¹³³ lactam/ lactone formation¹³⁴ and an internal Heck reaction,¹³⁵ demonstrating the wide variety of methodology that can be used to access these synthetically important molecules.

1.5 Aims and Objectives

Since the advent of DOS as a new way of developing compound libraries for screening, many strategies have been developed within its framework to enable the efficient construction of diverse libraries.

Medium ring-containing scaffolds have been shown to display a broad range of biological activities and yet are under-represented within approved pharmaceuticals. Therefore, construction of a library of medium-sized ring using the principles of DOS was highly desirable.

Combining both DOS and medium-ring methodology, keto-alkene **66** was identified as a key intermediate in the synthesis of our library, due to its pluripotent functionality allowing for a range of chemical transformations, and variability of X allowing for the investigation of various heteroatom analogues of the library (Figure 26).



66

Figure 26 – Key intermediate **66** in the design of the library.

With ketone **66** in hand, we planned to carry out reagent-based DOS on the scaffold to synthesise a library containing a wide variety of medium ring-containing scaffolds (Figure 27).

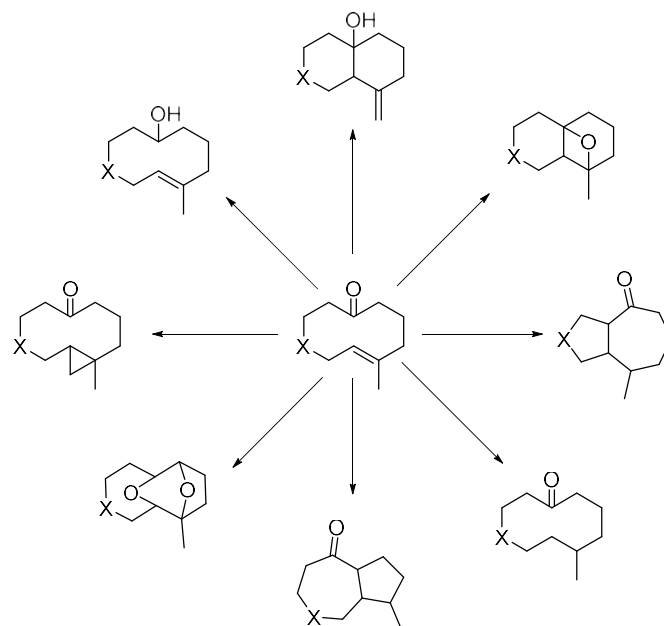


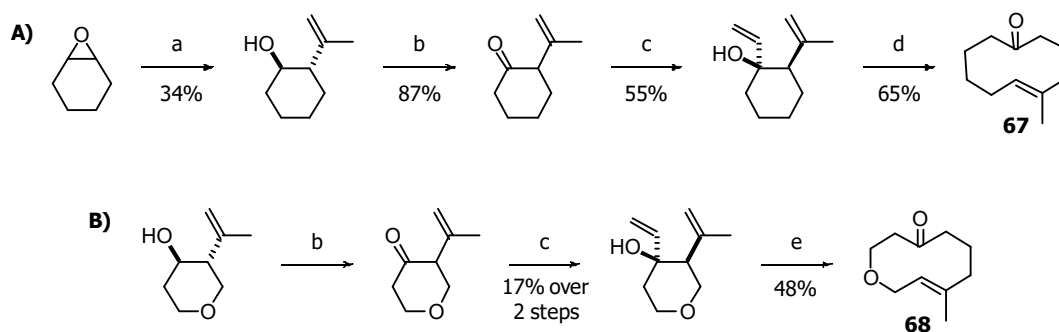
Figure 27 – Representation of some of the scaffolds that can be synthesised in 1–3 steps from scaffold **66** using reactions with literature precedent.

Once we have synthesised a library of scaffolds, a cheminformatics analysis and practical considerations will be used to determine which are suitable to advance for diversification. Virtual decoration of these scaffolds using LLAMA, followed by assessment of their chemical properties, chemical space coverage and ease of synthesis will direct the synthesis of a representative small library of compounds. Finally, these compounds will be placed into a screening library for future use in HTS.

Chapter Two: Design and Synthesis of a Library of Scaffolds

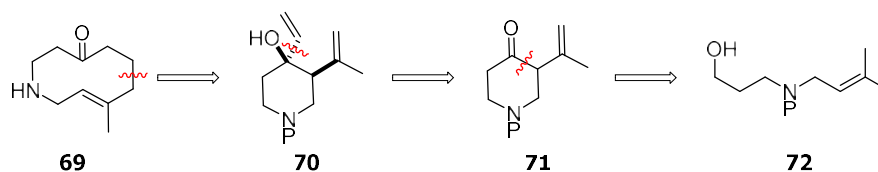
2.1 Introduction

As discussed in Section 1.5, the first aim of this project was to synthesise a ten-membered ring containing three points of diversity. The carbon and oxygen analogues **67** and **68** of our initial target have been synthesised previously by the Jacobsen group (Scheme 19).¹³⁶ Both routes featured the synthesis of a diene intermediate, which is then utilised in a Cope-like rearrangement to furnish the desired ten-membered ring.



Scheme 19 – Jacobsen’s synthesis of ten-membered ketones **67** and **68**. Reagents and conditions: a) CuI, isopropenylmagnesium bromide, THF; b) (COCl)₂, DMSO, NEt₃, CH₂Cl₂; c) vinylmagnesium bromide, THF; d) KH, 18-crown-6, THF; e) (C₆H₅CN)PdCl₂ (10 mol%), THF.

The first target contained an amine, **69** to allow for a greater scope of diversification once the library has been generated, as other atoms (such as C, O or S) would already be fully saturated and therefore unable to undergo further chemical reactions.^{iv} A retrosynthetic analysis of keto-alkene **69** based on the Jacobsen methodology is summarised in Scheme 20.



Scheme 20 – Retrosynthetic of keto-alkene **69**. P = protecting group

Ketone **71** was identified as a key intermediate, which would be accessed through a series of oxidations and cyclisation starting from amino alcohol **72**.

^{iv} Use of a sulfur heteroatom would however enable access to a sulfone or sulfoximine group.

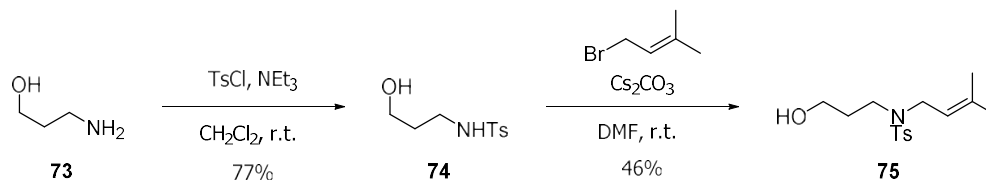
2.2 Synthesis of ten-membered ketone 69

2.2.1 Choice of Protecting Group

Protecting-group choice was key to the success of the proposed strategy. The *p*-toluenesulfonyl (Ts) protecting group was chosen due to its electron-withdrawing nature, which reduces the nucleophilicity/basicity of the nitrogen, removing potential chemoselectivity issues in subsequent oxidation steps.¹³⁷ The tosyl group also provides a chromophore, which is useful for reaction monitoring. Tosyl sulfonamides are stable to all but the most forcing conditions, which would allow for a wide array of chemistry to be explored during library development without deprotecting the amine prematurely.¹³⁸ We were aware that the stability of this protecting group might be problematic for later scaffold development and mindful that alternative, easier to remove protecting groups might need to be chosen once the full library of scaffolds had been generated and the synthetic route established.

2.2.2 Synthesis of the linear precursor amino alcohol 75

Alcohol **75** was first synthesised from commercially available 3-amino-1-propanol **73** (Scheme 21) utilising a procedure from Williams *et al.*¹³⁹ The Ts group was installed first to aid in monoalkylation in the subsequent prenylation step.



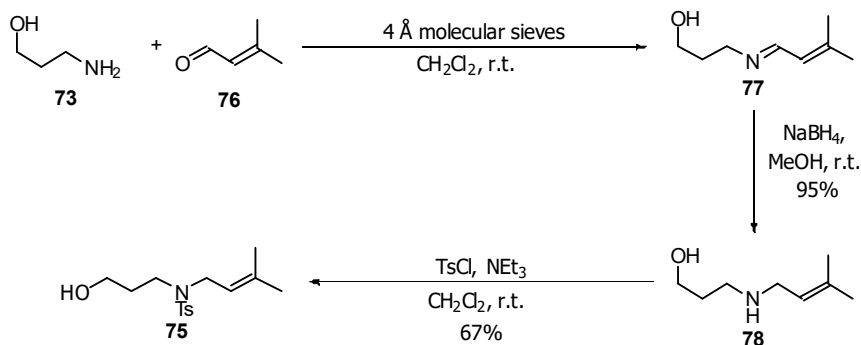
Scheme 21 – First synthetic route to alcohol **75** from amino alcohol **73** *via* an alkylation strategy

Chemoselective *N*-tosylation was successfully carried out following a procedure by Williams *et al.*, giving sulfonamide **74** in good yield.¹³⁹ Unfortunately, subsequent *N*-alkylation proceeded in poor yield, which was unexpected following literature precedent on similar substrates reporting high yields.^{140–142} Efforts to increase the yield, by increasing the number of equivalents of base or prenyl bromide resulted in the formation of the bis-prenylated product on oxygen as well as nitrogen instead of the desired alcohol **75**.

To overcome the low yield of the *N*-alkylation, it was decided to reverse the route and form the secondary amine bond first and then introduce the sulfonamide. The secondary amine

gave the possibility of introducing a range of protecting groups at this point in the synthesis, which could be utilised in the development of the final library.

A reductive amination was carried out using 3-amino-1-propanol **73** and 3-methyl-2-butenal **76**, adapting a procedure by Hayakawa *et al.*¹⁴³ Imine **77** was formed by stirring the two starting materials overnight in the presence of activated 4 Å molecular sieves. The sieves served to absorb the water generated in the reaction, shifting the equilibrium towards the desired product. The crude imine product was used directly in the next step, which involved treatment with sodium borohydride to give secondary amine **78** in 95% yield, which could be used without the need for purification (Scheme 22).



Scheme 22 – Modified synthetic procedure for accessing alcohol **75**.

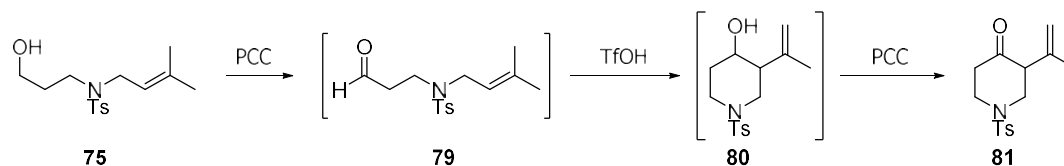
Chemoselective *N*-tosylation was achieved by subjecting amine **78** to *p*-toluenesulfonyl chloride (TsCl) in dichloromethane, to give the desired sulfonamide **75** in 67% yield. Increasing the number of equivalents of TsCl in an attempt to improve the yield, instead led to the tosylation of the hydroxyl as well as the amine.

Overall, the modified route represents a much higher yielding synthesis than the original route, with an overall yield of 64% compared to 35%. Protection of the amine after prenylation also allows for a much wider range of potential protecting groups to be used, as the effect of the protecting group on the subsequent *N*-alkylation step does not need to be considered.

2.2.3 Synthesis of piperidinone **81**

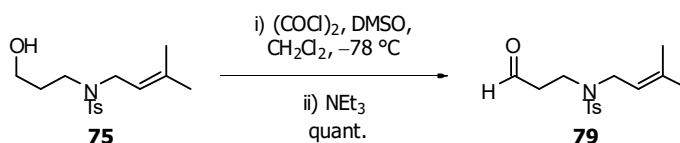
With alcohol **75** in hand, several viable routes to synthesise piperidinone **81** were identified. The Snaith group had previously used alcohol **75** in a one-pot oxidation-cyclisation-oxidation sequence to generate piperidone **81** directly in 61% yield.¹⁴⁴ In this one-pot procedure, alcohol

75 is treated with pyridinium chlorochromate (PCC) and triflic acid (TfOH) (Scheme 23).¹⁴⁴ PCC first oxidises alcohol **75** to the corresponding aldehyde **79**. A Prins cyclisation catalysed by TfOH then forms piperidinol **80** as a mixture of diastereomers which undergo further oxidation to the desired piperidinone **81**.



Scheme 23 – One-pot synthesis of piperidinone **81**.

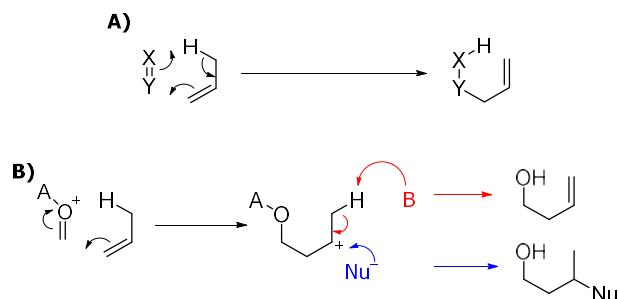
The benefit of this one-pot route is that three steps can be carried out consecutively with no need for any processing in between. Using the Snaith conditions, ketone **81** was first isolated in a yield of 36%. This one-pot reaction sequence proved capricious, with the isolated yield of ketone **81** varying from 19%–36%. Due to the low yields, toxicity of the reagents and difficulty of handling the crude material before purification, no efforts were made to optimise the reaction, and it was instead decided to carry out the reaction sequence in a stepwise manner. Swern oxidation of alcohol **75** to the corresponding aldehyde **79** proceeded in quantitative yield with no need for purification (Scheme 24).



Scheme 24 – Swern oxidation of alcohol **75** to aldehyde **76**

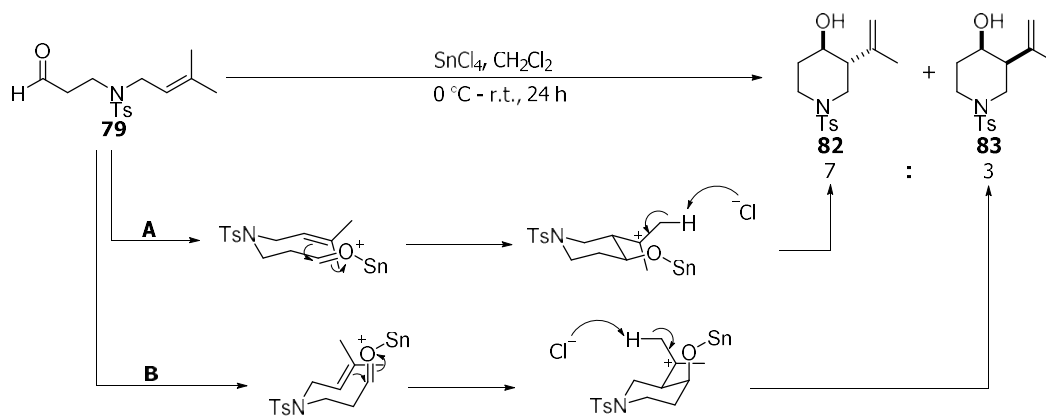
The subsequent cyclisation reaction between an olefin and an aldehyde has been extensively studied. Reaction can proceed *via* one of two mechanistic pathways: a carbonyl-ene reaction and a Prins reaction.^{145,146} The carbonyl-ene (Scheme 25A) describes a pericyclic reaction between an olefin bearing an allylic hydrogen (the ene) and an electron-deficient unsaturated functional group (the enophile). The reaction involves the concerted formation of two σ -bonds and the migration of a π -bond.¹⁴⁶ The Prins reaction (red route, Scheme 25B) describes a stepwise process involving the acid-catalysed addition of an olefin to a carbonyl and the formation of a carbocation intermediate, which undergoes deprotonation to deliver the end-product. Differentiation between the two reaction mechanisms is typically *via* observation of a

by-product generated by nucleophilic attack on the transient carbocation in the stepwise process (blue route, Scheme 25B).^{147,148}



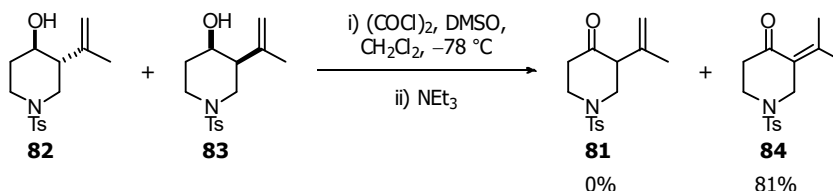
Scheme 25 – A) General representation of an ene reaction. X, Y = C, N, O; B) General representation of a Prins reaction. A = Lewis or Brønsted acid activator, B = base, Nu = nucleophile

Williams *et al.* have investigated the cyclisation of aldehyde **79** under both the carbonyl-ene and Prins cyclisation pathways.¹³⁹ The group showed that SnCl₄ was the best catalyst for the reaction, with this reaction proceeding in high yield *via* a Prins mechanism, with very little by-product formation. Our optimisation of the reaction conditions by increasing the reaction time to 24 h while reducing the catalyst loading to 10 mol% meant that the reaction proceeded in quantitative yield with no purification of the product required (Scheme 26). A mixture of both diastereomers **82:83** was obtained in a ratio of 7:3. We postulate the two diastereoisomers are formed through a chair-like T.S. in which the larger prenyl substituent adopts a pseudoequatorial orientation. The minor diastereoisomer is then formed through pathway B which incurs an unfavourable *syn*-pentane-like interaction between the pseudoaxially oriented Lewis acid-activated aldehyde and one of the methyl groups in the prenyl substituent.



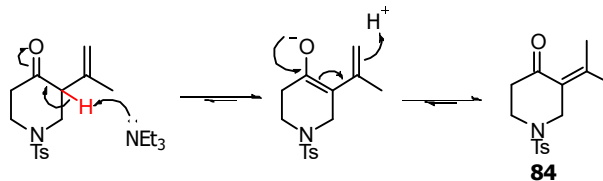
Scheme 26 – Prins cyclisation of aldehyde **79**

With alcohols **82** and **83** in hand, Swern oxidation using the conditions previously used to synthesise aldehyde **79** failed to yield desired piperidinone **81**; conjugated enone **84** was isolated instead (Scheme 27).



Scheme 27 – Swern oxidation of the diastereomeric mixture of alcohols **82** and **83** to enone **84**

Based on literature precedent, abstraction of the tertiary α proton (highlighted in red, Scheme 28) by the triethylamine base forms the corresponding enolate, which provides a pathway for forming the conjugated enone **84** upon re-protonation.¹⁴⁹ Utilising Hünig's base as a more bulky base, which it was hypothesised would increase the energy barrier of proton abstraction due to increased steric interactions, led to the formation of the desired piperidinone **81** in 33% yield; however, olefin isomerisation remained a problem. It was postulated that, due to the tertiary amines relatively higher boiling point compared to dichloromethane, there was a point during isolation of the crude at which the desired compound was dissolved in just amine, drastically increasing the rate of isomerisation. A modification to the work-up procedure addressed the problem: the crude product from the aqueous work-up was never isolated; instead, the reaction volume was reduced before direct loading on to a silica column. This modification to the work-up enabled isolation of the desired piperidinone **81** in 95% yield over three steps.



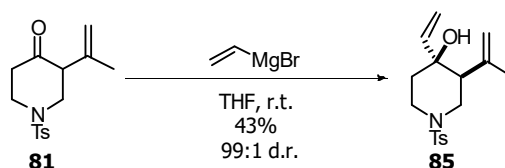
Scheme 28 – Formation of conjugated ketone **84**

Given the short reaction time for the oxidation steps and the ability to use the intermediates without purification, this stepwise oxidation–cyclisation–oxidation sequence can be carried out in just over 24 h. The overall reaction time is comparable to the one-pot method but avoids

the use of toxic reagents and provides a much-improved yield of 95%. The stepwise sequence has been carried out on a scale up to 6 g with a minimal (<5 %) reduction in yield observed.

2.2.4 Formation of alcohol **85**

With piperidinone **81** in hand, alcohol **85** could be accessed by vinyl addition into the ketone. Treatment of piperidinone **81** with vinylmagnesium bromide gave alcohol **85** in a 43% yield as a single diastereoisomer as determined by analysis of the ^1H NMR spectrum of the crude material (Scheme 30).



Scheme 29 - Vinyl addition to form alcohol **85**

The relative stereochemistry was confirmed by a NOESY experiment. NOe interactions (highlighted in blue in Figure 28) between the alkenyl protons and the axial protons in the piperidine enabled the assignment of the relative stereochemistry. The two axial protons on the top face (as drawn) only showed nOe interactions with one of the protons of the methylidene group, while the two axial protons on the opposite face only showed nOe interactions with the internal proton of the vinyl group. These interactions confirmed a *trans* relationship between the two alkene substituents with both substituents occupying equatorial positions. Additional information can be gleaned from coupling constants measured in the ^1H NMR spectrum of the product. The hydrogens bonded to the carbon highlighted in red display two resonances in the ^1H NMR spectrum; the axial proton appears as an apparent triplet, with a large coupling constant of 12.0 Hz. From COSY it can be seen that the axial proton couples to two different protons (red arrows in Figure 28), so for it to appear as an apparent triplet, the coupling constants to these two protons must be the same. Typically, a 3J coupling of this magnitude is observed between protons with a transdiaxial relationship, as dictated by the Karplus equation. If the protons had an axial-equatorial relationship the coupling constant would be much smaller, at around 5 Hz.

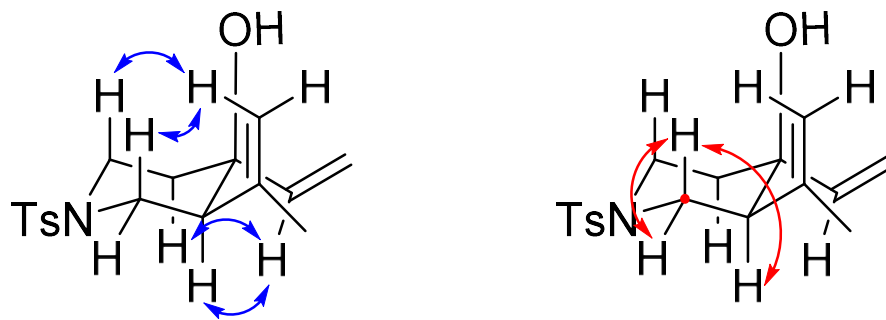
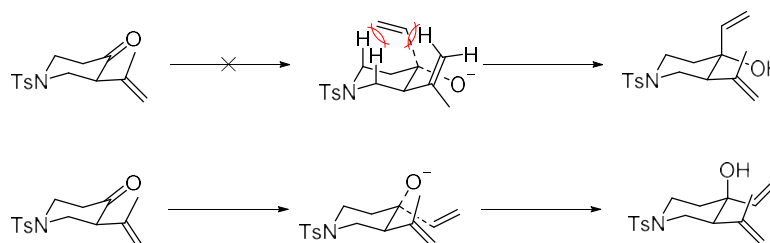


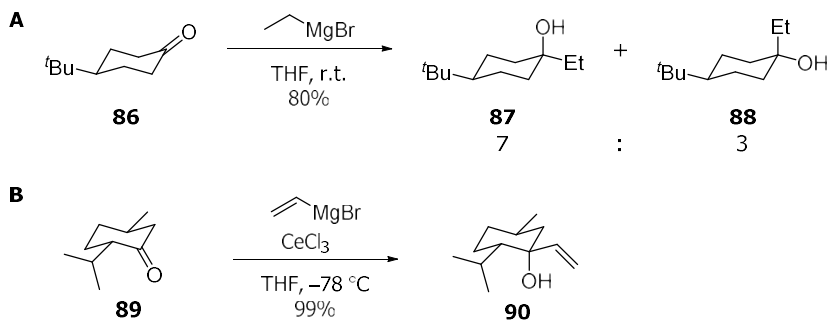
Figure 28 – Key nOes (blue) and coupling constants (red) used to determine the relative stereochemistry. The OH bond length is exaggerated for ease of viewing.

The observed diastereoselectivity can be rationalised by considering a multitude of factors, one of which is the steric differences within the two transition states (Scheme 30). Attack of the Grignard on the top face (as drawn) incurs steric interactions between the axial hydrogens on the beta-carbons but also a large steric clash with the alpha isoproprenyl group, increasing the energy of the transition state. Attack on the opposite face incurs lower steric interactions, reducing the energy of the transition state and favouring formation of the observed major diastereomer.



Scheme 30 – Rationalisation of the stereo vinyl addition to form alcohol **85**

The proposed rationalisation for the observed diastereoselectivity is reinforced by previously conducted research. Meakins *et al.* demonstrated that Grignard attack into cyclohexanone **86** proceeded with a 7:3 preference for the Grignard to add equatorially (Scheme 31A).¹⁵⁰ The increased preference for a Grignard reagent to add equatorially when an α -alkyl group is present has been shown by work conducted by multiple groups utilising isopulegone **89**, where Grignard addition has been found to be completely diastereoselective (Scheme 31B).^{151–153}



Scheme 31 – Previously observed diastereoselectivity of Grignard addition in cyclohexanone derivatives **86** and **89**

While steric interactions play a role in the observed outcome, stereoelectronic effects also need to be considered. The Cieplak model can be applied to rationalise the observed outcome.¹⁵⁴ Nucleophilic addition to the carbonyl causes a new C-C bond to form. The Cieplak model predicts that as the new bond is being formed, it will be stabilised by hyperconjugation with the σ bond that is antiperiplanar to it (Figure 29). Typically, the $\sigma_{\text{C-H}}$ HOMO is higher in energy than the $\sigma_{\text{C-C}}$ HOMO, so will be closer in energy to the $\sigma^*_{\text{C-C}}$ which in turn means there is a greater stabilising interaction between the two orbitals, lowering the overall energy of the transition state. However, vinylmagnesium bromide is electron rich so the energy gap between the $\sigma^*_{\text{C-C}}$ MO and either $\sigma_{\text{C-H}}$ or $\sigma_{\text{C-C}}$ MO is relatively large. The large energy gap means that the overlap of the molecular orbitals will be poor, causing little stabilisation of the transition state. Therefore, the stereoelectronic effects are minimised when vinylmagnesium bromide is used as the reagent, so steric effects become dominant. Attack of vinylmagnesium bromide equatorially is preferred sterically, rationalising the observed 99:1 d.r.

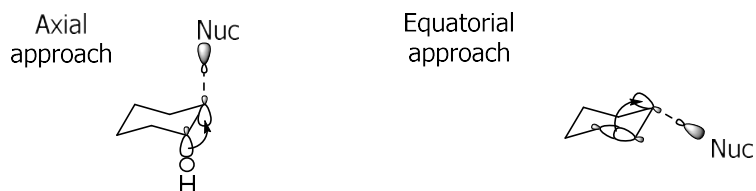


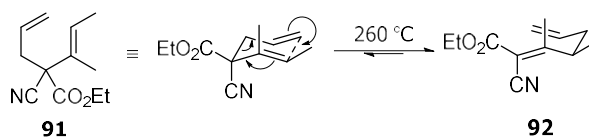
Figure 29 – Hyperconjugation stabilisation of axial and equatorial approaches in the Cieplak model

While the d.r. was pleasing, the low yield of the Grignard addition would prove to be a hindrance for a large-scale synthesis of our target ten-membered ketone. Therefore, the alternative organocerium reagent was explored. Organocerium reagents have been used for 40 years as a more nucleophilic, less basic alternative to traditional Grignard or lithium reagents.^{155–157} Addition of vinylmagnesium bromide to freshly prepared anhydrous CeCl_3 at

-78 °C, followed by addition of ketone **81** to the resultant solution, gave alcohol **85** in an increased 77% yield and comparable diastereoselectivity.

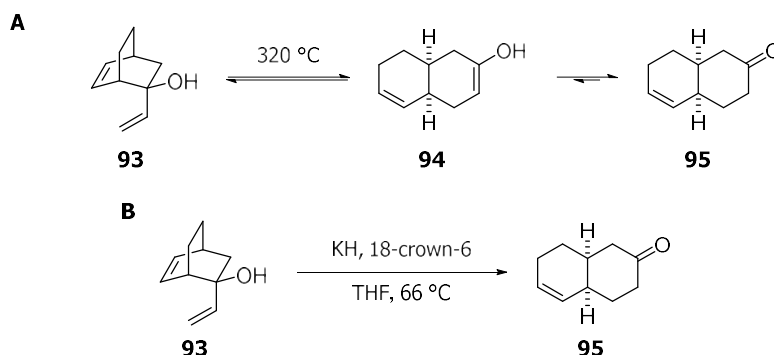
2.2.5 Formation of ten-membered ring ketone **96**

The Cope rearrangement describes a [3,3]-sigmatropic rearrangement. The reaction was discovered by Arthur Cope in 1940 (Scheme 32).¹⁵⁸ Overall, the reaction involves the rearrangement of a 1,5-diene *via* a chair-like transition state.¹⁵⁹ The Cope rearrangement is reversible, with the relative stability of the starting material and product determining the position of the equilibrium. For example, trisubstituted alkene **91** is less stable than tetrasubstituted alkene **92** by ~ 1 kcal mol⁻¹, so the equilibrium in this example is favoured towards the desired alkene.



Scheme 32 – The first Cope rearrangement of alkene **91** into alkene **92**

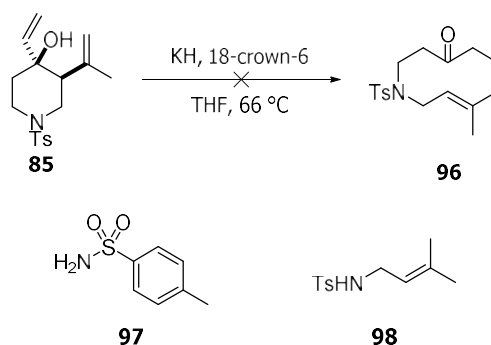
In 1964, Berson and Jones discovered the oxy-Cope rearrangement (Scheme 33A).¹⁶⁰ 1,5-Diene **93** was heated at 320 °C to generate the initial Cope product **94**, which contained an enol functional group, which rapidly tautomerises to ketone **95**, which can no longer undergo retro-Cope rearrangement. Since the keto-enol equilibrium lies heavily towards the ketone tautomer, the oxy-Cope rearrangement is essentially irreversible, allowing for the complete conversion of the starting material.



Scheme 33 – First discovered oxy-Cope and oxy-anion Cope rearrangements

In the following decade, Evans *et al.* discovered that conversion of an oxy-Cope substrate to the corresponding alkoxide increased the rate of reaction by $10^{10} - 10^{17} \text{ mol dm}^{-3} \text{ s}^{-1}$ (Scheme 33B).¹⁶¹ This discovery, named the oxy-anion Cope rearrangement, allowed for Cope rearrangements to be performed at much lower temperatures, broadening the scope of substrates that could be used.

Alcohol **85** was subjected to the Evans conditions (Scheme 34). Unfortunately, the desired ketone **96** was not isolated; the only identifiable, minor side-products were tosylamine **97** and alkene **98**. These products could have been generated by extensive fragmentation of alcohol **85**, so a brief optimisation was carried out to try and favour ring expansion over fragmentation (Table 1).



Scheme 34 – Evans's conditions and identified products

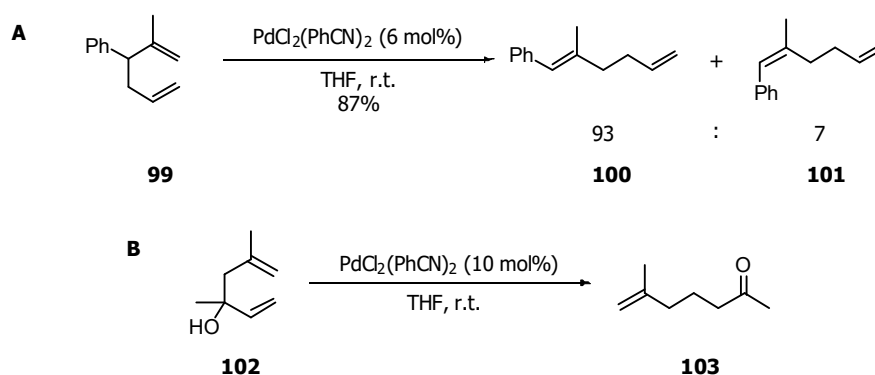
Table 1 – Attempted optimisation of the oxy-anion Cope ring expansion

Entry	Temp./ °C	Equiv. of KH	Outcome
1	66	3.0	Fragmentation
2	20	3.0	No reaction
3	66	1.0	No reaction

Since the original conditions had led to decomposition, the temperature of the reaction was reduced to see if the rearrangement could be favoured (entry 2, Table 1). Previous work has shown that the oxy-anion Cope can be conducted at temperatures as low as 0 °C,¹⁶² but even at 20 °C, no reaction was observed. It was therefore postulated that an elevated temperature was necessary for this substrate to undergo reaction. Next, the number of equivalents of KH was reduced from three to one (entry 3, Table 1). No reaction was observed after heating the

reaction at 66 °C for 17 h. As this investigation was ongoing, alternative ring-expansion conditions proved more fruitful, so further optimisation was discontinued.

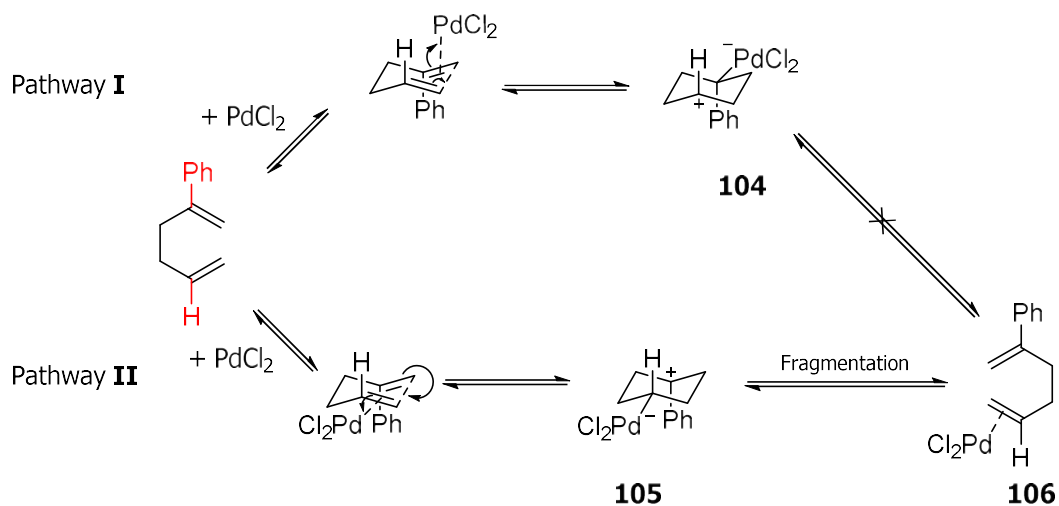
Cope-type rearrangements are not limited to thermal reaction conditions.^v Overman and Knoll demonstrated that palladium(II) chloride complexes catalyse a net Cope-type rearrangement at room temperature (r.t.) with low catalyst loading (Scheme 35A).¹⁶³ 1,5-Diene **99** rearranged into both the *E* **100** and *Z* **101** isomers in an 87% overall yield. Bluthe *et al.* further demonstrated that this methodology could be applied to oxy-Cope substrates (Scheme 35B).¹⁶⁴ Once again, keto-enol tautomerism ensures the reaction on these substrates progresses to completion.



Scheme 35 – Palladium-catalysed Cope rearrangements of alkenes **99** and **102**

One limitation of the Overman conditions is that an electron-donating R group must be present at either C-2 or C-5 of the 1,5-hexadiene (highlighted in red, Scheme 36). By consideration of the reaction mechanism, the necessity of the R group can be rationalised.^{165,166}

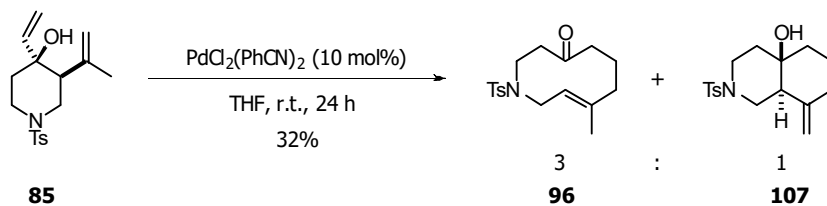
^v By definition Cope rearrangements are pericyclic processes. However, other reaction pathways, such as the one designed by Overman, deliver the same outcome in a stepwise fashion. Henceforth, these reactions will be referred to as Cope-type rearrangements.



Scheme 36 – Two reaction pathways for the PdCl₂-catalysed Cope rearrangement

In pathway I, palladium(II) co-ordinates to the more substituted (and more electron-rich) double bond. Intramolecular addition of the less substituted π bond would form intermediate palladacyclohexane intermediate **104**, which contains a secondary carbocation. Moreover, this cyclisation pathway results in the large palladium atom being σ -bonded to a tertiary carbon centre, which leads to significant steric crowding, which can be released by the reverse reaction. Since the formation of intermediate **104** involves a high activation energy, it is essentially a non-propagative pathway and if formed, the reverse reaction proceeds rapidly. In pathway II, the palladium(II) catalyst co-ordinates to the less substituted double bond, now rendering this alkene susceptible to nucleophilic addition. Intramolecular addition of the more substituted (and more nucleophilic) π bond forms intermediate **105**, where the positive charge is now stabilised by the electron-donating R group (3° carbocation and in this case also benzylic). Moreover, the palladium is now σ -bonded to a secondary carbon centre. Following ring fragmentation, the PdCl₂ is released and desired diene **106** is generated

Since alcohol **85** contained a methyl substituent at C-2, it was postulated that alcohol **85** should be a good substrate for rearrangement under Overman's conditions. The reaction indeed proved successful, providing (*E*)-keto-alkene **96**, albeit in a disappointing 32% yield (Scheme 37). A second product was observed in the ¹H NMR spectrum of the crude material, in a ratio of 1 : 3 with the product, which was subsequently identified as decalol **107** (Figure 30).



Scheme 37 – Oxy-Cope ring-expansion of alkene **85** using Overman conditions

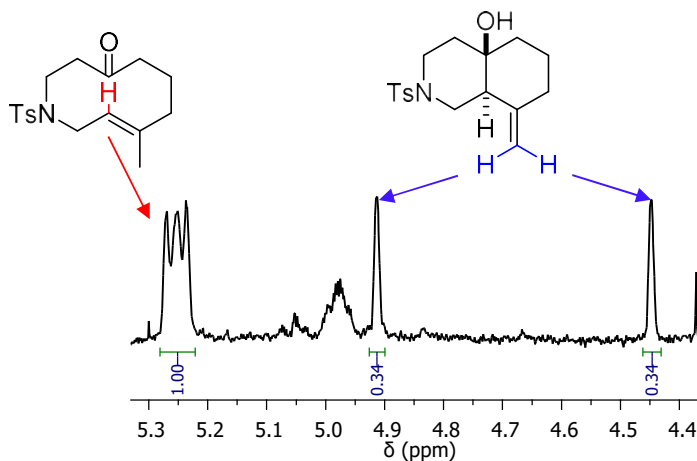
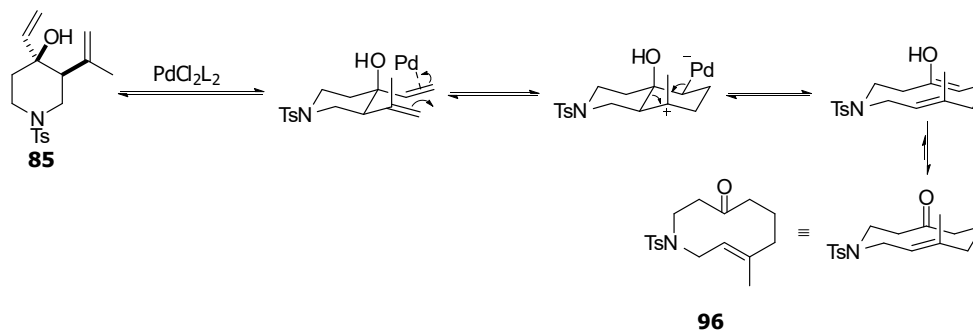


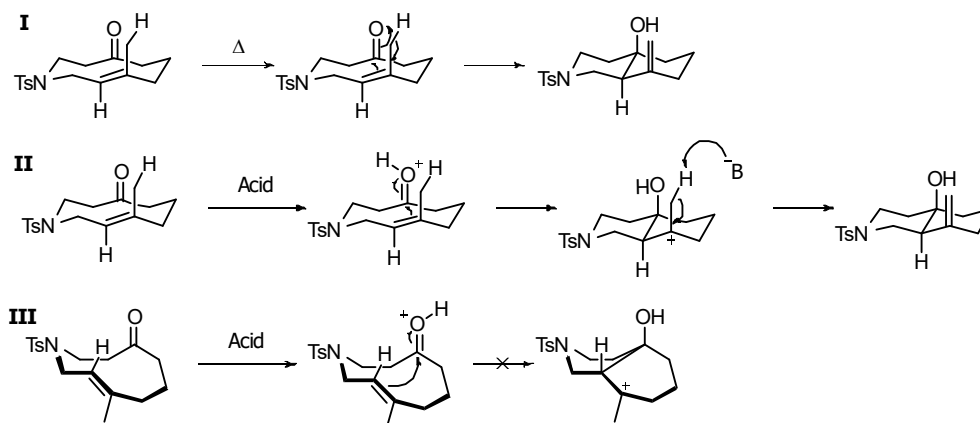
Figure 30 – A section of the ^1H NMR spectrum (400 MHz, CDCl_3) of the crude reaction mixture after work-up but prior to purification showing the alkene resonances of oxy-Cope product **96** and decalol **107**.

The exclusive formation of the (*E*)-alkene product can be rationalised by considering the reaction mechanism, in which the cyclisation step proceeds *via* a six-membered chair-like reactive conformation in which both alkene substituents occupy equatorial positions on the piperidine (Scheme 38).



Scheme 38 – Reaction mechanism to form (*E*)-keto-alkene **96**

Formation of decalol **107** can occur through a pericyclic ene reaction (in which the methyl group and carbonyl must be on the same face of the ring) or a stepwise Prins mechanism (see Section 2.2.3). From both reaction mechanisms, it can be seen that the products are predicted to provide a *trans*-fused bicyclic product (Scheme 39).

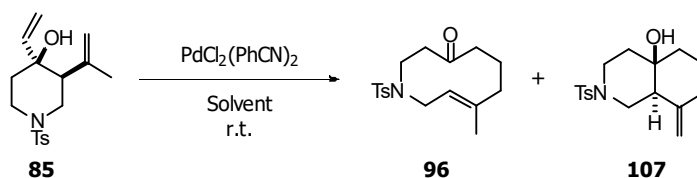


Scheme 39 – Reaction mechanisms for the formation of decalol **107**

Mechanism **I** in Scheme 39 demonstrates conversion of ketone **96** into decalol **107** via a thermal ene reaction. This reaction is a concerted process involving a six-atom cyclic transition state. The transition state can only be adopted when both the methyl group and the carbonyl are on the same face of the ring, so the ene reaction mechanism affords exclusively a product with a *trans* relative stereochemistry at the ring junction.

In theory it is possible to generate both *cis* and *trans* decalols **107** via a Prins-like mechanism; however, only the *trans* product is generated in the case of keto-alkene **96**. Consideration of pathways **II** and **III** reveals that while **II** progresses through a relatively unhindered chair-chair intermediate, **III** involves the formation of a higher energy boat-chair-like intermediate, and therefore a higher energy transition state which disfavours the formation of a *cis*-decalol.

While separable from the corresponding keto-alkene, the presence of decalol **107** warranted optimisation of the reaction conditions (Table 2). Reaction temperature was not assessed, as an increased temperature would have favoured the ene reaction pathway.

Table 2 – Optimisation of the Overman oxy-Cope reaction.^[a]

entry	time (h)	mol% of catalyst	solvent	yield (%) ^[b]	ratio of 96 : 107 ^[c]
1	4	10	THF	60	3:1
2	6	10	THF	35	2.5:1
3	2	10	THF	50	4:1
4 ^[d]	4	10	THF	12	not determined
5 ^[d]	24	10	THF	37	4:1
6	4	5	THF	64	9:1
7	4	2.5	THF	57	9:1
8	2	5	CH ₂ Cl ₂	64	4:1
9	24	5	toluene	71	19:1
10	2	5	benzene	77	39:1
11 ^[e]	2	5	benzene	73 ^[f]	25:1

[a] Unless otherwise noted, the reaction conditions were **85** (0.06 mmol), solvent (2 mL) at r.t. [b] Yields based on ¹H NMR spectroscopic analysis of the reaction mixture without purification using 2,4,6-trimethoxybenzene as an internal standard. [c] Ratio determined by integration of the alkenyl resonances in the ¹H NMR spectrum of the crude reaction material prior to any purification. [d] Pr₂NEt (40 mol%) was used as an additive. [e] Performed on a 4.1 mmol scale. [f] Isolated yield after purification by column chromatography.

The first variable that was examined was time, as it has previously been shown that analogues of keto-alkene **96** undergo further reaction to the corresponding decalol by Lewis and Brønsted acid catalysis.¹³⁶ Unfortunately, while decreasing the time did marginally improve the ratio, it also led to a decrease in overall yield due to an incomplete reaction. Increasing the reaction time led to both a worse yield due to the formation of more decalol **107** (entries 2 and 3, Table 2).

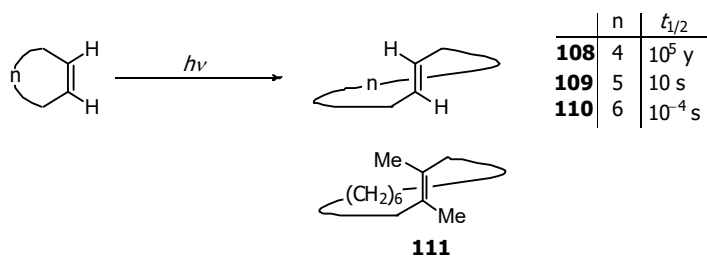
Suppression of Brønsted acid catalysis (through generation of small amounts of HCl from the catalyst) by addition of a base was attempted (entries 4 and 5, Table 2) but this led to increased reaction times with minimal improvement of product ratio or yield, which would suggest the base may be co-ordinating to the palladium(II) catalyst, reducing the turnover. Catalyst loading was also examined, and pleasingly, reducing the mol % catalyst increased the ratio threefold in favour of the target ketone while having a negligible effect on the yield (entries 6 and 7, Table 2). Finally, the role of solvent was assessed (entries 8-11, Table 2).

This solvent screen identified aromatic solvents as optimal, with high yields and a thirteenfold increase in the ratio in favour of the desired product. Scale up of the reaction under optimised conditions saw a small drop in product ratio, but maintenance of the high product yield (entry 11, Table 2).

2.2.6 Properties of the ten-membered ring

Before synthesising a library of scaffolds, it was thought to be useful to analyse the properties of keto-alkene **96**, so that subsequent transformations can be rationally designed.

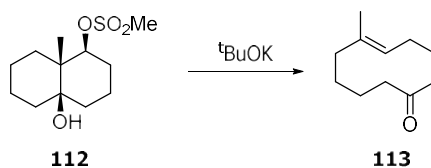
The first property that was assessed was whether a single enantiomer of keto-alkene **96** could be isolated. Cope *et al.* and Binsch *et al.* showed that the enantiomers of (*E*)-cyclooctene **108** can be isolated, and that the rate of racemisation is slow at r.t. ($t_{1/2} = 10^5$ y). By comparison, the rate of racemisation of (*E*)-cyclononene (**109**) is much faster ($t_{1/2} = 10$ s) at r.t. and of (*E*)-cyclodecene (**110**) much faster still ($t_{1/2} = 10^{-4}$ s at r.t.) (Scheme 40).^{167,168} Marshall *et al.* demonstrated that installation of methyl substituents to create a tetrasubstituted alkene increases the barrier to interconversion high enough that configurationally stable enantiomers^{vi} of 1,2-dimethylcyclodecene (**111**) could be isolated.¹⁶⁹



Scheme 40 – Configurational stability of various cycloalkenes and the configurationally stable dimethyl analogue of cyclodecene

Previous work by Westen attempted to synthesise optically active (*E*)-cyclodecenone **113** starting from a single enantiomer of methanesulfonate **112** (Scheme 41), but the product was found to be optically inactive.¹⁷⁰

^{vi} While the authors do not state a half-life, (+)-*trans*-1,2-dimethylcycloundecene showed no loss of optical activity after being heated to 100 °C for 72 h.



Scheme 41 – Westen’s synthesis of racemic **113** from enantiomerically pure starting material

Taking this literature precedent into account, it was highly unlikely that the enantiomers of keto-alkene **96**, a structural analogue of keto-alkene **113**, would be configurationally stable and efforts to separate the two enantiomers by HPLC with a variety of chiral columns proved unsuccessful.

The conformation of keto-alkene **96** is also important as it will dictate the reactivity of the various functional groups that are present within the molecule. Conformational analysis of structurally related cyclodecane has shown that it can adopt multiple low-energy conformations (Figure 31). The lowest energy conformation was found to be the boat-chair-boat (BCB) conformation, with half the population adopting this conformation at any given point at room temperature.^{171,172}

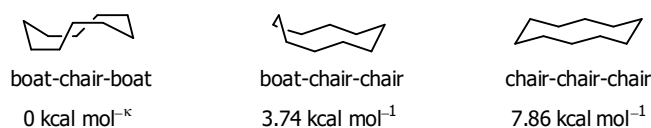


Figure 31 – The three lowest-energy conformations of cyclodecane. The relative strain energies are given below each conformation

With reference to the reaction mechanism (Scheme 38), we predicted that keto-alkene **96** will form in a chair-chair-chair (CCC) conformation, with the methyl group and ketone on the same face of the molecule (Scheme 38); indeed, X-ray crystallography confirmed (*E*)-keto-alkene **96** adopts this conformation in the solid phase (Figure 32). The adoption of the CCC formation over the lowest-energy BCB conformation adopted by cyclodecane can be explained by the presence of three sp² centres within keto-alkene **96**, which will alter the relative energies of the different conformations.

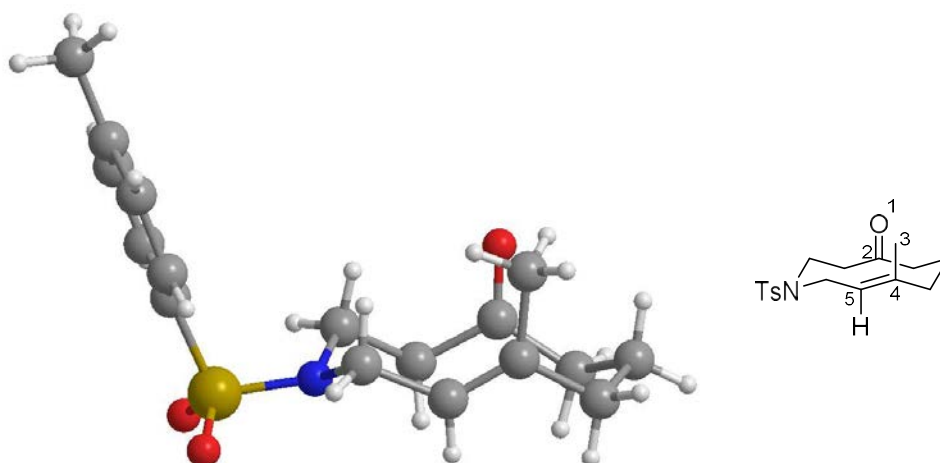


Figure 32 – Left: X-ray crystal structure of (*E*)-keto-alkene **96**; representation generated in Chem3D 17.1^{vii}
 Right: 3D representation of keto-alkene **96** with the relevant atoms labelled using an arbitrary numbering system

Analysis of the crystal structure showed that the carbonyl and the methyl group are on the same face of the molecule. The distance between O-1 and C-3 is 3.18 Å (the sum of the Van der Waals radii of oxygen and carbon is 3.22 Å). C-3 was measured to be -8.3° away from true vertical, indicating that the methyl group has moved out of the ring, presumably to lower transannular strain (Figure 33).

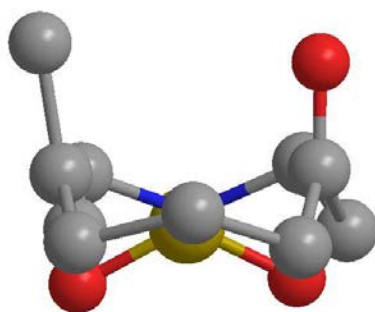


Figure 33 – View down the length of keto-alkene **96**. Hydrogens and the tosyl group have been removed for clarity.

This repulsion is exemplified by the distance between the two quaternary carbons, C-2 and C-4, which were found to have a distance between them of 2.92 Å (the sum of the Van der Waals radii of two carbons is 3.4 Å); a reduction of 0.26 Å compared to the O-1 – C-3 distance.

^{vii} Full crystallographic data for all X-ray crystal structures are collected together in the appendix

The nitrogen atom within keto-alkene **96** was found to have an average bond angle of 115.8° between each of the substituents. In comparison, the average bond angle of sulfonamides within the Cambridge Structural Database was measured as 117.4°. ¹⁷³ If the nitrogen was fully sp³ hybridised, then the bond angles would be expected to be 109.5°, while if it was sp² hybridised, bond angles of 120° would be observed. The observed bond angles of 115.8° could be due to overlap between the lone pair of the nitrogen and an empty d orbital on the sulfur, which partially hybridises the orbitals, leading to the observed geometry. ^{viii}

While the molecule crystallises in a single conformation in the solid phase, keto-alkene **96** is conformationally flexible in solution. The resonances in the ¹H NMR spectrum of keto-alkene **96** are broad and ill-defined at r.t., consistent with a molecule exhibiting more than one conformation that are in intermediate exchange, the region of exchange between fast and slow exchange. ¹⁷⁴⁻¹⁷⁶ To determine the effect of temperature on the population of these conformations, a solution of keto-alkene **96** in CDCl₃ was studied by variable-temperature NMR (VT-NMR).

The ¹H-NMR spectrum of keto-alkene **96** was recorded at temperatures between +25 °C and +65 °C (Figure 34). At the limit of fast exchange, well defined, population-weighted peaks would be expected to be observed in the ¹H-NMR spectrum. However, even at +65 °C, only broad peaks were seen in the ¹H-NMR spectrum, consistent with a molecule still in the intermediate exchange region. The amount of decalol **107** increased from 5% to 6% of the sample, which would be consistent with a thermal ene reaction.

^{viii} This hybridisation is consistent across all of the crystal structures obtained for the library of scaffolds

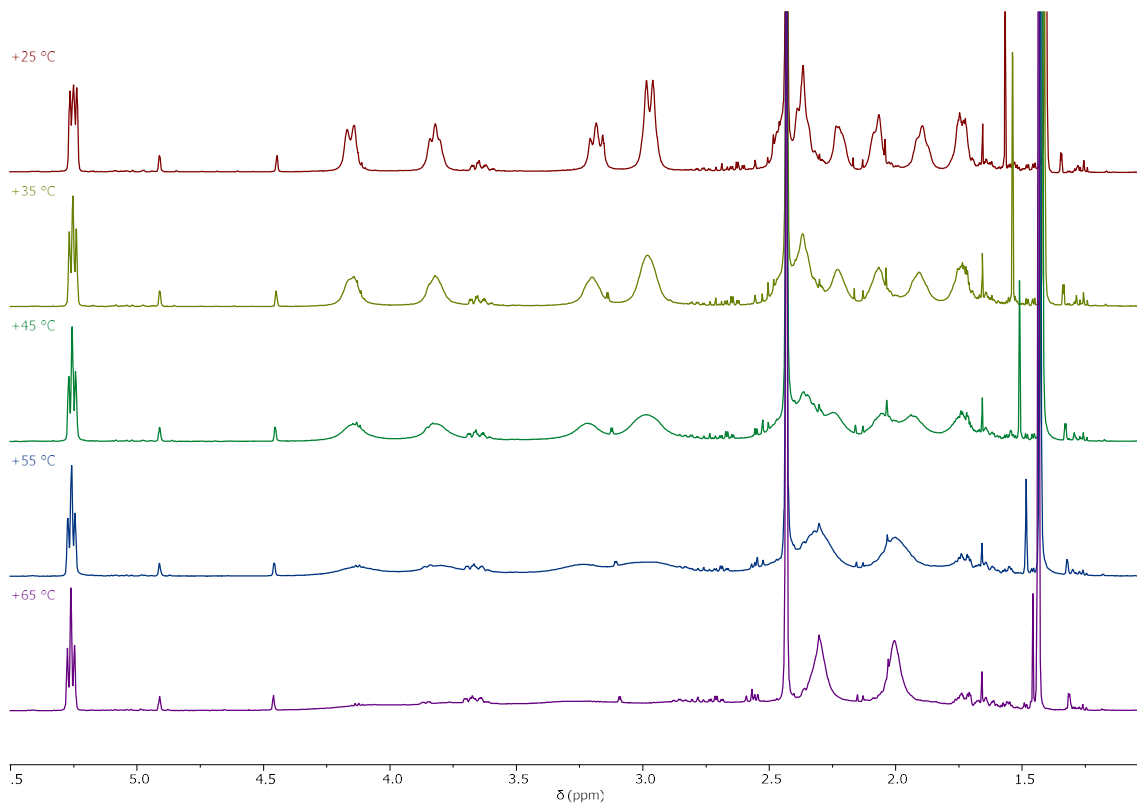


Figure 34 – VT-NMR (500 MHz, CDCl₃) of keto-alkene **96** containing 5% decalol **107**. Chemical shifts between 5.5 and 1.0 ppm are shown.

Decreasing the temperature of the NMR experiment brought the molecule into the region of slow exchange (Figure 35). While >1 conformations are populated at room temperature, only one conformation is visible and therefore significantly populated in the ¹H-NMR spectrum at –35 °C, which by definition must be the lowest energy conformation in CDCl₃. It was also observed from the resonance broadening seen within the ¹H-NMR spectra that multiple conformations begin to be significantly populated between 0 and +15 °C.

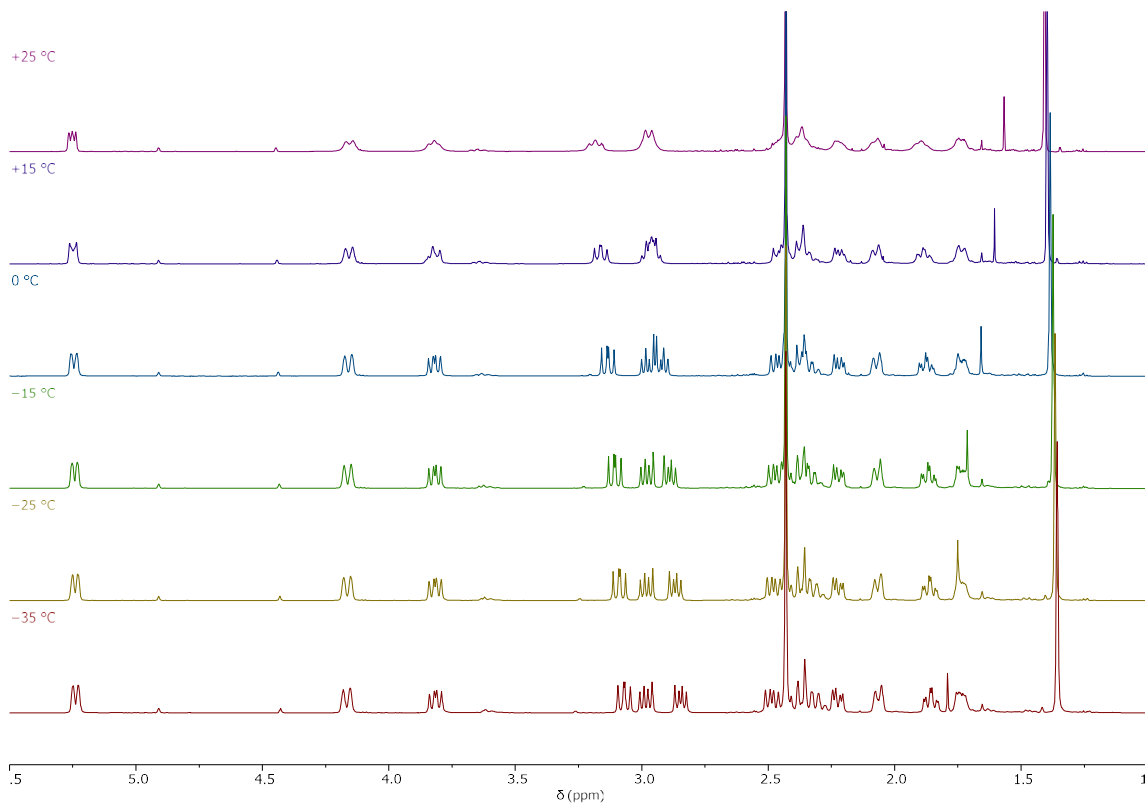


Figure 35 – VT NMR (500 MHz, CDCl_3) spectra of keto-alkene **96**. Chemical shifts between 5.5 and 1.0 ppm are shown.

A NOESY experiment conducted at $-35\text{ }^\circ\text{C}$ enabled identification of the adopted conformation. The methyl protons and the alkene proton displayed completely independent sets of nOe interactions, indicating their occupying two faces of the molecule (Figure 36). NOe interactions were observed between the pseudoaxial protons, which enabled the assignment of the chair-chair conformation, identical to the conformation seen in the solid phase.

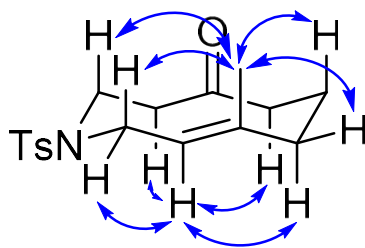


Figure 36 – Key nOes used to identify the low-energy solution CCC conformation of keto-alkene **96**

The CCC conformation had clearly been identified as the low-energy conformation for keto-alkene **96**, but other conformations are accessible as evidenced by the appearance of the

broad resonances in the ^1H -NMR spectrum at r.t. indicating intermediate exchange. Computational analysis using Forge¹⁷⁷ was conducted to ascertain the other possible conformations and their relative energies. Conformational analysis^{ix} generated eleven conformations within an energy window of 6 kcal mol⁻¹ of the lowest energy conformation.

An energy window is defined as the maximum energy difference between the lowest energy conformation and the highest energy conformation. If any conformations are found with a higher energy gap then they are discarded. When conformational analysis is conducted to assess the shape of a ligand upon binding to a biological target the energy window is kept large (> 10 kcal mol⁻¹) so that conformations that may be stabilised upon binding are not accidentally discarded. However, when assessing conformations in solution, any conformers that are > 1.5 kcal mol⁻¹ higher in free energy than the lowest energy conformation will be present at $< 1\%$ population at 25 °C. Forge generates conformers in the gas phase, so does not take solvent interactions into account. Therefore, the energy window has been increased to account for conformations that, while relatively high in energy in the gas phase, may be stabilised in solution and therefore adopted more readily.^{178,179}

Broadly, the calculated conformations can be placed into two categories differing only by changes in the bond angles and distances. The lowest energy conformation is the aforementioned CCC conformation (**96-I**, Figure 38) where both the methyl and carbonyl are on the same face of the molecule, which is identified as the lowest-energy conformation. The predicted conformation is broadly similar to the observed conformation in the crystal structure apart from the carbonyl oxygen – methyl carbon distance (Figure 37). The distance is predicted to be 2.8 Å while the measured distance is 3.18 Å. The difference in distance can be attributed to the change in angle relative to the plane of the ring of the two groups. Within the crystal structure the methyl group had an angle of -8.1° beyond vertical, while the predicted angle is -16.3° . The carbonyl, which is vertical in the crystal structure, is predicted to have an angle of -21.5° beyond vertical compared to 0° .

^{ix} For full details on how the computational analysis was carried out, please see Section 6.2

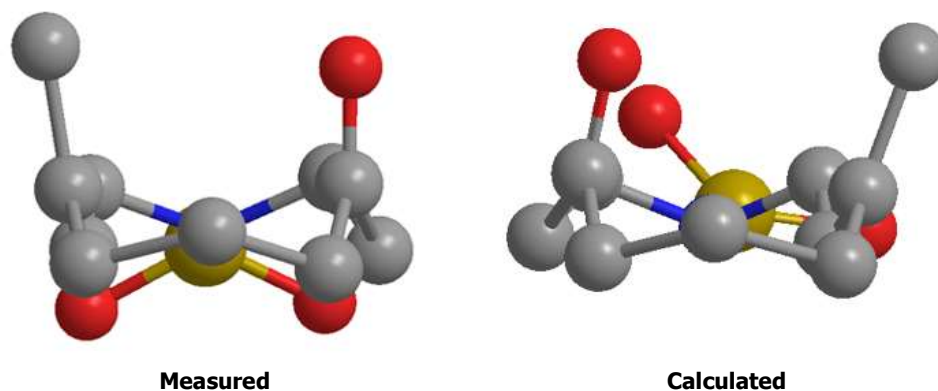


Figure 37 – View down the length of keto-alkene **96**, of both the measured crystal structure (left) and the predicted lowest energy conformation (right). Hydrogens and the tosyl group have been removed for clarity.

The other conformation is a BCC conformation where the carbonyl and methyl groups are on opposite faces of the molecule (**96-II**, Figure 38), of which the lowest energy representative is 0.37 kcal mol⁻¹ higher in energy than the lowest energy CCC conformation.

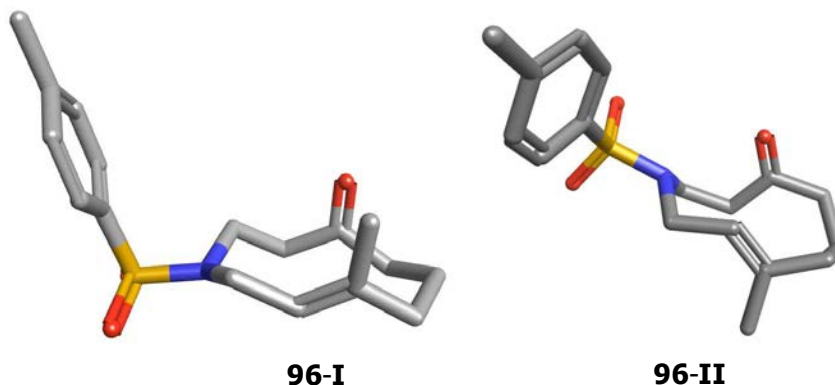


Figure 38 – Illustrative conformations from the two categories of conformations of keto-alkene **96**

From the energy difference between the eleven conformers, the relative populations of the two conformations at -35 °C can be calculated using equation 1. From the predicted energy difference, it would be expected that at -35 °C ~85% of the population had adopted the conformation **96-I**. However, experimentally, >99% of the population has adopted the conformation **96-I**, so the actual energy difference must be larger than that calculated.

$$\frac{p_2}{p_1} = e^{-\left(\frac{\Delta G}{RT}\right)} \quad (1)$$

Conformational analysis in Forge is conducted in the gas phase, whereas reactions take place in solution. For organic compounds of less than 1000 Da, vacuum models can have similar accuracy in estimating ΔE_0 for their stereoisomers as solution models.¹⁸⁰ For keto-alkene **96**,

as the predicted lowest energy conformation in the gas phase is also the conformation adopted at $-35\text{ }^{\circ}\text{C}$ in chloroform, it can be assumed that the conformational analysis is a good fit for non-coordinating solvents.

To conclude, keto-alkene **96** is a medium-sized ring which can adopt multiple conformations at room temperature. Its lowest-energy conformation is the CCC conformation, which has the methyl group and carbonyl on the same face of the ring. A second group of conformations, in which the methyl and the carbonyl occupy opposite faces of the ring in a BCC conformation, are accessible at temperatures $>0\text{ }^{\circ}\text{C}$. Therefore, when planning reactions for diversification of keto-alkene **96**, both groups of conformations were considered to see if a reaction was feasible.

2.3 Design and Synthesis of a Library of Scaffolds

2.3.1 Scaffold Definition

Before synthesising a library of scaffolds, the definition of a “scaffold” needs to be explored. In general terms, a scaffold is a molecular core to which functional groups are attached or embedded. A medicinal chemistry scaffold is often described as a core structure which is required for pharmacological activity (a pharmacophore).⁹⁸ However, there is no strict definition that is universally accepted. For the work presented within this thesis, the definition devised by Bemis and Murcko is used, as it is one of the most widely used and allows for easy comparisons between different libraries.¹⁸¹

The Bemis and Murcko definition of scaffolds provides a graph-based method which can be used to explore molecular hierarchy.¹⁸² For any ring-containing system, a graph representation can be drawn, which is made up of three components: ring systems, linkers and side-chains (Figure 39). A single scaffold is defined as a combination of ring systems and linkers.^x The formal definition utilised by Murcko scaffolds allows for direct comparison of different libraries of compounds, as well as compartmentalisation of core structures, which in turn can help elucidate the relevant pharmacophore in a drug-discovery project.

^x The formal definition also differentiates between sp^2 - and sp^3 -hybridised carbons. For example, cyclohexanone and cyclohexanol are counted as two different scaffolds.

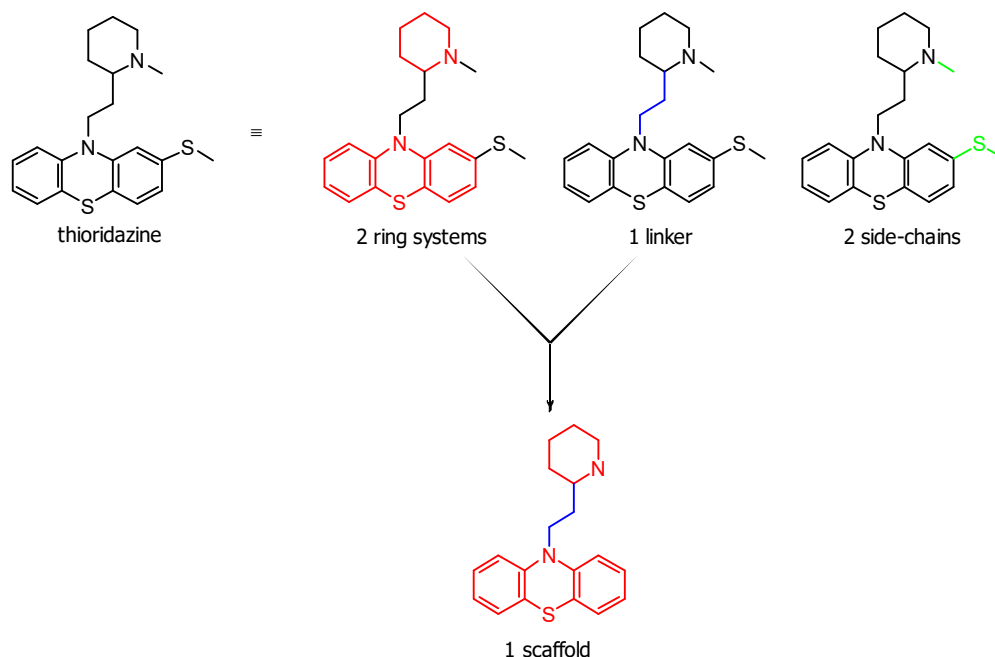


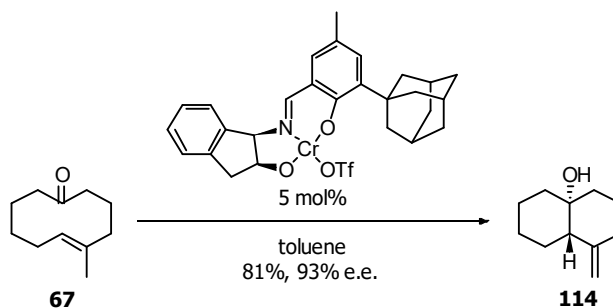
Figure 39 – Definition of a Bemis and Murcko scaffold as demonstrated by thioridazine

From the Murcko scaffold definition, it can be seen that the number and diversity of ring systems within a library are a key component of how many scaffolds, and in turn, how diverse is the generated library. Taking this into consideration, our design rationale when undertaking reactions to generate scaffolds was to maximise the number of ring systems generated or to introduce new linkers to which rings could be appended, rather than the manipulation of side-chains.

2.3.2 Carbonyl Transformations

Intramolecular carbonyl transformations

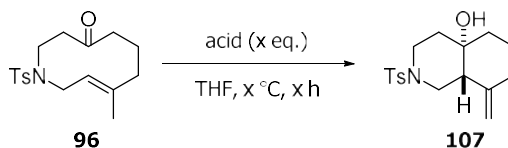
Our first focus was the side-product from the oxy-Cope reaction, namely decalol **107**. Structures of this type have been synthesised by the Jacobsen group, who transformed keto-alkene **67** into decalol **114** enantioselectivity *via* a transannulation reaction using a chiral chromium catalyst (Scheme 42).



Scheme 42 – Jacobsen's enantioselective synthesis of decalol **114**

As the formation of decalol **107** had already been observed as a side-product in the formation of keto-alkene **96**, conditions were screened to see whether decalol **107** could be formed directly from keto-alkene **96** (Table 3).

Table 3 – Exploration of reaction conditions to form decalol **107**^[a]



Entry	Acid	Eq. of acid	Temp (°C)	Time (h)	Yield (%)
1	PdCl ₂ (PhCN) ₂	0.05	r.t.	72	42
2	PdCl ₂ (PhCN) ₂	0.1	r.t.	72	49
3	TsOH•H ₂ O	0.1	r.t.	72	47
4 ^[b]	TsOH•H ₂ O	0.05	r.t.	24	66
5	none	N/A	66	72	61

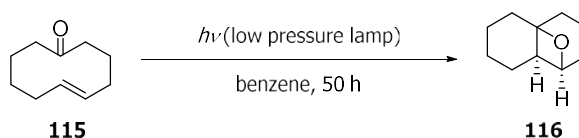
[a] Unless otherwise noted, the reaction conditions were **96** (0.12 mmol), THF (6 mL). [b] Carried out on a 0.5 mmol scale.

Since decalol **107** was already formed in small quantities in the synthesis of keto-alkene **96**, the initial conditions were the oxy-Cope reaction conditions. THF was chosen as the solvent as

it had previously delivered the largest amount of decalol **107**. The use of $\text{PdCl}_2(\text{PhCN})_2$, potentially acting as a Lewis acid, delivered low yields of decalol **107**, with starting material still observed after 72 h (entries 1 and 2, Table 3). The poor results with this palladium catalyst may have been due to competing co-ordination with the alkene, leading to low turnover of the catalyst. With that in mind $\text{TsOH}\cdot\text{H}_2\text{O}$, a Brønsted acid, was tried instead. An initial reaction delivered a 47% yield but with full consumption of starting material (entry 3, Table 3). It was suspected that decalol **107** was reacting further under the reaction conditions over the extended reaction time, due to the presence of non-product resonances within the ^1H NMR spectrum of the reaction material before purification. Gratifyingly, reducing the reaction time to 24 h and the number of equivalents of acid to 5 mol% afforded the product in 66% yield (entry 4, Table 3). To assess whether decalol **107** could be formed in high yield from an ene reaction, having already observed the possibility during V.T. NMR studies (Section 2.2.6), a solution of keto-alkene **96** in THF was heated at reflux for 72 h and afforded decalol **107** in 61% isolated yield; however, full conversion was not observed even after a week of heating.

Overall, decalol **107** was generated in moderate yield, utilising both Prins and thermal ene reaction conditions. The exocyclic double bond presents opportunities for further elaboration, but these have not yet been explored.

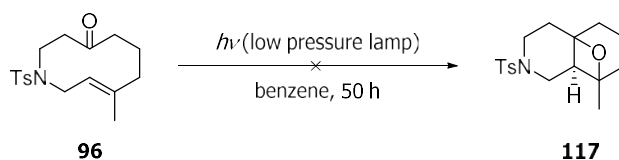
Other intramolecular reactions involving the ketone have also been shown to be possible. Lange and Bosch described an intramolecular Paternó–Büchi reaction with *trans*-5-cyclodecenone **115**, giving oxetane **116** in 55% yield (Scheme 43).¹⁸³



Scheme 43 – Synthesis of oxetane **116**

UV-Vis spectroscopic analysis of keto-alkene **96** revealed a λ_{max} at 232 nm and 275 nm. The peak at 232 nm can be attributed to the carbonyl absorption and the broad peak at 275 nm to the absorption of the tosyl group. Unfortunately, it was not possible to irradiate specifically at 232 nm, so a medium-pressure lamp was used, which covers a range of wavelengths from 200 to 500 nm. A vessel of quartz glass was used as standard borosilicate glass absorbs wavelengths up to 325 nm, which would have disabled the reaction. Quartz glass does not absorb in that region, so the light can pass through unimpeded to the reaction.^{184,185} Applying

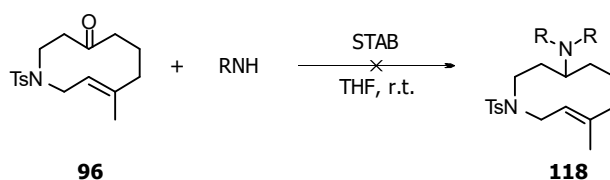
the methodology of Lange and Bosch to keto-alkene **96**, (Scheme 44), consumption of the starting material progressed slowly, taking ~50 h to reach completion. No identifiable product was isolated; the only identifiable functionality was a tolyl group, but it was not appended to the desired scaffold. It was speculated that the light excited the tosyl group, causing it to cleave into a tolyl radical, which then caused the decomposition of keto-alkene **96**. No further work was attempted on this substrate, however it is of interest for further work (see section 3.4.3).



Scheme 44 – Attempted Paternó-Büchi reaction to form oxetane **117**

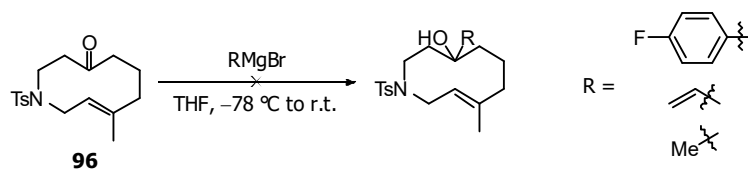
Intermolecular carbonyl transformations

Reductive amination with other nitrogen-containing rings was of interest. Therefore, a reductive amination between keto-alkene **96** and morpholine was attempted using standard one-pot conditions in an effort to generate tertiary amine **118** (Scheme 45). Only starting material was recovered after 24 h, so the less hindered 1° amine benzylamine was used as an alternative. Unfortunately, no reaction was observed under these conditions as well. The obvious avenue of increasing the reaction temperature was not available, as an increased temperature would also have increase the rate of the competing ene reaction.



Scheme 45 – Attempted one-pot reductive amination to generate amine **118**

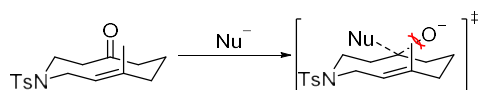
Since both primary and secondary amines had failed to react, it was speculated that a stronger nucleophile might react more effectively. With this in mind, a range of Grignard reagents was tried (Scheme 46).



Scheme 46 – Attempted nucleophilic addition reactions using Grignard reagents

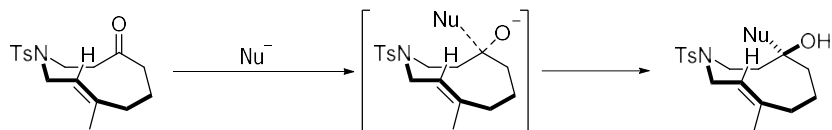
Initially, 4-fluorophenylmagnesium bromide was used, as a successful addition would generate a new aromatic-containing scaffold. However, no reaction was seen. Transmetalation to the corresponding organocerium reagent did not yield a result. As an alternative, both vinylmagnesium bromide and methylmagnesium bromide were tested. Both reagents also failed to react, even when these reagents were converted into their corresponding more nucleophilic organocerium reagents. Temperatures above room temperature were not probed, as it was suspected that the Grignard might act as a base and cause the keto-alkene **96** to decompose in a similar way to that observed for alcohol **85** (see Section 2.2.4).

The lack of reactivity at the carbonyl can be rationalised by consideration of the transition state (Scheme 47). Nucleophilic attack on the front face of the carbonyl (as drawn) is disfavoured as the rest of the ring blocks this face. Therefore, the nucleophile must attack the back face of the carbonyl. As the nucleophile attacks into the π^* molecular orbital, the carbonyl carbon transitions from sp^2 - to sp^3 -hybridisation, pushing the oxygen into the ring. In turn, this increases transannular strain, increasing the energy of the transition state. If, as shown in Scheme 47, the reactive conformation sees the methyl group and carbonyl oxygen on the same face, then there will also be a large steric clash between these two groups.



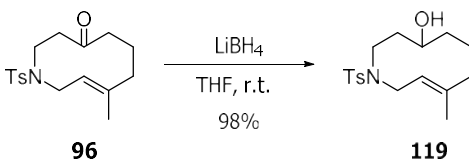
Scheme 47 – Transition state of nucleophilic attack on keto-alkene **96**

To avoid interactions with the transannular methyl substituent, the ring would need to adopt the alternative BCC conformation, where the carbonyl and methyl are on opposite faces (Scheme 48). However, addition into the carbonyl in this conformation will still be expected to create large transannular strain in the transition state.



Scheme 48 – Nucleophilic attack on the alternative BCC keto-alkene **96** conformation.

As nucleophilic addition with carbon- and nitrogen-containing nucleophiles had proven unsuccessful, we turned to an even smaller nucleophile. Reduction of the carbonyl to the corresponding alcohol using NaBH₄ was therefore attempted. Pleasingly, reduction occurred, although the reaction did not go to completion even after 48 h. Overall, a yield of 50% was obtained, with 35% recovery of starting material. Building on this success, a stronger reducing agent was investigated. Thus reaction with LiBH₄ proceeded smoothly, with desired alcohol **119** isolated in excellent yield (Scheme 49).¹⁸⁶



Scheme 49 – LiBH₄-mediated reduction of keto-alkene **96** to give alcohol **119**

Converting the sp² carbonyl carbon in keto-alkene **96** into an sp³ centre in alcohol **119** increases the number of sp³ centres in the molecule by one. In turn, this increases the conformational flexibility of the molecule. Conformational analysis using Forge was conducted to ascertain the low-energy conformations and their relative energies. This computational analysis^{xi} generated 76 different conformations within 6 kcal mol⁻¹ of the lowest-energy conformation. The lowest-energy conformation was again predicted to be the CCC conformation; however, the crystal structure obtained for alcohol **119** showed it crystallised in a twisted BCC conformation (Figure 40).

^{xi} For full details on how the computational analysis was carried out, please see Section 6.2

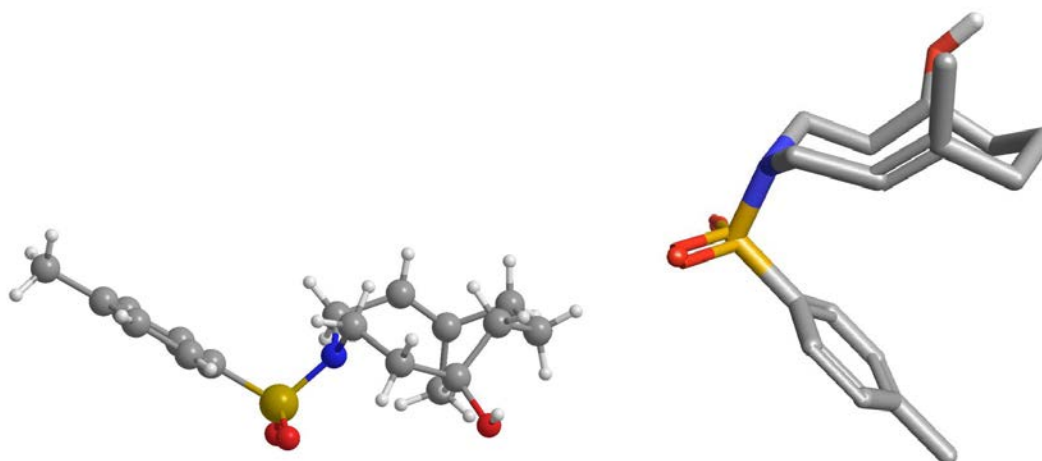


Figure 40 – Left: X-ray crystal structure of alcohol **119**, right: predicted lowest-energy conformation

A wide variety of conformations are predicted to be adopted by alcohol **119**, such as the CCC, BCB, BCC, crown and twisted varieties thereof, rather than the two adopted by the parent keto-alkene, demonstrating the greater conformational flexibility present in the molecule.

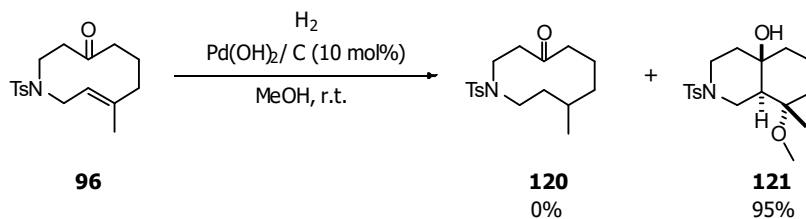
In terms of the overall goal of this project, a molecule with many accessible conformations can be a double-edged sword within a screening library. On the negative side, it incurs a greater entropic penalty upon binding with a biological target. On the other hand, libraries designed by DOS are typically prospecting libraries used to find new targets or new ways of interacting with old targets. Therefore, a molecule which can access multiple conformations can essentially be thought of as multiple different compounds that might be useful for interacting with – and therefore uncovering – multiple (potentially new) targets.^{187–189}

Overall, the carbonyl group within keto-alkene **96** proved to very unreactive towards intermolecular processes, which we hypothesise is primarily a consequence of transannular effects. While possible to reduce, the subsequently generated alcohol **119** was not explored for further scaffold generation. To further explore the scaffold potential of keto-alkene **96**, focus transferred to exploring the reactivity of the alkene.

2.3.3 Double Bond Transformations

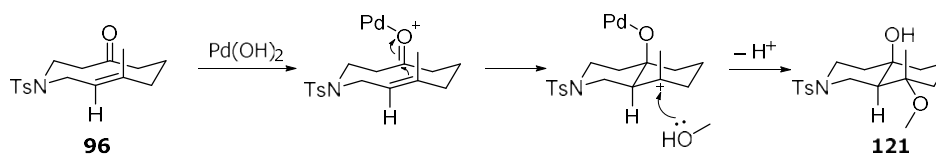
To increase the F_{sp^3} , reduction of the double bond in keto-alkene **96** was attempted. Standard hydrogenation conditions (10% Pd/C, H_2 , MeOH) returned only starting material, so a stronger

catalyst in Pd(OH)₂/C was utilised. This time, instead of returning desired ketone **120**, decalol **121** was isolated in 95% yield after 17 h (Scheme 50).



Scheme 50 – Synthesis of decalol **121**

The formation of decalol **121** and the proposed relative stereochemistry can be rationalised by the Pd²⁺ acting as a Lewis acid, facilitating a Prins type cyclisation on the reactive conformation of keto-alkene **96**, in which the methyl group is in a pseudoaxial position. The generated 3° carbocation is trapped by a molecule of methanol, which approaches from the less hindered face, delivering the observed stereochemistry (Scheme 51).



Scheme 51 – Proposed reaction mechanism for the formation of decalol **121**

Reduction of an alkene by Pd(OH)₂ and H₂ is typically rapid (<1 h). The inability to reduce the double bond in keto-alkene **96** can be rationalised in much the same way as the reasoning behind the low reactivity of the carbonyl. Palladium-catalysed addition of H₂ across a double bond is a *syn* process. Since only one face of the alkene is accessible, the hydrogen must approach from the outer face. We postulate that H₂ addition across the double bond increases transannular strain raising the activation barrier, so instead, reaction follows the Prins mechanism pathway.

From this and the previous results, transformations that convert the sp² centres of the carbonyl or the alkene into sp³ centres are challenging. This left a set of functional groups that had yet to be explored – three-membered rings. Three-membered rings are highly strained molecules that have a unique geometry, with idealised internal angles of 60° and external angles of 120° (Figure 41). Therefore, they have similar geometry to double bonds while still generating sp³ centres.

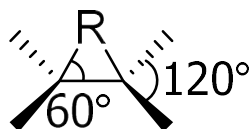
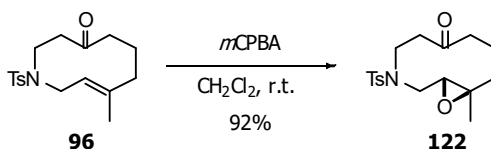


Figure 41 – Internal and external angles of a three-membered ring. R can = CH₂, NH, O

Keto-alkene **96** was treated with *meta*-chloroperbenzoic acid (*m*CPBA) in CH₂Cl₂. Epoxide **122** was generated in a 92% yield, with no starting material observed (Scheme 52).

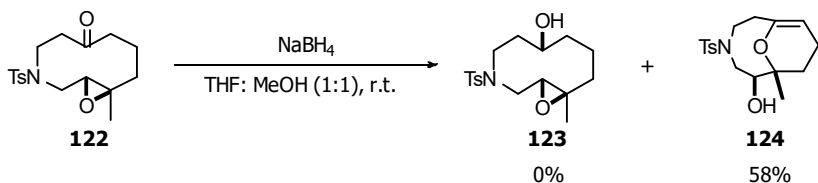


Scheme 52 – Synthesis of epoxide **122**

*m*CPBA is an electrophilic peracid which reacts with alkenes to form an epoxide in a *syn*-stereospecific reaction mechanism.¹⁹⁰ The concerted nature of the bond-forming process means that the geometry of the substituents around the alkene varies very little along the reaction coordinate, which we postulate minimises the build-up of unfavourable transannular interactions within the transition state, reducing the activation energy, and allowing reaction to proceed in high yield.

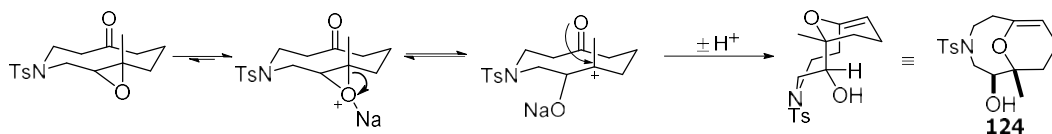
Comparison of the crystal structures of keto-alkene **96** and epoxide **122** demonstrate that the epoxide functionality geometrically acts as a double bond equivalent. The bond angles (within 1-2°) are the same in both crystal structures. The distance between the carbonyl and the methyl group is also unaffected (3.18 Å in keto-alkene **96** vs. 3.19 Å in epoxide **122**).

With epoxide **122** in hand, reduction of the carbonyl was attempted to synthesise another new scaffold. Treatment with LiBH₄ led to degradation of epoxide **122** with no identifiable products. Use of NaBH₄ did not lead to desired alcohol **123**, but unexpectedly generated enol ether **124** in 58% yield (Scheme 53). The structure and chemical reactivity of enol ether **124** is further discussed in section 2.3.4.



Scheme 53 – Attempted reduction of ketone **122** to alcohol **123** using NaBH₄ led to enol ether **124**

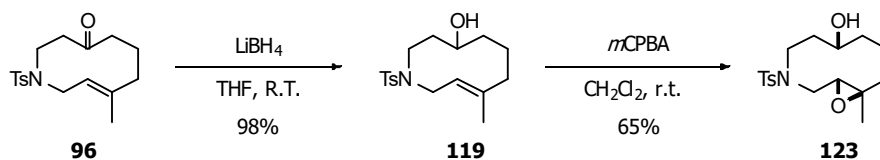
The formation of enol ether **124** was unexpected. To ensure the result was not a result of an impurity, the reaction was repeated with a different batch of epoxide **122** and the same product was observed. We postulate that the sodium ions in solution function as a weak Lewis acid and co-ordinate to the epoxide. The epoxide can then transiently ring open, creating a 3° carbocation, which is susceptible to nucleophilic attack *via* an S_N1 mechanism. Intramolecular attack of the carbonyl into the carbocation forms a transient oxocarbenium, which rapidly loses a proton to form enol ether **124** (Scheme 54). The reaction mechanism requires an intramolecular attack over the ring face, which will incur transannular strain, but leads to the release of ring strain in the epoxide, which is an overall reduction in energy.



Scheme 54 – Proposed reaction mechanism to form enol ether **124**

Both 6- and 7-*exo tet* cyclisations are possible according to Baldwin's rules, but the formation of a 6-membered ring is only observed. The distance between the carbonyl and each of the electrophilic centres in the epoxide is similar (3.2 Å for the quaternary centre and 3.4 Å for the tertiary centre). A tertiary carbocation is much more stable than a secondary carbocation, so there will be a much greater population of the former in solution than the latter. Formation of a 6-membered ring also incurs a smaller entropy loss than the formation of a 7-membered ring.¹⁹¹ Taken together, these could rationalise why only the 6-membered ring is observed.

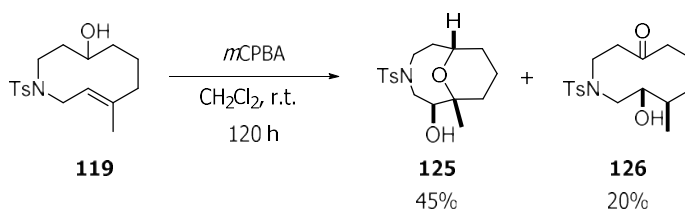
Alcohol **123** could not be generated by reduction of the carbonyl in epoxide **122**, so the order of chemical transformations was reversed, generating first alcohol **119** by reduction with LiBH₄ and then epoxidation with *m*CPBA to generate epoxide **123** in a 64% yield over two steps (Scheme 55).



Scheme 55 – Synthesis of epoxy alcohol **123**

Epoxide **123** is formed as a single diastereomer. The diastereoselectivity can be attributed to a phenomenon known as “macrocyclic stereocontrol,” which was first proposed by Clark Still.¹⁹² One face of the alkene in alcohol **119** is blocked by the surrounding macrocycle, inhibiting epoxidation on that face (Scheme 55).^{xii}

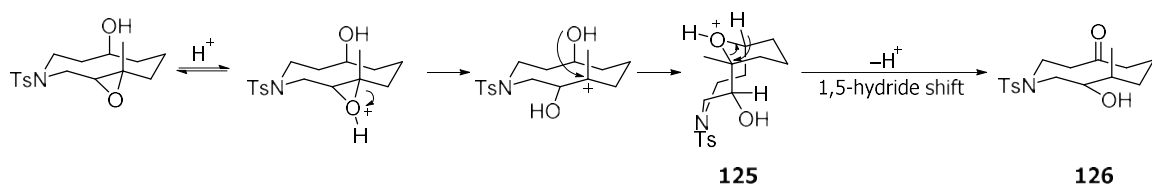
On one occasion, the reaction of alcohol **119** was left for 120 h (typical reaction length ~5 h). Instead of the expected epoxide **123**, ether **125** was isolated in 45% yield and ketone **126** in 20% yield (Scheme 56).



Scheme 56 – Serendipitous synthesis of ether **125** and ketone **126** from alcohol **119** through epoxide **123**

We postulate epoxide **123** formed along with the by-product of the epoxidation reaction *meta*-chlorobenzoic acid. The acid causes a cascade of subsequent reactions to form the identified scaffolds. Ether **125** can be formed from the Brønsted acid-mediated activation of epoxide **123** and subsequent regioselective ring-opening (Scheme 57). The structure of ketone **126** was confirmed *via* a HMBC interaction between the methyl protons and the carbinol carbon (the reverse signal is also observed), which confirmed the location of the alcohol on the adjoining carbon to the methyl group. To form a scaffold with the observed relationship between the functional groups, a 1,5-hydride shift within ether **126** could have occurred. Similar reactions have been observed with other six-membered cyclic ethers.^{193,194}

^{xii} Technically, alcohol **119** and the related scaffolds are not macrocycles, but medium-sized rings. The principle can still be applied in their case.

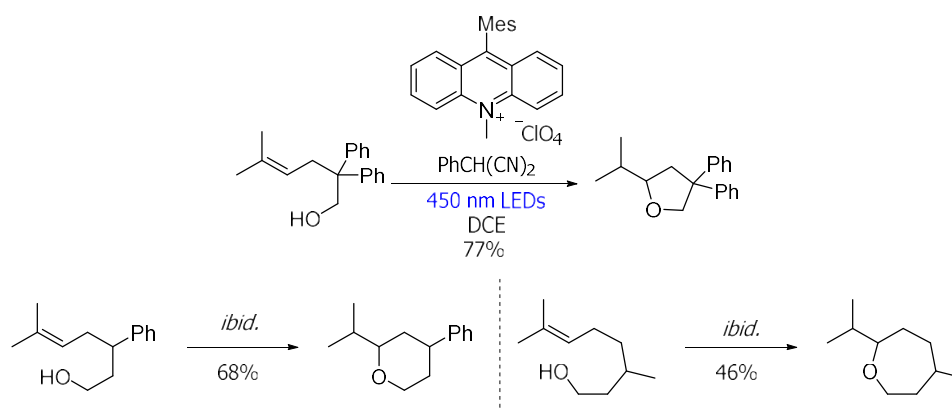


Scheme 57 – Proposed reaction mechanism for the formation of ether **125** and ketone **126**

Overall, several new scaffolds were obtained by chemical transformation of the double bond. Large transannular strain unfortunately caused a lack of reactivity in the alkene, mirroring the reactivity seen with the carbonyl. Some success was achieved with formation of epoxides, which showed a disposition towards intramolecular reactions, with formation of both enol ether **124** and ether **125** observed. These successes were built upon to further expand the library of scaffolds.

2.3.4 Intramolecular Reactions

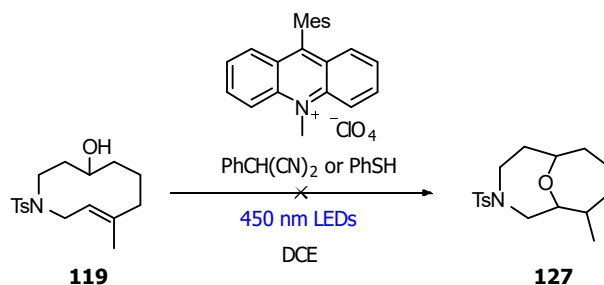
After some success with transformation of the double bond, we concentrated on building on the intramolecular reactions that had previously been successful. Hamilton and Nicewicz demonstrated that cyclic ethers can be generated *via* an anti-Markovnikov photocatalysed hydroetherification (Scheme 58).¹⁹⁵ Importantly, it was shown that seven-membered rings could be generated, albeit in lower yield.



Scheme 58 – Hamilton's and Nicewicz's anti-Markovnikov photocatalysed hydroetherification.

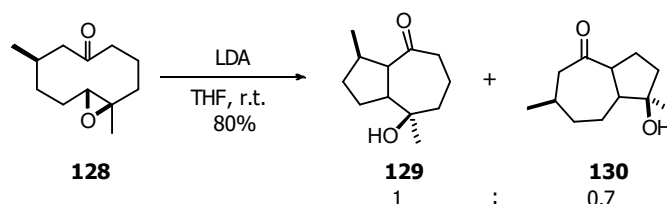
Building on their work, it was hoped that these hydroetherification conditions could be applied to alcohol **119** to generate the bridged ether scaffold **127**. Supplementary work by the group had shown that the use of thiophenol as the H atom transfer reagent could lead to reduced reaction times and increased yields.¹⁹⁶ Taking this into account two reactions were run in

parallel, with the H atom transfer reagent varied between the two (Scheme 59). Unfortunately, no reaction was seen after a week of irradiation. The pathlength of the light was reduced steadily throughout the week as no reaction was seen by TLC analysis, but this had no effect on the outcome. This was not investigated further.

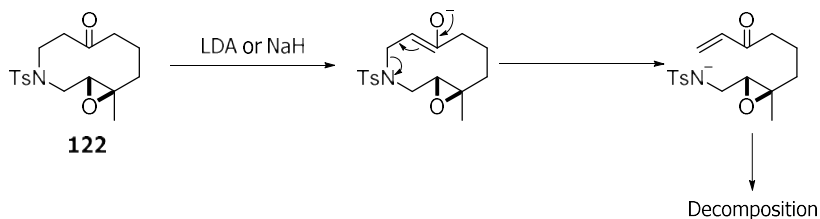


Scheme 59 – Attempted hydroetherification of alcohol **119**

It has been shown that intramolecular nucleophilic attack can be utilised to create fused ring systems within a medium sized ring. In Maier's synthesis of (–)-9-deoxy-englerin A, epoxide **128** was treated with LDA to give a mixture of ketones **129** and **130** *via* non-regioselective lithium enolate formation and subsequent S_N2 ring-opening of the epoxide *via* attack on the less-substituted carbon (Scheme 60).¹⁵³

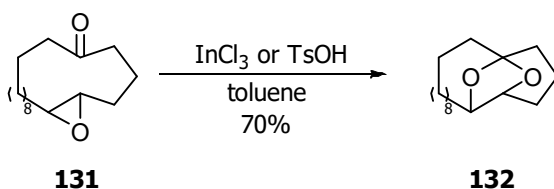


Scheme 60 – Formation of 5,7-fused ring systems from epoxide **128** in the synthesis of (–)-9-deoxy-englerin A. Application of these conditions to epoxide **122** led exclusively to decomposition; no products were identified. A further attempt using NaH as the base rather than LDA also proved unsuccessful. The failure of these reactions was postulated to be linked to the presence of the sulfonamide within the ring, which can act as a leaving group, leading to fragmentation and decomposition (Scheme 61).



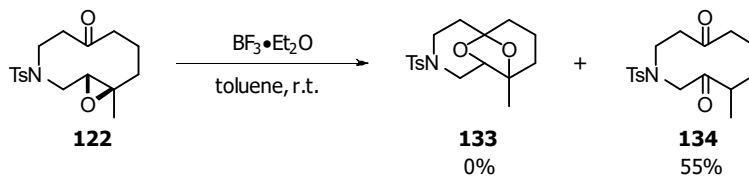
Scheme 61 – Proposed decomposition pathway of epoxide **122** under treatment with base

Since basic methods were causing decomposition, intramolecular reactions catalysed by acid were investigated as an alternative. Some success had already been seen with the formation of ether **125** (Section 2.3.3), but further optimisation and additional scaffolds were sought. Panten *et al.* had previously shown that ketal **132** could be formed from either a Lewis- or Brønsted acid-catalysed transformation of epoxide **131** (Scheme 62).¹⁹⁷



Scheme 62 – Synthesis of ketal **132** using either a Lewis or Brønsted acid

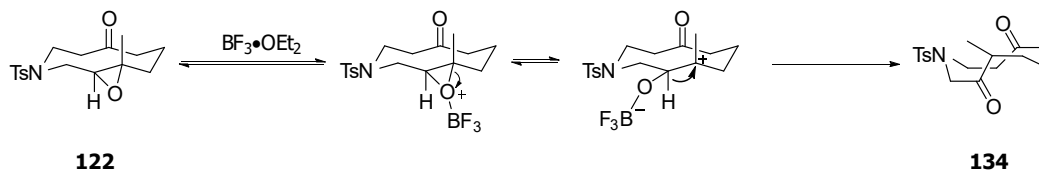
Panten *et al.* showed that the size of the ring could be varied dramatically as long as the chain length between the carbonyl and the epoxide was only two or three carbon atoms on the shortest side. Within epoxide **122** the chain length between the carbonyl and the epoxide is only three carbon atoms, so it should be a suitable substrate for this type of reaction. However, when epoxide **122** was subjected to $\text{BF}_3 \cdot \text{Et}_2\text{O}$ in toluene, the desired ketal **133** was not generated (Scheme 63). Instead, diketone **134** was preferentially formed in moderate yield.



Scheme 63 - Serendipitous synthesis of diketone **134** from epoxide **122** using $\text{BF}_3 \cdot \text{Et}_2\text{O}$

Diketone **134** is formed *via* an overall 1,2-hydride shift catalysed by $\text{BF}_3 \cdot \text{OEt}_2$, otherwise known as the Meinwald rearrangement (Scheme 64).^{198,199} The formation of a diketone was not described in the original paper. The explanation for this discrepancy could be due to

Panten's use of a disubstituted epoxide, which undergoes a Meinwald rearrangement less readily than the tri-substituted epoxide in our substrate. The formation of ketal **134** therefore dominates, leading to the observed results.



Scheme 64 – Proposed mechanism for the formation of diketone **134**

Interestingly, diketone **134** crystallises as a BCB structure rather than the CCC structures shared by the other 10-membered rings within the scaffold library (Figure 42). This conformation is the same as the lowest energy conformation for cyclodecane and cyclodecanone (see Section 2.2.6).²⁰⁰ In this solid-state structure, the two ketones orient in opposite directions, which presumably minimises the overall dipole of the molecule.

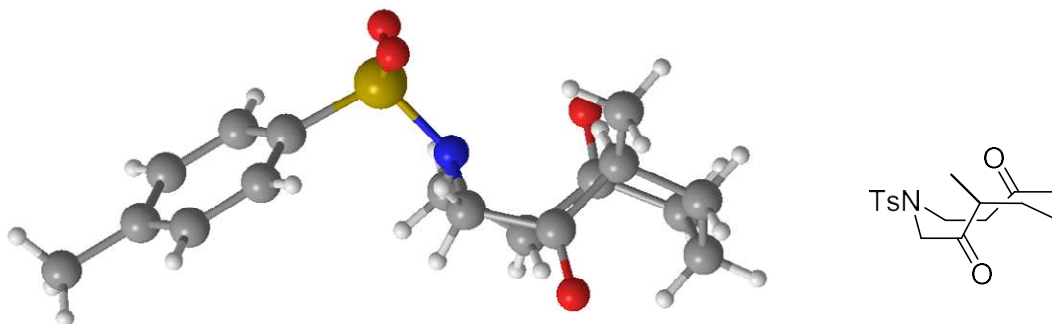
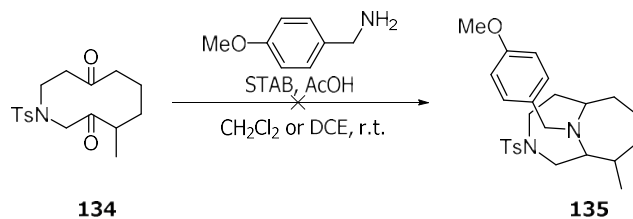


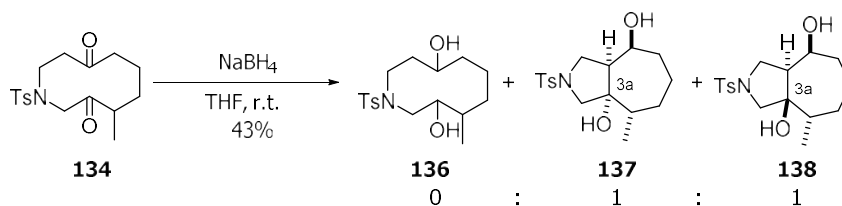
Figure 42 – Left: X-ray crystal structure of diketone **134**; representation generated in Chem3D 17.1. Right: 3D representation of diketone **134**

It was thought that reductive amination may have a higher chance of success on this substrate as the transannular interactions would be reduced relative to those seen in keto-alkene **96**. Since there were two ketones within the molecule, it was hypothesised that a double reductive amination cascade might lead directly to bridged azacycle **135**. Unfortunately, attempted reductive amination in both CH_2Cl_2 and DCE led to extensive decomposition (Scheme 65). No further work was carried out.



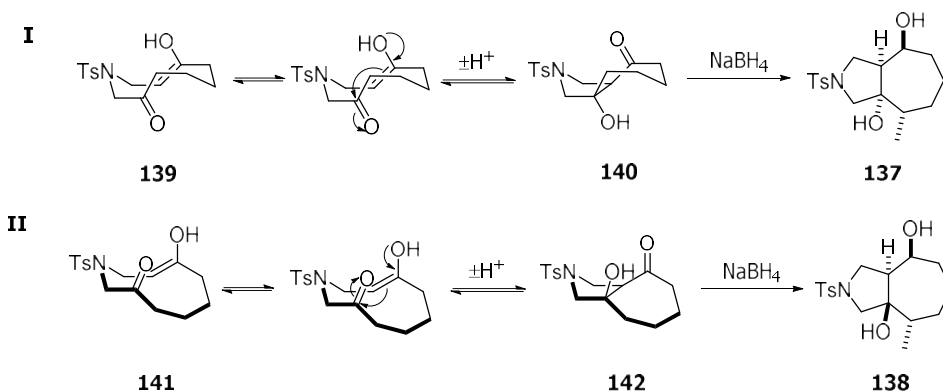
Scheme 65 – Attempted synthesis of azacycle **135**

To probe this reaction in more detail, diketone **134** was subjected to standard reduction conditions with NaBH_4 (Scheme 66). Unexpectedly, diol **136** was not obtained, instead a 1:1 mixture of diastereomeric diols **137** and **138** was obtained.



Scheme 66 – Attempted reduction of diketone **134** with NaBH_4 led to diols **137** and **138**.

Formation of diols **137** and **138** could be explained by the regioselective formation of enols **139** and **141**, followed by an intramolecular aldol condensation to give ketones **140** and **142** (Scheme 67). Subsequent stereoselective reduction of the resulting ketone gives the isolated diols **137** and **138**. The two diastereomers differ in the configuration of the alcohol at C-3a (Scheme 66), which is dictated by the reactive conformation of the macrocyclic scaffold.

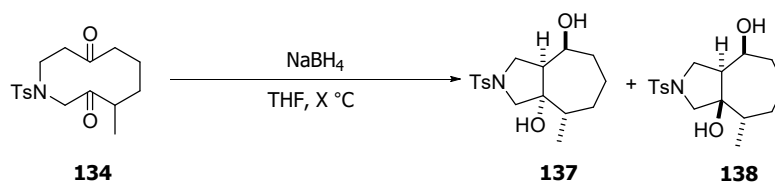


Scheme 67 – Conformational dependency of the outcome of treatment of diketone **134** with NaBH_4 . The methyl group is excluded in some diagrams for clarity

If conformer populations were dictating the ratio of products seen in the synthesis of diols **137** and **138**, then it can be reasoned that temperature might have an effect on the ratio of the products obtained. Alternatively, if the reaction does go *via* a reversible intramolecular aldol pathway and the reduction of ketones **140** or **142** is the rate determining step, then a change in product ratio may indicate the thermodynamic product was being formed at elevated temperatures.

Therefore, diketone **134** was treated with NaBH₄ at 0 °C and 35 °C to see how the ratio varied with temperature (Table 4). At 0 °C, a 5:1 ratio in favour of diol **137** was observed. At 35 °C the opposite result was observed, with a 5:1 product ratio in favour of diol **138**. The diastereomers were inseparable by standard techniques, so an alternative route to compounds of this type was sought.

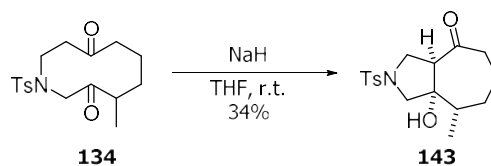
Table 4 – Exploration of how temperature affects the ratio of diols **137** and **138**



Entry	Temp (°C)	Yield (%)	Ratio 137:138 ^[a]
1	0	50	5:1
2	35	98	1:5

[a] The ratio of **137:138** was determined by integration of the respective methyl resonances in the ¹H-NMR spectrum of the crude material.

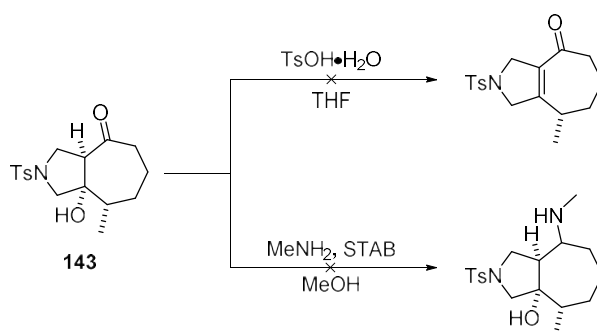
Postulating the 5,7-fused ring systems were synthesised from the corresponding enol, *via* an intramolecular aldol reaction, the reaction of diketone **134** in the presence of just an acid or base was studied. Treatment of diketone **134** with TsOH•H₂O in THF led to a complex mixture of products that could not be identified. Utilisation of LiBF₄ as a Lewis acid led to recovery of starting material, even after 48 h. The use of basic conditions was more successful; treatment of diketone **134** with NaH led to the formation of ketone **143** in 34% yield as a single diastereoisomer (Scheme 68).



Scheme 68 – Synthesis of ketone **143** from diketone **134** using NaH

The formation of a single regioisomer, ketone **143**, is noteworthy as four possible enolates could be formed; however, analysis of the crystal structure, only two hydrogens are orthogonal to a carbonyl, and therefore have the best orbital overlap to form the enolate. If the substrate adopts a similar conformation in solution, it can be postulated that only two enolates are viable on stereoelectronic grounds, of which only one is propagative. The observed diastereoselectivity follows from a pathway **I** (Scheme 67) type transition state. The lack of any pathway **II** reaction product may be due to the change from enol to enolate; previously, with an enol functionality an intramolecular hydrogen bond could potentially form in pathway **II**, whereas use of sodium hydride forms an enolate may make the relative energy of a pathway **II** transition state higher.

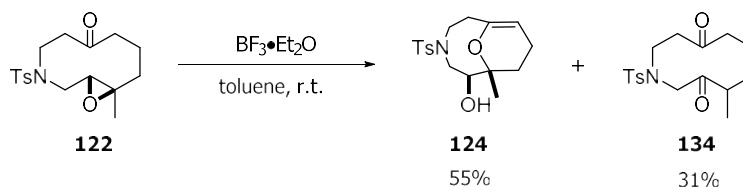
The reactivity of ketone **143** was briefly explored to ascertain whether it was worthwhile pursuing this family of scaffolds further. Firstly, ketone **143** was treated with TsOH•H₂O in THF to generate the corresponding enone *via* dehydration, but nothing identifiable was recovered. Finally, a reductive amination was attempted; however, reaction of methylamine and STAB in a one-pot reductive amination led to no product.



Scheme 69 – Unsuccessful attempted transformations of ketone **143** to an enone or amine

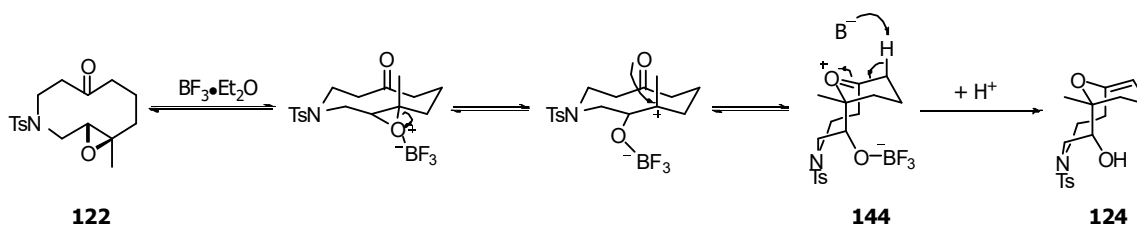
Enol ether and related compounds

The successful synthesis of diketone **134** proved to be condition dependent. On one occasion, a second product was identified as enol ether **124** (Scheme 70).



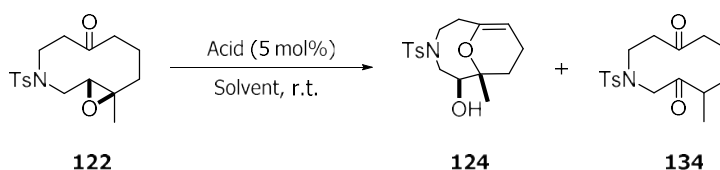
Scheme 70 – Synthesis of enol ether **124** and diketone **134** under the same reaction conditions

The proposed reaction mechanism for the formation of enol ether **124** can be seen in Scheme 71. BF_3 , acting as a Lewis acid, co-ordinates to the epoxide oxygen. The epoxide can then transiently ring open, creating a 3° carbocation, which is susceptible to nucleophilic attack in an $\text{S}_{\text{N}}1$ mechanism. Intramolecular attack of the carbonyl into the carbocation forms a transient oxocarbenium **144**, which rapidly loses a proton to form enol ether **124**. The regioselectivity of this reaction follows the same principles as previously discussed.



Scheme 71 – Proposed reaction mechanism for the formation of enol ether **124**

To probe the formation of enol ether, a range of different reaction conditions were trialled (Table 5).

Table 5 – Exploration of conditions to selectively generate enol ether **124** or diketone **134**^[a]

Entry	Solvent	Catalyst	Ratio of 124:134 ^[b]
1	toluene	BF ₃ •Et ₂ O	0.6:0.4
2	toluene	In(NTf ₂) ₃	Degraded
3	toluene	InCl ₃	1:0
4	toluene	SnCl ₂	Degraded
5	toluene	SnCl ₄	0.6:0.4
6	toluene	TMSOTf	Degraded
7	toluene	TsOH•H ₂ O	1:0
8	toluene	HCl (4 M in dioxane)	Degraded
9	CHCl ₃	BF ₃ •Et ₂ O	0:1
10	CH ₂ Cl ₂	BF ₃ •Et ₂ O	0:1
11	THF	BF ₃ •Et ₂ O	1:0 ^[c]
12	MeCN ^[d]	BF ₃ •Et ₂ O	0:1
13	toluene ^[d]	BF ₃ •Et ₂ O	0:1
14	toluene ^[e]	BF ₃ •Et ₂ O	0.45:0.55
15	toluene ^[f]	TsOH•H ₂ O	1:0 ^[g]
16 ^[h]	CHCl ₃	BF ₃ •Et ₂ O	N/A
17 ^[i]	toluene	TsOH•H ₂ O	N/A

[a] Unless otherwise noted, the reaction conditions were epoxide **122** (0.05 mmol), acid (5 mol%), solvent (2 mL) at r.t. for 17 h. Unless stated, the solvent was obtained from a Solvent Purification System (SPS). [b] Ratio determined by integration of the methyl resonances in the ¹H-NMR spectrum of the crude reaction material. [c] Reaction took 72 h [d] Dried over activated 3 Å molecular sieves for 72 h prior to use. [e] As in entry 13, but two drops of deionised water added. [f] Activated 3 Å molecular sieves added to the reaction. [g] 6% conversion seen after 72 h. [h] Conducted on a 0.61 mmol scale, 62% yield. [i] Conducted on a 0.85 mmol scale, 84% yield.

Initial exploration of the reaction conditions focused on different acid catalysts. The most useful results came with the use of InCl₃ and TsOH•H₂O, which both generated enol ether **124** exclusively (entries 3 and 7, Table 5). Interestingly, these were the same catalysts used in the original paper that reported the synthesis of ketal **132** (Scheme 62). Since the enol ether and ketal scaffold would have similar ¹H-NMR spectra, a re-evaluation of whether Panten *et al.* actually synthesised ketal **132** needs to be considered.

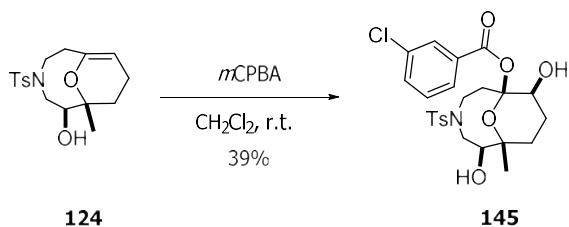
With little success in chemoselectively forming diketone **134**, a solvent screen with $\text{BF}_3 \cdot \text{Et}_2\text{O}$ as the catalyst was instituted instead (entries 9 – 12, Table 5). Chloroform, dichloromethane and acetonitrile all provided diketone **134** exclusively, while THF led to the formation of enol ether **124** exclusively, albeit at a reduced rate.

Halogenated solvents are less miscible with water than toluene, so have lower natural water content.²⁰¹ Suspecting that water may have caused an issue with the initial toluene reaction (entry 1, Table 5), a batch of toluene was dried over activated 3 Å molecular sieves for 72 h to reduce the water content below 10 ppm. Use of this solvent gave exclusively diketone **134**, while deliberately adding water to the reaction gave a mixture of products (entries 13 and 14, Table 5). To confirm the importance of water for the formation of enol ether **124**, the reaction was performed with $\text{TsOH} \cdot \text{H}_2\text{O}$ and activated 3 Å molecular sieves within the reaction mixture (entry 15, Table 5). The drying effect of the sieves severely retarded the rate of reaction, with only 6% conversion to the enol ether seen after 72 h as determined by analysis of the $^1\text{H-NMR}$ spectrum of the material before purification.

A number of observations can be made from this optimisation study. First, from entry 15 it can be seen that TsOH is not a sufficiently strong an acid to catalyse the Meinwald rearrangement (Scheme 64). Lewis acids are typically used to effect this transformation, hence the exclusive formation of enol ether **124** even after removal of H_2O .^{199,202} From entries 13 and 14, it is evident that minimising the water content in the reaction mixture is important for the efficient formation of diketone **134**. A further finding is the rate of formation of enol ether **124** is much greater than rate of formation of diketone **134**. It also suggests H_2O may play a role in the reaction mechanism to form enol ether **124**, possibly acting as the base (Scheme 71). The optimised conditions also proved amenable to scale up (entries 16 and 17, Table 5).

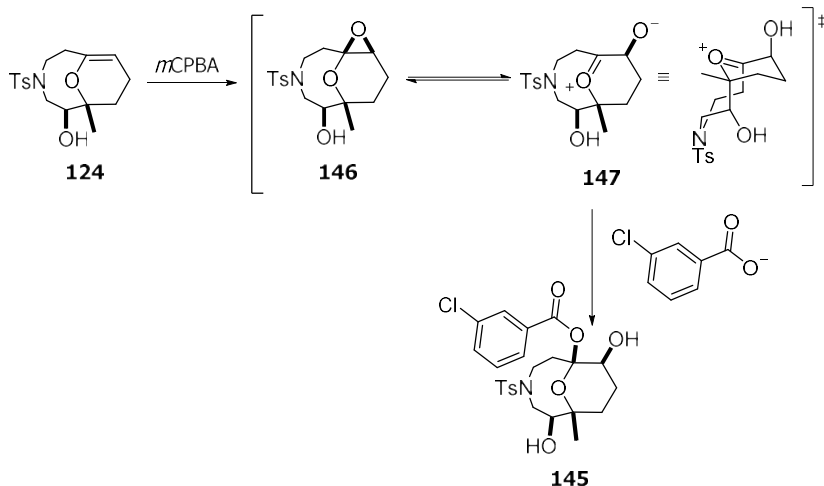
Enol ether **124** is a bridged bicyclic [5,3,1] system, which is a rare scaffold and completely novel with the level of functionality embedded within the scaffold.^{203,204} Therefore, diversification and transformation of the initial enol ether should give a unique library of scaffolds.

Diversification of enol ether **124** began with epoxidation of the enol ether, using standard electrophilic epoxidation conditions (Scheme 72).



Scheme 72 – Synthesis of acetal **145** from enol ether **124** using *m*CPBA

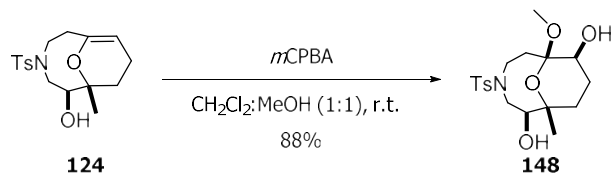
Acetal **145** was isolated in poor yield. Epoxidation of enol ether **124** presumably leads to an unstable acetal **146**. This intermediate is in equilibrium with oxocarbenium **147**, which is susceptible towards nucleophilic trapping. In the absence of another nucleophile, the carboxylate by-product from the epoxidation, a relatively poor nucleophile, reacts to form the isolated acetal **145** (Scheme 73). The relative stereochemistry can be rationalised by consideration of oxocarbenium **147** and substrate control; one face is completely blocked by the surrounding ring, so nucleophilic attack can only take place on one face of the ring.^{xiii}



Scheme 73 – Proposed reaction mechanism for the formation of acetal **145**

To test this mechanistic hypothesis, the reaction was performed with methanol as the co-solvent. Methanol is more nucleophilic than *m*-chlorobenzoate and if present in large excess, the methyl acetal was expected as the major product. Subjection of enol ether **124** to these reaction conditions gave methyl acetal **148** in an 88% yield as predicted (Scheme 74).

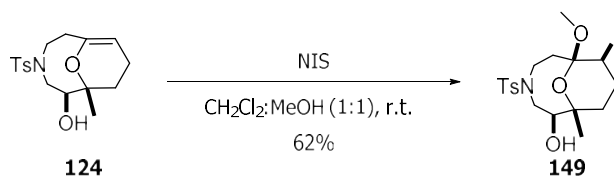
^{xiii} This selectivity is observed consistently for all scaffolds within this family.



Scheme 74 – Synthesis of methyl acetal **148**

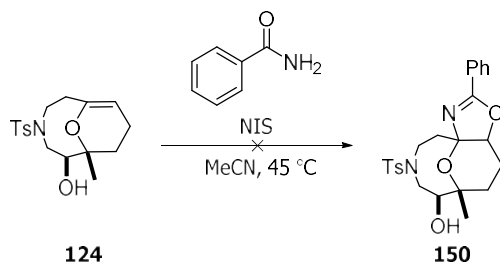
With the successful synthesis of acetal **148**, other nucleophiles were included in the reaction mixture. Acetonitrile, allyltrimethylsilane, triethylsilane and resorcinol were all attempted as alternative nucleophiles, but either led to the previously observed acetal **145** or degradation of the reactants. With these disappointing results, it was decided to move away from *m*CPBA and investigate other forms of double-bond activation.

Alkenes can also be activated by the formation of halonium species. Initially this was attempted with a reaction between *N*-iodosuccinimide (NIS) and enol ether **124** in CH₂Cl₂, to see whether the succinimide would act as a nucleophile. No identifiable products were isolated. Therefore, the reaction solvent was changed to a mixture of CH₂Cl₂ and MeOH. Reaction under these conditions led to the desired iodinated acetal **149** in 62% yield (Scheme 75).



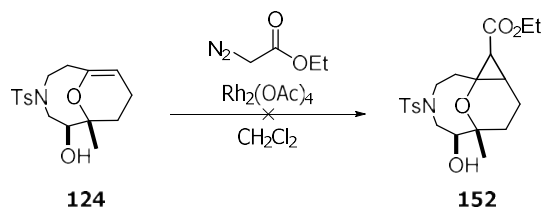
Scheme 75 – Synthesis of acetal **149** from enol ether **124**

De Castro and Marzabadi have demonstrated the reaction of a glycal with NIS and benzamide to generate an oxazoline ring;²⁰⁵ however, applying these conditions to enol ether **124**, led to degradation of the starting material with no identifiable products (Scheme 76).



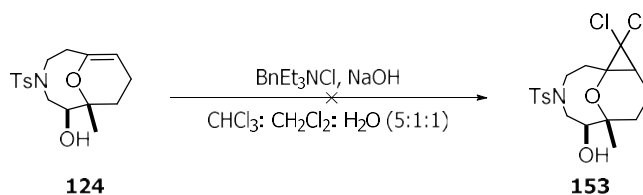
Scheme 76 – Attempted synthesis of oxazoline **150**

An alternative to epoxidation of the double bond is the formation of a cyclopropane functional group. Both copper- and rhodium-catalysed methods were attempted in conjunction with ethyl diazoacetate; however, both reactions resulted in a complicated mixture of products (Scheme 77).



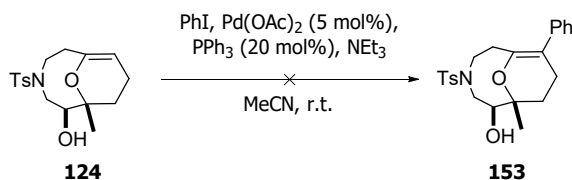
Scheme 77 – Attempted cyclopropane formation from enol ether **124** using a rhodium catalysed method

A metal-free route to generate a bis-chlorocyclopropane *via* a carbene intermediate was also attempted but degradation of the starting material was observed under the reaction conditions (Scheme 78).



Scheme 78 - Attempted dichlorocyclopropane formation from enol ether **124** using a basic method

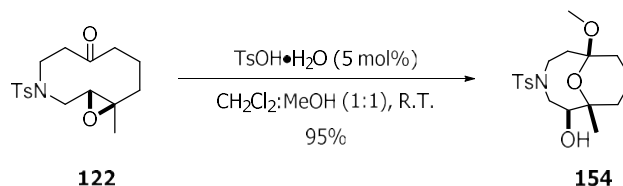
Heck couplings were briefly explored between enol ether **124** and iodobenzene to generate enol ether **153**, but only starting material were recovered (Scheme 79). The failure of enol ether **121** to react may be due to the steric bulk surrounding the alkene, which will inhibit the ability of palladium to co-ordinate to the alkene.²⁰⁶



Scheme 79 – Attempted Heck coupling to synthesise enol ether **153**

Since the formation of enol ether **124** was predicted to proceed *via* an oxocarbenium intermediate, the formation of enol ether **124** was run in a 1:1 solvent mixture of CH₂Cl₂ and MeOH to ascertain whether the transient oxocarbenium species could be trapped with

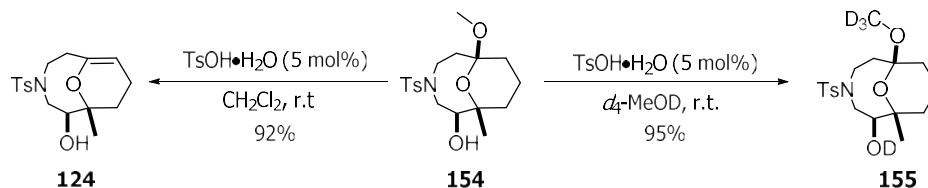
methanol to form methyl acetal **154** directly. The reaction proceeded in excellent yield, giving acetal **154** in 95% yield (Scheme 80).



Scheme 80 – Synthesis of acetal **154** under acidic conditions

With the formation of acetal **154**, the library now has access to two closely related scaffolds, namely acetals **148** and **154**, where the only difference is a selective oxidation at C-8. This can be useful for the exploration of functional group diversity or, looking to the future, if the SAR needs to be established, the total polar surface area can be varied by selective deletion or insertion of a hydroxyl group.

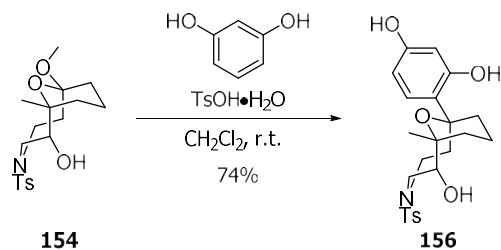
Two further reactions were carried out to test the reactivity of acetal **154**. First, treatment of acetal **154** with TsOH·H₂O in the absence of MeOH, selectively generated enol ether **124** in 92% yield. Second, acetal **154** was treated with TsOH·H₂O in the presence of *d*₄-MeOD to generate acetal **155** (Scheme 81).



Scheme 81 – Experiments probing the reactivity of acetal **154**

These two experiments show the expected reactivity of the acetal under mildly acidic conditions. Exploitation of this property coupled with the introduction of various masked nucleophiles, was utilised to generate a small library of new scaffolds.

Resorcinol was the first utilised nucleophile, as it would introduce an aromatic ring into the scaffold, while also providing further handles for diversification, if desired. Subjection of acetal **154** to resorcinol and TsOH·H₂O in CH₂Cl₂ gave alcohol **156** in 74% yield and as a single regioisomer (Scheme 82). The structure of alcohol **156** was confirmed by X-ray crystallography (Figure 43).



Scheme 82 – Synthesis of alcohol **156** from acetal **154** under acidic conditions

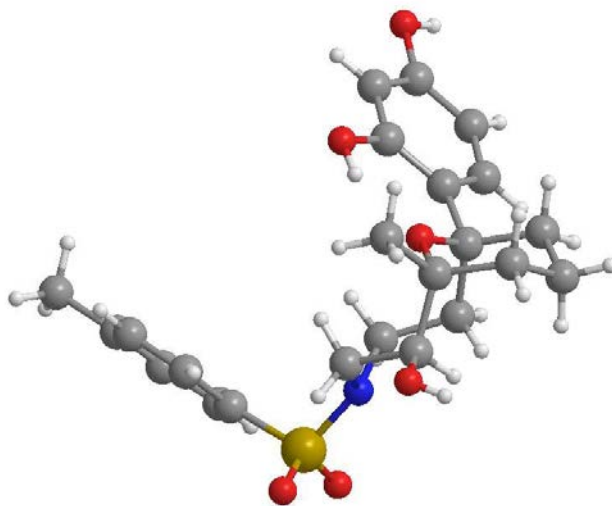
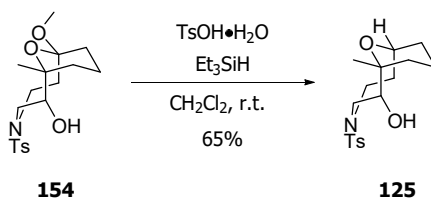


Figure 43 – X-ray crystal structure of alcohol **156**

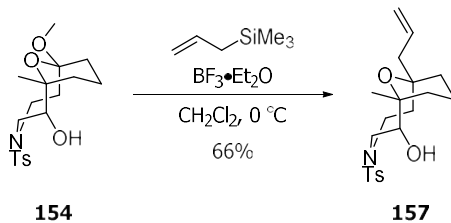
The regioselectivity of the addition can be explained by a steric argument. Attack through the 4-position of resorcinol leads to fewer steric interactions than attack through the alternative 2-position.

Successful synthesis of alcohol **156** led to the use of two more masked nucleophiles; allyltrimethylsilane and triethylsilane. Reaction with triethylsilane proceeded smoothly, giving ether **125** in 65% yield (Scheme 83). Interestingly, ether **125** is the same scaffold that was synthesised from epoxide **122** (Scheme 56, Section 2.3.3); synthesis starting from acetal cleanly gives ether **125**, while starting from epoxide **122** gives a mixture of compounds. This result demonstrates the relationship that exists between the scaffolds in this library.



Scheme 83 – Synthesis of ether **125** from acetal **154** under acidic conditions

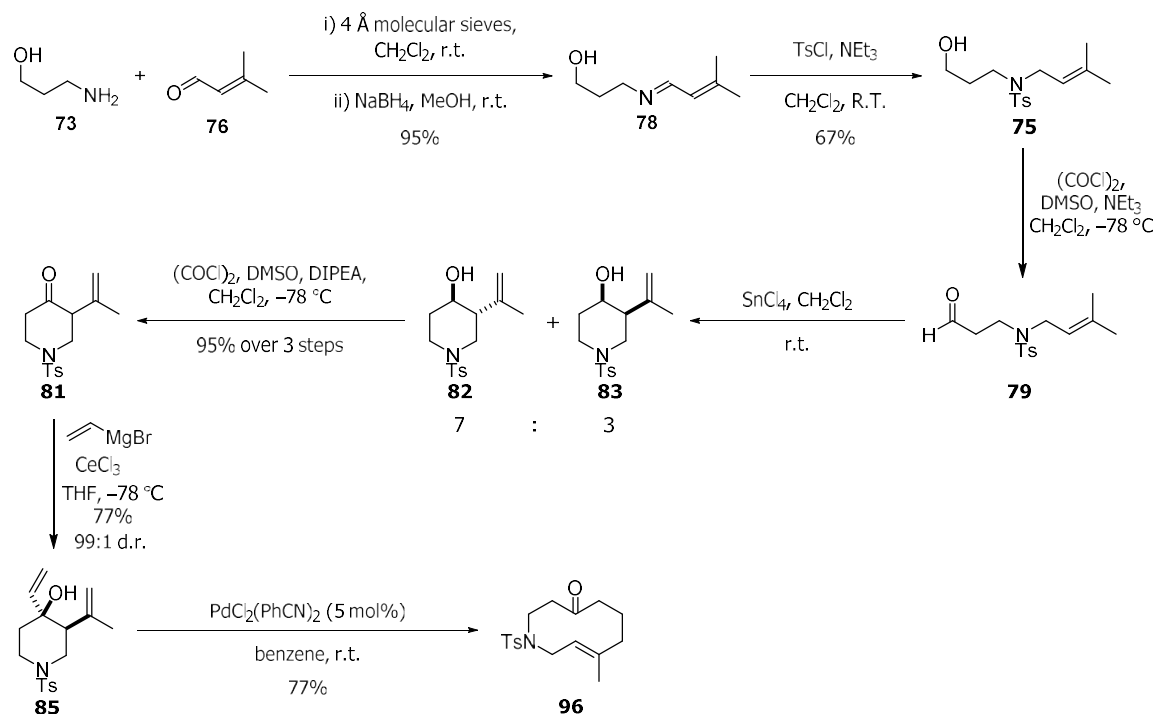
Use of allyltrimethylsilane under Brønsted-acid activation only generated enol ether **124**; however, the use of $\text{BF}_3\cdot\text{Et}_2\text{O}$ as a Lewis acid catalyst afforded homoallylic ether **157** in 66% yield (Scheme 84), with no enol ether **124** observed within the $^1\text{H-NMR}$ spectrum of the crude material. Looking forward, the allyl group provides an excellent handle to further develop this library of scaffolds.



Scheme 84 – Synthesis of alcohol **157** from acetal **154** under Lewis acidic conditions

2.4 Summary and conclusions

A route to keto-alkene **96** was designed and successfully used to access the target compound in 34% overall yield over seven steps (Scheme 85).



Scheme 85 – Optimised route to access keto-alkene **96** in multi-gram scale in 34% overall yield over seven steps.

Keto-alkene **96** was then utilised as the parent scaffold to prepare a library of other scaffolds. Use of either an ene or a Prins reaction allowed for the direct transformation of keto-alkene **96** into decalols **107** and **121**.

Nucleophilic addition into the ketone proved challenging, with reduction to alcohol **119** the only transformation that could be achieved. Functionalisation of the double bond was more successful, with the generation of epoxide **122** opening the door to a wide variety of intramolecular chemistry.

Meinwald rearrangement of epoxide **122** gave diketone **134**. Diketone **134** was then utilised further to synthesise a series of 5,7-fused rings, which while interesting, were isolated as a mixture of diastereomers.

Under optimised acidic conditions, intramolecular attack of the ketone to ring-open epoxide **122** gave enol ether **124**, a unique [5,3,1] bridged bicyclic scaffold, which was transformed into a further eight different scaffolds, with potential for further transformations.

Overall, keto-alkene **96** was transformed into a further eighteen different scaffolds (fourteen different Murcko scaffolds). The longest linear sequence to a single scaffold is three steps, showing the versatility of keto-alkene **96** as a starting point for DOS.

The nineteen scaffolds can be broadly grouped into four categories: ten-membered rings, decalols, 7,5-fused rings and [5,3,1]-bridged bicyclic systems (Figure 44).

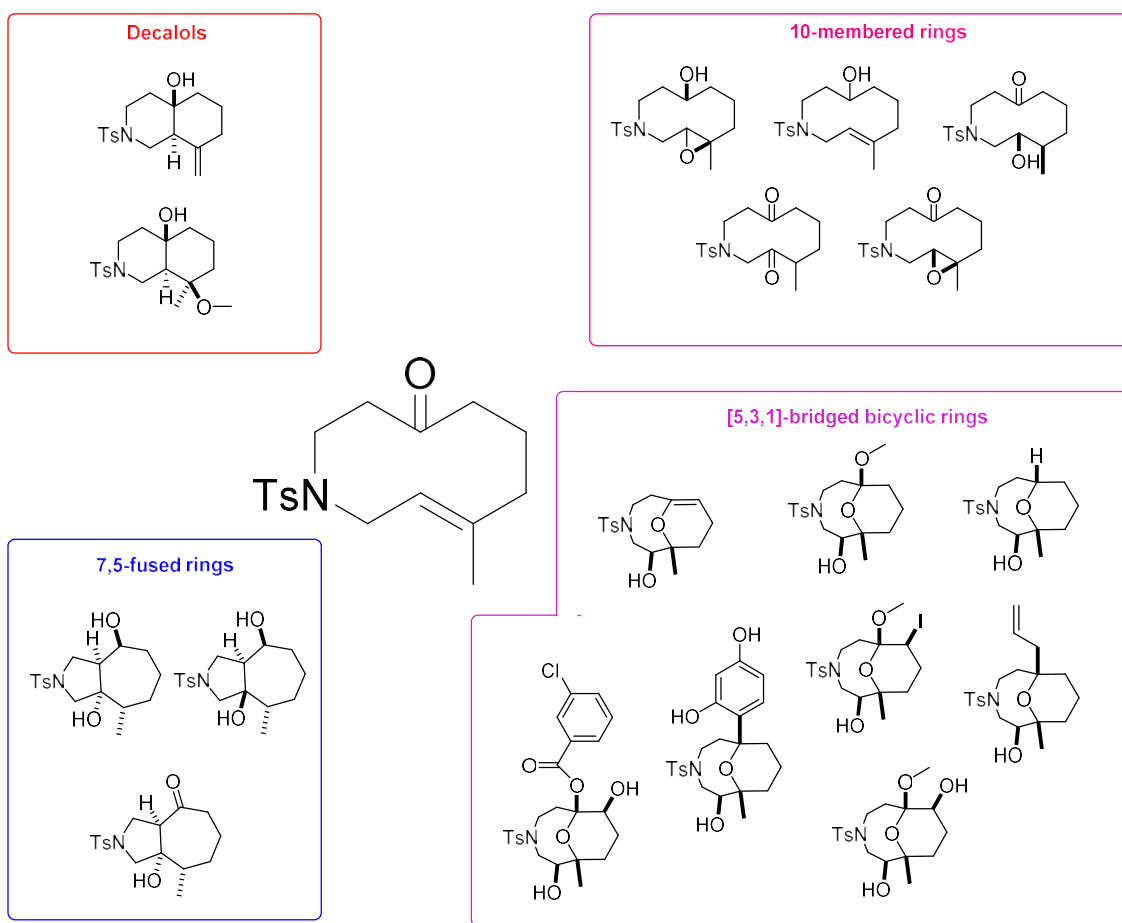


Figure 44 – Broad groupings of synthesised scaffolds.

Chapter Three: Synthesis of a Screening Library

3.1 Introduction

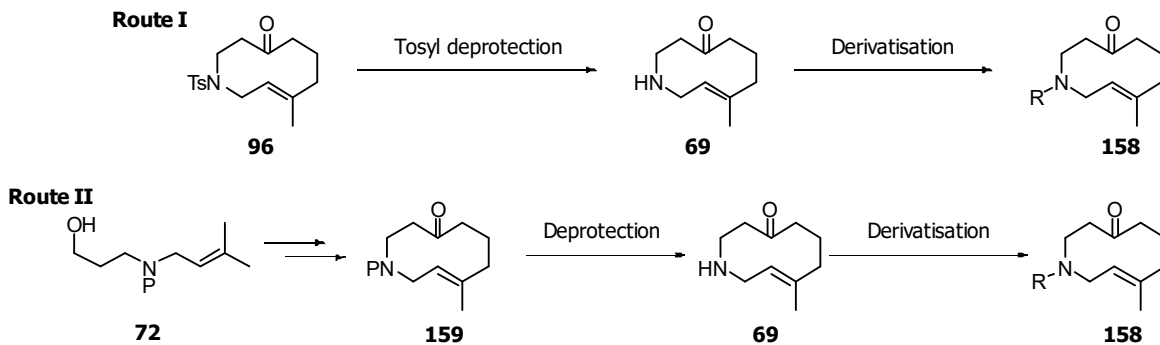
In Chapter 2 a library of eighteen different scaffolds was synthesised in one to three steps starting from keto-alkene **96**. Covering four different groups of ring systems, the library has broad scaffold diversity, but this is only one type of diversity with DOS. To fully realise a library of compounds that is suitable for use in high-throughput screening, the other types of diversity must also be taken into account.

In addition to the scaffolds that have been synthesised, some of the rings within the library exhibit conformational flexibility which allows for multiple conformations to be adopted by one scaffold (see Section 2.2.6). Once such a compound is screened, it can be thought of as multiple scaffolds being screened by one compound.

An element of stereochemical diversity has also already been incorporated within the library; all of the scaffolds have been synthesised in a racemic fashion, so although one diastereomer is submitted to the library, two enantiomers will be screened at the same time.

Building block and functional group diversity were not considered in the scaffold library described in Chapter 2. The scaffold transformations introduced a degree of functional group diversity within the library, such as the introduction of ethers in scaffolds **125**, **156** and **157**, but overall, the functionality was broadly similar across the synthesised library. The presence of the same (tosyl) sulfonamide group in every scaffold also limits the overall diversity of the library.

Therefore, to increase the diversity of the library and successfully turn it into a more attractive library for screening, the tosyl group either had to be removed to allow derivatisation of the resulting amine (Route I, Scheme 86), or replaced with an alternative amine protecting group that would enable more facile deprotection (Route II, Scheme 86).



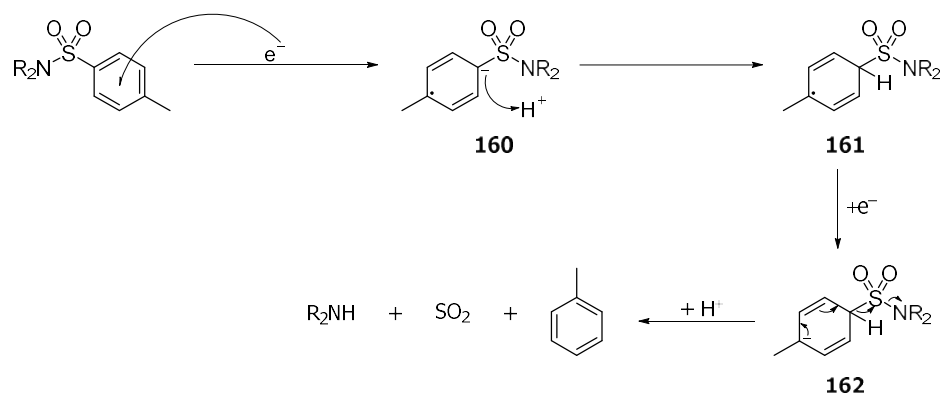
Scheme 86 – Proposed routes to enable derivatisation of the amine embedded in macrocycle **69**. P= undefined protecting group

3.2 Synthesis of Amine 69

3.2.1 Attempted tosyl removal

Initial focus for the synthesis of amine **69** was placed on deprotection of sulfonamide **96**. Although the tosyl group was primarily chosen for its stability whilst developing the synthetic route, the possibility of generating amine **69** from sulfonamide **96** in one step from known chemistry was nevertheless still attractive.

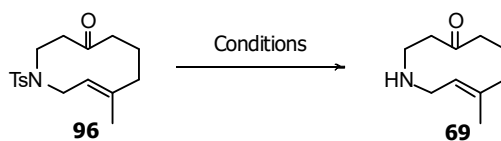
Various methods for deprotecting a tosylsulfonamide are known, mainly involving single-electron reduction processes.¹³⁸ Commonly used methods include dissolving metal reductions, samarium diiodide and sonication of magnesium in methanol.^{207–209} In each case, a single electron is donated into the aromatic system of the tosylsulfonamide, generating a radical anion that can be depicted as a tertiary radical and a stabilised carbanion **160** (Scheme 87). The carbanion is rapidly quenched to afford radical **161**, which accepts a second electron to form carbanion **162**, which can re-aromatise, generating toluene, SO₂ and the desired free amine.



Scheme 87 – Mechanism of tosyl removal from a sulfonamide *via* a single-electron reduction process.

The progenitor scaffold, keto-alkene **96**, was chosen as the scaffold on which to optimise the tosyl group removal as generating amine **69** at this stage would afford greater flexibility in scaffold choice for the final library. A range of deprotection methods were trialed (Table 6).

Table 6 – Attempted removal of the tosyl group^[a]



Entry	Conditions	Comment
1	96 , Mg (1.0 eq.), MeOH, sonication, 4 h ^[b]	5:1 mixture of 96 : unidentified compound ^[c]
2	96 , Mg (1.2 eq.), MeOH:THF (1:1), sonication, 6 h ^[b]	1:1 mixture of 96 : unidentified compound ^[c]
3	96 , Na/Hg amalgam (20% Na), Na ₂ HPO ₄ , MeOH, 48 h	No reaction
4	96 , Na, naphthalene, THF, 2 h	Degradation
5	96 , SmI ₂ (6 eq.), H ₂ O (18 eq.), pyrrolidine (18 eq.), THF, 20 min	Degradation
6	96 , SmI ₂ (4 eq.), H ₂ O (12 eq.), pyrrolidine (12 eq.), THF, 20 min	Degradation
7	96 , SmI ₂ (2.2 eq.), H ₂ O (6.6 eq.), pyrrolidine (6.6 eq.), THF, 20 min	Degradation

[a] All solvents were degassed prior to use. [b] Reaction began at r.t. but sonication warmed the water bath slowly to 43 °C. [c] By integration of the alkenyl peaks in the ¹H NMR spectrum of the crude material.

The first conditions tested were adapted from a method reported by Nyasse *et al.* (entry 1, Table 6).²⁰⁸ After 4 h, the reaction mixture contained majority starting material with ~17% conversion to a new product. It was postulated that the poor solubility of keto-alkene **96** in

MeOH contributed to the lack of reaction, so the reaction was repeated with THF as a co-solvent (entry 2, Table 6). Pleasingly, the reaction proceeded with greater conversion of starting material, to provide a 1:1 mixture of **96** and the unknown product after 6 h. To ascertain whether the new product was the desired amine **69**, the unpurified material was subjected to Boc protection conditions (Boc₂O, NEt₃, CH₂Cl₂). Only keto-alkene **96** was isolated, so it was inferred that the new product was not desired amine **69**. Comparison of the ¹H NMR spectrum of the new product with the ¹H NMR spectrum of alcohol **119** (see page 73) formed by ketone reduction confirmed that the observed product was not alcohol **119**.

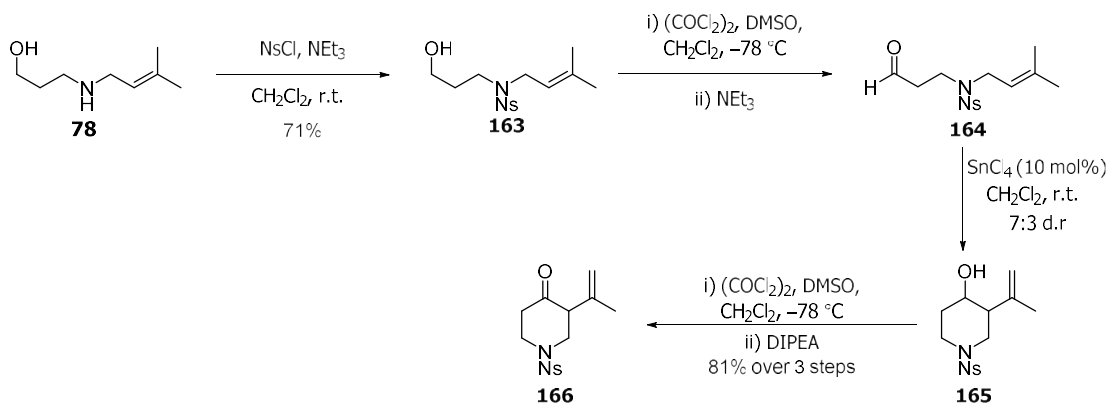
Conditions using Na as the electron source, rather than Mg, were tried, but led to either no reaction or degradation of the starting material (entries 3 and 4, Table 6).²⁰⁹ Samarium(II) iodide is a widely used reducing agent, which has previously been used to deprotect tosylamides in conjunction with H₂O and pyrrolidine in work by Ankner and Hilmersson.²⁰⁷ An initial attempt (entry 5, Table 6) led to degradation of keto-alkene **96** within 20 min, which was postulated to be caused by the large excess of SmI₂ causing degradation of the other electron acceptor functional groups (ketone, alkene) present in the molecule. To improve selectivity, the number of equivalents of SmI₂ was reduced (entries 6 and 7, Table 6); however, no change to the outcome was observed. From these results, it was concluded that selective reduction of the tosylsulfonamide would be hard to effect in a high yield, if at all, so efforts were diverted to the more promising use of a different protecting group.

3.2.2 Alternative protecting groups

Since the tosyl group could not be removed from sulfonamide **96**, an alternative option was to introduce a different protecting group directly after synthesising amino alcohol **78**. Analysis of the subsequent chemistry leading to the target keto-alkene suggested the chosen protecting group would need to be stable to both acidic and basic conditions. The initial focus was placed on the 4-nitrobenzenesulfonyl (nosyl) protecting group. Nosyl protecting groups are traditionally removed by thiolates or other soft nucleophiles in an S_NAr-type reaction mechanism,²¹⁰ so the risk of premature deprotection throughout the synthetic sequence was deemed low.

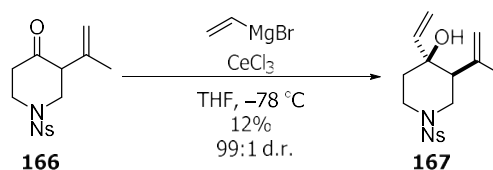
Chemoselective *N*-nosylation of amino alcohol **78** was achieved by subjecting amino alcohol **78** to 4-nitrobenzenesulfonyl chloride (NsCl) in dichloromethane, which afforded the desired sulfonamide **163** in 71% yield (Scheme 88). Sulfonamide **163** was then subjected to the

stepwise oxidation-cyclisation-oxidation procedure previously described in Section 2.2.3. The sequence proceeded smoothly with desired piperidinone **166** isolated in 81% yield over the three steps. Overall, synthesis of piperidinone **166** was achieved in 58% yield, compared to the 64% yield achieved with piperidinone **166**. Since the yields were comparable no further optimisation was carried out.



Scheme 88 – Synthesis of piperidinone **166**

With piperidinone **166** in hand, vinyl Grignard addition into the ketone was attempted. Unfortunately, application of the organocerium conditions described in Section 2.2.4 led to cleavage of the nosyl group and significant by-product formation (Scheme 89). The desired alcohol **167** was only isolated in 12% yield, although the d.r. of this product remained 99:1. No other products were positively identified.

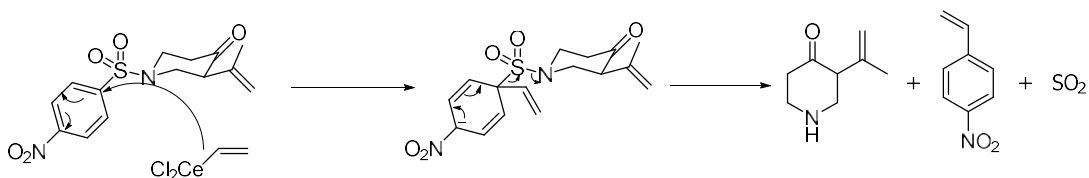


Scheme 89 – Synthesis of alcohol **167** *via* Grignard addition into piperidinone **166**

Resonances in the ^1H NMR spectrum of other isolated fractions suggested the side-products were aromatic in nature. One of the side-products was tentatively identified as 4-nitrostyrene, as resonances in the ^1H NMR spectrum of the reaction material before purification matched those reported in the literature.²¹¹

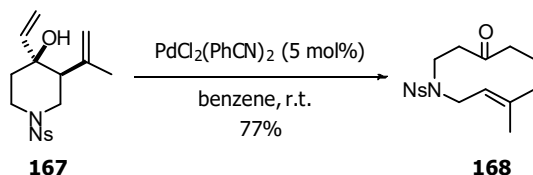
Cleavage of the nosyl group *via* nucleophilic attack on the aromatic ring ($\text{S}_{\text{N}}\text{Ar}$) is a possible pathway that would rationalise the observed results (Scheme 90) although organocerium

reagents are hard nucleophiles on the basis of HSAB theory, and nosyl groups are typically removed by soft nucleophiles.^{210,212,213}



Scheme 90 – Potential cleavage pathway

Despite its formation in disappointing yield, alcohol **167** reacted under the ring-expansion conditions previously developed (Scheme 91) to provide keto-alkene **168** in 77% yield, identical that seen with the tosyl analogue.



Scheme 91 – oxy-Cope like rearrangement of alcohol **167** to keto-alkene **168**

Keto-alkene **168** was synthesised in an overall yield of 5% in seven steps, compared with the 34% overall yield seen with tosyl analogue **96**. The unexpected cleavage of the nosyl group was responsible for this low overall yield and would prove to be a significant hindrance upon scale-up for library synthesis. Therefore, the decision was made to develop two separate series to alternative substrates in parallel, specifically using another alternative amine protecting group (Alloc) and replacing the amine with a different heteroatom (oxygen).

Synthesis of ether analogue **68**

If a suitable amine protecting group could not be realised, then replacing the amine with an ether would afford a similar but alternative progenitor scaffold for exploration. An all-carbon analogue **67** was also considered, but this analogue displayed a CLogP^{xiv} of 3.14 (Figure 45). Ideally, compounds within a screening library would have a CLogP between -1 and $+3.5$,⁶⁹ which encompasses keto-alkene **67**. However, derivatisation of a scaffold typically increases the CLogP, which would bring derivatives of keto-alkene **67** outside of the ideal range for

^{xiv} CLogP values were calculated using BioByte's algorithm within ChemDraw Professional 17.1

CLogP and therefore less desirable for a screening library.²¹⁴ The oxygen and sulfur analogues **68** and **169** were also considered. Oxygen analogue **68** has a similar CLogP to amine analogue **69**, and was amenable to the already developed chemistry, so the decision was made to focus on the synthesis of ether **68**.

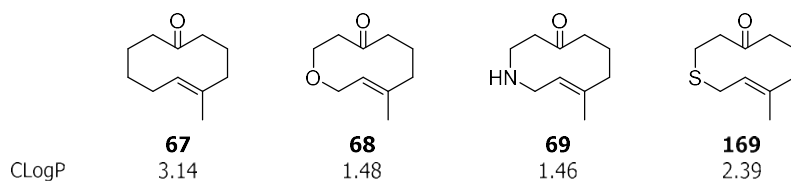
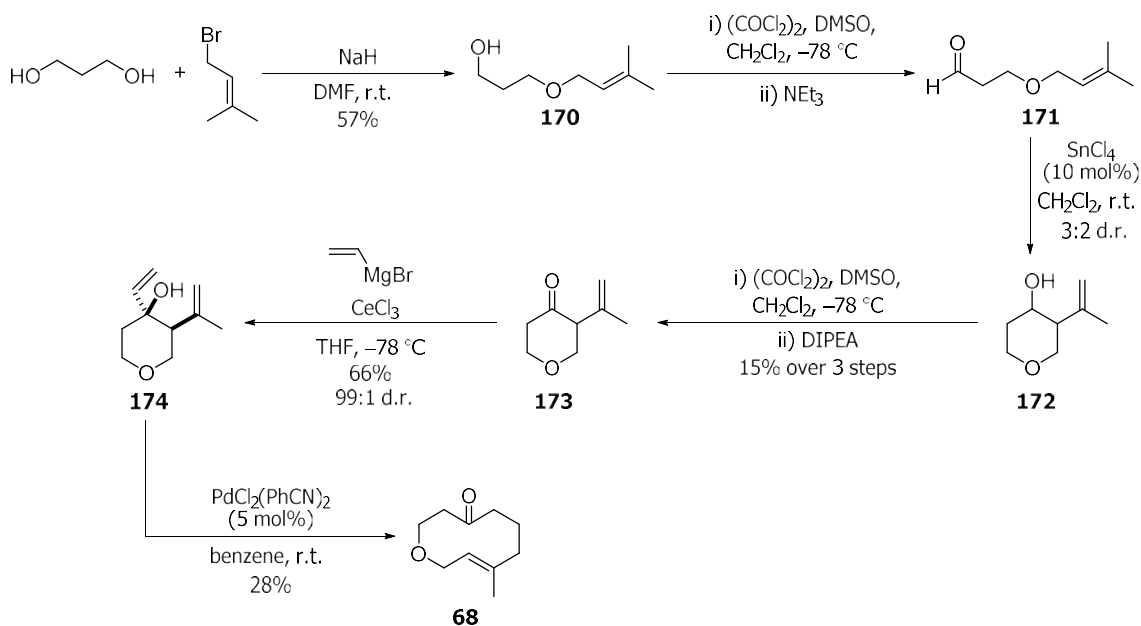


Figure 45 – Analogues of the progenitor scaffold and their CLogP values

Keto-alkene **68** has previously been synthesised by Jacobsen.¹³⁶ Adaption of their procedure in conjunction with our previously optimised conditions allowed for the successful synthesis of oxygen analogue **68** (Scheme 92).



Scheme 92 – Synthesis of oxygen analogue **68** in 2% overall yield over 6 steps

An excess of 1,3-propanediol, treated sequentially with NaH and prenyl bromide, afforded ether **170** in 57% yield. The use of a large excess of 1,3-propanediol reduced the likelihood of both alcohols reacting to form a bis-ether. With ether **170** in hand, the stepwise oxidation-cyclisation-oxidation sequence provided ketone **173** in 15% isolated yield over these three steps. The yield was disappointing but in line with other literature routes to this

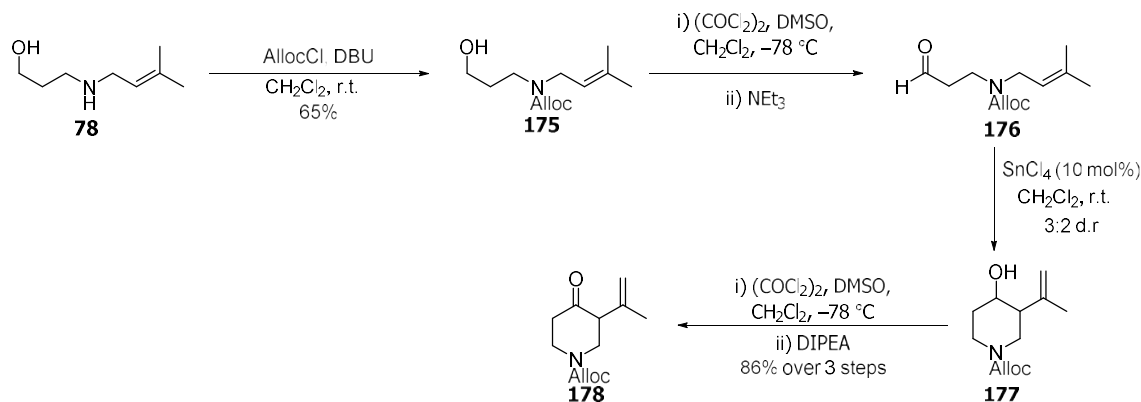
compound.^{136,215} Vinylcerium addition into ketone **173** gave alcohol **174** in excellent diastereoselectivity and in a comparable yield to that seen with tosyl sulfonamide **85**. Finally, application of the Cope-like rearrangement on alcohol **174** using the conditions previously developed, afforded keto-alkene **68** in 28% yield. The low yield was surprising when compared to the yield of sulfonamide **96** (77%) and was lower than the yield obtained by Jacobsen (48%). No other products were positively identified from the reaction.

Keto-alkene **68** was synthesised in 2% overall yield over six steps. Optimisation of the route would likely have increased the overall yield, but it was not prioritised as the ether functionality limited the further derivatisation that could be carried out on scaffolds derived from this keto-alkene. As the other route, which was being examined in parallel, proved more successful, ether scaffolds were not investigated further.

Synthesis of alloc-protected analogue **180**

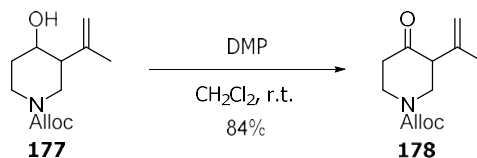
The allyloxycarbonyl (alloc) group, which has an orthogonal removal method to those already used, was chosen. Alloc carbamates are typically deprotected using Pd(0) catalysis, so the risk of premature deprotection along the synthesis route was deemed low.²¹⁶ Deprotection using Pd(II) catalysis has been observed, but requires transformation of the alloc group prior to deprotection (*e.g.* conversion to a silyl carbamate or hydrostannolysis).^{217,218} Therefore, it was argued there would be little risk of premature deprotection under the Overmann conditions.

As with the other syntheses, the route began with chemoselective alloc protection of the amine in amino alcohol **78**, which was achieved using allyl chloroformate (AllocCl) in the presence of DBU, to give desired alcohol **175** in 65% yield (Scheme 93). Alcohol **175** was then subjected to the stepwise oxidation-cyclisation-oxidation procedure developed in Section 2.2.3. The sequence proceeded smoothly, with desired piperidinone **178** isolated in 86% yield over the three steps. The synthesis of piperidinone **178** was achieved in 53% overall yield.



Scheme 93 – Synthesis of piperidinone **178** in 53% overall yield over 4 steps.

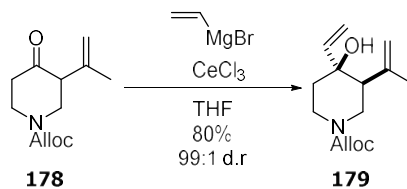
Unlike with sulfonamides **81** and **166**, the second oxidation step proved capricious, with yields variable by up to 25% depending on the batch of material used. Suspecting the problem was residual tin salts from the previous Prins cyclisation step,^{xv} alcohol **177** was purified by column chromatography prior to Swern oxidation; however, this did not make this reaction more reliable. Therefore, Dess-Martin periodinane (DMP) was utilised as an alternative oxidant (Scheme 94). Purification of alcohol **177** by column chromatography followed by oxidation with DMP now provided piperidinone **178** in a reproducible 84% yield.



Scheme 94 – DMP oxidation of alcohol **175** provided piperidinone **176** in a reproducible high yield.

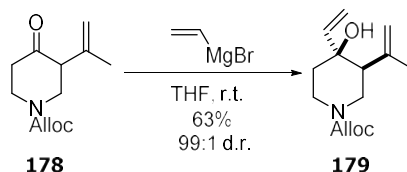
With piperidinone **178** in hand, vinyl addition using the developed organocerium methodology, afforded alcohol **179** in 80% yield and excellent diastereoselectivity (Scheme 95).

^{xv} A new batch of SnCl₄ had been obtained between the syntheses of piperidinones **81** and **164** and the synthesis piperidinone **176**, which could rationalise why the Swern reaction was capricious in this case, but the same result was not observed in the synthesis of piperidinones **81** and **164**.



Scheme 95 – Synthesis of alcohol **179** *via* Grignard addition into piperidinone **178**

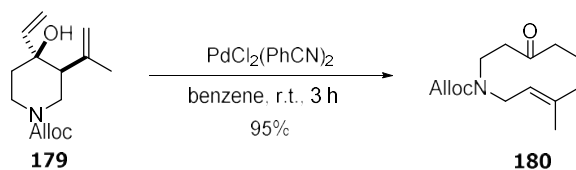
The organocerium chemistry gave comparable yields up to a scale of ~3 g of piperidinone **178**. Performing this reaction on larger scale required >7 g of $\text{CeCl}_3 \cdot 7\text{H}_2\text{O}$, which proved challenging to fully dehydrate with the equipment available. If not effectively dehydrated, the organocerium reagent autoquenched before use, which in turn led to an inseparable mixture of piperidinone **178** and alcohol **179**. Therefore, an alternative solution was to return to the Grignard reagent. To overcome the low yields previously seen, the reaction was performed at high concentration^{xvi} (0.65 – 0.75 M with respect to piperidinone **178**), which has previously been used successfully in the literature.¹⁵³ Using these conditions, full consumption of piperidinone **178** afforded desired alcohol **179** in 63% isolated yield, (Scheme 96).



Scheme 96 – Synthesis of alcohol **177** on large (> 15 mmol) scale

With alcohol **179** in hand, the final step was to carry out the Overman rearrangement chemistry to form the desired ten-membered ring. Treatment of alcohol **179** with $\text{PdCl}_2(\text{PhCN})_2$ in benzene delivered desired keto-alkene **180** in 95% yield (Scheme 97). The yield was much higher than that observed for the tosyl or nosyl analogues, which we postulate is caused by the alkene in the alloc group sequestering the palladium catalyst, reducing its ability to mediate the formation of the decalol side-product. Another observation which supports this hypothesis is the increased reaction time. Ring expansion of the tosyl and nosyl sulfonamides proceeded within 2 h, while the alloc analogue required 3 h, a 50% increase in reaction time. If the palladium catalyst is co-ordinating to the alloc group, then there is less available to catalyse the ring expansion reaction, which would rationalise the increased reaction time.

^{xvi} When these conditions were originally assessed the reaction was run at 0.1 M with respect to the piperidinone (see Section 2.2.4)

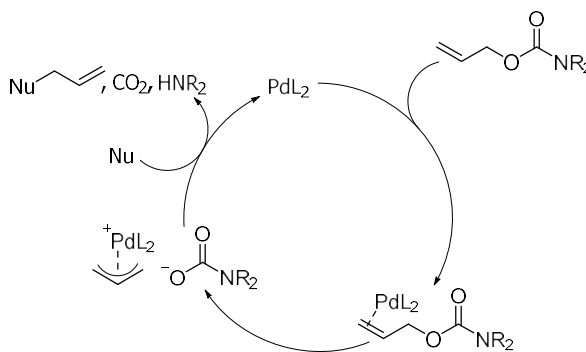


Scheme 97 – oxy-Cope like rearrangement of alcohol **179** to keto-alkene **180**

Keto-alkene **180** was successfully synthesised in 40% overall yield over seven steps. The chemistry could be performed on large (>3 g) scale, showing the suitability of the chemistry for library synthesis. However, like the tosyl scaffold, the ability to synthesise a library required the alloc protecting group to be removed selectively and in high yield. Focus therefore turned to identifying alloc removal conditions that would generate amine **69**.

3.2.3 Alloc cleavage

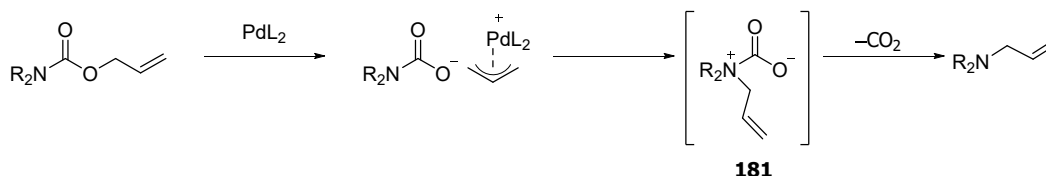
Removal of an alloc group is typically carried out using palladium(0) and a nucleophile (Scheme 98).^{216,219–222} The first part of the catalytic cycle involves co-ordination of the palladium catalyst to the double bond, generation of the π -allyl complex and the corresponding carbamate anion. Subsequent nucleophilic attack on the π -allyl complex, affords an allylated species and regenerates the catalyst. In addition, decarboxylation of the carbamate anion occurs to afford the desired amine.



Scheme 98 – Catalytic cycle for alloc removal

The alloc removal reaction is closely related to the Tsuji-Trost reaction, which is used to allylate nucleophiles. In the case of alloc removal, if the nucleophile additive is not sufficiently nucleophilic, then an alternative pathway can occur. Instead of nucleophilic attack on the π -allyl complex, palladium facilitates the transfer of the allyl group to the nitrogen, generating ammonium ion **181** (Scheme 99). Subsequent decarboxylation leads to the corresponding *N*-

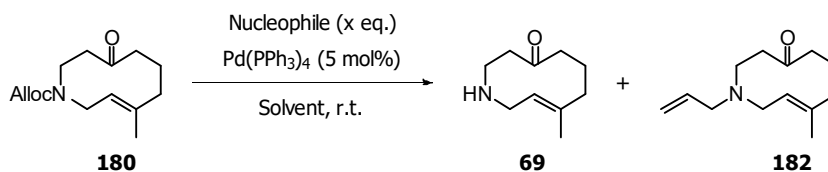
allylated species.²²² Another possible pathway to this *N*-allylated product is that the released amine competes with the sacrificial nucleophile.



Scheme 99 – Tsuji-Trost mechanistic pathway

The strength of the sacrificial nucleophile is therefore important in determining the outcome of the reaction. A variety of nucleophiles were tested (Table 7).

Table 7 – Optimisation of the alloc cleavage^[a]



Entry	Nucleophile	Eq.	Solvent	Ratio of 69:182 ^[b]
1	dimedone	2	THF	0:1
2	dimedone	6	THF	0:1
3	dimedone	10	THF	0:1
4	morpholine	5	THF	0:1
5	morpholine	5	CH ₂ Cl ₂	37:13
6	morpholine	5	toluene	3:1
7	morpholine	5	benzene	3:1
8	morpholine	10	CH ₂ Cl ₂	11:2
9	piperidine	5	CH ₂ Cl ₂	11:1
10	pyrrolidine	5	CH ₂ Cl ₂	47:3
11	pyrrolidine	10	CH ₂ Cl ₂	47:3
12	pyrrolidine	2	CH ₂ Cl ₂	2:1

[a] All solvents were degassed prior to use. [b] Determined by integration of the alkenyl peaks in the ¹H NMR spectrum of the reaction mixture after work-up but prior to purification by column chromatography.

Initially, alloc cleavage was studied utilising a procedure adapted from Kunz and Unverzagt.²²¹ Keto-alkene **180** was treated with Pd(PPh₃)₄ and 2 eq. of dimedone in THF, but only the undesired allyl amine **182** was observed in the ¹H NMR spectrum of the reaction mixture after work-up (entry 1, Table 7). Theorising that the poor ratio was due to the low number of

equivalents of dimedone, a larger excess of dimedone was used, but allyl amine **182** was still the only product formed (entries 2 and 3, Table 7). Morpholine was next used as an alternative, stronger nucleophile than dimedone (entry 4, Table 7). No free amine was observed; allyl amine **182** once again the exclusive product formed.

By consideration of the reaction mechanism, it was postulated that the polar solvent was favouring the formation of the ammonium intermediate **181**. Therefore, a range of non-polar solvents were tried (entries 5-7, Table 7). Now the desired amine **69** was generated as the major product. To try and further improve the ratio towards the desired amine **69**, the number of equivalents of morpholine was doubled (entry 8, Table 7). Pleasingly, the ratio improved significantly, giving a ratio of 11:2 in favour of the desired amine **69**. From the success of morpholine, further amine nucleophiles were investigated (entries 9 and 10, Table 7). Both piperidine and pyrrolidine gave increased ratios, with a ratio of 47:3 observed using pyrrolidine. To further optimise the conditions, the number of equivalents of pyrrolidine was varied (entries 11 and 12, Table 7). Ten equivalents produced the same result as when five equivalents were employed, while 2 equivalents showed a dramatic reduction in ratio, highlighting the importance of using a large excess of pyrrolidine. Consequently, the final conditions for alloc removal were found to be Pd(PPh₃)₄ (5 mol %) and pyrrolidine (5 eq.) in CH₂Cl₂.

To conclude, keto-alkene **180** was synthesised in 40% yield over seven steps. Alloc cleavage could be achieved selectively and in high yield to give amine **69**, which allows for the subsequent derivatisation of the scaffold library.

3.3 Chemoinformatic analysis of a potential library of scaffolds

With the progenitor scaffold in hand and having shown that the alloc carbamate could be deprotected, key decisions were undertaken to ensure that a high-quality high-throughput screening library was successfully synthesised.

In the original tosylsulfonamide library, nineteen different scaffolds were successfully synthesised. However, it was not possible to deploy all nineteen scaffolds in subsequent derivatisation owing to time constraints. Instead, it was decided to concentrate on using a smaller number of scaffolds (<5) for derivatisation, with ~10–15 derivatives of each scaffold to be synthesised. Synthesis of a large number of derivatives allows for exploration of chemical

space around each of the scaffolds. Careful selection would maximise the number of Murcko scaffolds entering the final library, fulfilling one of the main criteria of DOS.

To narrow down which scaffolds to use for derivatisation, the potential promiscuity of each scaffold was considered by reference to Pan-Assay Interference compounds (PAINS) filters. PAINS frequently produce a false positive within assays by being promiscuous. Therefore, by filtering them out, once the library has been fully developed, it increases the confidence that any potential hit is a true positive.^{60,223} PAINS usually contain reactive functional groups which are susceptible to nucleophilic attack or are unstable with the resulting degradation products leading to promiscuity. Examples of functional groups to be avoided are alkyl halides, acid halides, epoxides, anhydrides, triflates, aldehydes, 2- and 4-fluoropyridines and oxoniums.⁶⁰

Analysis of the previously synthesised library of scaffolds revealed seven were unsuitable after being subjected to the PAINS filter (Figure 46). While acetals are not directly removed by consideration of PAINS, within the acid environment of the body they have the potential to transform into oxonium-containing compounds, which are removed by the PAINS filter. Stability studies were not carried out on the acetals within our library of scaffolds, so their stability under *in vitro* conditions is unknown. Therefore, it was decided to remove them from contention to forgo the risk that unsuitable compounds would be submitted to the final library.

Ketones are also electrophilic and are usually not used in high-throughput screening assays. However, previous evidence had shown that the ketones present within the scaffold library are unreactive justifying their retention as viable scaffolds.

While the PAINS filter is an important consideration when deciding on which scaffolds to take forward, it is not the only criterion to consider. The stability of the scaffold also needs to be considered. Any derivatives of the keto-alkene scaffold (**69**) would likely not be stable, as slow conversion of the keto-alkene into the corresponding decalol had been observed (see Section 2.2.4). The allyl-containing [5,3,1]-bridged bicyclic ring (**157**) was also deemed unsuitable as it is likely susceptible to oxidation by P450 enzymes.²²⁴ Therefore, both of these scaffolds were not considered for further derivatisation.

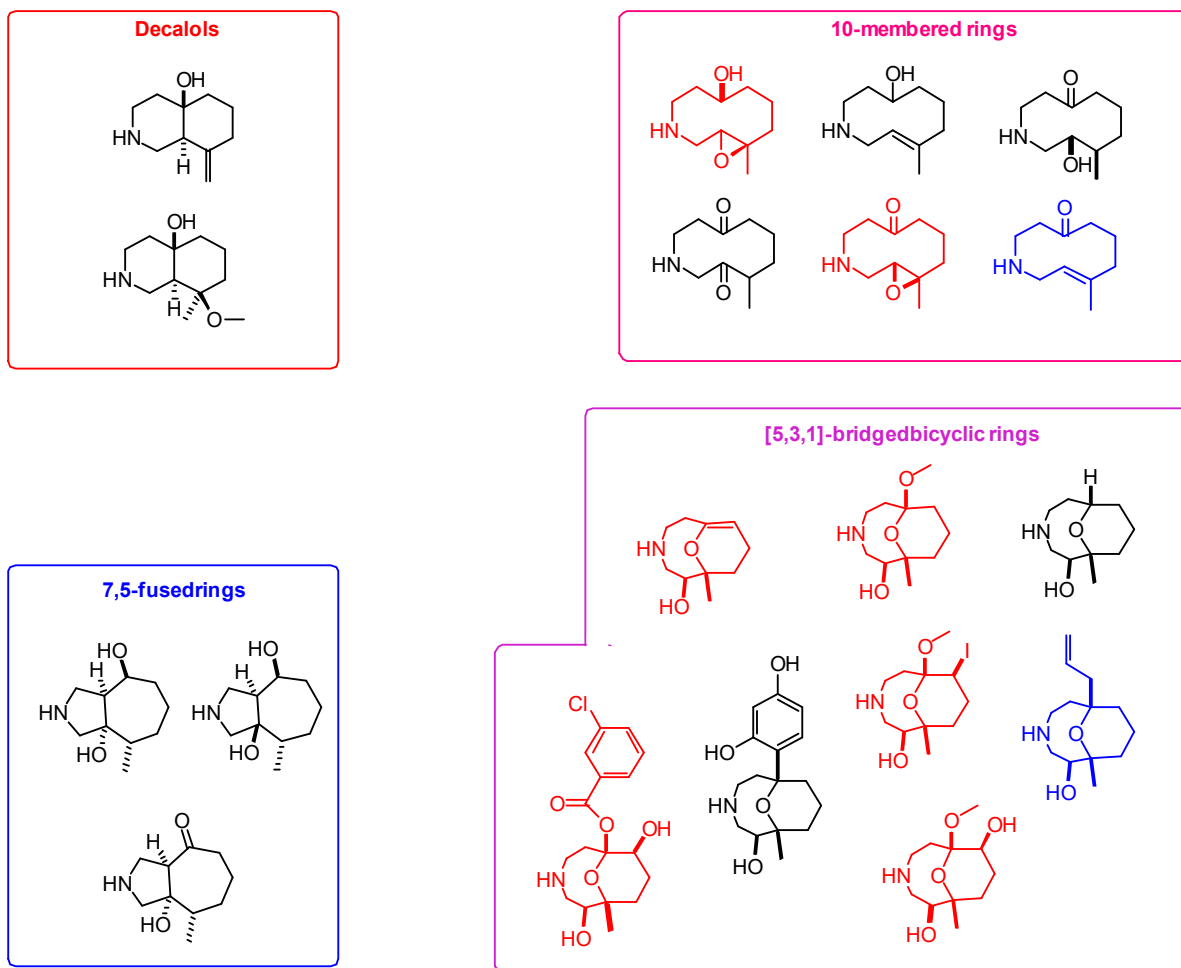


Figure 46 – Synthesised scaffolds. Unsuitable scaffolds due to the PAINS filter are highlighted in red; those cancelled out due to other considerations are highlighted in blue.

Of the ten remaining scaffolds under consideration, synthetic challenges (*i.e.* practicality) that would inhibit the facile creation of a library were next considered (Figure 47). The three 7,5-fused rings **184**, **185** and **189** were unable to be made consistently in high yield, and there were stereoselectivity issues (see Section 2.3.4). Therefore, they were discarded for derivatisation. Decalol **188** and ketone **192** had only previously been made serendipitously, with no further optimisation carried out, so were also not considered further. Finally, diketone **191** was made in a capricious reaction that proved very sensitive to water, which could limit its synthesis on a large scale, and so was also not considered further.

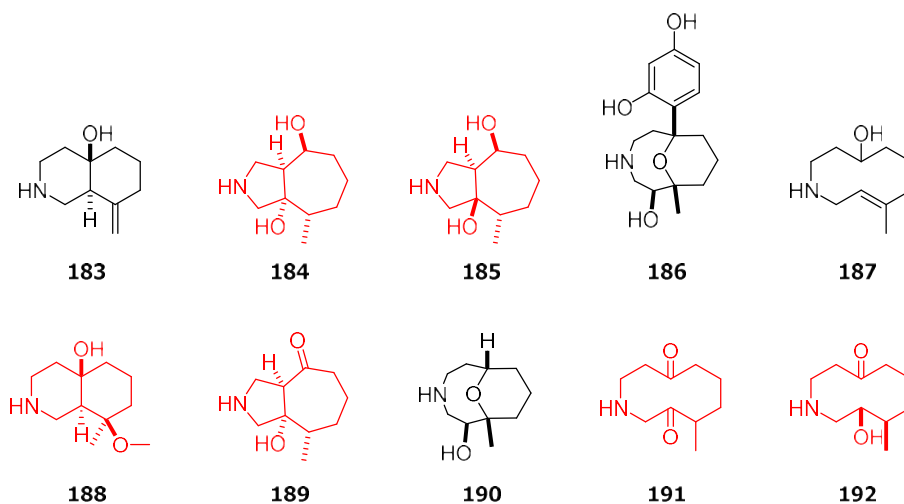


Figure 47 – Remaining scaffolds under consideration. Those that would likely present synthetic challenges are highlighted in red.

The four remaining scaffolds covered three of the four broad groupings that were originally established (Figure 46). To maximise the possibility of successfully synthesising a complete library it was decided to focus on three scaffolds, one from each of the broad groups. Therefore, ether **186** was excluded from further consideration due to its high molecular weight before derivatisation (293 Da), which limited the possible scope of derivatisation.

The three scaffolds advanced for derivatisation are a good representation of the library of scaffolds initially generated. Three of the four broad types of scaffold are represented. In terms of chemical space coverage, the three scaffolds have mean PMI co-ordinates that are close to the mean PMI co-ordinates for all nineteen scaffolds (Figure 48).^{xvii} Pleasingly, all three scaffolds also sit away from the rod-disk axis, a product of their high F_{sp^3} character.

^{xvii} PMI co-ordinates were generated using LLAMA. The data points do not exactly match as LLAMA does not rigorously minimise to the lowest energy conformation.

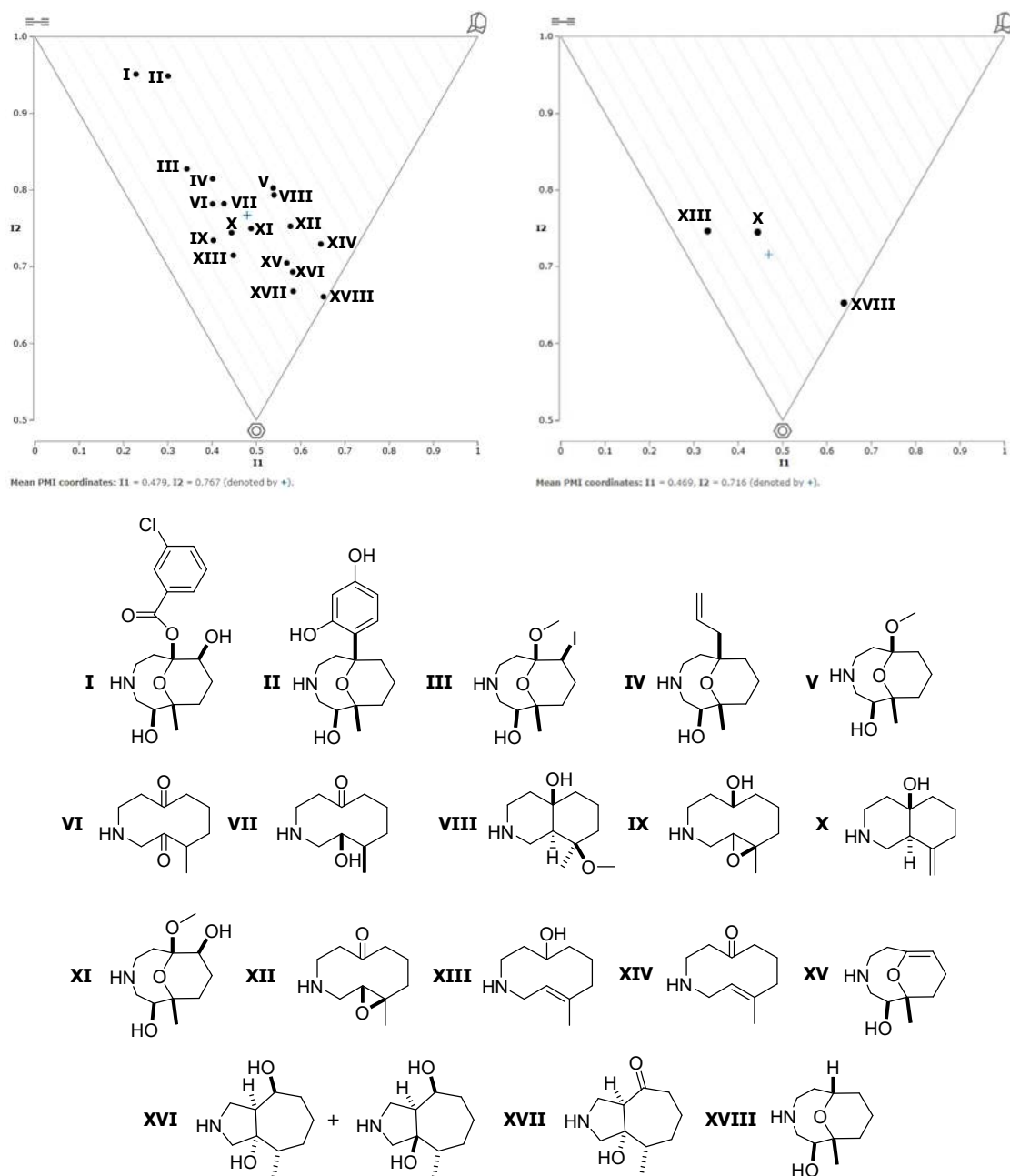


Figure 48 – Top left: PMI plot of all nineteen scaffolds. Top right: PMI plot of the three selected scaffolds. Bottom: Select identification of scaffolds

Having identified three scaffolds to focus on, the next step was to virtually decorate these scaffolds using LLAMA. Virtual decoration creates a library *in silico* of hundreds of compounds. Following the generation of the virtual library, fifteen compounds of each scaffold were selected for physical synthesis. The main criteria for selection of the compounds were

maximising the functional groups present within the library and having wide shape diversity as measured by a PMI plot.

Virtual decoration was conducted using LLAMA, which consisted of single-step diversification.^{xviii} To simplify the vast amount of data that could be generated, a few limitations were placed on the virtual decoration. First, only amine derivatisations were considered. Second, the reaction scope was limited to those reactions that would likely be high-yielding and have a wide substrate scope with little need for optimisation: sulfonamide formation, urea formation, amide formation and reductive amination. The counterpart in the derivatisations were chosen from an array of compounds contained within the "Scaffold Diversification Resource" at the University of Birmingham.^{xix}

Virtual decoration was carried out on each scaffold, with the constraints described above, to give a virtual library of 67 compounds per scaffold (Figure 49). All three virtual libraries shifted towards the rod-disc axis compared to their parent scaffolds. However, all three virtual libraries maintained 3D character with a wide range of chemical space coverage.

^{xviii} Multiple step derivatisation using LLAMA is possible, however it was decided for only one step to be considered to simplify the data generated and for ease of synthesis realisation.

^{xix} The Scaffold Diversification Resource is a collection of compounds within the University of Birmingham with favourable medicinal chemical properties created for the purposes of synthesising diversity-based libraries of high-value chemical compounds for drug discovery.

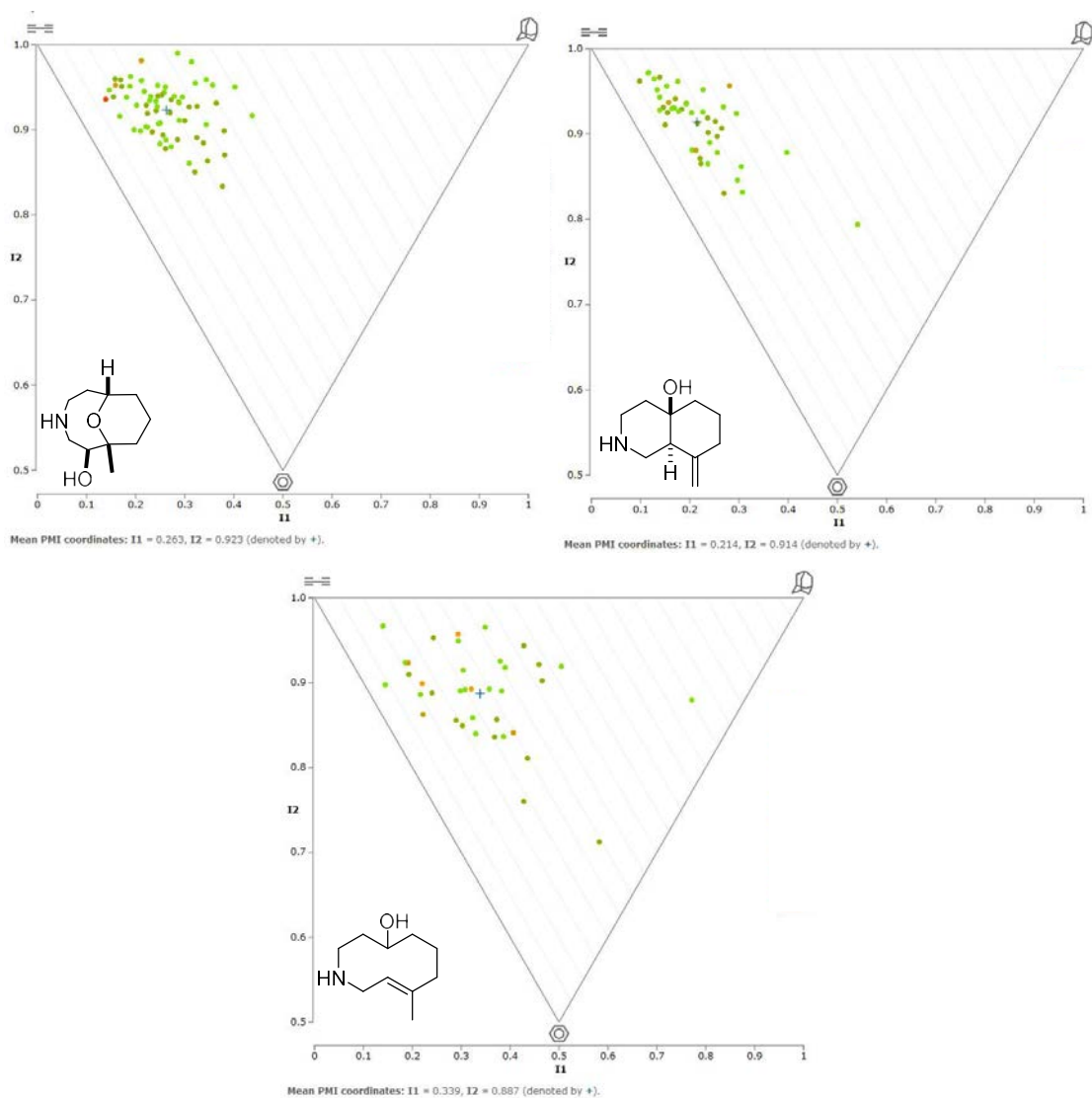


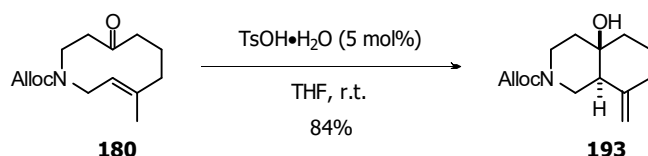
Figure 49 – Chemical space coverage of each of the virtual libraries. The corresponding parent scaffold is in the bottom left of the graph.

Following the generation of the three libraries *in silico*, compounds were selected for actual synthesis. To this end, fifteen compounds were selected from each of the three virtual libraries. The compounds selected were chosen based on a number of criteria; primarily they were chosen to maximise the spread of PMI co-ordinates, which were used as an analogy to chemical space coverage. Secondary criteria were considerations of the number of different functional groups that were to be incorporated into the realised libraries and the number of Murcko scaffolds that would be contained within them.

3.4 Synthesis of a screening library

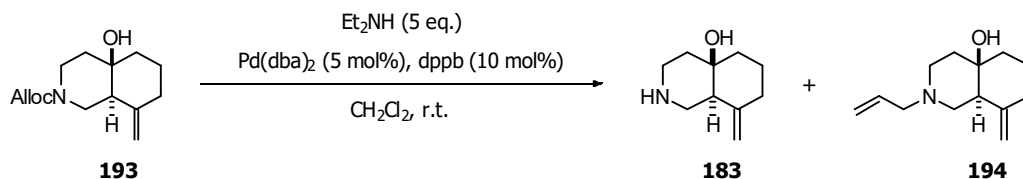
3.4.1 Synthesis of a compound library based on decalol scaffold **183**

Synthesis of decalol **193** was accomplished by treatment of keto-alkene **180** with TsOH•H₂O in THF in an 84% yield (Scheme 100).



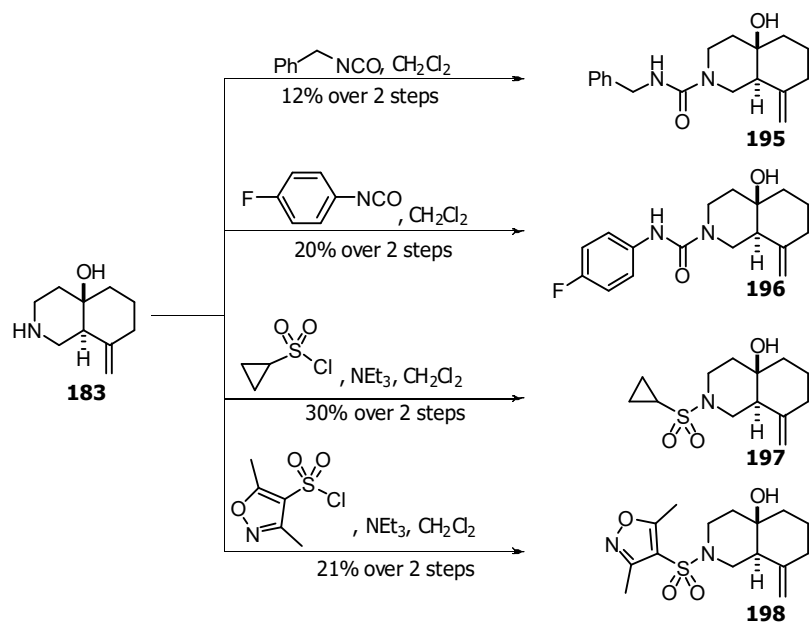
Scheme 100 – Synthesis of decalol **193** from keto-alkene **180**

With decalol **193** in hand, the next step was to deprotect the alloc carbamate. From concurrent work that was being carried out (see Section 3.4.2), it had been observed that the previously established Pd(PPh₃)₄/pyrrolidine conditions were not suitable for library synthesis. The yields obtained for the amine derivatisations were very low, as residual pyrrolidine competed with the generated free amine to react with the other component. Therefore, re-optimisation of the alloc cleavage was conducted and new conditions were found (see Section 3.4.2): Pd(dba)₂ (5 mol%), 1,4-bis(diphenylphosphino)butane (dppb) (10 mol%), Et₂NH (5 eq.) in CH₂Cl₂. Treatment of alloc carbamate **193** under these conditions successfully gave the desired amine **183**, although an accurate ratio with the undesired allyl amine **194** cannot be reported as the alkenyl resonances for the two products are coincident in the ¹H NMR spectrum of the crude reaction mixture (Scheme 101).



Scheme 101 – Synthesis of amine **181** and undesired side-product allyl amine **194**

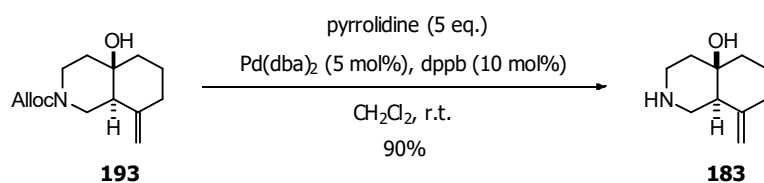
The solvent was removed from the reaction mixture on a rotary evaporator at a high temperature (> 60 °C) to remove the remaining Et₂NH. The residue was then directly submitted to derivatisation reactions (Scheme 102).



Scheme 102 – Synthesis of four derivatives of amine **183**

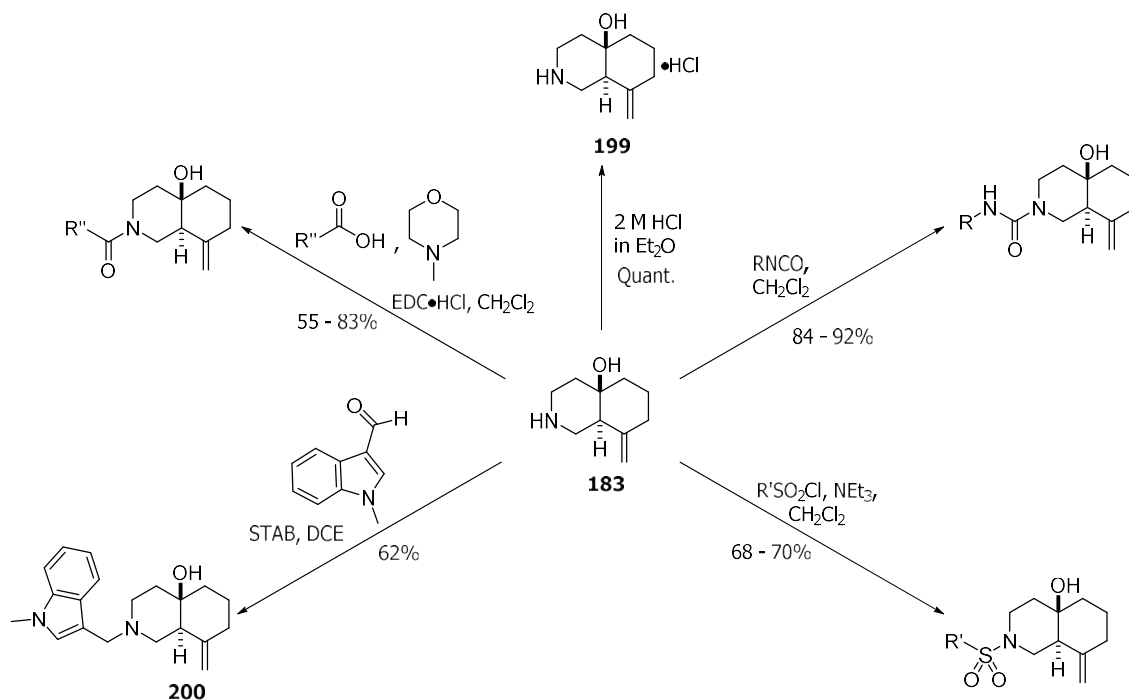
Ureas **195** and **196**, and sulfonamides **197** and **198** were synthesised from amine **183**. While all the reactions were successful, all four products were formed in low yield over two steps (12 – 30%). In each case, other products identified included allyl amine **194** and a derivative formed from the reaction of the derivatising agent with residual Et_2NH . The yields were unacceptably low for an efficient synthesis of a library of compounds. Therefore, it was decided to purify amine **183** before further derivatisation.

Since the alloc-cleavage product was now being purified, the nucleophile used in the alloc cleavage was changed back to pyrrolidine, as it was postulated that a higher yield would be achieved than with the less nucleophilic diethylamine (Scheme 103). Under these conditions, the desired amine **183** was isolated in 90% yield.



Scheme 103 – Optimised synthesis of amine **183**

With purified amine **183** in hand, a range of derivatisations were carried out on the scaffold to generate a small library of compounds (Scheme 104).



Scheme 104 – Synthesis of a library of decalols

Fifteen different compounds were synthesised, with five different functional groups installed. Unlike the low yields seen previously, much higher yields were obtained for the synthesis of sulfonamides and ureas (68–92%), showing the benefit of purifying amine **183** prior to derivatisation. Reductive amination was carried out using *N*-methylindole-3-carbaldehyde to generate amine **200** in 62% yield. Five amides were also generated using EDC as the coupling agent in a 55–83 % yield. Finally, the HCl salt of amine **183** was synthesised in quantitative yield by treating amine with HCl in Et₂O to give salt **199**.

Fifteen different compounds were successfully synthesised from scaffold **183** (Figure 50). The fifteen compounds contain five different linkage functionalities and 14 different Murcko scaffolds. The compounds were synthesised in yields ranging from 12 – 92%. A PMI plot of the library shows good shape diversity, with all of the products lying away from the rod-disc axis (Figure 51). The mean PMI co-ordinates are also similar to those of the *in silico* library (Figure 49); therefore, the fifteen compounds synthesised represent well the *in silico* library.

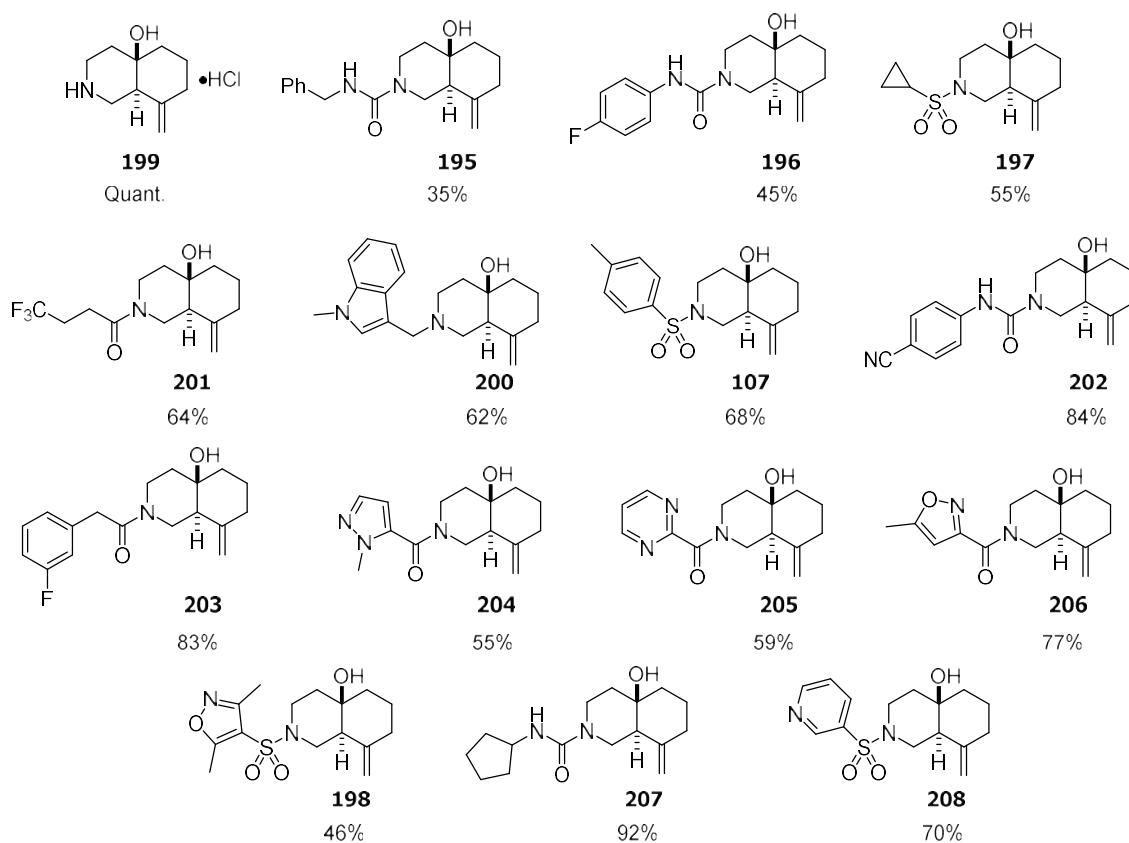


Figure 50 – All fifteen scaffolds synthesised from amine **183**.

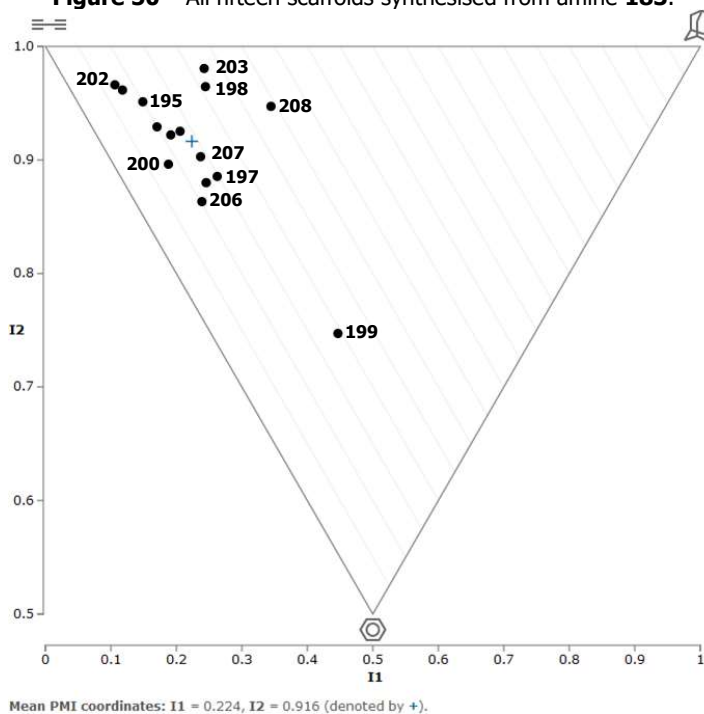
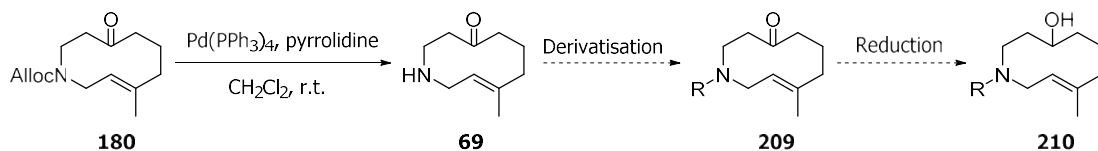


Figure 51 – PMI plot of the synthesised library of decalols

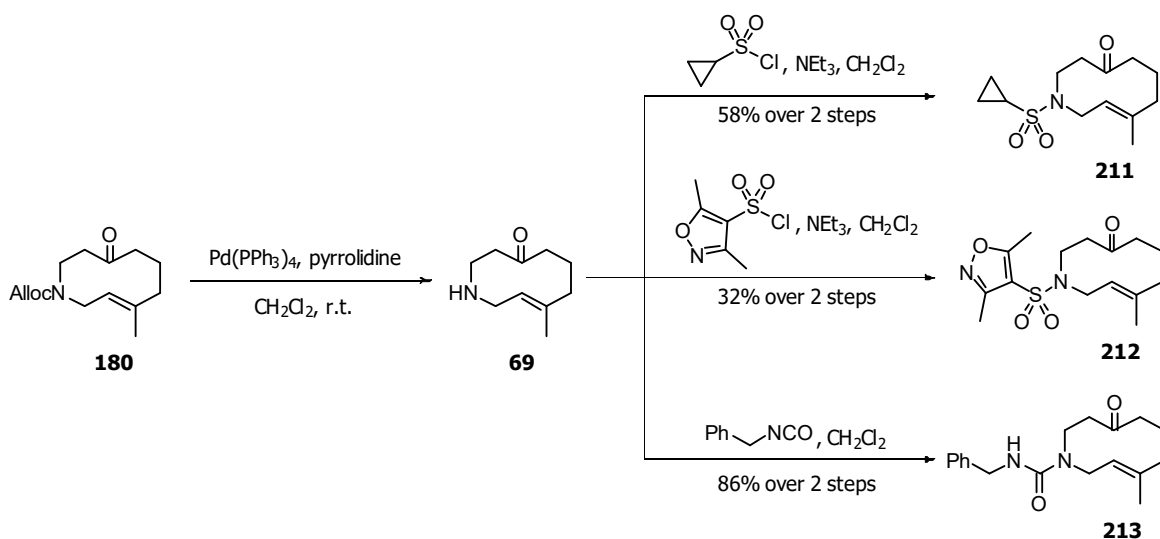
3.4.2 Synthesis of a compound library based on alcohol scaffold **187**

As the deprotection of keto-alkene **180** had already been optimised, it was initially planned to synthesise analogues of alcohol **187** by generation of amine **69**, followed by amine derivatisation and subsequent reduction of the ketone (Scheme 105).



Scheme 105 – Initial planned route to generate derivatives of alcohol **187**

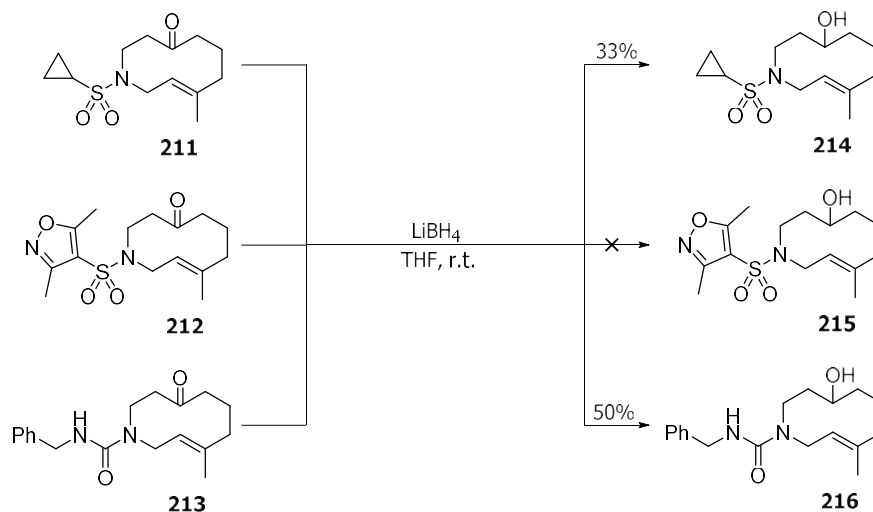
Amine **69** was synthesised using the optimised conditions (Section 3.2.3). The unpurified material was used directly for three different derivatisations (Scheme 106), all of which proceeded successfully, in 32 – 86% yield over the two steps. Urea **213**, however, was isolated alongside an impurity that was identified as triphenylphosphine oxide. Alternative column chromatography conditions failed to remove completely this impurity, highlighting the approach taken to library synthesis could present an issue if used for wholesale library assembly.



Scheme 106 – Synthesis of derivatives of amine **69**

To generate the respective alcohols, each derivative was treated with LiBH_4 in THF (Scheme 107). Alcohol **214** was formed in 33% yield, much lower than the 95% observed with the tosyl sulfonamide analogue **119**. Sulfonamide **212** degraded in the reaction, with no

identifiable products isolated. Ketone **213** was reduced to alcohol **216** in a moderate 50% yield. Overall, the results of the reduction were disappointing, with all reactions proceeding in $\leq 50\%$ yield or degrading.



Scheme 107 – Synthesis of derivatives of alcohol **187**

These results highlighted multiple problems with the route outlined in Scheme 105. First, the optimised route to amine **69** generated triphenylphosphine oxide as an impurity, which was difficult to remove. Second, ketone reduction proceeded in low yield. Therefore, to make the synthesis of a library of alcohols easier, the problems were tackled from two fronts: i) the deprotection of keto-alkene **180** was re-optimised to identify alternative Pd catalysts to $\text{Pd}(\text{PPh}_3)_4$ and ii) the alternative sequence of reactions, *i.e.* ketone reduction before alloc removal, was examined.

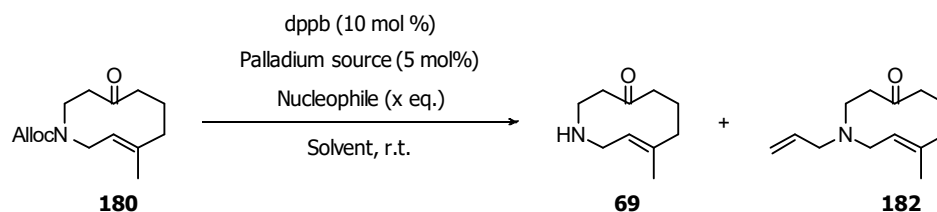
Re-optimisation of the alloc removal of keto-alkene **180**

Side-products from the reactions in Scheme 106 included triphenylphosphine oxide and the pyrrolidine analogues arising from reaction with the electrophile derivatisation agent. Therefore, it was decided to optimise the alloc cleavage with a view to identifying a different nucleophile that was easier to remove, and a different catalyst, which would not produce triphenylphosphine oxide as an oxidation by-product.

Within the previous optimisation study (Section 3.2.3) attention had focused on optimising the nucleophile additive. However, only carbon- and nitrogen-based nucleophiles had been considered. Adapting the work of Genet *et. al*/a sulfur-based nucleophile and another nitrogen-

based nucleophile were trialled, alongside alternative palladium sources (Table 8).²¹⁶ Dppb was chosen as the phosphine ligand, as the oxidation by-product would be more easily removed by column chromatography.

Table 8 – Re-optimisation of the alloc removal^[a]



Entry	Nucleophile	Eq.	Palladium Source	Solvent	Outcome
1	thiosalicylic acid	2	Pd ₂ (dba) ₃	THF	Unidentifiable product
2	thiosalicylic acid	2	Pd ₂ (dba) ₃	CH ₂ Cl ₂	Mixture of keto-alkene 69 and unknown product
3	thiosalicylic acid	2	Pd(dba) ₂	THF	Mixture of keto-alkene 69 and unknown product
4	thiosalicylic acid	2	Pd(dba) ₂	CH ₂ Cl ₂	Mixture of keto-alkene 69 and unknown product
5	thiosalicylic acid	2	Pd(PPh ₃) ₄	THF	Mixture of keto-alkene 69 and unknown product
6	Et ₂ NH	5	Pd(dba) ₂	THF	60:40 69:182 ^[b]
7	Et ₂ NH	5	Pd(dba) ₂	CH ₂ Cl ₂	67:33 69:182 ^[b]
8	Et ₂ NH	5	Pd(PPh ₃) ₄	CH ₂ Cl ₂	62:38 69:182 ^[b]

[a] All solvents were degassed prior to use. [b] Determined by integration of the alkenyl resonances in the ¹H NMR spectrum of the crude material prior to purification by column chromatography.

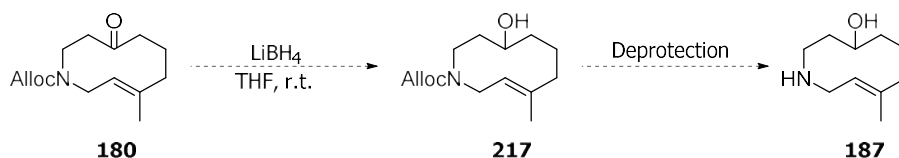
Thiosalicylic acid was used as a sulfur-based nucleophile, alongside either Pd₂(dba)₃ or Pd(dba)₂ as the palladium(0) sources (entries 1-4, Table 8). The attraction of using thiosalicylic acid was that it could be separated from the desired amine **69** by a base wash. Unfortunately, in all attempts to use thiosalicylic acid, the reaction failed to go to completion, even after extended reaction times (17 h). Attention therefore turned towards identifying an alternative nitrogen nucleophile.

Et₂NH has been used as an effective nucleophile in alloc removals.²¹⁶ The by-product, allyldiethylamine, is volatile and therefore more easily removed compared to the *N*-allyl pyrrolidine by-product generated under the previous optimised conditions. The boiling point of diethylamine 55 °C, lower than that for pyrrolidine, which boils at 87 °C, making it easier to remove the excess amine prior to derivatisation.

Use of Et₂NH was successful, albeit with a lower ratio of amine **69**: allyl amine **182** observed than with pyrrolidine as the nucleophile (entries 6-8, Table 8). A combination of Pd(dba)₂ and dppb proved to be a more effective catalytic system than Pd(PPh₃)₄ in CH₂Cl₂. Therefore, the final optimised conditions were Pd(dba)₂ (5 mol%), dppb (10 mol%), Et₂NH (5 eq.) in CH₂Cl₂. These conditions were ultimately not used on keto-alkene **180** for derivatisation purposes, as it was decided that derivatisation of amine **69** followed by reduction of the ketone was too inefficient a route. However, they were used for the derivatisations of other scaffolds (see Sections 3.4.1 and 3.4.4).

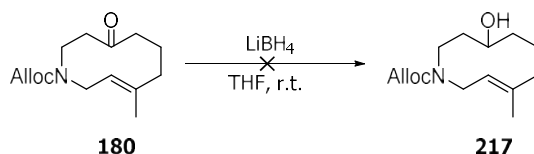
Reduction of keto-alkene **180**

Synthesising a library of alcohols starting from keto-alkene **180**, was deemed inefficient in terms of steps, as every final compound would require three reactions starting from keto-alkene **180** to be successfully synthesised. The number of steps could be effectively halved if alcohol **217** were synthesised prior to alloc removal (Scheme 108).



Scheme 108 – Planned synthetic route to generate amine **187**

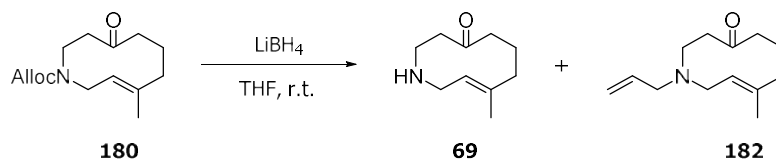
It was thought that the same reduction conditions that generated alcohol **119** could be used (see Section 2.3.2); however, no product was generated under these conditions and no identifiable side-products were isolated after column chromatography (Scheme 109).



Scheme 109 – Attempted synthesis of alcohol **215**

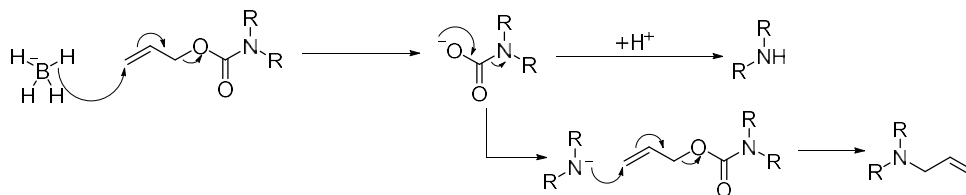
The reaction was repeated and closely monitored. Analysis of the ¹H NMR spectrum of the reaction mixture after work-up revealed no evidence for ketone reduction. Instead, the alloc group had been removed, giving amine **69** in a 17:3 ratio with allyl amine **182** (Scheme 110). Alloc cleavage has previously been observed using NaBH₄ or LiBH₄ in conjunction with Pd(PPh₃)₄.²¹⁹ To ascertain whether palladium residues were the cause of the observed reaction

outcome, all glassware was cleaned with 6 M HCl_(aq) prior to the reaction to ensure any palladium residues had been removed; however, the same result was observed.



Scheme 110 – Unexpected outcome from the attempted reduction of keto-alkene **180**

Cleavage of the alloc carbamate under these conditions was unexpected. No precedent for the observed outcome has been reported within the literature without the assistance of a metal catalyst. If the reducing agent were strong enough to attack the alloc carbamate, the expected outcome would be reduction of the carbamate to a methyl group, as is observed for the reduction of Boc groups with LiAlH₄.²²⁵ A potential mechanistic explanation of the observed outcome is shown in Scheme 111. Borohydride attack into the allyl could cause an S_N2 like mechanism, with the loss of propene and generation of a carbamate anion, which rapidly decarboxylates to give an amine anion. The amine anion could then either protonate, to give the observed amine, or attack into another alloc functional group, generating the observed allyl amine. While there is no direct precedent for this reaction, Bell and Brown have previously observed an S_N2 reaction between an alkyl halide and sodium borohydride.²²⁶

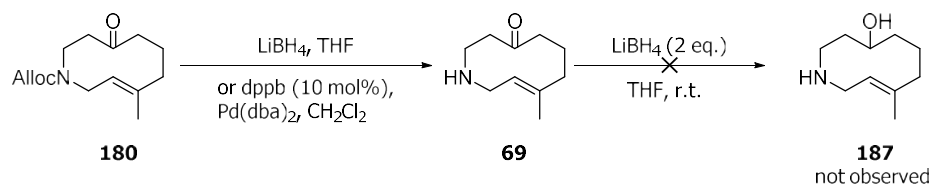


Scheme 111 – Potential mechanistic pathway to form amine **69** and allyl amine **182**

To assess whether this reaction was more broadly applicable, decalol **193** was subjected to the same conditions. No reaction was observed.

Brown and Narasimhan had previously shown that the addition of sub-stoichiometric amounts of LiEt_3BH to a mixture of LiBH_4 and an ester aids the reduction of the ester.²²⁸ However, nothing identifiable was recovered when LiBEt_3H was used as an additive in the reduction of keto-alkene **180** to alcohol **217** (entry 8, Table 9). Use of LiBEt_3H directly (entry 9, Table 9) produced a similar outcome.

As reduction of the ketone in the presence of the alloc carbamate was found to be difficult, an alternative pathway was also considered in which the alloc protecting group was removed first (Scheme 112). Amine **69** was generated by either the previously outlined Pd(0)-catalysed conditions (see Table 8) or by treatment of ketone **180** with LiBH_4 and subsequent work-up. In either case, the compound was used without further purification and subjected to the original reaction conditions (LiBH_4 , THF) to generate alcohol **187**. In both cases the reaction led to extensive decomposition.



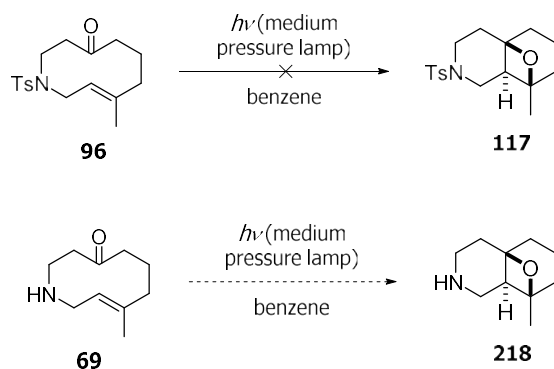
Scheme 112 – Attempted synthesis of amine **187**

In summary, it was not possible to synthesise a library of alcohols in an efficient manner. Amino alcohol **187** was unable to be accessed, while synthesis of a library of alcohols *via* the keto-alkene suffered from low yields and unpredictability about which derivatives would be stable enough to endure the subsequent reduction conditions.

3.4.3 Synthesis of a compound library based on oxetane scaffold **218**

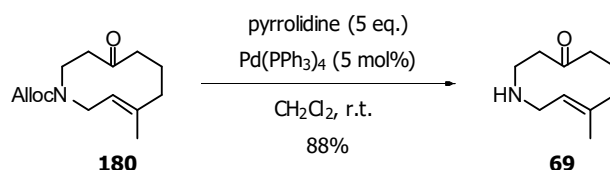
While it had been decided that generation of a library of alcohols *via* keto-alkene **180** would not be viable due to the inefficiency of the approach, the generation of amine **69** presented an opportunity to re-visit the synthesis of a scaffold that had previously been unsuccessful.

Previously, the synthesis of oxetane **117** had been attempted (see Section 2.3.2) but was unsuccessful, which we hypothesised was a result of the tosyl group absorbing light and causing degradation of the molecule (Scheme 113). Given amine **69** does not contain a tosyl group, it was theorised that oxetane **218** may now be accessible.



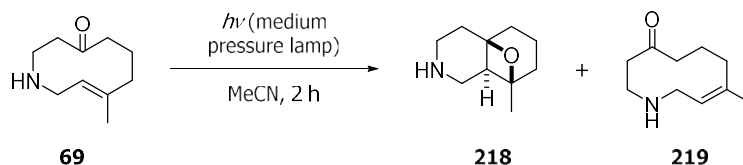
Scheme 113 – Previous and planned synthesis of an oxetane-containing scaffold

Keto-alkene **180** was subjected to the initially optimised alloc cleavage conditions (see Section 3.2.3) and then purified by column chromatography to give amine **69** in an 88% yield (Scheme 114).



Scheme 114 – Synthesis of amine **69** using the initially optimised conditions

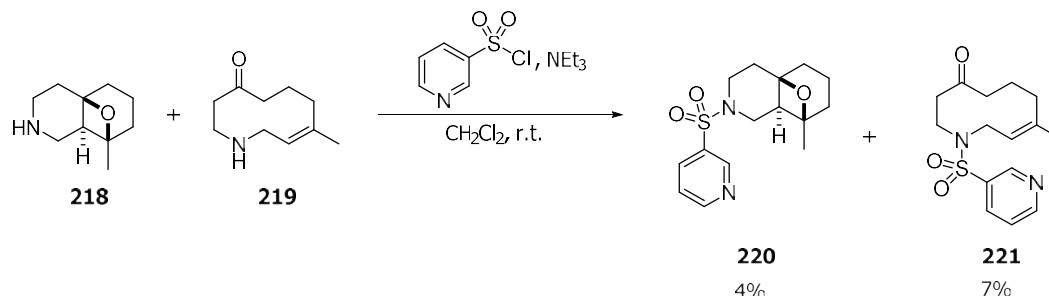
With amine **69** in hand, a Paternò-Büchi reaction was conducted, using similar conditions to those described in Section 2.3.2 (Scheme 115); the solvent was changed to acetonitrile for toxicity reasons, otherwise the conditions were identical. After 2 h of irradiation, the reaction was complete. The ¹H NMR spectrum of the material after removal of the solvent revealed at least two different products, the desired oxetane **218** and what was postulated to be (*Z*)-keto-alkene **219**. The unprotected amines were inseparable, so it was decided to derivatise both amines and then separate the products post-derivatisation.



Scheme 115 – Synthesis of oxetane **218** along with by-product (*Z*)-keto-alkene **219**

Amines **218** and **219** were converted to sulfonamides **220** and **221** by treatment with pyridine-3-sulfonyl chloride and NEt₃ (Scheme 116). The respective yields were 7% for keto-

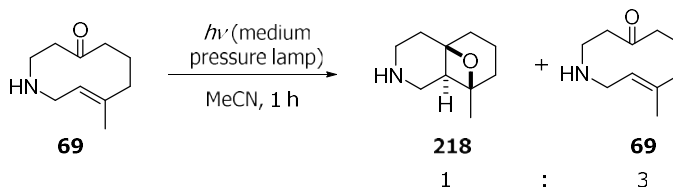
alkene **221** over two steps and 4% for oxetane **220** over two steps with the structures of the two compounds confirmed by 2D NMR experiments. Pleasingly, oxetane **218** had been successfully synthesised, albeit in a low yield.



Scheme 116 – Synthesis of oxetane **220** and keto-alkene **221**

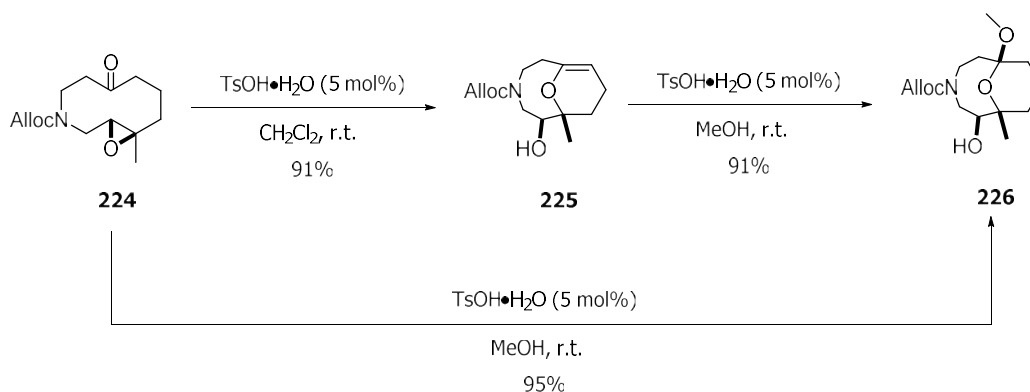
To try and improve the yield, the Paternò-Büchi reaction was repeated, with aliquots of the reaction mixture removed for analysis. Aliquots were taken every 30 minutes with the reaction proceeded rapidly. After 3 h the reaction material had completely degraded with no discernible product observed. It was theorised that the constant switching on and off of the lamp adversely affected the outcome of the reaction.

To try and obtain desired amine **218**, the reaction was run for 1 h with the lamp left constantly on (Scheme 117). Instead of the previously observed *E/Z* isomerisation (Scheme 115), amine **218** and (*E*)-keto-alkene **69** were the observed products, along with degradation products, in a ratio of ~ 1:3 amine **218**: amine **69** as determined by integration of a single resonance in the ¹H NMR spectrum of the material after the solvent had been removed.



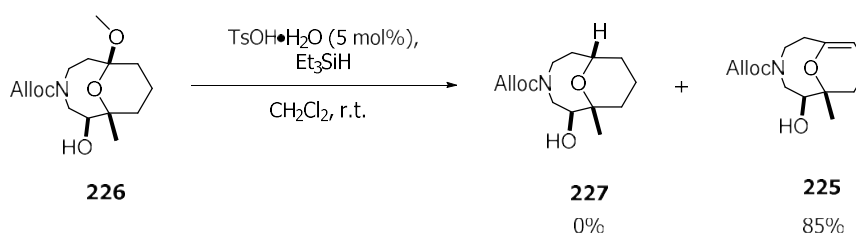
Scheme 117 – Modified synthesis of amine **218**

To ascertain whether the yield had been improved by modifications to the Paternò-Büchi reaction, the reaction material was converted to sulfonamides **222** and **223** by treatment with (4-fluorophenyl)methanesulfonyl chloride and NEt₃ (Scheme 118). The respective yields were 10% for keto-alkene **223** over two steps and 4% for oxetane **222** over two steps showing



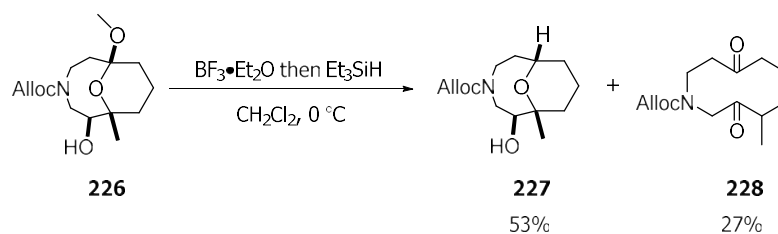
Scheme 120 – Synthesis of acetal **226** is possible *via* either a one or two step synthesis.

Following the successful synthesis of acetal **226**, the next aim was to generate alloc-protected ether scaffold **227**. Initially, the synthesis was attempted using the same conditions that had proved successful on the tosyl analogue (see Section 2.3.4) (Scheme 121). However, the only product generated was enol ether **225**.



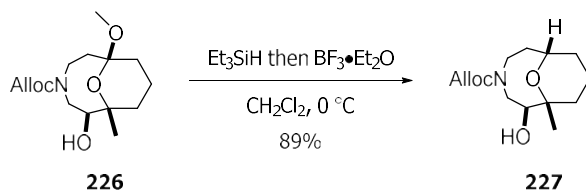
Scheme 121 – Attempted synthesis of ether **227** generated only enol ether **225**.

This result had been observed before in the attempted allylation of acetal **154** (see Section 2.3.4). Therefore, the same solution was applied, which was to use $\text{BF}_3\cdot\text{Et}_2\text{O}$ as an alternative acidic reagent to achieve the desired outcome. Treatment of acetal **226** with $\text{BF}_3\cdot\text{Et}_2\text{O}$ and triethylsilane generated the desired ether **227** in 53% yield alongside a second product, which was subsequently identified as diketone **228**, which was isolated in 27% yield (Scheme 122).



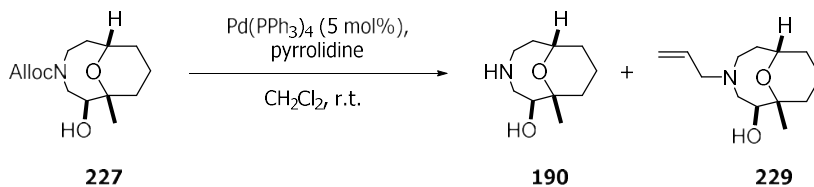
Scheme 122 – Synthesis of ether **227** and by-product diketone **228**

It was hypothesised that the addition of $\text{BF}_3 \cdot \text{Et}_2\text{O}$ before the addition of triethylsilane had led to the formation of diketone **228**. Therefore, the order of addition was reversed, with $\text{BF}_3 \cdot \text{Et}_2\text{O}$ added second. This modification eliminated the formation of the diketone side-product, with ether **227** synthesised in an 89% yield (Scheme 123).



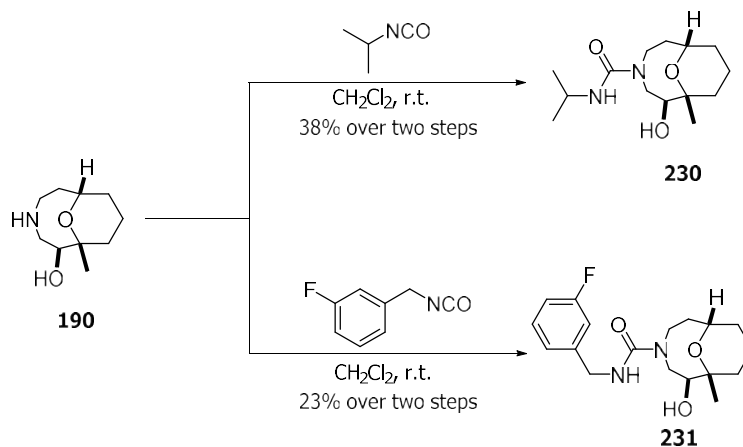
Scheme 123 – Synthesis of exclusively ether **227**

With ether **227** in hand, the final steps to realise a compound library were deprotection of the amine and subsequent derivatisation. Ether **227** was deprotected using the initial conditions of $\text{Pd}(\text{PPh}_3)_4$ and pyrrolidine (Scheme 124). These conditions successfully gave the desired amine **190**, although with the undesired allyl amine **229** in an unknown ratio as all possible diagnostic resonances for the two products are coincident in the ^1H NMR spectrum of the crude reaction mixture.



Scheme 124 – Synthesis of amine **188** and unwanted side-product allyl amine **229**

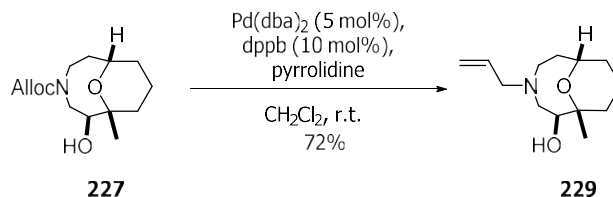
The solvent was removed from the reaction mixture on a rotary evaporator at a high temperature ($> 60\text{ }^\circ\text{C}$) to remove the remaining pyrrolidine. The residue was then directly submitted to derivatisation reactions (Scheme 125).



Scheme 125 – Synthesis of ureas **230** and **231**

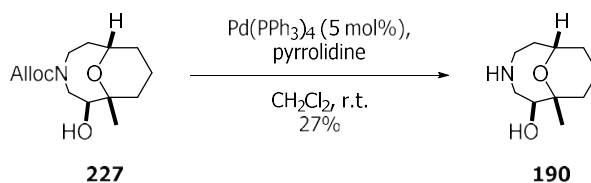
Ureas **230** and **231** were successfully synthesised, albeit in low yields of 38% and 23%, respectively. Due to these low yields seen with this route and taking into account the reaction outcomes that had previously been seen (see Sections 3.4.1 and 3.4.2), it was decided to switch to a reaction pathway where amine **190** was purified before its use in derivatisation reactions.

Deprotection of ether **227** was first attempted using the second optimised conditions of $\text{Pd}(\text{dba})_2$, dppb and pyrrolidine (Scheme 126); however, the only isolated product was allyl amine **229**, which was recovered in a 72% yield.



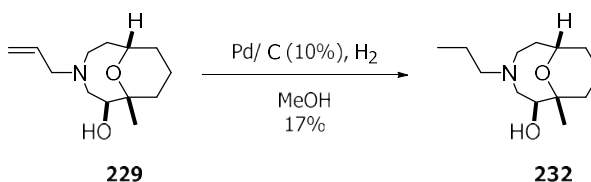
Scheme 126 – Accidental synthesis of allyl amine **229**

It was postulated that the poor outcome was due to the use of $\text{Pd}(\text{dba})_2$ over $\text{Pd}(\text{PPh}_3)_4$, so the reaction was repeated, with $\text{Pd}(\text{PPh}_3)_4$ (Scheme 127). The desired amine **190** was isolated in 27% yield after purification, which was very disappointing when compared to the yields seen with the other deprotections. Unfortunately, time constraints meant that no further optimisation of the deprotection could be carried out.



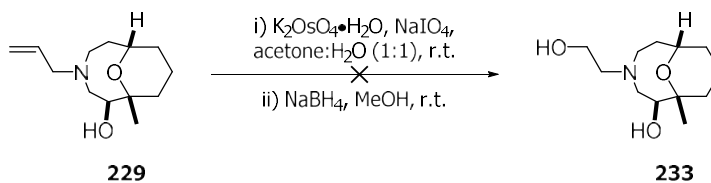
Scheme 127 – Synthesis of amine **190** using the second optimised deprotection conditions

While allyl amine **229** was not submitted to the final library due to its potential oxidation by P450 enzymes, it could act as a progenitor scaffold for further scaffold generation. Allyl amine **229** was reduced using Pd/C and H₂ to generate propyl amine **232** in 17% yield (Scheme 128).



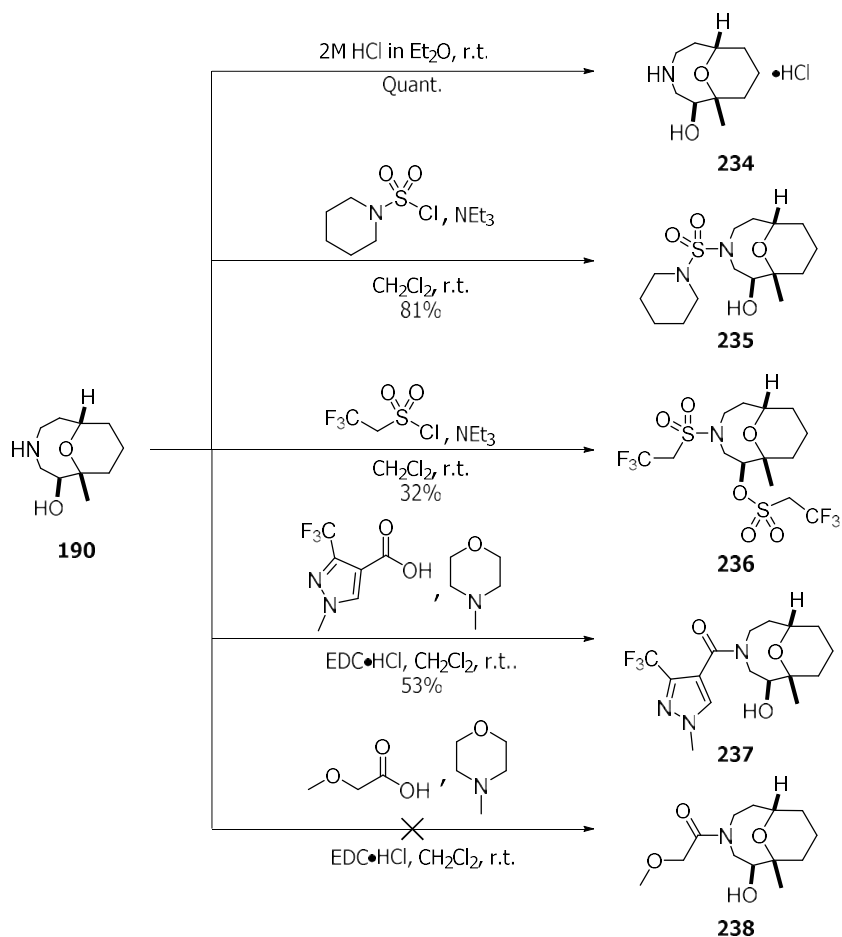
Scheme 128 – Synthesis of propyl amine **232** by reduction of allyl amine **229**

Attempted oxidative cleavage of allyl amine **229** to generate alcohol **233** using potassium osmate and sodium periodate was conducted by adapting a procedure from Trost and Li, led to no identifiable products (Scheme 129).²³⁰ No further manipulations of allyl amine **229** were attempted.



Scheme 129 – Attempted synthesis of alcohol **233** from allyl amine **229**

Returning concentration to amine **190**, a variety of derivatisations were conducted. Unfortunately, due to limitations in the quantity of material, a full complement of scaffolds could not be synthesised. Taking into account the scaffolds already synthesised and the initial *in silico* library, as diverse a representation of the *in silico* library as possible was attempted to be formed (Scheme 130).



Scheme 130 – Derivatisations of amine **190**

The synthesis of five different compounds was attempted. The HCl salt of amine **190** was synthesised in quantitative yield by treating amine with HCl in Et₂O to give salt **234**. Sulfamide **235** was generated in 81% yield using piperidine-1-sulfonyl chloride and triethylamine. Sulfonamide **236** was accidentally generated as the only isolable product in a 32% yield due to addition of a super-stoichiometric amount of 2,2,2-trifluoroethanesulfonyl chloride. Amide **237** was generated in 53% yield using EDC as the coupling agent. Generation of amide **238** was also attempted but resulted in degradation.

In conclusion, eight different compounds were successfully synthesised from scaffold **190** (Figure 52). The eight compounds contain five different linkage functionalities and five different Murcko scaffolds. A PMI plot of the library shows good shape diversity, with all scaffolds lying away from the rod-disc axis (Figure 53). The mean PMI co-ordinates are also

similar to those of the *in silico* library (Figure 49), therefore, the eight compounds synthesised represent well the *in silico* library.

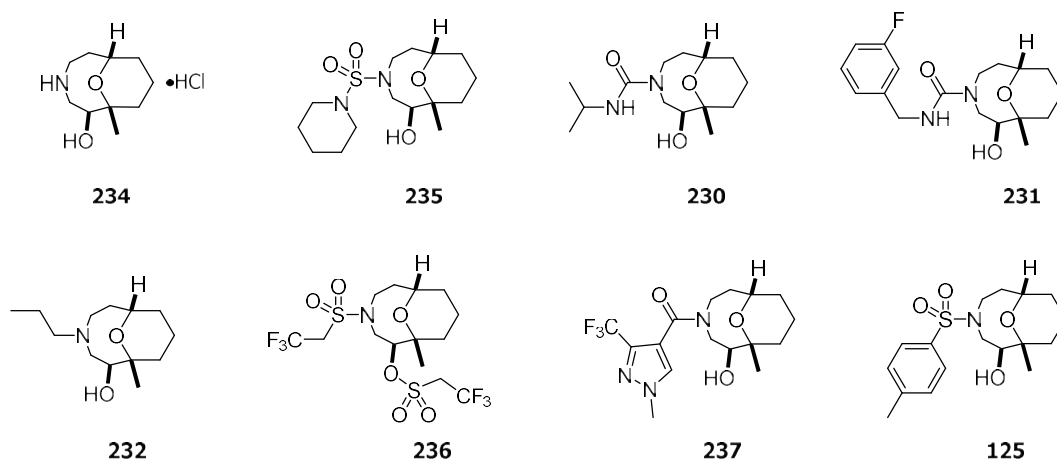


Figure 52 – Eight ether scaffolds synthesised for the library

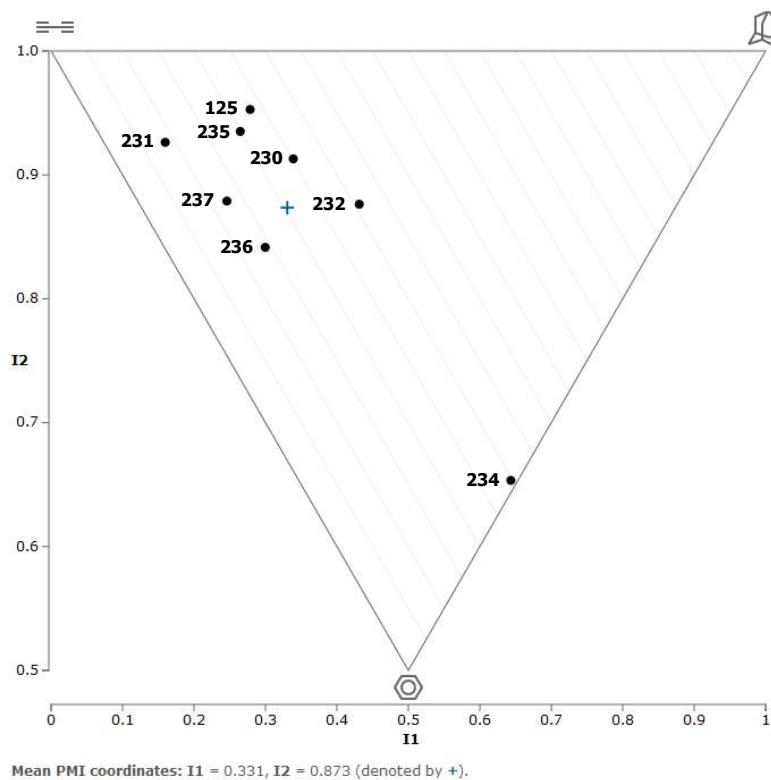


Figure 53 – PMI plot of the synthesised library of ethers

3.5 Summary and Conclusions

Deprotection of the amine of tosylated keto-alkene **96** was shown to be non-viable for the overall aim of construction of a library of scaffolds. Alternative reaction pathways, which used a nosyl protecting group or switched the amine for an ether were also shown to be non-viable for this purpose due to their low yields. Use of an alloc protecting group allowed for the synthesis of keto-alkene **180** in 40% overall yield over seven steps. It was then demonstrated that the alloc carbamate in keto-alkene **180** could be selectively deprotected in high yield, enabling its use as a progenitor scaffold for a compound library.

Chemoinformatic analysis and application of a series of filters enabled the selection of three different scaffolds, namely decalol **183**, alcohol **187** and ether **190**, as starting points for generating a small library of diverse compounds.

Alloc protected decalol **193** was synthesised. After alloc removal, derivatisation of the resulting amine afforded fifteen different analogues, encompassing five different functionalities and fourteen different Murcko scaffolds. The synthesised library was found to be a good representation of the *in silico* library that was generated using LLAMA.

Derivatives of alcohol **187** were originally accessed *via* deprotection of keto-alkene **180**, amine derivatisation, and reduction of the ketone; however, the route proved to be capricious, with low yields. A more general route, where alcohol **187** was generated before derivatisation was attempted, but resulted in alloc removal instead of the expected ketone reduction.

An alternative scaffold, oxetane **218**, was synthesised using a Paternò-Büchi reaction, but library generation was hampered by low yields of the oxetane scaffold.

Ether **227** was synthesised and successfully deprotected. Derivatisation of the resulting amine afforded eight analogues, encompassing five different functionalities and five different Murcko scaffolds.

Overall, thirty different compounds, representing 26 different Murcko scaffolds, were submitted to the compound library (Figure 54). They cover a wide range of functionality and occupy a large range of chemical space as measured by a PMI plot (Figure 55). A small but diverse compound library has therefore been successfully synthesised.

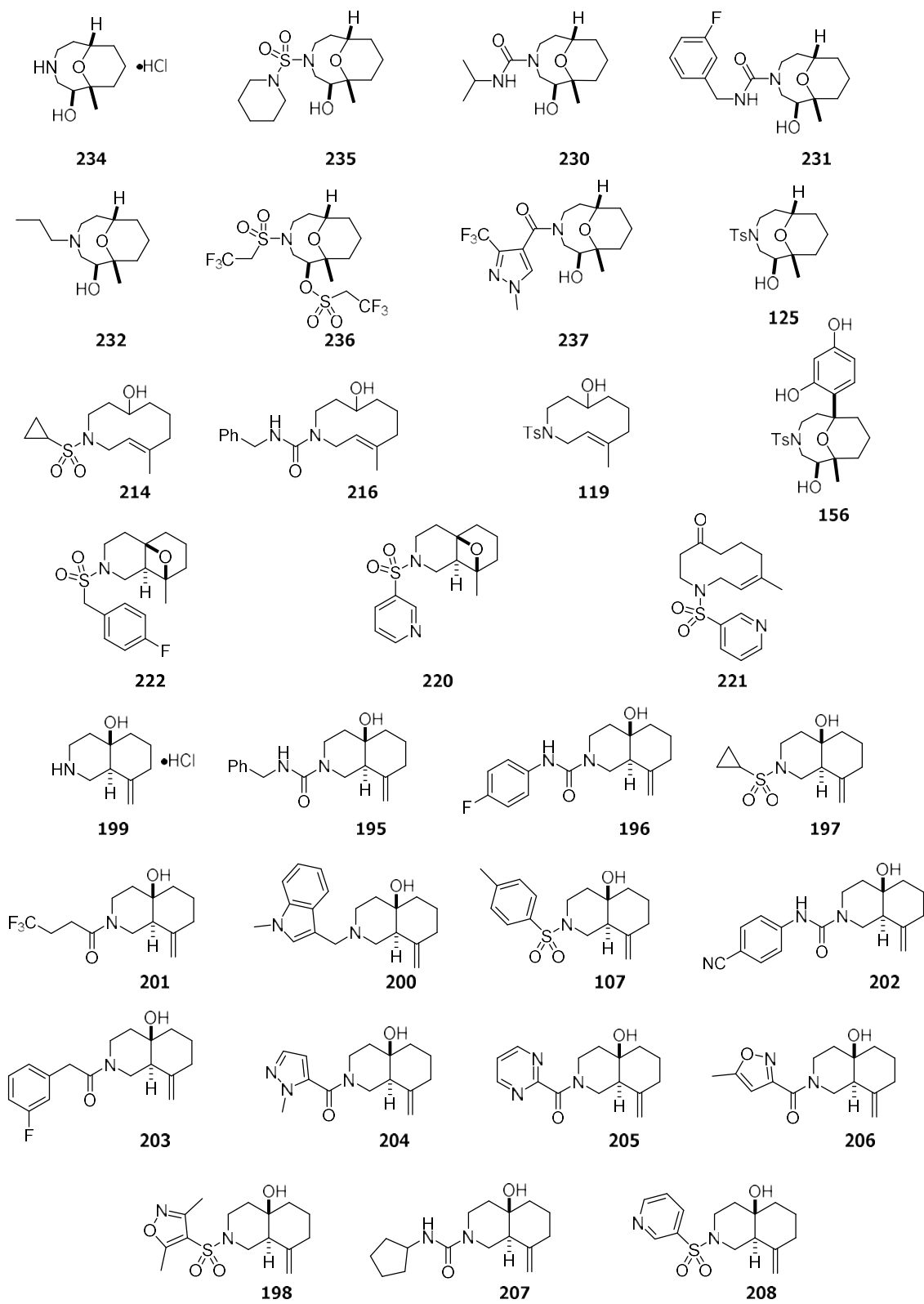


Figure 54 – All scaffolds submitted to the compound library

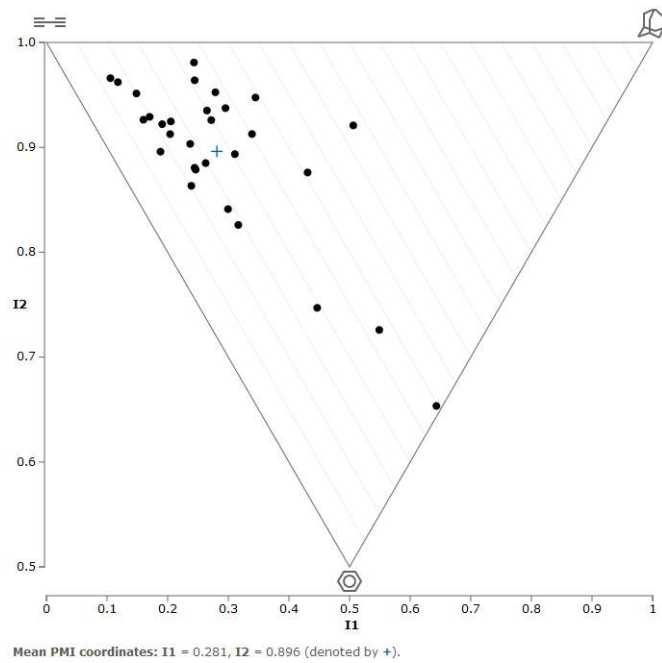


Figure 55 – PMI plot of all scaffolds submitted to the compound library.

Chapter Four: Summary and Future Work

4.1 Summary

Our original aim was to synthesise a library of medium-sized rings, which could then be derivatised to realise a compound library based on the principles of diversity-oriented synthesis.

Chapter Two documented the synthesis of the progenitor scaffold, keto-alkene **96**, which was transformed in turn into a further eighteen different medium-sized ring scaffolds, all of which were novel scaffolds. These scaffolds could be broadly grouped into four different categories, showing the diverse nature of the chemistry that we were able to achieve.

Chapter Three documented the attempted tosyl removal of keto-alkene **96**, which proved unsuccessful. After subsequent scaffold development, keto-alkene **180** containing an alloc carbamate was developed as an alternative candidate and successfully deprotected using Pd(0) catalysis.

Cheminformatic analysis and a series of filters allowed for the selection of three different scaffolds for derivatisation. Derivatisation of decalol **183** was successful and produced a library of fifteen analogues. Derivatisation of ether **190** produced eight analogues, while derivatisation of alcohol **187** was not possible.

Overall, a library of thirty compounds, comprising of a range of functionality and 26 different Murcko scaffolds, was synthesised and submitted to the Haworth Chemically-Enabled Compound Collection, a target-agnostic screening library being developed within the University of Birmingham.

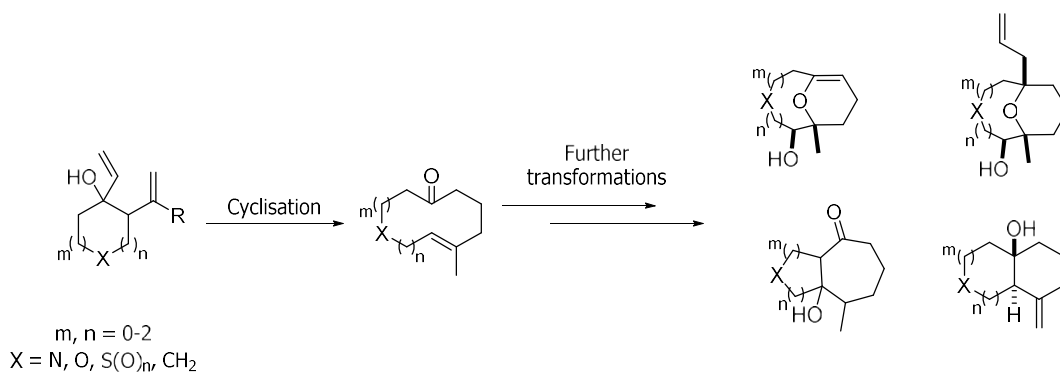
4.2 Future Work

Looking forward, a different protecting group is necessary for further library generation. Whilst the alloc protecting group can be removed, the deprotection reaction has proved capricious, limiting the number of compounds that could be synthesised. Further optimisation would be advisable if this protecting group is retained in future studies, for example studying the use of silanes instead of amines as the nucleophile present in the deprotection step.²³¹ The foremost candidate as an alternative protecting group is the carboxybenzyl (Cbz) group, which can be removed by hydrogenolysis.

A different amine protecting group may also enable the facile synthesis of alcohol **187** or oxetane **218**, two scaffolds which we were unable to synthesise in high yields although these reactions warrant further optimisation. Oxetane **218**, for example, could also be synthesised in higher yields by exploring different irradiation methods, such as a low-pressure lamp, which unfortunately we did not have access to.

Further work needs to be conducted on the 5,7-fused ring systems, which currently cannot be made diastereoselectively. A full screen of temperature, solvent and reagents should hopefully enable a single diastereomer to be synthesised, which in turn would allow a candidate from the fourth group of scaffolds to be used for compound library assembly.

Ideally, the methodology and transformations developed throughout this project would be generalised across a range of medium-sized rings, rather than just the single keto-alkene that was used within this project (Scheme 131).



Scheme 131 – Concept of a generalised version of the designed route which would enable access to a variety of different Murcko scaffolds.

Chapter Five: Experimental

5.1 General Experimental Details

Unless stated otherwise, all reactions were carried out in oven-dried glassware under an argon atmosphere using anhydrous solvents. Anhydrous THF, toluene and CH_2Cl_2 were collected from a PureSolv™ solvent purification system and stored over 3 Å molecular sieves, which were activated by heating at 250 °C under high vacuum (< 2 mbar) for at least 6 h prior to use following a procedure by Williams *et al.*²⁰¹ All other solvents were dried over 3 Å molecular sieves, which were activated by heating at 250 °C under high vacuum (< 2 mbar) for at least 6 h prior to use. All other reagents and solvents were purchased from commercial suppliers and used without further purification unless stated otherwise. Room temperature refers to a temperature range of 17–25 °C. Reaction temperatures of 0 °C were maintained using an ice-water bath and temperatures below 0 °C were maintained using an acetone-dry ice bath.

Reaction progress was monitored by thin-layer chromatography (TLC), which was performed on Merck silica gel 60 F₂₅₄ plates. Developed plates were visualised under UV irradiation (254 nm), followed by staining with either potassium permanganate, vanillin or ninhydrin dip. Flash column chromatography was performed using silica gel (Aldrich Silica Gel 60, 230-400 mesh, 40-63 µm) and the indicated eluent. All solutions are aqueous and saturated unless stated otherwise.

The concentration of vinylmagnesium bromide was determined by titration with menthol and phenanthroline, following a procedure published by Lin *et al.*²³² The concentration of SmI_2 was determined by titration with iodine, following a procedure published by Szostak *et al.*²³³

Degassing of solvents was carried out by passing a stream of argon through the bulk solvent for 10 min. When degassed solvents were to be transferred, the syringe was purged three times with argon before withdrawal of liquid into the syringe.

¹H-NMR, ¹³C-NMR and ¹⁹F-NMR spectra were recorded in commercially available deuterated solvents on a Bruker AVIII 300 (¹H = 300 MHz), AVIII 400 (¹H = 400 MHz, ¹³C = 101 MHz), AVANCE NEO 400 (¹H = 400 MHz, ¹³C = 101 MHz) or AVANCE NEO 500 (¹H = 500 MHz, ¹³C = 126 MHz) spectrometer. Variable temperature NMR studies were carried out using a CryoProbe Prodigy BBFO-500 MHz (−40 °C to +80 °C). Those spectra recorded in chloroform-*d* were calibrated using the solvent resonance, $\delta_{\text{H}} = 7.26$ ppm and $\delta_{\text{C}} = 77.16$ ppm. Those spectra recorded in acetone-*d*₆ were calibrated using the solvent resonance, $\delta_{\text{H}} = 2.05$ ppm and $\delta_{\text{C}} =$

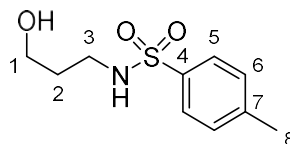
29.84 ppm. Those spectra recorded in methanol- d_4 were calibrated using the solvent resonance, $\delta_H = 3.31$ ppm and $\delta_C = 49.00$ ppm. Chemical shifts are reported in ppm and coupling constants in Hz, to the nearest 0.1 Hz. The following abbreviations are used to describe the multiplicity of resonances in 1H NMR spectra: s (singlet), d (doublet), t (triplet), q (quartet) and m (multiplet). Stack is used to describe resonances of two or more different protons which are coincident. The resonances for 1,4-disubstituted aromatics sometimes appear as doublets, other times as more complex forms. These resonances, which make up an AA'BB' system in the spectrum, are reported throughout as a range and assigned as "AA' of AA'BB' " and "BB' of AA'BB' ", irrespective of their appearance. Proton-decoupled ^{13}C -NMR spectra were recorded using the PENDANT pulse sequence and/or the UDEFT pulse sequence. Proton and carbon assignments were determined either on the basis of unambiguous chemical shift or coupling pattern, by patterns observed in 2D NMR experiments or by analogy with fully interpreted spectra for related compounds. NOESY experiments were used to determine relative stereochemistry when necessary. The numbering of compounds for NMR assignment is arbitrary.

Infrared spectra were recorded on a Perkin-Elmer Spectrum 100 FTIR spectrometer. Wavelengths (ν) are reported in cm^{-1} . ASAP and EI mass spectra were recorded on a VG ZabSpec magnetic sector mass spectrometer and ESI mass spectra were recorded on a Micromass LCT time of flight mass spectrometer. High-resolution mass spectrometry on all instruments was run with a tolerance of 5.0 ppm and calculated to find a monoisotopic mass.

Melting points were measured with a Gallenkamp melting point apparatus with an open capillary.

5.2 Synthetic Procedures

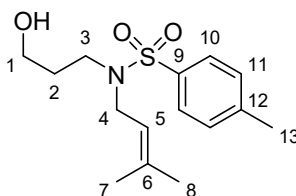
N-(3'-Hydroxypropyl)-4-methylbenzenesulfonamide (**74**)



NEt₃ (1.21 mL, 8.67 mmol) was added to a solution of 3-amino-1-propanol (0.500 g, 6.67 mmol) in CH₂Cl₂ (15 mL) and the resulting solution was cooled to 0 °C. A solution of TsCl (1.40 g, 7.33 mmol) in CH₂Cl₂ (10 mL) was added dropwise over 1 min and the resulting solution was stirred at 0 °C for 1 h. The reaction mixture was then washed sequentially with HCl_(aq) (1 M, 20 mL), H₂O (20 mL) and brine (20 mL). The organic layer was dried (MgSO₄), filtered and the solvent was then removed under reduced pressure to yield sulfonamide **74** as a colourless oil (1.183 g, 77%). *R*_f (50% EtOAc in hexane) = 0.2; IR (neat / cm⁻¹) 3492 br w (O-H), 3280 br w (N-H), 2944 w, 2880 w, 1318 m, 1151 s; ¹H NMR (400 MHz, CDCl₃) δ_H 7.77 – 7.73 (AA' of AA'BB', 2H, H-5), 7.33 – 7.29 (BB' of AA'BB', 2H, H-6), 5.04 (t, *J* = 6.1 Hz, 1H, NH), 3.74 (app. q, *J* = 5.2 Hz, 2H, H-1), 3.10 (app. q, *J* = 6.0 Hz, 2H, H-3), 2.43 (s, 3H, H-8), 1.87 (t, *J* = 5.2 Hz, 1H, OH), 1.71 (app. quintet, *J* = 5.6 Hz, 2H, H-2); ¹³C NMR (101 MHz, CDCl₃) δ_C 143.4 (C, C-7), 137.0 (C, C-4), 129.7 (CH, C-6), 127.1 (CH, C-5), 60.7 (CH₂, C-1), 41.1 (CH₂, C-3), 31.5 (CH₂, C-2), 21.5 (CH₃, C-8); LRMS (EI) *m/z* 229.1 [(M)⁺, 20%], 184.0 (50), 155.0 (90).

Data were in agreement with those reported in the literature.¹³⁹

***N*-(3'-Hydroxypropyl)-4-methyl-*N*-(3''-methylbut-2''-en-1''-yl)benzenesulfonamide (75)**



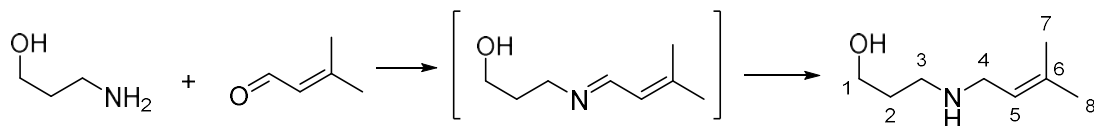
Method A: Cs₂CO₃ (1.98 g, 6.07 mmol) was added to a solution of sulfonamide **74** (1.16 g, 5.06 mmol) in anhydrous DMF (25 mL). The mixture was stirred for 30 min at r.t. Prenyl bromide (0.64 mL, 5.57 mmol) was then added and the resulting solution was stirred for 18 h at r.t. The solution was then poured into H₂O (20 mL) and the mixture was extracted with Et₂O (3 × 40 mL). The combined organic phases were washed with brine (40 mL), dried (MgSO₄), filtered and the solvent was then removed under reduced pressure to provide a yellow oil, which was purified by flash column chromatography (eluent: 50% EtOAc in hexane), to yield sulfonamide **75** as a clear oil (0.685 g, 46%). *R*_f (50% EtOAc in hexane) = 0.6; IR (neat / cm⁻¹) 3499 br w (O-H), 2929 w, 1331 m, 1153 s; ¹H NMR (400 MHz, CDCl₃) δ_H 7.76 – 7.70 (AA' of AA'BB', 2H, H-10), 7.31 – 7.27 (BB' of AA'BB', 2H, H-11), 4.92 (t with unresolved ⁴J coupling, *J* = 7.2 Hz, 1H, H-5), 3.80 (d, *J* = 7.2 Hz, 2H, H-4), 3.77 – 3.71 (m, 2H, H-1), 3.21 (t, *J* = 6.4 Hz, 2H, H-3), 2.47 (br s, 1H, OH), 2.43 (s, 3H, H-13), 1.71 (app. quintet, *J* = 6.0 Hz, 2H, H-2), 1.64 (s, 3H, H-7 or H-8), 1.61 (s, 3H, H-7 or H-8); ¹³C NMR (101 MHz, CDCl₃) δ_C 143.2 (C, C-12), [137.0, 136.9 (2 × C, C-6 & C-9)], 129.6 (CH, C-11), 127.2 (CH, C-10), 118.8 (CH, C-5), 58.7 (CH₂, C-1), 45.8 (CH₂, C-4), 43.7 (CH₂, C-3), 31.0 (CH₂, C-2), 25.7 (CH₃, C-7 or C-8), 21.5 (CH₃, C-13), 17.8 (CH₃, C-7 or C-8); LRMS (ESI) *m/z* 320.1 [(M + Na)⁺, 100%], 230.1 (80), 212.1 (30).

Data were in agreement with those reported in the literature.¹³⁹

Method B: NEt₃ (4.20 mL, 30.2 mmol) was added to a stirred solution of amine **78** (3.32 g, 23.2 mmol) in CH₂Cl₂ (115 mL). The solution was cooled to 0 °C. TsCl (4.19 g, 22.0 mmol) was added in one portion and the reaction mixture was warmed to r.t. After 2 h, the reaction mixture was washed sequentially with HCl_(aq) (1 M, 80 mL), H₂O (80 mL) and brine (80 mL). The organic layer was dried (MgSO₄), filtered and the solvent was then removed under reduced pressure to provide a yellow oil, which was purified by flash column chromatography (eluent: 50% EtOAc in hexane), to yield sulfonamide **75** as a clear oil (4.53 g, 69%).

Data were in agreement with those obtained for sulfonamide **75** that was prepared using method A and in agreement with those reported in the literature.¹³⁹

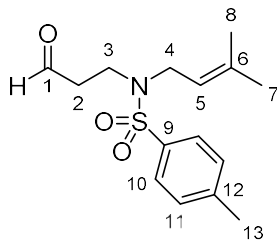
3-((3'-Methylbut-2'-en-1'-yl)amino)propan-1-ol (**78**)



3-Methyl-2-butenal (1.40 mL, 14.6 mmol) was added to a stirred solution of 3-amino-1-propanol (1.02 mL, 13.3 mmol) and activated 3 Å molecular sieves in CH₂Cl₂ (100 mL) at r.t. After 24 h, the solution was filtered through a pad of Celite and the solvent was then removed under reduced pressure to give the intermediate imine as a clear oil. The crude imine was dissolved in MeOH (20 mL) and the resulting solution cooled to 0 °C. NaBH₄ (1.00 g, 26.6 mmol) was added in one portion and the reaction temperature was raised to r.t. After 1 h, H₂O (15 mL) was added to the reaction mixture, the layers were separated, and the aqueous layer was washed with CH₂Cl₂ (3 × 15 mL). The organic phases were combined, dried (MgSO₄), filtered and the solvent was then removed under reduced pressure to yield amine **78** as a pale yellow oil, which was used without further purification (1.80 g). *R_f* (10% MeOH in CH₂Cl₂) = 0.1; IR (neat / cm⁻¹) 3288 br m (O-H, N-H), 2922 m, 1445 m, 1065 s; ¹H NMR (400 MHz, CDCl₃) δ_H 5.20 (t with unresolved ⁴*J* coupling, *J* = 6.9 Hz, 1H, H-5), 3.79 (t, *J* = 5.4 Hz, 2H, H-1), 3.19 (d, *J* = 6.9 Hz, 2H, H-4), 2.86 (t, *J* = 5.7 Hz, 2H, H-3), 1.70 (s, 3H, H-7 or H-8), 1.68 – 1.64 (m, 2H, H-2), 1.63 (s, 3H, H-7 or H-8), exchangeable protons not observed; ¹³C NMR (101 MHz, CDCl₃) δ_C 135.4 (C, C-6), 121.8 (CH, C-5), 63.8 (CH₂, C-1), 48.9 (CH₂, C-3), 46.9 (CH₂, C-4), 30.6 (CH₂, C-2), 25.7 (CH₃, C-7 or C-8), 17.9 (CH₃, C-7 or C-8); LRMS (EI) *m/z* 143.1 [(M)⁺, 30%], 128.1 (100), 69.1 (100).

Data were in agreement with those reported in the literature.¹⁴³

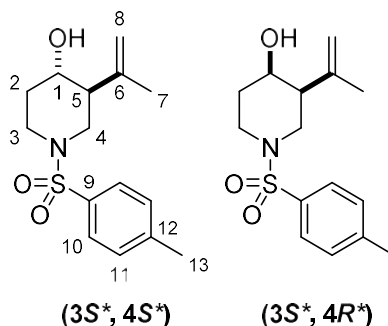
4-Methyl-*N*-(3'-methylbut-2'-en-1'-yl)-*N*-(3''-oxopropyl)benzenesulfonamide (**79**)



DMSO (3.6 mL, 51 mmol) was added dropwise over 2 min to a solution of oxalyl chloride (2.1 mL, 25 mmol) in CH₂Cl₂ (65 mL) at -78 °C. The resultant solution was stirred for 10 min, after which time, a solution of alcohol **75** (6.08 g, 20.4 mmol) in CH₂Cl₂ (15 mL) was added dropwise over 5 min. After 1 h, NEt₃ (14 mL, 102 mmol) was added and the resulting solution was warmed to r.t. over 5 min. H₂O (60 mL) was added to the reaction mixture and the layers were separated. The aqueous layer was extracted with CH₂Cl₂ (3 × 40 mL). The organic layers were combined, dried (MgSO₄), filtered and the solvent was then removed under reduced pressure to give aldehyde **79** as a pale yellow oil, which was used without further purification in the following cyclisation (see p 152). *R*_f (50% EtOAc in hexane) = 0.5; IR (neat / cm⁻¹) 2925 w, 1722 s (C=O), 1336 s, 1154 s; ¹H NMR (400 MHz, CDCl₃) δ_H 9.75 (s, 1H, H-1), 7.70 – 7.75 (AA' of AA'BB', 2H, H-10), 7.33 – 7.28 (BB' of AA'BB', 2H, H-11), 4.98 (t with unresolved ⁴*J* coupling, *J* = 7.1 Hz, 1H, H-5), 3.76 (d, *J* = 6.1 Hz, 2H, H-4), 3.36 (t, *J* = 7.5 Hz, 2H, H-3), 2.82 – 2.76 (m, 2H, H-2), 2.43 (s, 3H, H-13), 1.66 (s, 3H, H-8 or H-7), 1.61 (s, 3H, H-7 or H-8); ¹³C NMR (101 MHz, CDCl₃) δ_C 200.6 (CH, C-1), 143.5 (C, C-12), 137.8 (C, C-6), 136.5 (C, C-9), 129.8 (CH, C-11), 127.4 (CH, C-10), 118.8 (CH, C-5), 46.6 (CH₂, C-4), 44.2 (CH₂, C-3), 41.1 (CH₂, C-2), 25.9 (CH₃, C-7 or C-8), 21.7 (CH₃, C-13), 17.9 (CH₃, C-7 or C-8); LRMS (ESI) *m/z* 318.1 [(M + Na)⁺, 100%].

Data were in agreement with those reported in the literature.¹³⁹

(3*S, 4*S**)-3-(Prop-1'-en-2'-yl)-1-tosylpiperidin-4-ol (82) & (3*S**, 4*R**)-3-(prop-1'-en-2'-yl)-1-tosylpiperidin-4-ol (83)**

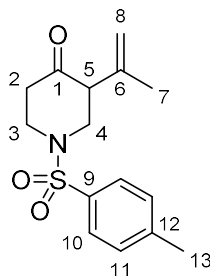


SnCl₄ (1 M solution in heptanes, 2.1 mL, 2.1 mmol) was added to a solution of aldehyde **79** (6.03 g, 20.4 mmol, used without purification, see p 151) in CH₂Cl₂ (200 mL) at 0 °C. The resulting solution was stirred for 16 h, after which time NH₄Cl_(aq) (100 mL) was added. The phases were separated and the aqueous phase was extracted with CH₂Cl₂ (3 × 70 mL). The combined organic phases were washed with brine, dried (MgSO₄), filtered and evaporated under reduced pressure to give a dark orange oil, which was used without further purification (6.03 g). By integration of the isopropenyl resonances at 4.88 and 4.58 ppm in the ¹H NMR spectrum of the crude product the diastereomeric ratio of (3*S**, 4*S**)-**82** to (3*R**, 4*S**)-**83** was determined to be 7:3.

Normally, the product was used as a mixture since both diastereomers converge to the same product in the next oxidation step; however, the major isomer (3*S**, 4*S**)-**82** was once isolated by flash column chromatography (eluent: 40% EtOAc in hexane), to yield piperidinol **82** as a white crystalline solid. *R*_f (50% EtOAc in hexane) = 0.4; m.p. 149 – 151 °C (lit.¹³⁹ m.p. 149 – 151 °C); IR (neat / cm⁻¹) 3393 br (O-H), 2952 m, 1450 w, 1335 m, 1161 s; ¹H NMR (400 MHz, CDCl₃) δ_H 7.67 – 7.63 (AA' of AA'BB', 2H, H-10), 7.34 – 7.30 (BB' of AA'BB', 2H, H-11), 4.97 (s, 1H, H-8_a or H-8_b), 4.58 (s, 1H, H-8_b or H-8_a), 3.98 – 3.95 (m, 1H, H-1), 3.62 – 3.54 (stack, 2H, H-3_a and H-4_a), 2.63 – 2.53 (stack, 2H, H-3_b and H-4_b), 2.44 – 2.35 (stack, 4H, H-13 and H-5), 1.98 – 1.80 (stack, 2H, H-2), 1.77 (s, 3H, H-7), *OH* not observed; ¹³C NMR (101 MHz, CDCl₃) δ_C 144.0 (C, C-12), 143.6 (C, C-6), 133.5 (C, C-9), 129.8 (CH, C-11), 127.7 (CH, C-10), 112.4 (CH₂, C-8), 63.1 (CH, C-1), 46.9 (CH, C-5), 43.6 (CH₂, C-4), 40.7 (CH₂, C-3), 31.3 (CH₂, C-2), 23.0 (CH₃, C-7), 21.6 (CH₃, C-13); LRMS (ESI) *m/z* 318.1 [(M + Na)⁺, 100%].

Data were in agreement with those reported in the literature.¹³⁹

3-(Prop-1'-en-2'-yl)-1-tosylpiperidin-4-one (**81**)



Method A: TfOH (0.55 mL, 6.3 mmol) was added to a suspension of PCC (4.38 g, 20.3 mmol) in CH₂Cl₂ (120 mL). The mixture was stirred for 5 min before being cooled to 0 °C. A solution of alcohol **75** (1.34 g, 4.52 mmol) in CH₂Cl₂ (30 mL) was then added in one portion and the resulting reaction mixture was warmed to r.t. and stirred vigorously. After 24 h, NaHCO₃ (3.00 g) and Et₂O (50 mL) were added. The mixture was vigorously stirred for 15 min and then filtered through a pad of silica, washing the residue with Et₂O (200 mL). The solvent was then removed under reduced pressure to give a brown oil, which was purified by flash column chromatography (eluent: 35% EtOAc in hexane) to yield piperidinone **81** as a white crystalline solid (0.48 g, 36%). *R_f* (50% EtOAc in hexane) = 0.5; m.p. 82 – 83 °C (lit.¹⁴⁴ m.p. 82 – 83 °C); IR (neat / cm⁻¹) 2952 m, 1721 s (C=O), 1337 m, 1155 s; ¹H NMR (400 MHz, CDCl₃) δ_H 7.68 – 7.64 (AA' of AA'BB', 2H, H-10), 7.36 – 7.32 (BB' of AA'BB', 2H, H-11), 5.06 – 5.03 (m, 1H, H-8_a or H-8_b), 4.91 – 4.89 (m, 1H, H-8_b or H-8_a), 3.73 – 3.61 (stack, 2H, H-3), 3.24 – 3.04 (stack, 3H, H-4 & H-5), 2.61 – 2.54 (stack, 2H, H-2), 2.44 (s, 3H, H-13), 1.72 (s, 3H, H-7); ¹³C NMR (101 MHz, CDCl₃) δ_C 205.4 (C, C-1), 144.2 (C, C-12), 139.7 (C, C-6), 133.3 (C, C-9), 130.0 (CH, C-11), 127.6 (CH, C-10), 115.2 (CH₂, C-8), 56.5 (CH, C-5), 49.7 (CH₂, C-3), 46.4 (CH₂, C-4), 40.0 (CH₂, C-2), 21.7 (CH₃, C-13), 21.6 (CH₃, C-7); LRMS (ASAP) *m/z* 294.1 [(M + H)⁺, 100%].

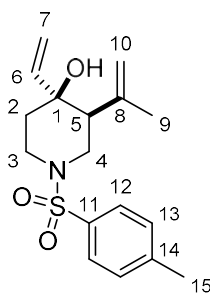
Data were in agreement with those reported in the literature.¹⁴⁴

Method B: DMSO (2.7 mL, 38 mmol) was added dropwise over 2 min to a solution of oxalyl chloride (1.6 mL, 18 mmol) in CH₂Cl₂ (40 mL) at –78 °C. The resultant solution was stirred for 10 min, after which time, a solution of alcohol **80** (4.45 g, 15.1 mmol, used without purification, see p 152) in CH₂Cl₂ (20 mL) was added dropwise over 10 min. After 1 h, *n*-Pr₂NEt (13.2 mL, 75.3 mmol) was added in one portion. After stirring for 15 min at –78 °C, the temperature of the solution was raised to 0 °C by replacing the cooling bath with an ice-water

bath. The mixture was stirred for 30 min at this temperature. $\text{HCl}_{(\text{aq})}$ (1 M, 60 mL) was then added and the solution was vigorously stirred for 15 min at 0 °C. The two phases were then separated and the aqueous phase was washed with CH_2Cl_2 (3 × 40 mL). The combined organic phases were dried (MgSO_4), filtered and the solution concentrated under reduced pressure to a volume of *ca.* 15 mL. This solution was then added directly to a column containing silica and the compound was purified by flash column chromatography (eluent: 35% EtOAc in hexane) to yield piperidinone **81** as a white, crystalline solid (3.580 g, 81% over 3 steps).

Data were in agreement with those obtained for piperidinone **81** that was prepared using method A and in agreement with those reported in the literature.¹⁴⁴

(3*S, 4*S**)-3-(Prop-1'-en-2'-yl)-1-tosyl-4-vinylpiperidin-4-ol (85)**



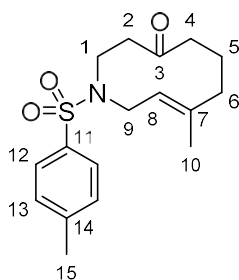
Method A: Vinylmagnesium bromide (0.80 M solution in THF, 2.7 mL, 2.1 mmol) was added dropwise over 1 min to a solution of piperidinone **81** (0.479 g, 1.63 mmol) in THF (4 mL) at –78 °C. The reaction mixture was warmed to r.t. and then stirred for 17 h, before being quenched by the sequential addition of $\text{NH}_4\text{Cl}_{(\text{aq})}$ (6 mL) and H_2O (6 mL). The aqueous layer was extracted with EtOAc (3 × 7 mL). The combined organic phases were washed with brine (6 mL), dried (MgSO_4), filtered and evaporated under reduced pressure to give a dark yellow oil, which contained only one diastereomer upon analysis of the ^1H NMR spectrum of the crude product. The crude product was purified by flash column chromatography (eluent: 30% EtOAc in hexane) to yield allylic alcohol **85** as a white crystalline solid (0.223 g, 43%). R_f (50% EtOAc in hexane) = 0.5; mp 104 – 106 °C; IR (neat / cm^{-1}) 3532 s (O-H), 2860 w, 1330 m, 1158 s; ^1H NMR (400 MHz, CDCl_3) δ_{H} 7.65 – 7.61 (AA' of AA'BB', 2H, H-12), 7.33 – 7.28 (BB' of AA'BB', 2H, H-13), 5.84 (dd, J = 17.2, 10.8 Hz, 1H, H-6), 5.19 (dd, J = 17.2, 0.8 Hz, 1H, H-7_{trans}), 5.07 (dd, J = 10.8, 0.8 Hz, 1H, H-7_{cis}), 4.94 (app. t, J = 1.2 Hz, 1H, H-10_a or H-10_b), 4.60 (s, 1H, H-10_b or H-10_a), 3.65 – 3.58 (m, 1H, H-3_a), 3.49 (ddd, J = 11.2, 4.0, 2.0 Hz, 1H, H-4_a), 2.66 – 2.59 (m, 1H, H-3_b), 2.55 (app. t, J = 12.0 Hz, 1H, H-4_b), 2.43-2.35 (stack, 4H, H-5 and H-

15), 1.92 – 1.82 (m, 1H, H-2_a), 1.76 (s, 3H, H-9), 1.69 (s, 1H, *OH*), 1.64 (app. dt, *J* = 14.0, 2.4 Hz, 1H, H-2_b); ¹³C NMR (101 MHz, CDCl₃) δ_c 144.3 (C, C-8), 143.9 (CH, C-6), 143.5 (C, C-14), 133.4 (C, C-11), 129.7 (CH, C-13), 127.7 (CH, C-12), 113.1 (CH₂, C-10), 112.6 (CH₂, C-7), 70.4 (C, C-1), 50.2 (CH, C-5), 45.7 (CH₂, C-4), 41.8 (CH₂, C-3), 36.3 (CH₂, C-2), 26.3 (CH₃, C-9), 21.5 (CH₃, C-15); LRMS (ESI) *m/z* 344.1 [(M + Na)⁺, 100%], 322.1 (15), 304.1 (10); HRMS (ESI) calc'd for C₁₇H₂₃NO₃SNa (M + Na)⁺ 344.1296, found 344.1298.

Method B: CeCl₃·7H₂O (2.22 g, 5.96 mmol) was heated at 140 °C under high vacuum (< 2 mbar) for 2 h, and then cooled to r.t. THF (25 mL) was added and the resulting slurry was stirred vigorously for 2 h, before being cooled to –78 °C. Vinylmagnesium bromide (0.76 M solution in THF, 6.9 mL, 5.5 mmol) was added. The resulting mixture was stirred for 30 min, after which time a solution of piperidinone **81** (1.34 g, 4.58 mmol) in THF (10 mL) was added dropwise over 5 min. The resulting mixture was stirred at –78 °C for 4 h before being poured into a solution of AcOH_(aq) (5%, 40 mL). The aqueous layer was extracted with EtOAc (3 × 45 mL). The combined organic fractions were washed with NaHCO_{3(aq)} (2 × 50 mL), dried (MgSO₄), filtered and the solvent was then removed under reduced pressure to give a dark yellow oil, which contained only one diastereomer by analysis of the ¹H NMR spectrum of the crude product. The crude product was purified by flash column chromatography (eluent: 25% EtOAc in hexane) to yield allylic alcohol **85** as a white crystalline solid (1.29 g, 88%).

Data were in agreement with those obtained for allylic alcohol **85** that was prepared using method A.

(*E*)-8-Methyl-1-tosyl-2,3,5,6,7,10-hexahydroazecin-4(1*H*)-one (**96**)

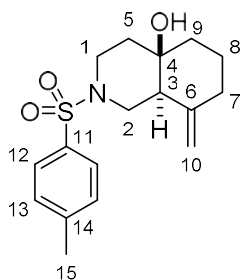


[(C₆H₅CN)₂PdCl₂] (78 mg, 0.20 mmol) was added in one portion to a stirred solution of allylic alcohol **85** (1.305 g, 4.06 mmol) in benzene (40 mL). After 2 h, the solvent was removed under reduced pressure to give an orange oil, which was purified by flash column chromatography (eluent: 30% EtOAc in hexane), to yield ketone **96** as a white crystalline solid

(0.944 g, 73%). R_f (50% EtOAc in hexane) = 0.5; mp 110 – 112 °C; IR (neat / cm^{-1}) 2938 m, 1701 s (C=O), 1340 m, 1160 s; ^1H NMR (400 MHz, CDCl_3) δ_{H} 7.66 – 7.63 (AA' of AA'BB', 2H, H-12), 7.33 – 7.28 (BB' of AA'BB', 2H, H-13), 5.28 – 5.22 (m, 1H, H-8), 4.20 – 4.05 (m, 1H, H-9_a), 3.86 – 3.74 (m, 1H, H-1_a), 3.23 – 3.11 (m, 1H, H-9_b), 3.03 – 2.91 (stack, 2H, H-1_b, H-2_a), 2.46 – 2.40 (stack, 4H, H-2_b, H-15), 2.39 – 2.33 (stack, 2H, H-4_a, H-5_a), 2.25 – 2.21 (m, 1H, H-4_b), 2.21 – 2.16 (m, 1H, H-6_a), 2.11 – 2.01 (m, 1H, H-6_b), 1.94 – 1.85 (m, 1H, H-5_b), 1.40 (s, 3H, H-10); ^{13}C NMR (101 MHz, CDCl_3) δ_{C} 208.3 (C, C-3), 146.3 (C, C-14), 146.1 (C, C-7), 136.6 (C, C-11), 129.8 (CH, C-13), 127.2 (CH, C-12), 121.4 (CH, C-8), 48.0 (CH_2 , C-9), 45.9 (CH_2 , C-2), 44.3 (CH_2 , C-1), 43.1 (CH_2 , C-4), 40.8 (CH_2 , C-6), 25.4 (CH_2 , C-5), 21.5 (CH_3 , C-15), 15.8 (CH_3 , C-10); LRMS (ESI) m/z 344.1 [(M + Na)⁺, 100%], 322.2 (20), 304.1 (10); HRMS (ESI) calc'd for $\text{C}_{17}\text{H}_{23}\text{NO}_3\text{SNa}$ (M + Na)⁺ 344.1296, found 344.1299.

NMR data (–35 °C): ^1H NMR (500 MHz, CDCl_3) δ_{H} 7.65 – 7.61 (AA' of AA'BB', 2H, H-12), 7.35 – 7.29 (BB' of AA'BB', 2H, H-13), 5.27 – 5.21 (m, 1H, H-8), 4.17 (d, J = 14.4 Hz, 1H, H-9_a), 3.82 (dd, J = 14.4, 9.4 Hz, 1H, H-1_a), 3.07 (dd, J = 14.4, 10.9 Hz, 1H, H-9_b), 2.98 (dd, J = 16.1, 8.4 Hz, 1H, H-2_a), 2.85 (dd, J = 14.4, 8.4 Hz, 1H, H-1_b), 2.49 (dd, J = 16.1, 9.4 Hz, 1H, H-2_b), 2.43 (s, 3H, H-15), 2.39 – 2.27 (stack, 2H, H-4_a and H-5_a), 2.22 (dd, J = 14.3, 5.8 Hz, 1H, H-4_b), 2.10 – 2.03 (m, 1H, H-6_a), 1.86 (app. td, J = 12.4, 3.9 Hz, 1H, H-6_b), 1.90 – 1.82 (m, 1H, H-5_b), 1.36 (s, 3H, H-10); ^{13}C NMR (126 MHz, CDCl_3) δ_{C} 209.1 (C, C-3), 143.6 (C, C-14), 143.3 (C, C-7), 135.2 (C, C-11), 129.9 (CH, C-13), 126.8 (CH, C-12), 120.9 (CH, C-8), 48.2 (CH_2 , C-9), 45.6 (CH_2 , C-2), 44.3 (CH_2 , C-1), 43.2 (CH_2 , C-4), 40.7 (CH_2 , C-6), 25.6 (CH_2 , C-5), 21.8 (CH_3 , C-15), 16.0 (CH_3 , C-10).

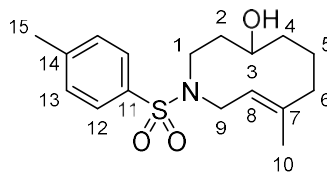
(4a*R, 8a*S**)-8-Methylene-2-tosyloctahydroisoquinolin-4a(2*H*)-ol (107)**



TsOH·H₂O (6.0 mg, 30 μmol) was added to a solution of ketone **96** (200 mg, 0.62 mmol) in THF (12 mL). After 12 h, NaHCO₃ (aq) (6 mL) was added. The layers were separated and the aqueous layer was washed with CH₂Cl₂ (3 × 7 mL). The combined organic phases were dried

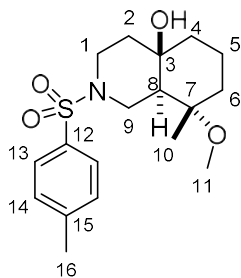
(MgSO₄), filtered and the solvent was then removed under reduced pressure to give a colourless oil, which was purified by flash column chromatography (eluent: 25% EtOAc in hexane) to yield decalol **107** as a white crystalline solid (132 mg, 66%). *R*_f (50% EtOAc in hexane) = 0.5; mp 123 – 125 °C; IR (neat / cm⁻¹) 3516 br w (O-H), 2928 w, 1338 m, 1152 s, 920 s, 744 s; ¹H NMR (400 MHz, CDCl₃) δ_H 7.66 – 7.62 (AA' of AA'BB', 2H, H-12), 7.32 – 7.29 (BB' of AA'BB', 2H, H-13), 4.88 (s, 1H, H-10_a), 4.42 (s, 1H, H-10_b), 3.66 – 3.57 (stack, 2H, H-1_a and H-2_a), 2.60 (app. td, *J* = 11.4, 4.4 Hz, 1H, H-1_b), 2.47 (app. t, *J* = 11.2 Hz, 1H, H-2_b), 2.41 (s, 3H, H-15), 2.36 – 2.24 (stack, 2H, H-3 and H-7_a), 2.04 – 1.94 (m, 1H, H-7_b), 1.74 – 1.57 (stack, 5H, H-5_a, H-8_a, H-9 and OH), 1.48 – 1.41 (m, 1H, H-8_b), 1.40 – 1.38 (m, 1H, H-5_b); ¹³C NMR (101 MHz, CDCl₃) δ_C 146.4 (C, C-6), 143.5 (C, C-14), 133.6 (C, C-11), 129.7 (CH, C-13), 127.7 (CH, C-12), 109.2 (CH₂, C-10), 69.7 (C, C-4), 47.8 (CH, C-3), 43.7 (CH₂, C-2), 42.1 (CH₂, C-1), 38.5 (CH₂, C-5), 37.3 (CH₂, C-9), 36.0 (CH₂, C-7), 23.3 (CH₂, C-8), 21.6 (CH₃, C-15); LRMS (ESI) *m/z* 322.1 [(M + H)⁺, 100%], 304.1 (50); HRMS (ESI) calc'd for C₁₇H₂₄NO₃S (M + H)⁺ 322.1477, found 322.1481.

(E)-8-Methyl-1-tosyl-1,2,3,4,5,6,7,10-octahydroazecin-4-ol (119)



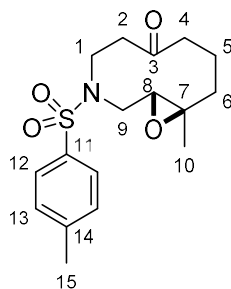
LiBH₄ (2.0 M in THF, 0.23 mL, 0.46 mmol) was added to a cooled (0 °C) solution of ketone **96** (100 mg, 0.31 mmol) in THF (2 mL) and the resulting mixture was stirred. The cooling bath was removed and the solution allowed to warm to r.t. After 3 h, H₂O (6 mL) was added. The two phases were separated and the aqueous layer was washed with EtOAc (3 × 7 mL). The combined organic phases were dried (MgSO₄), filtered and the solvent was then removed under reduced pressure to give a colourless oil, which was purified by flash column chromatography (eluent: 40% EtOAc in hexane) to yield alcohol **119** as a crystalline white solid (100 mg, 98%). *R_f* (50% EtOAc in hexane) = 0.3; mp 133 – 135 °C; IR (neat / cm⁻¹) 3393 br w (O-H), 2932 w, 1450 w, 1334 m, 1160 s; ¹H NMR (400 MHz, CDCl₃) δ_H 7.72 – 7.68 (AA' of AA'BB', 2H, H-12), 7.35 – 7.31 (BB' of AA'BB', 2H, H-13), 5.18 (app. t, *J* = 7.5 Hz, 1H, H-8), 4.31 – 4.15 (m, 1H, H-9_a), 3.57 – 3.39 (m, 1H, H-3), 3.21 (app. d, *J* = 14.9 Hz, 1H, H-1_a), 2.94 – 2.77 (m, 1H, H-9_b), 2.69 (app. t, *J* = 13.0 Hz, 1H, H-1_b), 2.43 (s, 3H, H-15), 2.25 (app. dt, *J* = 12.1, 4.2 Hz, 1H, H-6_a), 2.13 – 1.92 (stack, 2H, H-2_a and H-6_b), 1.78 (s, 3H, H-10), 1.75 – 1.61 (stack, 2H, H-2_b and OH), 1.52 – 1.46 (stack, 2H, H-5), 1.46 – 1.38 (stack, 2H, H-4); ¹³C NMR (101 MHz, CDCl₃) δ_C 145.2 (C, C-7), 143.4 (C, C-14), 129.8 (CH, C-13), 133.8 (C, C-11), 127.7 (CH, C-12), 118.1 (CH, C-8), 70.2 (CH, C-3), 45.9 (CH₂, C-9), 44.0 (CH₂, C-1), 40.6 (CH₂, C-6), 39.2 (CH₂, C-2), 33.9 (CH₂, C-4), 22.3 (CH₂, C-5), 21.6 (CH₃, C-15), 16.8 (CH₃, C-10); LRMS (ESI) *m/z* 346.1 [(M + Na)⁺, 100%], 324.2 (20), 306.2 (20); HRMS (ESI) calc'd for C₁₇H₂₅NO₃Na (M + Na)⁺ 346.1453, found 346.1456.

(4a*R, 8*S**, 8a*S**)-8-Methoxy-8-methyl-2-tosyloctahydroisoquinolin-4a(2*H*)-ol (121)**



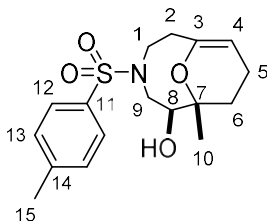
Pd(OH)₂/C (10% Pd, 5 mg) was added to a solution of ketone **96** (50 mg, 0.16 mmol) in a mixture of MeOH (2 mL) and THF (1 mL) and the resulting mixture was stirred. Hydrogen was directly bubbled through the solution for 5 min, after which time the reaction mixture was maintained under an atmosphere of H₂. After 24 h, the solution was filtered through a pad of Celite, washing with MeOH (10 mL), dried (MgSO₄), filtered and the solvent was then removed under reduced pressure to give a colourless oil, which was purified by flash column chromatography (eluent: 35% EtOAc in hexane) to yield decalol **121** as a colourless oil (50 mg, 95%). *R_f* (50% EtOAc in hexane) = 0.4; IR (neat / cm⁻¹) 3522 br w (O-H), 2916 w, 1334 m, 1126 s, 737 s; ¹H NMR (400 MHz, CDCl₃) δ_H 7.68 – 7.64 (AA' of AA'BB', 2H, H-13), 7.33 – 7.28 (BB' of AA'BB', 2H, H-14), 3.79 (ddd, *J* = 11.1, 3.7, 1.9 Hz, 1H, H-9_a), 3.64 (app. dq, *J* = 11.5, 2.4 Hz, 1H, H-1_a), 3.16 (s, 3H, H-11), 2.69 – 2.60 (m, 1H, H-1_b), 2.42 (s, 3H, H-16), 2.39 (app. t, *J* = 11.5 Hz, 1H, H-9_b), 1.80 – 1.69 (stack, 3H, H-2_a, H-6_a and H-8), 1.67 – 1.57 (m, 2H, H-5), 1.54 – 1.43 (stack, 3H, H-2_b, H-4_a and H-6_b), 1.38 – 1.59 (m, 1H, H-4_b), 1.13 (s, 3H, H-10), *OH* not observed; ¹³C NMR (101 MHz, CDCl₃) δ_C 143.4 (C, C-15), 133.9 (C, C-12), 129.7 (CH, C-14), 127.8 (CH, C-13), 75.2 (C, C-7), 69.8 (C, C-3), 48.4 (CH, C-8), 48.0 (CH₃, C-11), 42.0 (CH₂, C-1), 41.7 (CH₂, C-9), 40.6 (CH₂, C-2), 39.5 (CH₂, C-4), 36.1 (CH₂, C-6), 21.7 (CH₃, C-16), 19.5 (CH₃, C-10), 18.9 (CH₂, C-5); LRMS (ASAP) *m/z* 354.2 [(M + H)⁺, 100%], 304.1 (40); HRMS (ASAP) calc'd for C₁₈H₂₈NO₄S (M + H)⁺ 354.1739, found 354.1740.

(1*R, 10*R**)-10-Methyl-3-tosyl-11-oxa-3-azabicyclo[8.1.0]undecan-6-one (122)**



*m*CPBA (70%, 0.440 g, 1.78 mmol) was added to a solution of ketone **96** (0.441 g, 1.37 mmol) in CH₂Cl₂ (16 mL). The resultant solution was stirred for 4 h at r.t., after which time, Na₂S₂O₃ (aq) (10 mL) was added and the mixture was stirred for 10 min. The two phases were then separated and the organic phase was washed sequentially with NaHCO₃ (aq) (10 mL), H₂O (10 mL) and brine (10 mL). The organic phase was dried (MgSO₄), filtered and the solvent was then removed under reduced pressure to give a white solid, which was purified by flash column chromatography (eluent: 35% EtOAc in hexane) to yield epoxide **122** as a white, crystalline solid (0.425 g, 92%). *R*_f (50% EtOAc in hexane) = 0.5; mp 105 – 108 °C; IR (neat / cm⁻¹) 2932 br, 1707 s (C=O), 1337 s, 1158 s, 1090 s; ¹H NMR (400 MHz, CDCl₃) δ_H 7.69 – 7.64 (AA' of AA'BB, 2H, H-12), 7.33 – 7.28 (BB' of AA'BB', 2H, H-13), 3.77 – 3.64 (stack, 2H, H-1_a and H-9_a), 3.39 – 3.30 (m, 1H, H-1_b), 2.97 – 2.87 (m, 1H, H-2_a), 2.86 – 2.80 (m, 1H, H-8), 2.66 – 2.54 (stack, 4H, H-2_b, H-4 and H-9_b), 2.42 (s, 3H, H-15), 2.17 – 2.05 (stack, 2H, H-5_a and H-6_a), 1.74 – 1.63 (m, 1H, H-5_b), 1.17 (s, 3H, H-10), 1.05 – 0.94 (m, 1H, H-6_b); ¹³C NMR (101 MHz, CDCl₃) δ_C 210.6 (C, C-3), 143.8 (C, C-14), 136.1 (C, C-11), 130.0 (CH, C-13), 127.1 (CH, C-12), 61.9 (CH, C-8), 61.2 (C, C-7), 47.6 (CH₂, C-9), 46.2 (CH₂, C-1), 45.2 (CH₂, C-2), 43.3 (CH₂, C-4), 38.5 (CH₂, C-6), 21.6 (CH₃, C-15), 19.0 (CH₂, C-5), 15.9 (CH₃, C-10); LRMS (ESI) *m/z* 360.1 [(M + Na)⁺, 100%], 338.2 (30), 320.1 (25); HRMS (ESI) calc'd for C₁₇H₂₃NO₄SNa (M + Na)⁺ 360.1245, found 360.1246.

(1*R, 2*S**)-1-Methyl-4-tosyl-11-oxa-4-azabicyclo[5.3.1]undec-7-en-2-ol (124)**

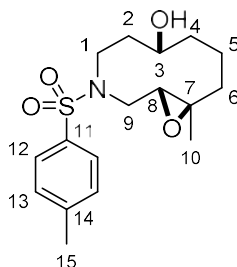


Method A: NaBH₄ (47 mg, 1.2 mmol) was added in one portion to a cooled (0 °C) solution of epoxide **122** (0.21 g, 0.62 mmol) in THF and MeOH (1:1, 4 mL total). The cooling bath was removed, and the reaction mixture was warmed to r.t. After 5 h, H₂O (5 mL) was added to the reaction mixture. The layers were separated and the aqueous layer was washed with CH₂Cl₂ (3 × 5 mL). The combined organic phases were dried (MgSO₄), filtered and the solvent was then removed under reduced pressure to give a colourless oil which was purified by flash column chromatography (eluent: 35% EtOAc in hexane) to yield enol ether **124** as a crystalline white solid (52 mg, 25%). *R_f* (50% EtOAc in hexane) = 0.5; mp 82 – 84 °C; IR (neat / cm⁻¹) 3337 br (O-H), 2938 m, 1701 m, 1324 s, 1153 s; ¹H NMR (400 MHz, CDCl₃) δ_H 7.71 – 7.67 (AA' of AA'BB, 2H, H-12), 7.32 – 7.27 (BB' of AA'BB', 2H, H-13), 4.82 (app. s, 1H, H-4), 4.38 (dd, *J* = 9.0, 3.4 Hz, 1H, H-8), 3.69 (app. dd, *J* = 14.5, 6.0 Hz, 1H, H-1_a), 3.47 (app. d, *J* = 14.5 Hz, 1H, H-9_a), 3.14 – 2.99 (stack, 2H, H-1_b and H-9_b), 2.42 (s, 3H, H-15), 2.40 – 2.32 (m, 1H, H-2_a), 2.31 – 2.23 (m, 1H, H-2_b), 2.22 – 2.11 (stack, 2H, H-5), 2.06 – 1.99 (m, 1H, H-6_a), 1.85 – 1.72 (stack, 2H, H-6_b and OH), 1.17 (s, 3H, H-10); ¹³C NMR (101 MHz, CDCl₃) δ_C 149.3 (C, C-3), 143.3 (C, C-14), 137.7 (C, C-11), 129.8 (CH, C-13), 126.7 (CH, C-12), 104.1 (CH, C-4), 76.1 (C, C-7), 72.8 (CH, C-8), 55.6 (CH₂, C-9), 49.9 (CH₂, C-1), 34.4 (CH₂, C-2), 29.7 (CH₂, C-6), 21.6 (CH₃, C-15), 20.5 (CH₃, C-10), 18.7 (CH₂, C-5); LRMS (ESI) *m/z* 360.1 [(M + Na)⁺, 100%], 338.1 (90), 320.1 (100), 292.1 (20), 218.6 (50), 209.1 (40); HRMS (ESI) calc'd for C₁₇H₂₃NO₄Na (M + Na)⁺ 360.1245, found 360.1244.

Method B: TsOH·H₂O (8.1 mg, 0.042 mmol) was added to a solution of epoxide **122** (286 mg, 0.848 mmol) in toluene (10 mL). After 2 h, NaHCO₃ (aq) (15 mL) was added. The layers were separated and the aqueous layer was washed with EtOAc (3 × 10 mL). The combined organic phases were dried (MgSO₄), filtered and the solvent was then removed under reduced pressure to give a colourless oil, which was purified by flash column chromatography (eluent: 25% EtOAc in hexane) to yield enol ether **124** as a crystalline white solid (241 mg, 84%).

Data were in agreement with those obtained for enol ether **124** that was prepared using method A.

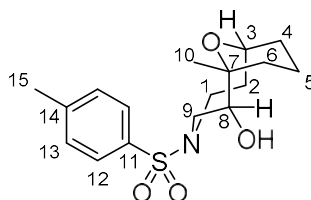
(1*R, 6*R**, 10*R**)-10-Methyl-3-tosyl-11-oxa-3-azabicyclo[8.1.0]undecan-6-ol
(**123**)^{xx}**



*m*CPBA (70%, 75 mg, 0.30 mmol) was added to a solution of alkene **119** (70 mg, 0.22 mmol) in CH₂Cl₂ (5 mL). The resultant solution was stirred for 4 h at r.t., after which time, Na₂S₂O₃ (aq) (5 mL) was added and the mixture was stirred for 10 min. The two phases were then separated and the organic phase was washed sequentially with NaHCO₃ (aq) (5 mL), H₂O (5 mL) and brine (5 mL). The organic phase was dried (MgSO₄), filtered and the solvent was then removed under reduced pressure to give a colourless oil, which was purified by flash column chromatography (eluent: 50% EtOAc in hexane) to yield epoxide **123** as a colourless oil (47 mg, 65%). *R*_f (50% EtOAc in hexane) = 0.2; IR (neat / cm⁻¹) 3471 br w (O-H), 2935 br, 1338 m, 1161 s, 720 m; ¹H NMR (400 MHz, CDCl₃) δ_H 7.68 – 7.63 (AA' of AA'BB', 2H, H-13), 7.34 – 7.30 (BB' of AA'BB', 2H, H-12), 4.06 – 3.99 (m, 1H, H-3), 3.39 – 3.27 (stack, 2H, H-1_a and H-9_a), 3.12 (dd, *J* = 12.4, 4.6 Hz, 1H, H-9_b), 2.98 (dd, *J* = 9.2, 4.6 Hz, 1H, H-8), 2.77 – 2.66 (m, 1H, H-1_b), 2.61 (br s, 1H, OH), 2.41 (s, 3H, H-15), 2.29 – 2.15 (stack, 2H, H-2_a and H-6_a), 1.83 – 1.64 (stack, 2H, H-5), 1.63 – 1.52 (stack, 2H, H-2_b and H-4_a), 1.50 – 1.45 (m, 1H, H-4_b), 1.43 (s, 3H, H-10), 1.07 – 0.96 (m, 1H, H-6_b); ¹³C NMR (101 MHz, CDCl₃) δ_C 143.9 (C, C-14), 133.3 (C, C-11), 129.9 (CH, C-12), 127.7 (CH, C-13), 69.3 (CH, C-3), 60.8 (C, C-7), 60.3 (CH, C-8), 48.9 (CH₂, C-9), 45.0 (CH₂, C-1), 40.1 (CH₂, C-6), 38.6 (CH₂, C-2), 34.4 (CH₂, C-4), 22.2 (CH₂, C-5), 21.6 (CH₃, C-15), 15.9 (CH₃, C-10); LRMS (ASAP) *m/z* 340.2 [(M + H)⁺, 20%], 322.1 (100); HRMS (ASAP) calc'd for C₁₇H₂₆NO₄S (M + H)⁺ 340.1583, found 340.1584.

^{xx} The relative stereochemistry has not been confirmed but has been inferred from other scaffolds. Please see Section 2.3.3.

(1*R, 2*S**, 7*S**)-1-Methyl-4-tosyl-11-oxa-4-azabicyclo[5.3.1]undecan-2-ol (125)**

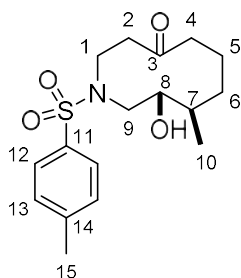


Method A: TsOH·H₂O (4.0 mg, 21 μmol) was added to a solution of acetal **152** (77 mg, 0.21 mmol) in CH₂Cl₂ (2 mL). Et₃SiH (160 μL, 1.0 mmol) was then added dropwise over 1 min. The resultant solution was stirred for 3 h at r.t., after which time, NaHCO_{3(aq)} (5 mL) was added. The solution was diluted with CH₂Cl₂ (8 mL) and the layers were separated. The aqueous layer was washed with CH₂Cl₂ (3 × 8 mL). The combined organic phases were dried (MgSO₄), filtered and the solvent was then removed under reduced pressure to give a colourless oil. Purification by flash column chromatography (eluent: 35% EtOAc in hexane) yielded ether **125** as a white, crystalline solid (46 mg, 65%). *R*_f (50% EtOAc in hexane) = 0.4; mp 97 – 99 °C; IR (neat / cm⁻¹) 3490 br (O-H), 2936 br m, 1329 m, 1158 s; ¹H NMR (400 MHz, CDCl₃) δ_H 7.69 – 7.65 (AA' of AA'BB', 2H, H-12), 7.31 – 7.28 (BB' of AA'BB', 2H, H-13), 4.24 (app. t, *J* = 5.6 Hz, 1H, H-8), 4.01 (app. dd, *J* = 14.2, 8.3 Hz, 1H, H-1_a), 3.88 (app. quintet, *J* = 6.1 Hz, 1H, H-3), 3.61 (dd, *J* = 14.5, 1.7 Hz, 1H, H-9_a), 3.30 (dd, *J* = 14.5, 6.4 Hz, 1H, H-9_b), 2.84 (ddd, *J* = 14.2, 7.9, 1.5 Hz, 1H, H-1_b), 2.42 (s, 3H, H-15), 2.23 (d, *J* = 4.9 Hz, 1H, OH), 1.97 – 1.84 (stack, 3H, H-2 and H-6_a), 1.76 – 1.66 (stack, 2H, H-4_a and H-5_a), 1.56 – 1.52 (m, 1H, H-5_b), 1.40 – 1.30 (stack, 2H, H-4_b and H-6_b), 1.04 (s, 3H, H-10); ¹³C NMR (101 MHz, CDCl₃) δ_C 143.3 (C, C-14), 137.3 (C, C-11), 129.8 (CH, C-13), 127.0 (CH, C-12), 75.3 (CH, C-8), 73.4 (C, C-7), 70.7 (CH, C-3), 53.7 (CH₂, C-9), 46.2 (CH₂, C-1), 36.4 (CH₂, C-2), 32.6 (CH₂, C-6), 27.6 (CH₂, C-4), 23.2 (CH₃, C-10), 21.6 (CH₃, C-15), 14.3 (CH₂, C-5); LRMS (ESI) *m/z* 362.5 [(M + Na)⁺, 100%], 340 (28); HRMS (ESI) calc'd for C₁₇H₂₅NO₄NaS (M + Na)⁺ 362.1402, found 362.1405.

Method B: *m*CPBA (70%, 101 mg, 0.411 mmol) was added in one portion to a stirred solution of alcohol **119** (95 mg, 0.29 mmol) in CH₂Cl₂ (5 mL). The resultant solution was stirred for 120 h, after which time, Na₂S₂O_{3(aq)} (5 mL) was added. The solution was stirred for 10 min before the layers were separated. The organic layer was washed sequentially with NaHCO_{3(aq)} (5 mL) and brine (5 mL), then dried (MgSO₄), filtered and the solvent was then removed under reduced pressure to give a cloudy yellow oil. Purification by flash column chromatography (eluent: 30% EtOAc in hexane) yielded ether **125** as a white, crystalline solid (45 mg, 45%).

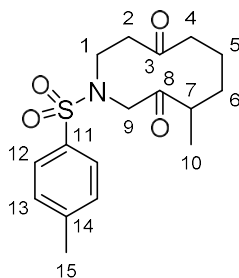
Data were in agreement with those obtained for ether **125** that was prepared using method A.

(8*R, 9*S**)-9-hydroxy-8-methyl-1-tosylazecan-4-one (126)**



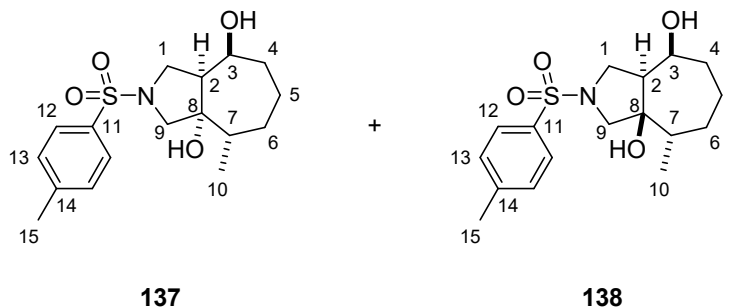
*m*CPBA (70%, 100 mg, 0.41 mmol) was added in one portion to a stirred solution of alcohol **119** (95 mg, 0.29 mmol) in CH₂Cl₂ (5 mL). The resultant solution was stirred for 120 h, after which time, Na₂S₂O_{3(aq)} (5 mL) was added. The solution was stirred for 10 min and then the layers were separated. The organic layer was washed sequentially with NaHCO_{3(aq)} (5 mL) and brine (5 mL), then dried (MgSO₄), filtered and the solvent was then removed under reduced pressure to give a cloudy yellow oil. Purification by flash column chromatography (eluent: 30% EtOAc in hexane) yielded alcohol **126** as a white, crystalline solid (20 mg, 20%). *R*_f (50% EtOAc in hexane) = 0.2; mp 111 – 113 °C; IR (neat / cm⁻¹) 3518 br w, 2929 br, 1704 m (C=O), 1322 s, 1157 s; ¹H NMR (400 MHz, CDCl₃) δ_H 7.72 – 7.66 (AA' of AA'BB', 2H, H-12), 7.36 – 7.31 (BB' of AA'BB', 2H, H-13), 3.58 – 3.45 (stack, 2H, H-1_a and H-8), 3.27 – 3.12 (stack, 2H, H-1_b and H-9_a), 3.01 – 2.86 (stack, 2H, H-2_a and H-9_b), 2.81 – 2.70 (m, 1H, H-4_a), 2.64 – 2.57 (m, 1H, H-2_b), 2.52 (ddd, *J* = 15.2, 7.5, 3.3 Hz, 1H, H-4_b), 2.43 (s, 3H, H-15), 2.00 – 1.85 (stack, 2H, H-5_a and H-7), 1.84 – 1.74 (m, 1H, H-5_b), 1.43 – 1.24 (stack, 2H, H-6), 1.17 (d, *J* = 6.7 Hz, 3H, H-10); ¹³C NMR (101 MHz, CDCl₃) δ_C 214.6 (C, C-3), 144.3 (C, C-14), 133.9 (C, C-11), 130.1 (CH, C-13), 127.7 (CH, C-12), 73.4 (CH, C-8), 56.3 (CH₂, C-9), 50.3 (CH₂, C-1), 45.1 (CH₂, C-2), 42.8 (CH₂, C-4), 33.1 (CH, C-7), 30.5 (CH₂, C-6), 21.7 (CH₃, C-15), 20.7 (CH₂, C-5), 15.7 (CH₃, C-10); LRMS (ASAP) *m/z* 322.1 [(M – H₂O + H)⁺, 100%], 340.2 (15); HRMS (ASAP) calc'd for C₁₇H₂₆NO₄S (M + H)⁺ 340.1583, found 340.1584.

4-Methyl-1-tosylazecane-3,8-dione (**134**)



BF₃·OEt₂ (4.0 μL, 31 μmol) was added to a solution of epoxide **122** (210 mg, 0.61 mmol) in CHCl₃ (2 mL) at r.t. The resultant solution was stirred for 1.5 h at r.t., after which time, NaHCO_{3(aq)} (5 mL) was added. The solution was diluted with CH₂Cl₂ (8 mL) and the layers were separated. The aqueous layer was washed with CH₂Cl₂ (3 × 8 mL). The combined organic phases were dried (MgSO₄), filtered and the solvent was then removed under reduced pressure to give a colourless oil. Purification by flash column chromatography (eluent: 30% EtOAc in hexane) yielded diketone **134** as a white, crystalline solid (128 mg, 62%). *R*_f (50% EtOAc in hexane) = 0.4; mp 107 – 110 °C; IR (neat / cm⁻¹) 2926 br m, 1701 s (C=O), 1341 m, 1160 s; ¹H NMR (400 MHz, CDCl₃) δ_H 7.73 – 7.70 (AA' of AA'BB', 2H, H-12), 7.35 – 7.31 (BB' of AA'BB', 2H, H-13), 4.07 (d, *J* = 17.6 Hz, 1H, H-9_a), 3.93 (app. t, *J* = 11.8 Hz, 1H, H-1_a), 3.55 (d, *J* = 17.6 Hz, 1H, H-9_b), 3.12 – 2.97 (stack, 2H, H-1_b and H-7), 2.71 (ddd, *J* = 16.9, 10.2, 2.3 Hz, 1H, H-2_a), 2.50 – 2.37 (stack, 6H, H-2_b, H-4 and H-15), 2.01 – 1.73 (stack, 3H, H-5 and H-6_a), 1.46 – 1.37 (m, 1H, H-6_b), 1.08 (d, *J* = 6.9 Hz, 3H, H-10); ¹³C NMR (101 MHz, CDCl₃) δ_C 213.0 (C, C-8), 211.0 (C, C-3) 144.0 (C, C-14), 135.5 (C, C-11), 130.0 (CH, C-13), 127.6 (CH, C-12), 57.6 (CH₂, C-9), 45.6 (CH₂, C-1), 43.5 (CH₂, C-4), 40.3 (CH₂ and CH, C-2 and C-7), 32.5 (CH₂, C-6), 22.9 (CH₂, C-5), 21.7 (CH₃, C-15), 19.2 (CH₃, C-10); LRMS (ESI) *m/z* 360.1 [(M + Na)⁺, 100%], 338.2 (10), 320.1 (10); HRMS (ESI) calc'd for C₁₇H₂₃NO₄NaS (M + Na)⁺ 360.1245, found 360.1243.

(3a*S, 4*S**, 8*S**, 8a*S**)-4-Methyl-2-tosyloctahydrocyclohepta[*c*]pyrrole-3a,8(1*H*)-diol (**137**) and (3a*R**, 4*S**, 8*S**, 8a*S**)-4-methyl-2-tosyloctahydrocyclohepta[*c*]pyrrole-3a,8(1*H*)-diol (**138**)**



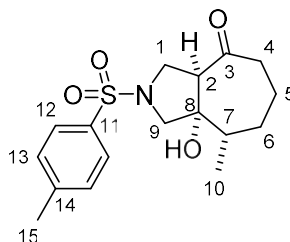
Method A: NaBH₄ (18 mg, 0.48 mmol) was added in one portion to a solution of diketone **134** (81 mg, 0.24 mmol) in THF (1.8 mL) at 0 °C and the resulting mixture was stirred. After 2 h, H₂O (3 mL) was added. The two phases were separated and the aqueous layer was washed with EtOAc (3 × 5 mL). The combined organic phases were dried (MgSO₄), filtered and the solvent was then removed under reduced pressure to give a white solid, which was purified by flash column chromatography (eluent: 30% EtOAc in hexane) to yield diol **137** as a white, crystalline solid (47 mg, 50%) as a mixture with diol **138** (ratio 5:1).^{xxi} *R*_f (50% EtOAc in hexane) = 0.4; mp 161 – 163 °C; IR (neat / cm⁻¹) 3460 br w (O-H), 2930 w, 1330 m, 1153 s; ¹H NMR (400 MHz, CDCl₃) δ_H 7.75 – 7.71 (AA' of AA'BB', 2H, H-12), 7.33 – 7.30 (BB' of AA'BB', 2H, H-13), 4.05 – 3.99 (m, 1H, H-3), 3.80 (app. t, *J* = 9.8 Hz, 1H, H-1_a), 3.45 – 3.37 (stack, 2H, H-1_b and H-9_a), 3.12 (d, *J* = 10.8 Hz, 1H, H-9_b), 2.42 (s, 3H, H-15), 2.19 – 2.06 (stack, 2H, H-2 and H-4_a), 1.80 – 1.71 (m, 1H, H-5_a), 1.69 – 1.58 (stack, 2H, H-4_b and H-6_a), 1.54 – 1.41 (stack, 2H, H-6_b and H-7), 1.35 – 1.26 (m, 1H, H-5_b), 0.89 (d, *J* = 6.3 Hz, 3H, H-10), exchangeable protons not observed; ¹³C NMR (101 MHz, CDCl₃) δ_C 143.6 (C, C-14), 133.8 (C, C-11), 129.8 (CH, C-13), 127.8 (CH, C-12), 84.3 (C, C-8), 69.2 (CH, C-3), 62.8 (CH₂, C-9), 49.5 (CH₂, C-1), 48.9 (CH, C-2), 42.5 (CH, C-7), 36.7 (CH₂, C-4), 34.3 (CH₂, C-6), 22.8 (CH₂, C-5), 21.7 (CH₃, C-15), 17.3 (CH₃, C-10); LRMS (ESI) *m/z* 362.1 [(M + Na)⁺, 100%], 403.1 (30); HRMS (ESI) calc'd for C₁₇H₂₅NO₄SNa (M + Na)⁺ 362.1402, found 362.1404.

^{xxi} By integration of the methyl resonances at 0.92 and 0.89 ppm in the ¹H NMR spectrum of the product, the diastereomeric ratio of diol **137** to diol **138** was determined to be 5:1.

Method B: NaBH₄ (5.0 mg, 0.130 mmol) was added in one portion to a solution of diketone **134** (23 mg, 67 μmol) in THF (0.7 mL) and the resulting mixture was heated to 35 °C and stirred. After 2 h, H₂O (3 mL) was added. The two phases were separated and the aqueous layer was washed with EtOAc (3 × 4 mL). The combined organic phases were dried (MgSO₄), filtered and the solvent was then removed under reduced pressure to give diol **138** as a white, crystalline solid (21 mg, 98%) as a mixture with diol **137** (ratio 5:1).^{xxii} *R*_f (50% EtOAc in hexane) = 0.4; mp 148 – 151 °C; IR (neat / cm⁻¹) 3495 br w (O-H), 2928 w, 1332 m, 1156 s; ¹H NMR (400 MHz, CDCl₃) δ_H 7.75 – 7.68 (AA' of AA'BB', 2H, H-12), 7.36 – 7.27 (BB' of AA'BB', 2H, H-13), 3.91 – 3.87 (m, 1H, H-3), 3.76 – 3.71 (stack, 2H, H-1_a and OH), 3.33 (dd, *J* = 10.0, 1.1 Hz, 1H, H-9_a), 3.12 (dd, *J* = 9.8, 4.6 Hz, 1H, H-1_b), 3.01 (dd, *J* = 10.0, 1.0 Hz, 1H, H-9_b), 2.42 (s, 3H, H-15), 2.23 (app. ddt, *J* = 8.7, 4.6, 1.3 Hz, 1H, H-2), 2.03 – 1.97 (m, 1H, H-7), 1.92 – 1.86 (m, 1H, H-4_a), 1.66 – 1.58 (stack, 3H, H-5 and H-6_a), 1.50 – 1.42 (m, 1H, H-4_b), 1.32 – 1.23 (m, 1H, H-6_b), 0.92 (d, *J* = 7.1 Hz, 3H, H-10), 1 × OH was not observed; ¹³C NMR (101 MHz, CDCl₃) δ_C 143.7 (C, C-14), 132.7 (C, C-11), 129.7 (CH, C-13), 128.0 (CH, C-12), 84.5 (C, C-8), 72.9 (CH, C-3), 62.2 (CH₂, C-9), 54.8 (CH, C-2), 53.1 (CH₂, C-1), 40.0 (CH, C-7), 36.1 (CH₂, C-4), 31.8 (CH₂, C-6), 24.4 (CH₂, C-5), 21.6 (CH₃, C-15), 18.2 (CH₃, C-10); LRMS (ESI) *m/z* 362.1 [(M + Na)⁺, 100%]; HRMS (ESI) calc'd for C₁₇H₂₅NO₄SNa (M + Na)⁺ 362.1402, found 362.1405.

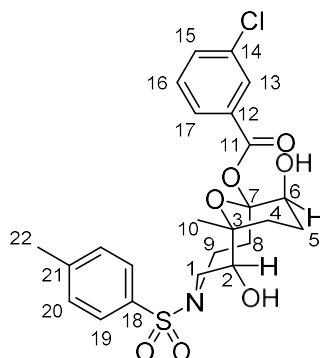
^{xxii} By integration of the methyl resonances at 0.92 and 0.89 ppm in the ¹H NMR spectrum of the crude product, the diastereomeric ratio of diol **138** to diol **137** was determined to be 5:1.

(3a*R, 8*S**, 8a*S**)-8a-Hydroxy-8-methyl-2-tosyloctahydrocyclohepta[*c*]pyrrol-4(1*H*)-one (143)**



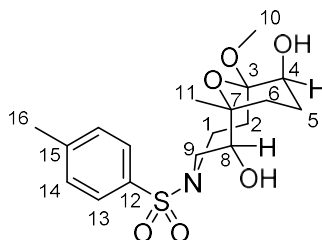
NaH (50% dispersion in mineral oil, 14 mg, 0.30 mmol) was added in one portion to a solution of diketone **134** (100 mg, 0.30 mmol) in THF (5 mL) and the resulting mixture was stirred. After 2 h, H₂O (3 mL) was added. The two phases were separated and the aqueous layer was washed with EtOAc (3 × 5 mL). The combined organic phases were dried (MgSO₄), filtered and the solvent was then removed under reduced pressure to give a yellow oil, which was purified by flash column chromatography (eluent: 30% EtOAc in hexane) to yield ketone **143** as a white, crystalline solid (34 mg, 34%). *R*_f (50% EtOAc in hexane) = 0.4; mp 156 – 158 °C; IR (neat / cm⁻¹) 3489 br w (O-H), 2925 w, 1700 s (C=O), 1333 m, 1159 s; ¹H NMR (400 MHz, CDCl₃) δ_H 7.76 – 7.71 (AA' of AA'BB', 2H, H-12), 7.37 – 7.33 (BB' of AA'BB', 2H, H-13), 4.83 (br s, 1H, OH), 4.04 – 3.95 (m, 1H, H-1_a), 3.47 (d, *J* = 10.9 Hz, 1H, H-9_a), 3.33 – 3.24 (stack, 2H, H-1_b and H-2), 3.13 (d, *J* = 10.9 Hz, 1H, H-9_b), 2.57 – 2.47 (m, 1H, H-4_a), 2.44 (s, 3H, H-15), 2.40 – 2.31 (m, 1H, H-4_b), 1.87 – 1.82 (m, 1H, H-5_a), 1.78 – 1.67 (stack, 3H, H-5_b, H-6_a and H-7), 1.57 – 1.48 (m, 1H, H-6_b), 0.97 (d, *J* = 6.6 Hz, 3H, H-10); ¹³C NMR (101 MHz, CDCl₃) δ_C 207.5 (C, C-3), 144.1 (C, C-14), 133.1 (C, C-11), 130.0 (CH, C-13), 127.9 (CH, C-12), 81.2 (C, C-8), 62.2 (CH₂, C-9), 58.4 (CH, C-2), 47.1 (CH₂, C-1), 43.4 (CH, C-7), 43.0 (CH₂, C-4), 33.1 (CH₂, C-6), 22.5 (CH₂, C-5), 21.7 (CH₃, C-15), 17.4 (CH₃, C-10); LRMS (ESI) *m/z* 360.1 [(M + Na)⁺, 100%], 401.2 (60); HRMS (ESI) calc'd for C₁₇H₂₃NO₄SNa (M + Na)⁺ 360.1245, found 360.1246.

(1'S*, 6'R*, 7'R*, 10'S*)-6',10'-Dihydroxy-7'-methyl-4'-tosyl-11'-oxa-4'-azabicyclo[5.3.1]undecan-1'-yl 3-chlorobenzoate (145)



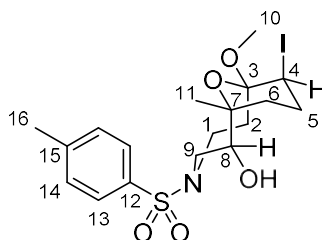
*m*CPBA (70%, 62 mg, 0.25 mmol) was added to a solution of enol ether **124** (65 mg, 0.19 mmol) in CH₂Cl₂ (2.5 mL). The resultant solution was stirred for 1.5 h at r.t., after which time, Na₂S₂O₃ (aq) (5 mL) was added and the mixture was stirred for 10 min. The two phases were then separated, and the organic phase was washed sequentially with NaHCO₃ (aq) (5 mL), H₂O (5 mL) and brine (5 mL). The organic phase was dried (MgSO₄), filtered and the solvent was then removed under reduced pressure to give a white solid, which was purified by flash column chromatography (eluent: 35% EtOAc in hexane) to yield acetal **145** as a white, crystalline solid (38 mg, 39%). *R*_f (50% EtOAc in hexane) = 0.4; mp 113 – 116 °C; IR (neat / cm⁻¹) 3458 br w (O-H), 2961 m, 1721 s (C=O), 1598 w, 1575 w, 1258 s, 751 s; ¹H NMR (400 MHz, CDCl₃) δ_H 8.00 (app. t, *J* = 1.8 Hz, 1H, H-13), 7.93 (app. dt, *J* = 7.7, 1.4 Hz, 1H, H-17), 7.70 – 7.64 (AA' of AA'BB', 2H, H-19), 7.56 (ddd, *J* = 8.0, 2.2, 1.1 Hz, 1H, H-15), 7.40 (app. t, *J* = 7.8 Hz, 1H, H-16), 7.33 – 7.28 (BB' of AA'BB', 2H, H-20), 4.96 (app. t, *J* = 5.7 Hz, 1H, H-6), 4.26 (app. d, *J* = 4.5 Hz, 1H, H-2), 3.89 (app. dd, *J* = 15.3, 9.0 Hz, 1H, H-9_a), 3.70 (app. d, *J* = 14.7 Hz, 1H, H-1_a), 3.38 (dd, *J* = 14.7, 6.4 Hz, 1H, H-1_b), 3.15 – 3.05 (m, 1H, H-9_b), 3.02 – 2.95 (stack, 2H, 2 × OH), 2.42 (s, 3H, H-22), 2.22 – 2.02 (stack, 4H, H-8 and H-5), 1.89 – 1.80 (m, 1H, H-4_a), 1.72 – 1.59 (m, 1H, H-4_b), 1.22 (s, 3H, H-10); ¹³C NMR (101 MHz, CDCl₃) δ_C 164.3 (C, C-11), 143.6 (C, C-21), 136.8 (C, C-18), 134.9 (C, C-14), 133.6 (CH, C-15), 131.7 (C, C-12), 130.1 (CH, C-17), 129.9 (CH, C-20), 129.8 (CH, C-13), 127.9 (CH, C-16), 126.9 (CH, C-19), 95.4 (C, C-7), 77.2 (C, C-3), 74.3 (CH, C-2), 71.2 (CH, C-6), 53.8 (CH₂, C-1), 43.2 (CH₂, C-9), 38.8 (CH₂, C-8), 25.7 (CH₂, C-4), 23.3 (CH₃, C-10), 22.1 (CH₂, C-5), 21.6 (CH₃, C-22); LRMS (ESI) *m/z* 532.1 [(M + Na)⁺, 100%], 492.1 (10); HRMS (ESI) calc'd for C₂₄H₂₈³⁵ClNO₇Na (M + Na)⁺ 532.1173, found 532.1174.

(1*R, 2*S**, 7*R**, 8*S**)-7-Methoxy-1-methyl-4-tosyl-11-oxa-4-azabicyclo[5.3.1]undecane-2,8-diol (148)**



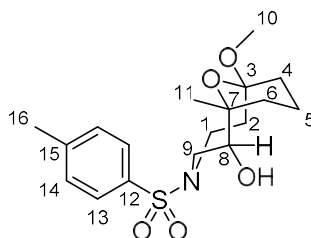
*m*CPBA (70%, 47 mg, 190 μ mol) was added to a solution of enol ether **124** (50 mg, 150 μ mol) in a 1:1 mixture of CH_2Cl_2 (1.2 mL) and MeOH (1.2 mL). The resultant solution was stirred for 45 min at r.t., after which time, $\text{Na}_2\text{S}_2\text{O}_3$ (aq) (3 mL) was added and the mixture was stirred for 10 min. The two phases were then separated and the organic phase was washed sequentially with NaHCO_3 (aq) (5 mL), H_2O (5 mL) and brine (5 mL). The organic phase was dried (MgSO_4), filtered and the solvent was then removed under reduced pressure to give a white solid, which was purified by flash column chromatography (eluent: 35% EtOAc in hexane) to yield acetal **148** as a white, crystalline solid (50 mg, 88%). R_f (50% EtOAc in hexane) = 0.5; mp 96 – 98 $^\circ\text{C}$; IR (neat / cm^{-1}) 3452 br m, 2941 m, 1325 m, 1156 s, 1044 s; ^1H NMR (400 MHz, CDCl_3) δ_{H} 7.68 – 7.64 (AA' of AA'BB', 2H, H-13), 7.32 – 7.28 (BB' of AA'BB', 2H, H-14), 4.15 (app. d, J = 6.7 Hz, 1H, H-8), 3.79 (app. dd, J = 14.3, 8.3 Hz, 1H, H-1_a), 3.64 – 3.55 (stack, 2H, H-4 and H-9_a), 3.36 – 3.30 (stack, 4H, H-9_b and H-10), 3.10 – 3.01 (m, 1H, H-1_b), 2.74 (br s, 2H, OH), 2.42 (s, 3H, H-16), 2.21 – 2.13 (m, 1H, H-2_a), 1.94 – 1.78 (stack, 4H, H-2_b, H-5 and H-6_a), 1.75 – 1.64 (m, 1H, H-6_b), 1.17 (s, 3H, H-11); ^{13}C NMR (101 MHz, CDCl_3) δ_{C} 143.4 (C, C-15), 136.9 (C, C-12), 129.8 (CH, C-14), 126.8 (CH, C-13), 98.7 (C, C-3), 76.8 (C, C-7), 74.5 (CH, C-8), 66.4 (CH, C-4), 53.7 (CH_2 , C-9), 50.7 (CH_3 , C-10), 44.1, (CH_2 , C-1), 36.6 (CH, C-2), 25.3 (CH_2 , C-6), 23.1 (CH_2 , C-5), 22.7 (CH_3 , C-11), 21.5 (CH_3 , C-16); LRMS (ESI) m/z 408.2 [(M + Na)⁺, 40%], 397.2 (10), 336.1 (30); HRMS (ESI) calc'd for $\text{C}_{18}\text{H}_{27}\text{NO}_6\text{SNa}$ (M + Na)⁺ 408.1457, found 408.1455.

(1*R, 2*S**, 7*R**, 8*S**)-8-Iodo-7-methoxy-1-methyl-4-tosyl-11-oxa-4-azabicyclo[5.3.1]undecan-2-ol (**149**)**



NIS (20 mg, 89 μmol) was added to a solution of enol ether **124** (20 mg, 59 μmol) in a 1:1 mixture of CH_2Cl_2 (0.5 mL) and MeOH (0.5 mL). The resultant solution was stirred for 1.5 h at r.t., after which time, $\text{Na}_2\text{S}_2\text{O}_3$ (aq) (3 mL) was added and the mixture was stirred for 10 min. The two phases were separated and the organic phase was washed sequentially with NaHCO_3 (aq) (5 mL), H_2O (5 mL) and brine (5 mL). The organic phase was dried (MgSO_4), filtered and the solvent was then removed under reduced pressure to give a white solid, which was purified by flash column chromatography (eluent: 35% EtOAc in hexane) to yield acetal **149** as a white, crystalline solid (18 mg, 62%). R_f (50% EtOAc in hexane) = 0.4; mp 82 – 84 $^\circ\text{C}$; IR (neat / cm^{-1}) 3469 br (O-H), 2943 br w, 1448 w, 1323 m, 1157 s, 1047 s; ^1H NMR (400 MHz, CDCl_3) δ_{H} 7.67 – 7.63 (AA' of AA'BB', 2H, H-13), 7.31 – 7.27 (BB' of AA'BB', 2H, H-14), 4.40 (app. t, $J = 3.6$ Hz, 1H, H-4), 4.20 (app. d, $J = 6.7$ Hz, 1H, H-8), 3.77 (dd, $J = 14.6, 7.9$ Hz, 1H, H-1_a), 3.62 (app. d, $J = 14.4$ Hz, 1H, H-9_a), 3.30 (dd, $J = 14.5, 6.9$ Hz, 1H, H-9_b), 3.20 (s, 3H, H-10), 2.95 (ddd, $J = 14.6, 7.5, 1.7$ Hz, 1H, H-1_b), 2.42 (s, 3H, H-16), 2.26 – 1.86 (stack, 6H, H-2, H-5, H-6), 1.22 (s, 3H, H-11), *OH* not observed; ^{13}C NMR (101 MHz, CDCl_3) δ_{C} 143.6 (C, C-15), 136.6 (C, C-12), 129.9 (CH, C-14), 126.8 (CH, C-13), 98.2 (C, C-3), 77.3 (C, C-7), 76.0 (CH, C-8), 53.8 (CH_2 , C-9), 50.4 (CH_3 , C-10), 44.8, (CH_2 , C-1), 36.3 (CH, C-4), 34.0 (CH_2 , C-2), 29.1 (CH_2 , C-5), 28.2 (CH_2 , C-6), 23.1 (CH_3 , C-11), 21.6 (CH_3 , C-16); LRMS (ESI) m/z 518.1 [(M + Na)⁺, 100%], 464.1 (10); HRMS (ESI) calc'd for $\text{C}_{18}\text{H}_{26}^{127}\text{INO}_5\text{SNa}$ (M + Na)⁺ 518.0474, found 518.0472.

(1*R, 2*S**, 7*S**)-7-Methoxy-1-methyl-4-tosyl-11-oxa-4-azabicyclo[5.3.1]undecan-2-ol (**154**)**

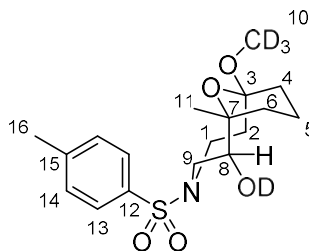


Method A: TsOH·H₂O (3.1 mg, 0.016 mmol) was added to a solution of epoxide **122** (109 mg, 0.323 mmol) in MeOH (5 mL). The resultant solution was stirred for 6 h at r.t., after which time, NaHCO_{3(aq)} (5 mL) was added. The solution was diluted with EtOAc (8 mL) and the layers were separated. The aqueous layer was washed with EtOAc (3 × 8 mL). The combined organic phases were dried (MgSO₄), filtered and the solvent was then removed under reduced pressure to give a white crystalline solid. Purification by flash column chromatography (eluent: 35% EtOAc in hexane) yielded acetal **154** as a white, crystalline solid (113 mg, 95%). *R_f* (50% EtOAc in hexane) = 0.4; mp 85 – 86 °C; IR (neat / cm⁻¹) 3460 br (O-H), 2938 m, 1449 w, 1326 s, 1158 s; ¹H NMR (400 MHz, CDCl₃) δ_H 7.68 – 7.64 (AA' of AA'BB', 2H, H-13), 7.30 – 7.26 (BB' of AA'BB', 2H, H-14), 4.21 – 4.16 (m, 1H, H-8), 3.80 (app. dd, *J* = 14.6, 7.9 Hz, 1H, H-1_a), 3.60 (dd, *J* = 14.5, 1.4 Hz, 1H, H-9_a), 3.32 (dd, *J* = 14.5, 6.7 Hz, 1H, H-9_b), 3.19 (s, 3H, H-10), 3.00 (ddd, *J* = 14.6, 7.5, 1.7 Hz, 1H, H-1_b), 2.42 (s, 3H, H-16), 2.03 – 1.97 (stack, 2H, H-2), 1.93 – 1.86 (m, 1H, H-6_a), 1.75 – 1.65 (stack, 3H, H-5 and H-4_a), 1.56 (br s, 1H, OH), 1.37 – 1.33 (m, 1H, H-4_b), 1.29 – 1.22 (m, 1H, H-6_b), 1.12 (s, 3H, H-11); ¹³C NMR (101 MHz, CDCl₃) δ_C 143.2 (C, C-15), 137.2 (C, C-12), 129.8 (CH, C-14), 126.9 (CH, C-13), 99.3 (C, C-3), 76.6 (C, C-7), 74.9 (CH, C-8), 53.8 (CH₂, C-9), 48.2 (CH₃, C-10), 44.1 (CH₂, C-1), 40.8 (CH₂, C-2), 31.8 (CH₂, C-6), 28.6 (CH₂, C-4), 22.9 (CH₃, C-11), 21.6 (CH₃, C-16), 17.4 (CH₂, C-5); LRMS (ESI) *m/z* 392.5 [(M + Na)⁺, 100%]; HRMS (ESI) calc'd for C₁₈H₂₇NO₅NaS (M + Na)⁺ 392.1508, found 392.1505.

Method B: TsOH·H₂O (2.1 mg, 0.01 mmol) was added to a solution of enol ether **124** (34 mg, 0.10 mmol) in MeOH (1 mL). The resultant solution was stirred for 2 h at r.t., after which time, NaHCO_{3(aq)} (2 mL) was added. The solution was diluted with EtOAc (5 mL) and the layers were separated. The aqueous layer was washed with EtOAc (3 × 5 mL). The combined organic phases were dried (MgSO₄), filtered and the solvent was then removed under reduced pressure to give acetal **154** as a white crystalline solid (36 mg, quant.), which required no further

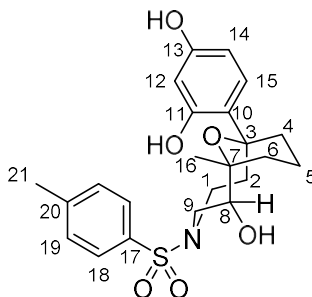
purification. Data were in agreement with those obtained for acetal **154** that was prepared using method A.

(1*R, 2*S**, 7*S**)-7-(Methoxy-*d*₃)-1-methyl-4-tosyl-11-oxa-4-azabicyclo[5.3.1]undecan-2-ol-*d* (155)**



TsOH·H₂O (0.60 mg, 3.1 μmol) was added to a solution of acetal **154** (13 mg, 36 μmol) in MeOD-*d*₄ (1 mL). The resultant solution was stirred for 2 h at r.t., after which time, NaHCO_{3(aq)} (2 mL) was added. The solution was diluted with EtOAc (5 mL) and the layers were separated. The aqueous layer was washed with EtOAc (3 × 5 mL). The combined organic phases were dried (MgSO₄), filtered and the solvent was then removed under reduced pressure to give a white crystalline solid (13 mg, quant.), which required no further purification. NMR data were in agreement with those for acetal **154**, except for the absence of the resonances at δ_H = 3.19 ppm and 1.56 ppm in the ¹H NMR spectrum, and the presence of a septet at δ_C = 48.2 ppm in the ¹³C NMR spectrum; LRMS (ESI) *m/z* 396.2 [(M + Na)⁺, 100%]; HRMS (ESI) calc'd for C₁₈H₂₃²H₄NO₅NaS (M + Na)⁺ 396.1759, found 396.1760.

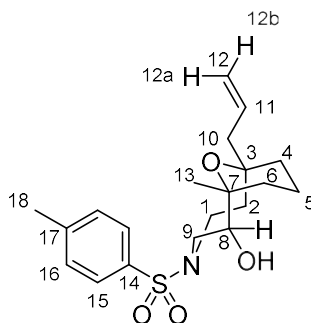
4-((1'S*, 6'S*, 7'R*)-6'-Hydroxy-7'-methyl-4'-tosyl-11'-oxa-4'-azabicyclo[5.3.1]undecan-1'-yl)benzene-1,3-diol (156)



TsOH·H₂O (4.0 mg, 21 μmol) was added to a solution of acetal **154** (80 mg, 0.22 mmol) in CH₂Cl₂ (2 mL). Resorcinol (120 mg, 1.1 mmol) was added in one portion and the resultant solution was stirred for 3 h at r.t., after which time, NaHCO_{3(aq)} (5 mL) was added. The solution was diluted with CH₂Cl₂ (8 mL) and the layers were separated. The aqueous layer was washed with CH₂Cl₂ (3 × 8 mL). The organic phases were combined, dried (MgSO₄), filtered and the solvent was then removed under reduced pressure to give a white crystalline solid. The crude product was washed with CHCl₃ (3 × 8 mL) and isolated by suction filtration to afford alcohol **156** as a white crystalline solid (72 mg, 74%). *R_f* (50% EtOAc in hexane) = 0.3; mp 91 – 93 °C; IR (neat / cm⁻¹) 3460 br w (O-H), 3259 br w (O-H), 2940 br m, 1692 s, 1318 m, 1153 s; ¹H NMR (400 MHz, acetone – *d*₆) δ_H 9.22 (br s, 1H, ArOH), 8.13 (s, 1H, ArOH), 7.69 – 7.65 (AA' of AA'BB', 2H, H-18), 7.39 – 7.35 (BB' of AA'BB', 2H, H-19), 7.01 – 6.90 (m, 1H, H-15), 6.25 (dd, *J* = 8.6, 2.6 Hz, 1H, H-14), 6.22 – 6.19 (m, 1H, H-12), 4.70 (br s, 1H, OH), 4.35 (app. t, *J* = 6.2 Hz, 1H, H-8), 3.86 – 3.77 (stack, 2H, H-1_a and H-9_a), 3.20 (dd, *J* = 14.1, 6.8 Hz, 1H, H-9_b), 2.62 – 2.48 (stack, 2H, H-1_b and H-2_a), 2.39 (s, 3H, H-21), 2.18 – 2.08 (stack, 2H, H-2_b and H-6_a), 1.88 – 1.77 (m, 1H, H-5_a), 1.74 – 1.60 (stack, 3H, H-4 and H-5_b), 1.43 – 1.31 (m, 1H, H-6_b), 1.21 (s, 3H, H-16); ¹³C NMR (101 MHz, acetone – *d*₆) δ_C 158.3 (2 × C, C-11 and C-13), 144.0 (C, C-20), 138.1 (C, C-17), 130.6, (CH, C-19), 128.3 (CH, C-15), 127.8 (CH, C-18), 107.4 (CH, C-14), 104.7 (CH, C-12), 73.8 (CH, C-8), 73.7 (C, C-3), 54.3 (CH₂, C-9), 45.5 (CH₂, C-1), 38.3 (CH₂, C-2), 35.7 (CH₂, C-4), 32.8 (CH₂, C-6), 24.1 (CH₃, C-16), 21.4

(CH₃, C-21), 16.5 (CH₂, C-5)^{xxiii}; LRMS (ESI) *m/z* 470.2 [(M + Na)⁺, 100%], 448.2 (12), 360.1 (12); HRMS (ESI) calc'd for C₂₃H₂₉NO₆NaS (M + Na)⁺ 470.1613, found 470.1615.

(1*R, 2*S**, 7*R**)-7-Allyl-1-methyl-4-tosyl-11-oxa-4-azabicyclo[5.3.1]undecan-2-ol (157)**

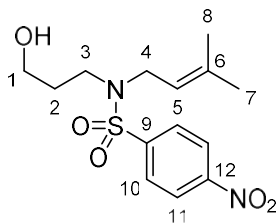


BF₃·OEt₂ (20 μL, 0.19 mmol) was added to a solution of acetal **154** (69 mg, 0.19 mmol) in CH₂Cl₂ (2 mL) at 0 °C. Allyltrimethylsilane (150 μL, 0.94 mmol) was then added dropwise over 1 min. The resultant solution was stirred for 2 h at 0 °C, after which time, NaHCO_{3(aq)} (5 mL) was added. The solution was diluted with CH₂Cl₂ (8 mL) and the layers were separated. The aqueous layer was washed with CH₂Cl₂ (3 × 8 mL). The combined organic phases were dried (MgSO₄), filtered and the solvent was then removed under reduced pressure to give a colourless oil. Purification by flash column chromatography (eluent: 35% EtOAc in hexane) yielded alcohol **157** as a white, crystalline solid (47 mg, 66%). *R*_f (50% EtOAc in hexane) = 0.4; mp 89 – 91 °C; IR (neat / cm⁻¹) 3490 br (O-H), 2935 br m, 1324 m, 1155 s; ¹H NMR (400 MHz, CDCl₃) δ_H 7.69 – 7.64 (AA' of AA'BB', 2H, H-15), 7.32 – 7.27 (BB' of AA'BB', 2H, H-16), 5.78 – 5.64 (m, 1H, H-11), 5.04 (d, *J* = 10.5 Hz, 1H, H-12_b), 4.97 (d, *J* = 17.4 Hz, 1H, H-12_a), 4.24 (app. t, *J* = 5.6 Hz, 1H, H-8), 3.85 (app. dd, *J* = 14.7, 9.1 Hz, 1H, H-1_a), 3.62 (dd, *J* = 14.4, 1.7 Hz, 1H, H-9_a), 3.25 (dd, *J* = 14.4, 6.6 Hz, 1H, H-9_b), 2.83 (app. dd, *J* = 14.3, 7.9 Hz, 1H, H-1_b), 2.43 (br s, 1H, OH), 2.42 (s, 3H, H-18), 2.14 (dd, *J* = 14.2, 5.8 Hz, 1H, H-10_a), 1.97 – 1.85 (stack, 3H, H-2_a, H-4_a and H-10_b), 1.77 – 1.62 (stack, 2H, H-2_b and H-5_a), 1.59 – 1.51

^{xxiii} Within the HMBC spectrum a correlation between H-14 and a ¹³C resonance at 77.0 ppm can be seen, believed to be C-7. However, as the carbon resonance cannot be seen in the standard ¹³C NMR spectrum, the carbon resonance has not been explicitly assigned. C-10 is also not observed.

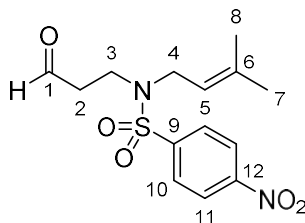
(m, 1H, H-5_b), 1.43 (app. td, $J = 13.4, 4.3$ Hz, 1H, H-6_a), 1.32 – 1.24 (m, 1H, H-4_b), 1.18 (app. td, $J = 13.5, 4.3$ Hz, 1H, H-6_b), 1.03 (s, 3H, H-13); ¹³C NMR (101 MHz, CDCl₃) δ_c 143.3 (C, C-17), 137.3 (C, C-14), 134.3 (CH, C-11), 129.8 (CH, C-16), 126.9 (CH, C-15), 118.2 (CH₂, C-12), 75.0 (CH, C-8), 74.3 (C, C-7), 73.5 (C, C-3), 53.7 (CH₂, C-9), 47.1 (CH₂, C-10), 44.5 (CH₂, C-1), 37.9 (CH₂, C-2), 32.3 (CH₂, C-6), 32.2 (CH₂, C-4), 23.5 (CH₃, C-13), 21.6 (CH₃, C-18), 15.3 (CH₂, C-5); LRMS (ESI) m/z 402.2 [(M + Na)⁺, 100%], 380.2 (30), 360.1 (20); HRMS (ESI) calc'd for C₂₀H₂₉NO₄NaS (M + Na)⁺ 402.1715, found 402.1719.

***N*-(3'-Hydroxypropyl)-*N*-(3''-methylbut-2''-en-1''-yl)-4-nitrobenzenesulfonamide (163)**



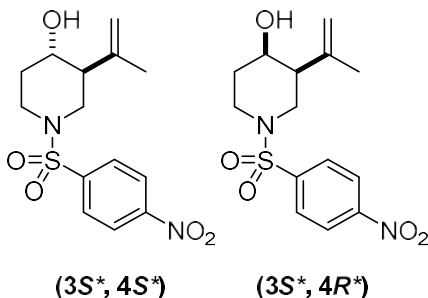
NEt₃ (3.90 mL, 28.3 mmol) was added to a solution of amine **78** (3.13 g, 21.8 mmol) in CH₂Cl₂ (105 mL). The solution was cooled to 0 °C. *p*NsCl (4.59 g, 20.7 mmol) was added in one portion and the reaction mixture was warmed to r.t. After 12 h, the reaction mixture was washed sequentially with HCl_(aq) (1 M, 80 mL), H₂O (80 mL) and brine (80 mL). The organic layer was dried (MgSO₄), filtered and the solvent was then removed under reduced pressure to provide an orange oil, which was purified by flash column chromatography (eluent: 50% EtOAc in hexane) to yield sulfonamide **163** as an orange oil (4.84 g, 71%). *R*_f (50% EtOAc in hexane) = 0.5; IR (neat / cm⁻¹) 3546 br w (O-H), 2933 w, 1734 br, 1527 s, 1346 s, 1156 s; ¹H NMR (400 MHz, CDCl₃) δ_H 8.37 – 8.33 (AA' of AA'BB', 2H, H-11), 8.00 – 7.96 (BB' of AA'BB', 2H, H-10), 4.90 (t with unresolved ⁴*J* coupling, *J* = 7.2 Hz, 1H, H-5), 3.88 (d, *J* = 7.2 Hz, 2H, H-4), 3.74 (app. q, *J* = 5.6 Hz, 2H, H-1), 3.29 (t, *J* = 6.5 Hz, 2H, H-3), 2.17 (t, *J* = 5.6 Hz, 1H, OH), 1.80 – 1.72 (m, 2H, H-2), 1.64 (app. s, 6H, H-8 and H-7); ¹³C NMR (101 MHz, CDCl₃) δ_C 150.1 (C, C-12), 146.2 (C, C-9), 138.2 (C, C-6), 129.6 (CH, C-10), 124.4 (CH, C-11), 118.0 (CH, C-5), 58.9 (CH₂, C-1), 45.7 (CH₂, C-4), 44.0 (CH₂, C-3), 31.0 (CH₂, C-2), 25.9 (CH₃, C-8 or C-7), 18.0 (CH₃, C-7 or C-8); LRMS (ESI) *m/z* 351.1 [(M + Na)⁺, 100%], 261.1 (20), 243.1 (30); HRMS (ESI) calc'd for C₁₄H₂₀N₂O₅Na (M + Na)⁺ 351.0991, found 351.0992.

***N*-(3'-Methylbut-2'-en-1'-yl)-4-nitro-*N*-(3''-oxopropyl)benzenesulfonamide (164)**



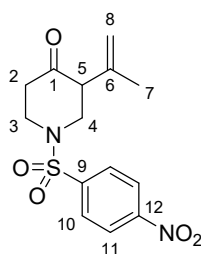
DMSO (2.6 mL, 37 mmol) was added dropwise over 2 min to a solution of oxalyl chloride (1.5 mL, 18 mmol) in CH₂Cl₂ (45 mL) at -78 °C. The resultant solution was stirred for 10 min, after which time, a solution of alcohol **163** (4.84 g, 14.7 mmol) in CH₂Cl₂ (15 mL) was added dropwise over 5 min. After 1 h, NEt₃ (10 mL, 74 mmol) was added and the resulting solution was warmed to r.t. over 5 min. H₂O (40 mL) was added to the reaction mixture and the layers were separated. The aqueous layer was extracted with CH₂Cl₂ (3 × 30 mL), the organic fractions were combined, dried (MgSO₄) and filtered. The solvent was then removed under reduced pressure to give an orange oil which was used without further purification in the following cyclisation reaction (see p 179) (4.81 g). *R*_f (50% EtOAc in hexane) = 0.4; IR (neat / cm⁻¹) 2939 w, 1722 s (C=O), 1529 s, 1349 s, 1161 s; ¹H NMR (400 MHz, CDCl₃) δ_H 9.76 (s, 1H, H-1), 8.38 – 8.33 (AA' of AA'BB', 2H, H-11), 8.00 – 7.95 (BB' of AA'BB', 2H, H-10), 4.92 (t with unresolved ⁴J coupling, *J* = 7.2 Hz, 1H, H-5), 3.86 (d, *J* = 7.2 Hz, 2H, H-4), 3.42 (t, *J* = 7.0 Hz, 2H, H-3), 2.84 (td, *J* = 7.0, 1.0 Hz, 2H, H-2), 1.65 (s, 3H, H-8 or H-7), 1.63 (s, 3H, H-7 or H-8); ¹³C NMR (101 MHz, CDCl₃) δ_C 200.0 (CH, C-1), 150.1 (C, C-12), 145.7 (C, C-9), 138.7 (C, C-6), 128.5 (CH, C-10), 124.4 (CH, C-11), 118.0 (CH, C-5), 46.6 (CH₂, C-4), 44.0 (CH₂, C-2), 41.2 (CH₂, C-3), 25.8 (CH₃, C-8 or C-7), 18.1 (CH₃, C-7 or C-8); LRMS (ESI) *m/z* 381.1 [(M + Na + MeOH)⁺, 100%]; HRMS (ESI) calc'd for C₁₅H₂₂N₂O₆SNa (M + Na + MeOH)⁺ 381.1096, found 381.1101.

(3*S, 4*S**)-1-((4-Nitrophenyl)sulfonyl)-3-(prop-1'-en-2'-yl)piperidin-4-ol (165A)**
& (3*S, 4*R**)-1-((4-nitrophenyl)sulfonyl)-3-(prop-1'-en-2'-yl)piperidin-4-ol**
(165B)



SnCl₄ (1 M solution in heptanes, 2.9 mL, 2.9 mmol) was added to a solution of aldehyde **164** (4.79 g, 14.7 mmol, used without purification, see p 178) in CH₂Cl₂ (140 mL) at 0 °C. The resulting solution was stirred for 16 h, after which time, NH₄Cl_(aq) (100 mL) was added. The phases were separated and the aqueous phase was extracted with CH₂Cl₂ (3 × 70 mL). The combined organic phases were washed with brine (100 mL), dried (MgSO₄), filtered and evaporated under reduced pressure to give a bright yellow oil, which was used without further purification in the following oxidation step (4.56 g). By integration of the isopropenyl resonances at 4.91 and 4.50 ppm in the ¹H NMR spectrum of the crude product, the diastereomeric ratio of (3*S**, 4*S**) to (3*R**, 4*S**) was determined to be 7: 3.

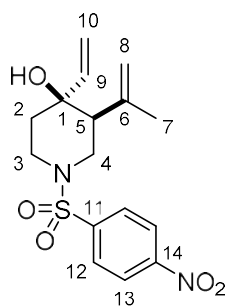
1-((4-Nitrophenyl)sulfonyl)-3-(prop-1'-en-2'-yl)piperidin-4-one (166)



DMSO (2.5 mL, 35 mmol) was added dropwise over 2 min to a solution of oxalyl chloride (1.4 mL, 17 mmol) in CH₂Cl₂ (45 mL) at -78 °C. The resultant solution was stirred for 10 min, after which time, a solution of alcohol **165** (4.56 g, 14.0 mmol, used without purification) in CH₂Cl₂ (15 mL) was added dropwise over 10 min. After 1 h, Pr₂NEt (13.2 mL, 75.3 mmol) was added in one portion. After stirring for 15 min at -78 °C, the temperature of the solution was raised to 0 °C by replacing the cooling bath with an ice-water bath. The mixture was stirred for 30

min at this temperature. $\text{HCl}_{(\text{aq})}$ (1 M, 60 mL) was then added and the solution was vigorously stirred for 15 min at 0 °C. The two phases were then separated and the aqueous phase was washed with CH_2Cl_2 (3 × 40 mL). The combined organic phases were dried (MgSO_4), filtered and the solution concentrated under reduced pressure to a volume of *ca.* 15 mL. This solution was then added directly to a column containing silica and the compound was purified by flash column chromatography (eluent: 40% EtOAc in hexane) to yield piperidinone **166** as a cream, crystalline solid (3.670 g, 81% over 3 steps). R_f (50% EtOAc in hexane) = 0.4; m.p. 84 – 86 °C; IR (neat / cm^{-1}) 2982 w, 1721 s (C=O), 1533 s, 1342 s, 1159 s; ^1H NMR (400 MHz, CDCl_3) δ_{H} 8.43 – 8.40 (AA' of AA'BB', 2H, H-11), 8.02 – 7.98 (BB' of AA'BB', 2H, H-10), 5.08 – 5.06 (m, 1H, H-8_a or H-8_b), 4.92 – 4.90 (m, 1H, H-8_b or H-8_a), 3.80 – 3.71 (stack, 2H, H-3_a and H-4_a), 3.29 – 3.16 (stack, 3H, H-3_b, H-4_b & H-5), 2.65 – 2.60 (stack, 2H, H-2), 1.74 (s, 3H, H-7); ^{13}C NMR (101 MHz, CDCl_3) δ_{C} 204.5 (C, C-1), 150.6 (C, C-12), 142.7 (C, C-6), 139.4 (C, C-9), 128.8 (CH, C-10), 124.8 (CH, C-11), 115.7 (CH_2 , C-8), 56.7 (CH, C-5), 49.6 (CH_2 , C-3), 46.3 (CH_2 , C-4), 40.1 (CH_2 , C-2), 21.8 (CH_3 , C-7); LRMS (ESI) m/z 325.1 [(M + H)⁺, 100%], 261.2 (10); HRMS (ASAP) calc'd for $\text{C}_{14}\text{H}_{26}\text{N}_2\text{O}_5\text{S}$ (M + H)⁺ 325.0858, found 325.0863.

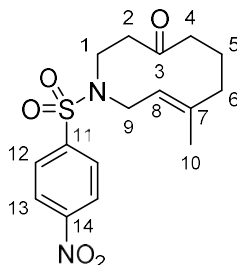
(3S*, 4S*)-1-((4-Nitrophenyl)sulfonyl)-3-(prop-1'-en-2'-yl)-4-vinylpiperidin-4-ol (167)



$\text{CeCl}_3 \cdot 7\text{H}_2\text{O}$ (5.48 g, 14.7 mmol) was heated at 140 °C under high vacuum (< 2 mbar) for 2 h, and then cooled to r.t. THF (45 mL) was added and the resulting slurry was stirred vigorously for 2 h, before being cooled to –78 °C. Vinylmagnesium bromide (0.76 M solution in THF, 17.8 mL, 13.5 mmol) was added and the resulting mixture was stirred for 30 min, after which time, a solution of piperidinone **166** (3.66 g, 11.3 mmol) in THF (25 mL) was added dropwise over 4 min. The resulting mixture was stirred at –78 °C for 4 h before being poured into a solution of acetic acid_(aq) (5%, 50 mL). The aqueous layer was extracted with EtOAc (3 × 50 mL). The combined organic fractions were washed with $\text{NaHCO}_{3(\text{aq})}$ (2 × 50 mL), dried (MgSO_4), filtered

and the solvent was then removed under reduced pressure to give a dark yellow oil, which contained only one diastereomer by analysis of the ^1H NMR spectrum of the crude product. The crude product was purified by flash column chromatography (eluent: 30% EtOAc in hexane) to yield allylic alcohol **167** as a white crystalline solid (0.484 g, 12%). R_f (50% EtOAc in hexane) = 0.6; mp 107 – 109 °C; IR (neat / cm^{-1}) 3522 s (O-H), 2856 w, 1328 m, 1154 s; ^1H NMR (400 MHz, CDCl_3) δ_{H} 8.42 – 8.38 (AA' of AA'BB', 2H, H-13), 7.98 – 7.94 (BB' of AA'BB', 2H, H-12), 5.85 (dd, $J = 17.2, 10.8$ Hz, 1H, H-9), 5.21 (dd, $J = 17.2, 0.9$ Hz, 1H, H-10_{trans}), 5.10 (dd, $J = 10.8, 0.9$ Hz, 1H, H-10_{cis}), 4.97 (s, 1H, H-8_a or H-8_b), 4.61 (s, 1H, H-8_b or H-8_a), 3.75 – 3.68 (m, 1H, H-3_a), 3.61 (ddd, $J = 11.3, 4.1, 2.0$ Hz, 1H, H-4_a), 2.75 – 2.67 (m, 1H, H-3_b), 2.63 (app. t, $J = 12.0$ Hz, 1H, H-4_b), 2.42 (dd, $J = 12.2, 4.0$ Hz, 1H, H-5), 1.94 – 1.84 (m, 1H, H-2_a), 1.77 (s, 3H, H-7), 1.70 – 1.68 (m, 1H, H-2_b), 1.66 (app. t, $J = 2.6$ Hz, 1H, OH); ^{13}C NMR (101 MHz, CDCl_3) δ_{C} 150.4 (C, C-14), 144.1 (C, C-6), 143.7 (CH, C-9), 142.8 (C, C-11), 128.9 (CH, C-12), 124.6 (CH, C-13), 113.5 (CH_2 , C-8), 113.2 (CH_2 , C-10), 70.5 (C, C-1), 50.3 (CH, C-5), 45.8 (CH_2 , C-4), 42.0 (CH_2 , C-3), 36.5 (CH_2 , C-2), 26.4 (CH_3 , C-7); LRMS (ESI) m/z 353.1 [(M + H)⁺, 55%], 335.1 (70); HRMS (ESI) calc'd for $\text{C}_{16}\text{H}_{21}\text{N}_2\text{O}_5\text{S}$ (M + H)⁺ 353.1171, found 353.1174.

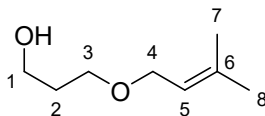
(E)-8-Methyl-1-((4-nitrophenyl)sulfonyl)-2,3,5,6,7,10-hexahydroazecin-4(1H)-one (168)



[(C₆H₅CN)₂PdCl₂] (26 mg, 0.067 mmol) was added in one portion to a stirred solution of allylic alcohol **167** (0.470 g, 1.33 mmol) in benzene (50 mL). After 2 h, the solvent was removed under reduced pressure to give an orange oil, which was purified by flash column chromatography (eluent: 35% EtOAc in hexane) to yield ketone **168** as a cream crystalline solid (0.362 g, 77%). *R_f* (50% EtOAc in hexane) = 0.5; mp 117 – 119 °C; IR (neat / cm⁻¹) 2942 w, 1692 (C=O), 1523 s, 1345 s, 1160 s; ¹H NMR (400 MHz, CDCl₃) δ_H 8.39 – 8.35 (AA' of AA'BB', 2H, H-13), 7.98 – 7.95 (BB' of AA'BB', 2H, H-12), 5.27 – 5.22 (m, 1H, H-8), 4.18 (app. d, *J* = 14.2 Hz, 1H, H-9_a), 3.88 – 3.76 (m, 1H, H-1_a), 3.28 (app. t, *J* = 12.5 Hz, 1H, H-9_b), 3.16 – 3.05 (m, 1H, H-1_b), 3.04 – 2.93 (m, 1H, H-2_a), 2.53 – 2.20 (stack, 4H, H-2_b, H-4, H-5_a), 2.15 – 2.06 (m, 1H, H-6_a), 1.97 – 1.86 (m, 1H, H-6_b), 1.79 – 1.72 (m, 1H, H-5_b), 1.43 (s, 3H, H-10); ¹³C NMR (101 MHz, CDCl₃) δ_C 208.0 (C, C-3), 145.8 (C, C-11), 144.1, (C, C-7), 128.2 (CH, C-12), 124.7 (CH, C-13), 120.8 (CH, C-8), 48.2 (CH₂, C-9), 45.9 (CH₂, C-2), 44.7 (CH₂, C-1), 43.1 (CH₂, C-4), 40.8 (CH₂, C-6), 25.4 (CH₂, C-5), 15.9 (CH₃, C-10), C-14 resonance not observed^{xxiv}; LRMS (ASAP) *m/z* 353.1 [(M + H)⁺, 55%], 335.1 (90); HRMS (ASAP) calc'd for C₁₆H₂₁N₂O₅S (M + H)⁺ 353.1171, found 353.1169.

^{xxiv}Within the HMBC spectrum a correlation between H-13 and a ¹³C resonance at 150.3 ppm can be seen, believed to be C-14; however, as the carbon resonance cannot be seen in the standard ¹³C NMR spectrum, the carbon resonance has not been explicitly assigned.

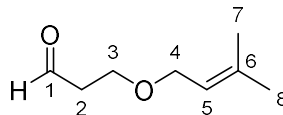
3-((3'-Methylbut-2'-en-1'-yl)oxy)propan-1-ol (**170**)



NaH (50% dispersion in mineral oil, 1.41 g, 29.4 mmol) was added in one portion to a solution of 1,3-propanediol (2.41 mL, 33.6 mmol) in DMF (50 mL) at 0 °C. The resultant solution was stirred for 20 min, after which time, prenyl bromide (1.62 mL, 14.0 mmol) was added dropwise over 1 min. The reaction mixture was then warmed to r.t. by removal of the cooling bath. After 3 h, $\text{NH}_4\text{Cl}_{(\text{aq})}$ (50 mL) was added. The phases were separated and the aqueous phase was extracted with EtOAc (3 × 70 mL). The combined organic phases were washed with brine (70 mL), dried (MgSO_4), filtered and evaporated under reduced pressure to give a yellow oil, which was purified by flash column chromatography (eluent: 40% EtOAc in hexane) to yield ether **170** as a pale yellow oil (1.14 g, 57%). R_f (50% EtOAc in hexane) = 0.5; IR (neat / cm^{-1}) 3381 br w (O-H), 2929 w, 2860 w, 1377 m, 1074 br s; ^1H NMR (400 MHz, CDCl_3) δ_{H} 5.33 (t with unresolved 4J coupling, $J = 7.0$ Hz, 1H, H-5), 3.96 (d, $J = 7.0$ Hz, 2H, H-4), 3.77 (app. q, $J = 5.4$ Hz, 2H, H-1), 3.60 (t, $J = 5.8$ Hz, 2H, H-3), 2.41 (t, $J = 5.4$ Hz, 1H, OH), 1.83 (app. quintet, $J = 5.7$ Hz, 2H, H-2), 1.74 (s, 3H, H-7 or H-8), 1.67 (s, 3H, H-7 or H-8); ^{13}C NMR (101 MHz, CDCl_3) δ_{C} 137.3 (C, C-6), 131.0 (CH, C-5), 69.5 (CH_2 , C-3), 67.7 (CH_2 , C-4), 62.4 (CH_2 , C-1), 32.2 (CH_2 , C-2), 25.9 (CH_3 , C-7 or C-8), 18.2 (CH_3 , C-7 or C-8); LRMS (ASAP) m/z 145.1 [(M + H) $^+$, 100%].

Data were in agreement with those reported in the literature.²¹⁵

3-((3'-Methylbut-2'-en-1'-yl)oxy)propanal (**171**)

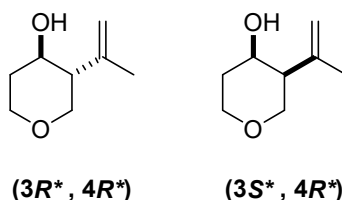


DMSO (1.36 mL, 19.1 mmol) was added dropwise over 2 min to a solution of oxalyl chloride (0.82 mL, 9.5 mmol) in CH_2Cl_2 (25 mL) at -78 °C. The resultant solution was stirred for 10 min, after which time, a solution of alcohol **170** (1.10 g, 7.63 mmol) in CH_2Cl_2 (10 mL) was added dropwise over 5 min. After 1 h, NEt_3 (14 mL, 102 mmol) was added and the solution was warmed to r.t. over 5 min. H_2O (30 mL) was added to the reaction mixture and the layers

were separated. The aqueous layer was extracted with CH₂Cl₂ (3 × 30 mL). The organic layers were combined, dried (MgSO₄), filtered and the solvent was then removed under reduced pressure to give aldehyde **171** as a yellow oil (1.09 g), which was used without further purification in the following cyclisation. *R_f* (50% EtOAc in hexane) = 0.5; IR (neat / cm⁻¹) 2860 br w, 1724 s (C=O), 1377 s, 1084 s; ¹H NMR (400 MHz, CDCl₃) δ_H 9.79 (t, *J* = 1.9 Hz, 1H, H-1), 5.33 (t with unresolved ⁴*J* coupling, *J* = 7.0 Hz, 1H, H-5), 3.98 (d, *J* = 7.0 Hz, 2H, H-4), 3.75 (t, *J* = 6.1 Hz, 2H, H-3), 2.67 (td, *J* = 6.2, 1.9 Hz, 2H, H-2), 1.74 (s, 3H, H-7 or H-8), 1.67 (s, 3H, H-7 or H-8); ¹³C NMR (101 MHz, CDCl₃) δ_C 201.4 (CH, C-1), 137.6 (C, C-6), 120.6 (CH, C-5), 67.6 (CH₂, C-4), 63.6 (CH₂, C-3), 44.0 (CH₂, C-2), 25.8 (CH₃, C-7 or C-8), 18.0 (CH₃, C-7 or C-8); LRMS (EI) *m/z* 142.1 [(M)⁺, 100%].

Data were in agreement with those reported in the literature.²¹⁵

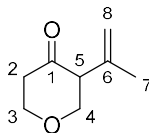
(3*R, 4*R**)-3-(Prop-1'-en-2'-yl)tetrahydro-2*H*-pyran-4-ol (172A) and (3*S**, 4*R**)-3-(prop-1'-en-2'-yl)tetrahydro-2*H*-pyran-4-ol (172B)**



SnCl₄ (1 M solution in heptanes, 0.76 mL, 0.76 mmol) was added to a solution of aldehyde **171** (1.09 g, 7.63 mmol, used without purification) in CH₂Cl₂ (76 mL) at 0 °C. The resulting solution was stirred for 16 h, after which time, NH₄Cl_(aq) (50 mL) was added. The aqueous phase was extracted with CH₂Cl₂ (3 × 40 mL) and the combined organic phases were washed with brine (100 mL), dried (MgSO₄) and evaporated under reduced pressure to give a bright yellow oil that was used in the following oxidation step (see p. 185) without further purification (1.68 g). By integration of the isopropenyl resonances at 4.92 and 4.62 ppm in the ¹H NMR spectrum of the crude product the diastereomeric ratio of the (3*R**, 4*R**) to (3*S**, 4*R**) stereoisomers was determined to be 3: 2.^{xxv}

^{xxv} These compounds have been previously synthesised, but were never isolated, so a comparison to a literature value for the diastereomeric ratio cannot be made.

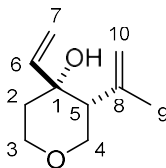
3-(Prop-1'-en-2'-yl)tetrahydro-4H-pyran-4-one (173)



DMSO (1.36 mL, 19.1 mmol) was added dropwise over 2 min to a solution of oxalyl chloride (0.82 mL, 9.54 mmol) in CH₂Cl₂ (20 mL) at -78 °C. The resultant solution was stirred for 10 min, after which time, a solution of alcohol **172** (1.09 g, 7.63 mmol, used without purification, see p 184) in CH₂Cl₂ (12 mL) was added dropwise over 5 min. After 1 h, Pr₂NEt (6.7 mL, 38 mmol) was added. After stirring for 15 min at -78 °C, the temperature of the solution was raised to 0 °C by replacing the cooling bath with an ice-water bath. The mixture was stirred for 30 min at this temperature. HCl_(aq) (1 M, 20 mL) was then added and the solution was vigorously stirred for 15 min at 0 °C. The two phases were then separated and the aqueous phase was washed with CH₂Cl₂ (3 × 30 mL). The combined organic phases were dried (MgSO₄), filtered and the solution concentrated under reduced pressure to a volume of *ca.* 15 mL. This solution was then added directly to a column containing silica and the compound was purified by flash column chromatography (eluent: 40% EtOAc in hexane) to yield pyranone **173** as a bright yellow oil (0.158 g, 15% over 3 steps). *R_f* (50% EtOAc in hexane) = 0.5; IR (neat / cm⁻¹) 2968 br w, 2858 br w, 1717 s (C=O), 1375 m, 1098 s; ¹H NMR (400 MHz, CDCl₃) δ_H 5.03 (app. quintet, *J* = 1.6 Hz, 1H, H-8_a or H-8_b), 4.89 – 4.87 (m, 1H, H-8_b or H-8_a), 4.16 – 4.09 (stack, 2H, H-3_a and H-4_a), 3.91 – 3.82 (stack, 2H, H-3_b and H-4_b), 3.18 – 3.13 (m, 1H, H-5), 2.57 – 2.52 (stack, 2H, H-2), 1.76 (s, 3H, H-7); ¹³C NMR (101 MHz, CDCl₃) δ_C 206.2 (C, C-1), 140.0 (C, C-6), 114.9 (CH₂, C-8), 71.6 (CH₂, C-3 or C-4), 68.4 (CH₂, C-3 or C-4), 59.0 (CH, C-5), 42.0 (CH₂, C-2), 22.0 (CH₃, C-7); LRMS (EI) *m/z* 140.1 [(M)⁺, 30%], 110.1 (10), 82.0 (20).

Data were in agreement with those reported in the literature.²¹⁵

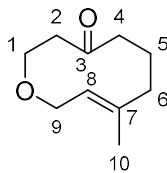
(3*R**, 4*R**)-3-(Prop-1'-en-2'-yl)-4-vinyltetrahydro-2H-pyran-4-ol (174)



CeCl₃·7H₂O (0.518 g, 1.39 mmol) was heated at 140 °C under high vacuum (< 2 mbar) for 2 h, and then cooled to r.t. THF (4 mL) was added and the resulting slurry was stirred vigorously for 2 h, before being cooled to -78 °C. Vinylmagnesium bromide (0.76 M solution in THF, 1.7 mL, 1.28 mmol) was added and the resulting mixture was stirred for 30 min, after which time, a solution of ketone **173** (0.150 g, 1.07 mmol) in THF (5 mL) was added dropwise over 4 min. The resulting mixture was stirred at -78 °C for 4 h before being poured into a solution of acetic acid_(aq) (5%, 18 mL). The aqueous layer was extracted with EtOAc (3 × 20 mL). The combined organic fractions were washed with NaHCO_{3(aq)} (2 × 20 mL), dried (MgSO₄), filtered and the solvent was then removed under reduced pressure to give a yellow oil, which contained only one diastereomer by analysis of the ¹H NMR spectrum of the crude product. The crude product was purified by flash column chromatography (eluent: 35% EtOAc in hexane) to yield allylic alcohol **174** as a clear oil (0.119 g, 66%). *R*_f (30% EtOAc in hexane) = 0.4; IR (neat / cm⁻¹) 3442 br w (O-H), 2951 m, 2865 m, 1639 m, 1375 m, 1116 s; ¹H NMR (400 MHz, CDCl₃) δ_H 5.89 (dd, *J* = 17.2, 10.6 Hz, 1H, H-6), 5.25 (dd, *J* = 17.2, 1.2 Hz, 1H, H-7_a), 5.07 (dd, *J* = 10.6, 1.2 Hz, 1H, H-7_b), 4.97 (app. t, *J* = 1.6 Hz, 1H, H-10_a), 4.68 (s, 1H, H-10_b), 3.82 – 3.77 (stack, 2H, H-3), 3.70 – 3.65 (stack, 2H, H-4), 2.36 (dd, *J* = 11.0, 5.3 Hz, 1H, H-5), 1.90 (d, *J* = 2.5 Hz, 1H, OH), 1.88 – 1.79 (m, 1H, H-2_a), 1.77 (dd, *J* = 1.5, 0.9 Hz, 3H, H-9), 1.54 – 1.50 (m, 1H, H-2_b); ¹³C NMR (101 MHz, CDCl₃) δ_C 144.9 (CH, C-6), 144.1 (C, C-8), 113.1 (CH₂, C-10), 112.2 (CH₂, C-7), 70.6 (C, C-1), 66.8 (CH₂, C-4), 63.6 (CH₂, C-3), 50.9 (CH, C-5), 37.0 (CH₂, C-2), 26.8 (CH₃, C-9); LRMS (ASAP) *m/z* 235.2 (100), 199.2 (20), 181.2 (20).

Data were in agreement with those reported in the literature.¹³⁶

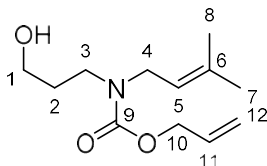
(E)-8-Methyl-2,3,5,6,7,10-hexahydro-4H-oxecin-4-one (68)



$[(C_6H_5CN)_2PdCl_2]$ (10 mg, 0.027 mmol) was added in one portion to a stirred solution of allylic alcohol **174** (91 mg, 0.54 mmol) in benzene (5 mL). After 3 h, the solvent was removed under reduced pressure to give an orange oil, which was purified by flash column chromatography (eluent: 25% EtOAc in hexane) to yield ketone **68** as a clear oil (25 mg, 28%). R_f (50% EtOAc in hexane) = 0.6; IR (neat / cm^{-1}) 2925 br m, 2863 m, 1699 s (C=O), 1103 s, 1076 s; 1H NMR (400 MHz, $CDCl_3$) δ_H 5.35 – 5.29 (m, 1H, H-8), 4.16 – 4.08 (m, 1H, H-9_a), 3.96 – 3.85 (stack, 2H, H-1_a and H-9_b), 3.74 – 3.66 (m, 1H, H-1_b), 2.94 (dd, J = 15.7, 8.8 Hz, 1H, H-2_a), 2.48 – 2.37 (stack, 2H, H-4_a and H-5_a), 2.30 (dd, J = 15.7, 7.8 Hz, 1H, H-2_b), 2.26 – 2.16 (m, 1H, H-4_b), 2.14 – 2.03 (m, 1H, H-6_a), 1.95 – 1.85 (m, 1H, H-6_b), 1.83 – 1.75 (m, 1H, H-5_b), 1.51 (s, 3H, H-10); ^{13}C NMR (101 MHz, $CDCl_3$) δ_C 208.6 (C, C-3), 143.1 (C, C-7), 123.9 (CH, C-8), 68.6 (CH₂, C-9), 66.9 (CH₂, C-1), 47.4 (CH₂, C-2), 43.5 (CH₂, C-4), 41.1 (CH₂, C-6), 26.3 (CH₂, C-5), 16.3 (CH₃, C-10); LRMS (ESI) m/z 191.1 [(M + Na)⁺, 100%], 289.2 (50), 307.2 (30), 325.2 (50).

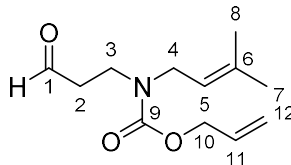
Data were in agreement with those reported in the literature.¹³⁶

Allyl (3'-hydroxypropyl)(3''-methylbut-2''-en-1''-yl)carbamate (**175**)



DBU (2.10 mL, 14.1 mmol) was added to a stirred solution of amine **78** (1.68 g, 11.8 mmol) in CH₂Cl₂ (24 mL), which was cooled to 0 °C. A solution of allyl chloroformate (1.4 mL, 13 mmol) in CH₂Cl₂ (4 mL) was added dropwise over 3 min. The cooling bath was removed and the reaction mixture warmed to r.t. After 12 h, the reaction mixture was washed sequentially with HCl_(aq) (1 M, 15 mL), NaHCO_{3(aq)} (15 mL) and brine (15 mL). The organic layer was dried (MgSO₄), filtered and the solvent was then removed under reduced pressure to provide a yellow oil, which was purified by flash column chromatography (eluent: 40% EtOAc in hexane) to afford carbamate **175** as a pale yellow oil (1.73 g, 65%). *R_f* (50% EtOAc in hexane) = 0.3; IR (neat / cm⁻¹) 3441 br w (O-H), 2935 br, 1670 br s (C=O), 1415 s, 1057 s; ¹H NMR (400 MHz, CDCl₃) δ_H 5.98 – 5.87 (m, 1H, H-11), 5.34 – 5.18 (stack, 2H, H-12), 5.17 – 5.11 (m, 1H, H-5), 4.59 (d, *J* = 5.5 Hz, 2H, H-10), 3.90 – 3.79 (m, 2H, H-4), 3.60 – 3.51 (m, 2H, H-1), 3.43 – 3.33 (m, 2H, H-3), 1.74 – 1.63 (stack, 8H, H-2, H-7 and H-8), *OH* not observed; ¹³C NMR (101 MHz, CDCl₃) δ_C 157.4 (C, C-9), 135.8 (C, C-6), 133.0 (CH, C-11), 120.2 (CH, C-5), 117.4 (CH₂, C-12), 66.4 (CH₂, C-10), 58.5 (CH₂, C-1), 44.6 (CH₂, C-4), 42.7 (CH₂, C-3), 30.5 (CH₂, C-2), 25.9 (CH₃, C-8 or C-7), 17.9 (CH₃, C-7 or C-8); LRMS (ESI) *m/z* 250.7 [(M + Na)⁺, 100%]; HRMS (ESI) calc'd for C₁₂H₂₁NO₃Na (M + Na)⁺ 250.1419, found 250.1417.

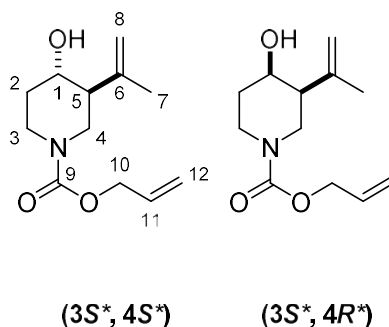
Allyl (3'-methylbut-2'-en-1'-yl)(3''-oxopropyl)carbamate (**176**)



DMSO (1.3 mL, 19 mmol) was added dropwise over 2 min to a solution of oxalyl chloride (0.80 mL, 9.0 mmol) in CH₂Cl₂ (25 mL) at -78 °C. The resultant solution was stirred for 10 min, after which time, a solution of alcohol **175** (1.70 g, 7.48 mmol) in CH₂Cl₂ (10 mL) was added dropwise over 5 min. After 1 h, NEt₃ (5.2 mL, 37 mmol) was added and the solution was warmed to r.t. over 5 min. H₂O (30 mL) was added to the reaction mixture and the resulting

layers were separated. The aqueous layer was extracted with CH_2Cl_2 (3×20 mL). The combined organic layers were dried (MgSO_4), filtered and the solvent was then removed under reduced pressure to give a yellow oil, which was used in the subsequent cyclisation step without further purification (1.68 g). R_f (50% EtOAc in hexane) = 0.5; IR (neat / cm^{-1}) 2928 br, 1693 br s (C=O), 1413 s, 1121 s; ^1H NMR (400 MHz, CDCl_3) δ_{H} 9.77 (s, 1H, H-1), 5.97 – 5.85 (m, 1H, H-11), 5.31 – 5.16 (stack, 2H, H-12), 5.15 – 5.09 (m, 1H, H-5), 4.57 (d, $J = 5.6$ Hz, 2H, H-10), 3.92 – 3.84 (m, 2H, H-4), 3.52 (t, $J = 6.7$ Hz, 2H, H-3), 2.71 (app. t, $J = 6.7$ Hz, 2H, H-2), 1.72 (s, 3H, H-7 or H-8), 1.67 (s, 3H, H-8 or H-7); ^{13}C NMR (101 MHz, CDCl_3) δ_{C} 201.2 (CH, C-1), 155.9 (C, C-9), 133.1 (CH, C-11), 120.2 (CH, C-5), 117.8 (C, C-6), 117.4 (CH_2 , C-12), 66.2 (CH_2 , C-10), 53.6 (CH_2 , C-4), 45.9 (CH_2 , C-3), 45.3 (CH_2 , C-2), 25.9 (CH_3 , C-8 or C-7), 17.9 (CH_3 , C-7 or C-8); LRMS (ESI) m/z 226.2 [(M + H) $^+$, 80%], 143.9 (100), 13.9 (60); HRMS (ESI) calc'd for $\text{C}_{12}\text{H}_{19}\text{NO}_3\text{Na}$ (M + Na) $^+$ 248.1257, found 248.1260.

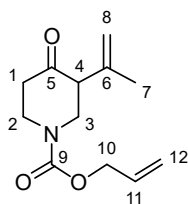
(3*S, 4*S**) Allyl 4-hydroxy-3-(prop-1'-en-2'-yl)piperidine-1-carboxylate (177A) & allyl (3*S**, 4*R**)-4-hydroxy-3-(prop-1'-en-2'-yl)piperidine-1-carboxylate (177B)**



SnCl_4 (1 M solution in heptanes, 0.75 mL, 0.75 mmol) was added to a solution of aldehyde **176** (1.70 g, 7.48 mmol, used without purification) in CH_2Cl_2 (75 mL) at 0 °C. The resulting solution was stirred for 16 h, after which time, $\text{NH}_4\text{Cl}_{(\text{aq})}$ (50 mL) was added. The aqueous phase was extracted with CH_2Cl_2 (3×40 mL) and the combined organic phases were washed with brine (100 mL), dried (MgSO_4) and evaporated under reduced pressure to give a bright yellow oil that was used in the subsequent oxidation step (see p 190) without further purification (1.68 g). By integration of the isopropenyl resonances at 4.93 and 4.72 ppm in the ^1H NMR spectrum of the crude product the diastereomeric ratio of (3*S**, 4*S**)-**177A** to (3*R**, 4*S**)-**177B** was determined to be 3: 2.

Normally, the product was used as a mixture since both diastereomers converge to the same product in the next oxidation step; however, the major (3*S**, 4*S**) isomer was once isolated by flash column chromatography (eluent: 40% EtOAc in hexane) to yield piperidinol **177A** as a yellow oil. R_f (50% EtOAc in hexane) = 0.3; IR (neat / cm^{-1}) 3230 br (O-H), 2935 w, 1684 br s (C=O), 1421 m, 1213 m; ^1H NMR (400 MHz, CDCl_3) δ_{H} 6.04 – 5.90 (m, 1H, H-11), 5.37 – 5.18 (stack, 2H, H-12), 5.05 (s, 1H, H-8_a), 4.75 (s, 1H, H-8_b), 4.65 – 4.56 (m, 2H, H-10), 4.09 (app. d, $J = 2.9$ Hz, 1 H, H-1), 4.07 – 3.90 (stack, 2H, H-3_a and H-4_a), 3.26 – 3.07 (stack, 2H, H-3_b and H-4_b), 2.27 – 2.18 (m, 1H, H-5), 1.98 – 1.89 (m, 1H, H-2_a), 1.82 (s, 3H, H-7), 1.77 – 1.67 (m, 1H, H-2_b), *OH* not observed; ^{13}C NMR (101 MHz, CDCl_3) δ_{C} 144.3 (C, C-6), 133.3 (CH, C-11), 117.4 (CH_2 , C-12), 112.5 (CH_2 , C-8), 66.1 (CH_2 , C-10), 64.0 (CH, C-1), 47.0 (CH, C-5), 41.7 (CH_2 , C-4), 38.5 (CH_2 , C-3), 31.4 (CH_2 , C-2), 23.0 (CH_3 , C-7)^{xxvi}; LRMS (ASAP) m/z 226.1 [(M + H)⁺, 60%], 208.1 (50), 164.1 (100); HRMS (ASAP) calc'd for $\text{C}_{12}\text{H}_{20}\text{NO}_3$ (M + H)⁺ 226.1443, found 226.1459.

Allyl 4-oxo-3-(prop-1'-en-2'-yl)piperidine-1-carboxylate (**178**)



Method A: DMSO (1.7 mL, 24 mmol) was added dropwise over 5 min to a solution of oxalyl chloride (1.0 mL, 12 mmol) in CH_2Cl_2 (30 mL) at -78 °C. The resultant solution was stirred for 10 min, after which time, a solution of alcohol **177** (2.13 g, 9.44 mmol, used without purification, see p 189) in CH_2Cl_2 (10 mL) was added dropwise over 5 min. After 1 h, Pr_2NEt (8.2 mL, 47 mmol) was added. After stirring for 15 min at -78 °C, the temperature of the solution was raised to 0 °C by replacing the cooling bath with an ice-water bath. The mixture was stirred for 30 min at this temperature. $\text{HCl}_{(\text{aq})}$ (1 M, 20 mL) was then added and the solution was vigorously stirred for 15 min at 0 °C. The two phases were then separated and the aqueous phase was washed with CH_2Cl_2 (3 \times 40 mL). The combined organic phases were dried (MgSO_4), filtered and the solution concentrated under reduced pressure to a volume of *ca.* 15 mL. This solution was then added directly to a column containing silica and the compound was purified by flash column chromatography (eluent: 40% EtOAc in hexane) to

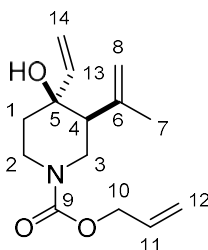
^{xxvi} C-9 not observed

yield piperidinone **178** as a bright yellow oil (1.82 g, 86% over 3 steps). R_f (50% EtOAc in hexane) = 0.5; IR (neat / cm^{-1}) 2946 w, 1693 br s (C=O), 1648 s, 1415 m, 1218 m; ^1H NMR (400 MHz, CDCl_3) δ_{H} 6.01 – 5.90 (m, 1H, H-11), 5.35 – 5.19 (stack, 2H, H-12), 5.02 – 5.00 (m, 1H, H-8_a or H-8_b), 4.82 – 4.80 (m, 1H, H-8_b or H-8_a), 4.66 – 4.61 (stack, 2H, H-10), 4.17 – 4.05 (stack, 2H, H-2_a and H-3_a), 3.56 – 3.45 (stack, 2H, H-2_b and H-3_b), 3.14 – 3.06 (m, 1H, H-4), 2.55 – 2.46 (stack, 2H, H-1), 1.75 (s, 3H, H-7); ^{13}C NMR (101 MHz, CDCl_3) δ_{C} 206.9 (C, C-5), 155.1 (C, C-9), 140.2 (C, C-6), 132.8 (CH, C-11), 118.0 (CH_2 , C-12), 114.8 (CH_2 , C-8), 66.6 (CH_2 , C-10), 57.3 (CH, C-4), 47.1 (CH_2 , C-2 or C-3), 43.6 (CH_2 , C-3 or C-2), 40.6 (CH_2 , C-1), 21.8 (CH_3 , C-7); LRMS (EI) m/z 223.2 [(M)⁺, 20%], 182.1 (60), 128.1 (65); HRMS (EI) calc'd for $\text{C}_{12}\text{H}_{17}\text{NO}_3$ (M)⁺ 223.1207, found 223.1208.

Method B: DMP (8.67 g, 20.4 mmol) was added in portions over 10 min to a solution of alcohol **177** (4.19 g, 18.6 mmol, used without purification, see p 189) in CH_2Cl_2 (160 mL). The resultant solution was stirred for 4 h, after which time the reaction was cooled to 0 °C and $\text{NaOH}_{(\text{aq})}$ (1 M, 50 mL) was added. The solution was vigorously stirred for 15 min at 0 °C. The resultant suspension was filtered through a pad of Celite and the solvent washed sequentially with H_2O (100 mL) and brine (100 mL). The organic phase was dried (MgSO_4), filtered and the solvent was then removed under reduced pressure to give a yellow oil, which was purified by flash column chromatography (eluent: 30% EtOAc in hexane) to yield ketone **178** as a yellow oil (3.48 g, 84%).

Data were in agreement with those obtained for ketone **178** that was prepared using method A.

(3*S, 4*S**) Allyl 4-hydroxy-3-(prop-1'-en-2'-yl)-4-vinylpiperidine-1-carboxylate
(179)**

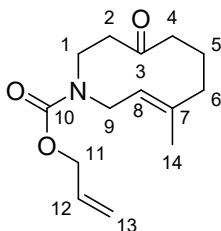


Method A: CeCl₃·7H₂O (6.35 g, 17.1 mmol) was heated at 140 °C under high vacuum (< 2 mbar) for 2 h, and then cooled to r.t. THF (28 mL) was added and the resulting slurry was stirred vigorously for 2 h, before being cooled to –78 °C. Vinylmagnesium bromide (0.80 M solution in THF, 19.8 mL, 15.8 mmol) was added and the resulting mixture was stirred for 30 min, after which time, a solution of piperidinone **178** (2.72g, 12.2 mmol) in THF (12 mL) was added dropwise over 4 min. The resulting mixture was stirred at –78 °C for 4 h before being poured into a solution of acetic acid_(aq) (5%, 25 mL). The aqueous layer was extracted with EtOAc (3 × 35 mL). The combined organic fractions were washed with NaHCO_{3(aq)} (2 × 30 mL), dried (MgSO₄), filtered and the solvent was then removed under reduced pressure to give a dark yellow oil, which contained only one diastereomer by analysis of the ¹H NMR spectrum of the crude product. The crude product was purified by flash column chromatography (eluent: 35% EtOAc in hexane) to yield allylic alcohol **179** as a light yellow oil (2.45 g, 80%). *R*_f (50% EtOAc in hexane) = 0.4; IR (neat / cm⁻¹) 3457 br w (O-H), 2947 bw w, 1679 br s (C=O), 1416 m, 1244 m; ¹H NMR (400 MHz, CDCl₃) δ_H 6.00 – 5.80 (stack, 2H, H-11 and H-13), 5.32 – 5.17 (stack, 3H, H-14_a and H-12), 5.06 (dd, *J* = 10.7, 1.1 Hz, 1H, H-14_b), 4.99 – 4.96 (m, 1H, H-8_a), 4.74 – 4.72 (m, 1H, H-8_b), 4.61 – 4.57 (stack, 2H, H-10), 4.09 – 3.82 (stack, 2H, H-2_a and H-3_a), 3.24 – 3.03 (stack, 2H, H-2_b and H-3_b), 2.26 – 2.16 (m, 1H, H-4), 1.89 (s, 1H, OH), 1.77 (s, 3H, H-7), 1.69 – 1.54 (stack, 2H, H-1); ¹³C NMR (101 MHz, CDCl₃) δ_C 155.2 (C, C-9), 144.7 (C, C-6), 144.5 (CH, C-13), 133.3 (CH, C-11), 117.4 (CH₂, C-12), 113.0 (CH₂, C-8), 112.3 (CH₂, C-14), 71.3 (C, C-5), 66.1 (CH₂, C-10), 50.5 (CH, C-4), 43.8 (CH₂, C-2 or C-3), 39.7 (CH₂, C-3 or C-2), 36.6 (CH₂, C-1), 26.4 (CH₃, C-7); LRMS (ESI) *m/z* 274.1 [(M + Na)⁺, 100%], 234.2 (20); HRMS (ESI) calc'd for C₁₄H₂₁NO₃Na (M + Na)⁺ 274.1419, found 274.1422.

Method B: Vinylmagnesium bromide (0.89 M solution in THF, 22 mL, 18.7 mmol) was added dropwise over 1 min to a solution of piperidinone **178** (3.48 g, 15.6 mmol) in THF (4 mL) at $-78\text{ }^{\circ}\text{C}$. The reaction mixture was warmed to r.t. and then stirred for 3 h, before being quenched by the sequential addition of $\text{NH}_4\text{Cl}_{(\text{aq})}$ (6 mL) and H_2O (6 mL). The aqueous layer was extracted with EtOAc ($3 \times 7\text{ mL}$). The combined organic phases were washed with brine (6 mL), dried (MgSO_4), filtered and evaporated under reduced pressure to give a dark yellow oil, which contained only one diastereomer upon analysis of the ^1H NMR spectrum of the crude product. The crude product was purified by flash column chromatography (eluent: 35% EtOAc in hexane) to yield allylic alcohol **179** as a light yellow oil (2.48 g, 63%).

Data were in agreement with those obtained for allylic alcohol **179** that was prepared using method A.

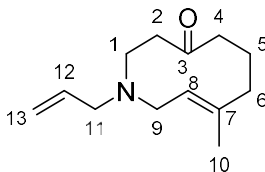
Allyl (*E*)-8-methyl-4-oxo-3,4,5,6,7,10-hexahydroazecine-1(2*H*)-carboxylate (180**)**



$[(\text{C}_6\text{H}_5\text{CN})_2\text{PdCl}_2]$ (32 mg, 0.084 mmol) was added in one portion to a stirred solution of allylic alcohol **179** (0.420 g, 1.67 mmol) in benzene (15 mL). After 3 h, the solvent was removed under reduced pressure to give an orange oil, which was purified by flash column chromatography (eluent: 25% EtOAc in hexane) to yield ketone **180** as a yellow oil (0.397 g, 95%). R_f (50% EtOAc in hexane) = 0.4; IR (neat / cm^{-1}) 2935 w, 1694 s (C=O), 1413 s, 1240 s, 1111 m; ^1H NMR (400 MHz, CDCl_3) δ_{H} 6.00 – 5.89 (m, 1H, H-12), 5.34 – 5.18 (stack, 2H, H-13), 5.13 – 5.01 (m, 1H, H-8), 4.62 (d, $J = 5.5\text{ Hz}$, 2H, H-11), 4.51 – 4.32 (m, 1H, H-9_a), 4.09 – 3.90 (m, 1H, H-1_a), 3.46 – 3.26 (m, 1H, H-9_b), 3.19 – 3.01 (m, 1H, H-1_b), 2.81 – 2.61 (m, 1H, H-2_a), 2.44 – 2.17 (stack, 4H, H-2_b, H-4 and H-5_a), 2.15 – 2.05 (m, 1H, H-6_a), 1.89 – 1.78 (m, 1H, H-6_b), 1.78 – 1.67 (m, 1H, H-5_b), 1.49 (s, 3H, H-14); ^{13}C NMR (101 MHz, CDCl_3) δ_{C} 209.0 (C, C-3), 155.8 (C, C-10), 141.8 (C, C-7), 133.2 (CH, C-12), 122.0 (CH, C-8), 117.4 (CH₂, C-13), 66.2 (CH₂, C-11), 46.6 (CH₂, C-9), 44.9 (CH₂, C-2), 43.6 (CH₂, C-1), 43.5 (CH₂, C-4), 40.8 (CH₂, C-6), 25.0 (CH₂, C-5), 15.9 (CH₃, C-14); LRMS (ESI) m/z 274.1 $[(\text{M} + \text{Na})^+]$,

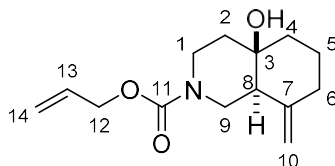
100%], 252.1 (10), 234.1 (10), 194.2 (15); HRMS (ESI) calc'd for C₁₄H₂₁NO₃Na (M + Na)⁺ 274.1419, found 274.1422.

(E)-1-Allyl-8-methyl-2,3,5,6,7,10-hexahydroazecin-4(1H)-one (182)



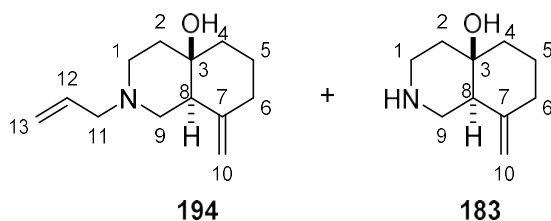
Pd(PPh₃)₄ (4.8 mg, 4.1 μmol) and dimedone (23 mg, 0.17 mmol) were added sequentially to a solution of ketone **180** (21 mg, 83 μmol) in degassed THF (1.8 mL). The resulting mixture was stirred at r.t. After 30 min, NaOH_(aq) (1.0 M, 2 mL) was added. The aqueous layer was washed with EtOAc (3 × 5 mL). The combined organic phases were dried (MgSO₄), filtered and the solvent was then removed under reduced pressure to give a yellow oil, which was purified by flash column chromatography (eluent: 100% EtOAc) to yield allyl amine **182** as a yellow oil (5.2 mg, 27%). *R_f* (100% EtOAc) = 0.2; IR (neat / cm⁻¹) 2925 br m, 1699 s (C=O), 1437 m, 1099 m; ¹H NMR (400 MHz, CDCl₃) δ_H 5.93 – 5.82 (m, 1H, H-12), 5.35 (app. t, *J* = 6.7 Hz, 1H, H-8), 5.22 – 5.12 (stack, 2H, H-13), 3.20 – 3.09 (stack, 3H, H-9_a and H-11), 3.00 – 2.85 (stack, 2H, H-2_a and H-9_b), 2.77 – 2.68 (stack, 2H, H-1), 2.40 – 2.24 (stack, 3H, H-2_b, H-4_a and H-5_a), 2.22 – 2.11 (m, 1H, H-4_b), 2.10 – 2.00 (m, 1H, H-6_a), 1.95 – 1.83 (m, 1H, H-6_b), 1.77 – 1.65 (m, 1H, H-5_b), 1.47 (s, 3H, H-10); ¹³C NMR (101 MHz, CDCl₃) δ_C 208.6 (C, C-3), 140.6 (C, C-7), 136.0 (CH, C-12), 124.1 (CH, C-8), 117.9 (CH₂, C-13) 61.9 (CH₂, C-11), 54.7 (CH₂, C-9), 50.2 (CH₂, C-1), 45.3 (CH₂, C-2), 43.4 (CH₂, C-4), 41.2 (CH₂, C-6), 26.3 (CH₂, C-5), 16.4 (CH₃, C-10); LRMS (ASAP) *m/z* 208.2 [(M + H)⁺, 100%]; HRMS (ASAP) calc'd for C₁₃H₂₂NO (M + H)⁺ 208.1701, found 208.1698.

Allyl (4a*R, 8a*S**)-4a-hydroxy-8-methyleneoctahydroisoquinoline-2(1*H*)-carboxylate (**193**)**



TsOH·H₂O (27 mg, 140 μmol) was added to a solution of ketone **180** (709 mg, 2.82 mmol) in THF (28 mL). After 12 h, NaHCO₃ (aq) (20 mL) was added. The layers were separated and the aqueous layer was washed with CH₂Cl₂ (3 × 15 mL). The combined organic phases were dried (MgSO₄), filtered and the solvent was then removed under reduced pressure to give a yellow oil, which was purified by flash column chromatography (eluent: 30% EtOAc in hexane) to yield decalol **193** as a yellow oil (599 mg, 84%). *R*_f (50% EtOAc in hexane) = 0.4; IR (neat / cm⁻¹) 3466 br (O-H), 2929 w, 1677 s (C=O), 1246 s, 1080 s; ¹H NMR (400 MHz, CDCl₃) δ_H 5.99 – 5.88 (1H, H-13), 5.53 (br s, 1H, OH), 5.33 – 5.17 (stack, 2H, H-14), 4.94 (s, 1H, H-10_a), 4.62 – 4.53 (stack, 3H, H-10_b and H-12), 4.15 – 3.91 (stack, 2H, H-1_a and H-9_a), 3.23 – 2.92 (stack, 2H, H-1_b and H-9_b), 2.35 – 2.29 (m, 1H, H-6_a), 2.19 – 2.07 (m, 1H, H-8), 2.07 – 1.96 (m, 1H, H-6_b), 1.77 – 1.53 (stack, 5H, H-2, H-4_a and H-5), 1.44 (app. td, *J* = 13.3, 4.5 Hz, 1H, H-4_b); ¹³C NMR (101 MHz, CDCl₃) δ_C 155.3 (C, C-11), 146.7 (C, C-7), 133.3 (CH, C-13), 117.4 (CH₂, C-14), 109.4 (CH₂, C-10), 70.5 (C, C-3), 66.1 (CH₂, C-12), 48.2 (CH, C-8), 41.7 (CH₂, C-9), 40.0 (CH₂, C-1), 38.9 (CH₂, C-4), 37.6 (CH₂, C-2), 36.2 (CH₂, C-6), 23.5 (CH₂, C-5); LRMS (ASAP) *m/z* 234.1 [(M – H₂O + H)⁺, 100%], 252.2 (5); HRMS (ASAP) calc'd for C₁₄H₂₂NO₃ (M + H)⁺ 252.1600, found 252.1591.

(4a*R, 8a*S**)-2-Allyl-8-methyleneoctahydroisoquinolin-4a(2*H*)-ol (194) and
(4a*R**, 8a*S**)-8-methyleneoctahydroisoquinolin-4a(2*H*)-ol (183)**



Pd(dba)₂ (28 mg, 49 μmol) and 1,4-bis(diphenylphosphino)butane (21 mg, 49 μmol) were added sequentially to a solution of decalol **193** (250 mg, 0.98 mmol) in degassed CH₂Cl₂ (6.5 mL) and the resulting mixture was stirred until a yellow colour persisted (typically 5 min). At that time, pyrrolidine (0.40 mL, 4.9 mmol) was added rapidly and the resulting solution stirred. After 30 min, the solvent was removed under reduced pressure to give a brown oil, which was purified by flash column chromatography (eluent: 5 to 20% MeOH (with 1% NH₃) in CH₂Cl₂) to afford, in order of elution, allyl amine **194** as a yellow oil (16 mg, 8%). *R_f* (20% MeOH in CH₂Cl₂) = 0.6; IR (neat / cm⁻¹) 3396 br (O-H), 2935 s, 1644 m, 1439 m; ¹H NMR (400 MHz, CDCl₃) δ_H 5.93 – 5.82 (m, 1H, H-12), 5.22 – 5.11 (stack, 2H, H-13), 4.88 (d, *J* = 1.6 Hz, 1H, H-10_a), 4.51 (d, *J* = 1.6 Hz, 1H, H-10_b), 3.04 (app. dq, *J* = 6.5, 1.2 Hz, 2H, H-11), 2.76 – 2.68 (stack, 2H, H-1_a and H-9_a), 2.33 – 2.25 (stack, 3H, H-1_b, H-6_a and H-8), 2.15 (app. t, *J* = 11.2 Hz, 1H, H-9_b), 2.06 – 1.96 (m, 1H, H-6_b), 1.75 – 1.64 (stack, 4H, H-2, H-4_a and H-5_a), 1.64 – 1.54 (m, 1H, H-5_b), 1.46 – 1.38 (m, 1H, H-4_b), *OH* not observed; ¹³C NMR (101 MHz, CDCl₃) δ_C 147.9 (C, C-7), 135.5 (CH, C-12), 117.9 (CH₂, C-13), 108.6 (CH₂, C-10), 70.2 (CH₂, C-3), 62.2 (CH₂, C-11), 51.0 (CH₂, C-9), 49.2 (CH₂, C-1), 48.4 (CH, C-8), 38.9 (CH₂, C-4), 37.9 (CH₂, C-2), 36.3 (CH₂, C-6), 23.7 (CH₂, C-5); LRMS (ASAP) *m/z* 208.2 [(*M* + *H*)⁺, 60%], 190.2 (50); HRMS (ASAP) calc'd for C₁₃H₂₂NO (*M* + *H*)⁺ 208.1701, found 208.1701, and then amine **183** as a white crystalline solid (147 mg, 90%). *R_f* (20% MeOH in CH₂Cl₂) = 0.1; mp 142 – 143 °C; IR (neat / cm⁻¹) 3281 br (N-H and O-H), 2929 s, 1645 m, 1437 m, 1269 m, 959 s, 729 s; ¹H NMR (400 MHz, CDCl₃) δ_H 4.84 (d, *J* = 1.6 Hz, 1H, H-10_a), 4.46 (d, *J* = 1.6 Hz, 1H, H-10_b), 2.96 (app. td, *J* = 12.4, 3.2 Hz, 1H, H-1_a), 2.85 – 2.76 (stack, 3H, H-1_b and H-9), 2.27 (app. ddt, *J* = 13.0, 4.1, 2.2 Hz, 1H, H-6_a), 2.18 (br. s, 2H, *NH* and *OH*), 2.15 – 2.09 (m, 1H, H-8), 2.05 – 1.94 (m, 1H, H-6_b), 1.71 – 1.38 (stack, 6H, H-2, H-4 and H-5); ¹³C NMR (101 MHz, CDCl₃) δ_C 147.9 (C, C-7), 108.5 (CH₂, C-10), 70.7 (C, C-3), 49.4 (CH, C-8), 43.7 (CH₂, C-9), 41.9 (CH₂, C-1), 39.4 (CH₂, C-4), 38.7 (CH₂, C-2), 36.4 (CH₂, C-6), 23.5 (CH₂, C-5); LRMS

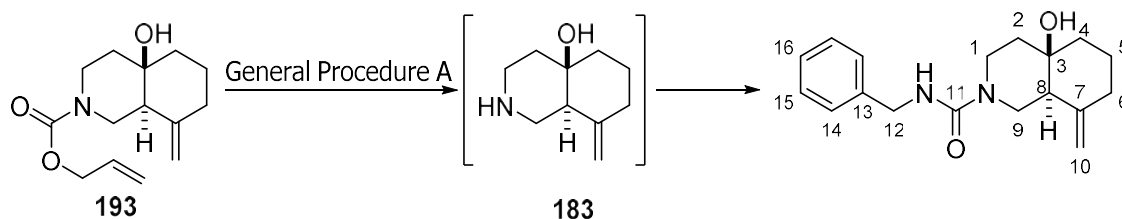
(ASAP) m/z 150.1 [(M - H₂O + H)⁺, 100%], 168.1 (75); HRMS (ASAP) calc'd for C₁₀H₁₈NO (M + H)⁺ 168.1388, found 168.1388.

General Procedures for Alloc Cleavage

Method A: Pd(dba)₂ (0.05 eq) and 1,4-bis(diphenylphosphino)butane (0.05 eq) were added sequentially to a solution of alloc-protected amine (1 eq) in degassed CH₂Cl₂ (0.1 M). The resulting mixture was stirred until a yellow colour persisted (typically 5 min). At that point, Et₂NH (5 eq) was added rapidly and the resulting solution was stirred at r.t. After 30 min, the solvent was removed under reduced pressure and the residue used directly without further purification.

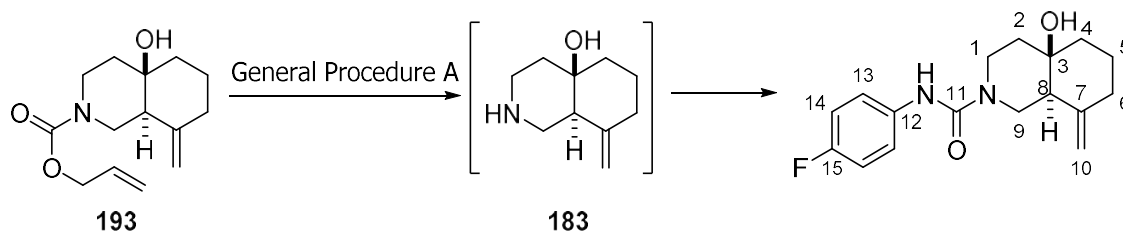
Method B: Pd(PPh₃)₄ (0.05 eq) was added to a solution of alloc-protected amine (1 eq) in degassed CH₂Cl₂ (0.1 M) and the resulting mixture was stirred. After 5 min, pyrrolidine (5 eq) was added rapidly and the resulting solution was stirred at r.t. After 30 min, the solvent was removed under reduced pressure and the residue used directly without further purification.

(4a*R, 8a*S**)-*N*-Benzyl-4a-hydroxy-8-methyleneoctahydroisoquinoline-2(1*H*)-carboxamide (195)**



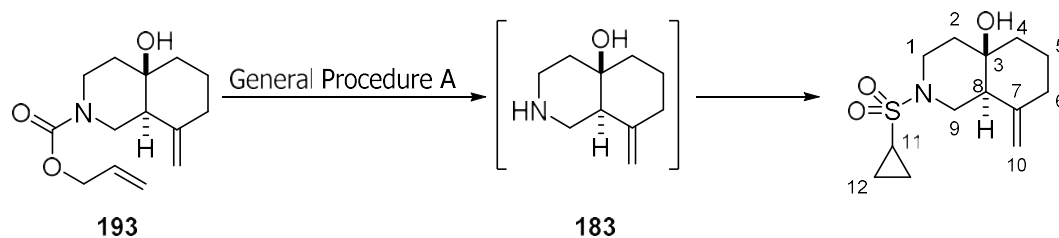
Carbamate **193** was deprotected according to general procedure **A** and the amine product **183** used without purification. Benzyl isocyanate (52 μL , 0.42 mmol) was added to a solution of amine **183** (70 mg, 0.42 mmol) in CH_2Cl_2 (4 mL) and the resulting solution was stirred at r.t. for 3 h. The solvent was then removed under reduced pressure to afford a brown oil, which was purified by flash column chromatography (eluent: 60% EtOAc in hexane) to yield urea **195** as a colourless oil (15 mg, 12% over two steps from carbamate **193**). R_f (70% EtOAc in hexane) = 0.3; IR (neat / cm^{-1}) 3364 br (O-H, N-H), 2929 br w, 1624 s (C=O), 1535 s, 1264 s; ^1H NMR (400 MHz, CDCl_3) δ_{H} 7.36 – 7.26 (stack, 5H, H-14, H-15 and H-16), 4.95 (s, 1H, H-10_a), 4.76 (br s, 1H, *NH*), 4.57 (s, 1H, H-10_b), 4.43 (app. d, J = 6.0 Hz, 2H, H-12), 3.91 – 3.85 (m, 1H, H-9_a), 3.76 – 3.69 (m, 1H, H-1_a), 3.20 (app. td, J = 13.0, 3.2 Hz, 1H, H-1_b), 3.02 (dd, J = 12.9, 11.7 Hz, 1H, H-9_b), 2.35 – 2.29 (m, 1H, H-6_a), 2.21 – 2.15 (m, 1H, H-8), 2.07 – 1.98 (m, 1H, H-6_b), 1.79 – 1.72 (m, 1H, H-5_a), 1.71 – 1.58 (stack, 4H, H-2, H-4_a and H-5_b), 1.49 – 1.41 (m, 1H, H-4_b), *OH* not observed; ^{13}C NMR (101 MHz, CDCl_3) δ_{C} 157.5 (C, C-11), 146.9 (C, C-7), 139.6 (C, C-13), 128.6 (CH, C-15 or C-16), 127.8 (CH, C-14), 127.3 (CH, C-15 or C-16), 109.3 (CH_2 , C-10), 70.5 (C, C-3), 47.9 (CH, C-8), 45.1 (CH_2 , C-12), 41.9 (CH_2 , C-9), 40.3 (CH_2 , C-1), 38.8 (CH_2 , C-4), 37.4 (CH_2 , C-2), 36.2 (CH_2 , C-6), 23.4 (CH_2 , C-5); LRMS (ASAP) m/z 301.2 [($\text{M} + \text{H}$)⁺, 15%], 205.1 (100); HRMS (ASAP) calc'd for $\text{C}_{18}\text{H}_{25}\text{N}_2\text{O}_2$ ($\text{M} + \text{H}$)⁺ 301.1916, found 301.1920.

(4a*R, 8a*S**)-*N*-(4'-Fluorophenyl)-4a-hydroxy-8-methyleneoctahydroisoquinoline-2(1*H*)-carboxamide (196)**



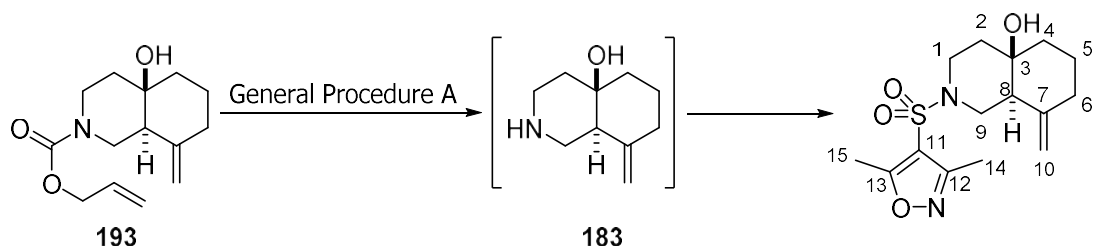
Carbamate **193** was deprotected according to general procedure **A** and the amine product **183** used without purification. 4-Fluorophenyl isocyanate (52 μL , 0.42 mmol) was added to a solution of amine **183** (70 mg, 0.42 mmol) in CH_2Cl_2 (4 mL) and the resulting solution was stirred at r.t. for 3 h. The solvent was then removed under reduced pressure to provide a brown oil, which was purified by flash column chromatography (eluent: 60% EtOAc in hexane) to yield urea **196** as a colourless oil (20 mg, 20% over two steps from carbamate **193**). R_f (70% EtOAc in hexane) = 0.3; IR (neat / cm^{-1}) 3312 br (O-H, N-H), 2931 br w, 1636 m (C=O), 1508 s, 1214 m; ^1H NMR (400 MHz, CDCl_3) δ_{H} 7.33 – 7.26 (AA' of AA'BB, 2H, H-13 or H-14), 7.01 – 6.93 (BB' of AA'BB, 2H, H-13 or H-14), 5.54 (br s, 1H, *NH*), 4.97 (s, 1H, H-10_a), 4.59 (s, 1H, H-10_b), 4.00 – 3.92 (m, 1H, H-9_a), 3.88 – 3.80 (m, 1H, H-1_a), 3.28 (app. td, $J = 13.1, 3.2$ Hz, 1H, H-1_b), 3.10 (dd, $J = 13.0, 11.7$ Hz, 1H, H-9_b), 2.38 – 2.31 (m, 1H, H-6_a), 2.25 – 2.18 (m, 1H, H-8), 2.08 – 1.98 (m, 1H, H-6_b), 1.81 – 1.54 (stack, 5H, H-2, H-4_a and H-5), 1.46 (app. td, $J = 13.0, 4.4$ Hz, 1H, H-4_b), *OH* not observed; ^{13}C NMR (101 MHz, CDCl_3) δ_{C} 159.0 (CF, d, $J = 242$ Hz, C-15), 155.2 (C, C-11), 146.9 (C, C-7), 135.2 (C, d, $J = 2$ Hz, C-12), 122.0 (CH, d, $J = 8$ Hz, C-13), 115.6 (CH, d, $J = 22$ Hz, C-14), 109.5 (CH_2 , C-10), 70.6 (C, C-3), 48.1 (CH, C-8), 42.2 (CH_2 , C-9), 40.8 (CH_2 , C-1), 38.8 (CH_2 , C-4), 37.6 (CH_2 , C-2), 36.2 (CH_2 , C-6), 23.5 (CH_2 , C-5); ^{19}F NMR (377 MHz, CDCl_3) δ_{F} -120.2 (CF); LRMS (ASAP) m/z 305.2 [(M + H)⁺, 100%], 287.2 (30); HRMS (ASAP) calc'd for $\text{C}_{17}\text{H}_{22}\text{FN}_2\text{O}_2$ (M + H)⁺ 305.1665, found 305.1662.

(4a*R, 8a*S**)-2-Cyclopropylsulfonyl-8-methyleneoctahydroisoquinolin-4a(2*H*)-ol
(**197**)**



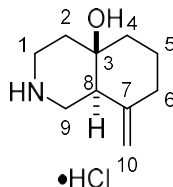
Carbamate **193** was deprotected according to general procedure **A** and the amine product **183** used without purification. NEt_3 (65 μL , 0.47 mmol) was added to a solution of amine **183** (65 mg, 0.39 mmol) in CH_2Cl_2 (4 mL) and the resulting solution was cooled to 0 $^\circ\text{C}$. Cyclopropanesulfonyl chloride (42 μL , 0.41 mmol) was added dropwise over 1 min and the resulting solution was stirred at r.t. for 17 h. The reaction mixture was then washed sequentially with $\text{HCl}_{(\text{aq})}$ (1 M, 2 mL), H_2O (2 mL) and brine (2 mL). The organic layer was dried (MgSO_4), filtered and the solvent was then removed under reduced pressure to provide a yellow oil, which was purified by flash column chromatography (eluent: 30% EtOAc in hexane) to yield sulfonamide **197** as a clear, colourless oil (32 mg, 30% over two steps from carbamate **193**). R_f (50% EtOAc in hexane) = 0.3; IR (neat / cm^{-1}) 3516 br (O-H), 2931 m, 1335 s, 1142 s, 923 s, 890 s; ^1H NMR (400 MHz, CDCl_3) δ_{H} 4.89 (s, 1H, H-10_a), 4.46 (s, 1H, H-10_b), 3.62 – 3.52 (stack, 2H, H-1_a and H-9_a), 3.12 (app. td, J = 11.2, 5.1 Hz, 1H, H-1_b), 2.98 (app. t, J = 11.4 Hz, 1H, H-9_b), 2.31 – 2.21 (stack, 3H, H-6_a, H-8 and H-11), 2.02 – 1.93 (m, 1H, H-6_b), 1.71 – 1.50 (stack, 5H, H-2, H-4_a and H-5), 1.43 (app. td, J = 12.9, 4.1 Hz, 1H, H-4_b), 1.15 – 1.09 (m, 2H, H-12_a), 0.97 – 0.89 (m, 2H, H-12_b), *OH* not observed; ^{13}C NMR (101 MHz, CDCl_3) δ_{C} 146.4 (C, C-7), 104.3 (CH_2 , C-10), 69.9 (C, C-3), 48.2 (CH, C-8), 43.9 (CH_2 , C-9), 42.2 (CH_2 , C-1), 38.6 (CH_2 , C-4), 37.5 (CH_2 , C-2), 36.1 (CH_2 , C-6), 25.9 (CH, C-11), 23.4 (CH_2 , C-5), 4.5 (CH_2 , C-12); LRMS (ASAP) m/z 272.1 [(M + H)⁺, 100%], 254.1 (15); HRMS (ASAP) calc'd for $\text{C}_{13}\text{H}_{22}\text{NO}_3\text{S}$ (M + H)⁺ 272.1320, found 272.1326.

(4a*R, 8a*S**)-2-((3',5'-Dimethylisoxazol-4'-yl)sulfonyl)-8-methyleneoctahydroisoquinolin-4a(2*H*)-ol (**198**)**



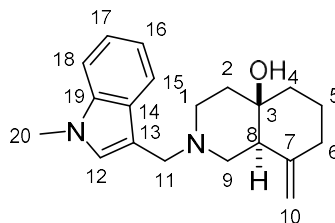
Carbamate **193** was deprotected according to general procedure **A** and the amine product **183** used without purification. NEt₃ (65 μL, 0.47 mmol) was added to a solution of amine **183** (65 mg, 0.39 mmol) in CH₂Cl₂ (4 mL) and the resulting solution was cooled to 0 °C. 3,5-Dimethylisoxazole-4-sulfonyl chloride (80 mg, 0.41 mmol) was added in one portion and the resulting solution was stirred at r.t. for 17 h. The reaction mixture was then washed sequentially with HCl_(aq) (1 M, 2 mL), H₂O (2 mL) and brine (2 mL). The organic layer was dried (MgSO₄), filtered and the solvent was then removed under reduced pressure to provide a yellow oil, which was purified by flash column chromatography (eluent: 25% EtOAc in hexane) to yield sulfonamide **198** as a white, crystalline solid (26 mg, 21% over two steps). *R*_f (50% EtOAc in hexane) = 0.4; mp 112 – 114 °C; IR (neat / cm⁻¹) 3531 br (O-H), 2934 br, 1587 m, 1342 m, 1179 s, 1120 s, 923 s; ¹H NMR (400 MHz, CDCl₃) δ_H 4.89 (s, 1H, H-10_a), 4.36 (s, 1H, H-10_b), 3.60 – 3.50 (stack, 2H, H-1_a and H-9_a), 2.85 – 2.77 (m, 1H, H-1_b), 2.67 (app. t, *J* = 11.4 Hz, 1H, H-9_b), 2.59 (s, 3H, H-15), 2.35 (s, 3H, H-14), 2.31 – 2.24 (stack, 2H, H-6_a and H-8), 2.02 – 1.92 (m, 1H, H-6_b), 1.75 – 1.41 (stack, 6H, H-2, H-4 and H-5), *OH* not observed; ¹³C NMR (101 MHz, CDCl₃) δ_C 173.6 (C, C-13), 158.1 (C, C-12), 146.2 (C, C-7), 113.9 (C, C-11), 109.4 (CH₂, C-10), 69.7 (C, C-3), 47.7 (CH, C-8), 43.3 (CH₂, C-9), 41.6 (CH₂, C-1), 38.4 (CH₂, C-4), 37.2 (CH₂, C-2), 36.0 (CH₂, C-6), 23.3 (CH₂, C-5), 13.1 (CH₃, C-15), 11.5 (CH₃, C-14); LRMS (ASAP) *m/z* 327.1 [(M + H)⁺, 100%], 309.1 (15); HRMS (ASAP) calc'd for C₁₅H₂₃N₂O₄S (M + H)⁺ 327.1379, found 327.1383.

(4a*R, 8a*S**)-8-Methyleneoctahydroisoquinolin-4a(2*H*)-ol hydrochloride (199)**



Amine **183** (37 mg, 0.218 mmol) was dissolved in Et₂O (1.0 mL) and HCl (2.0 M in Et₂O, 1 mL) was added dropwise over 1 min. The solvent was immediately removed under reduced pressure to yield hydrochloride salt **199** as a white crystalline solid (44 mg, 100; mp 187 – 190 °C dec.; IR (neat / cm⁻¹) 3370 br (N-H and O-H), 2937 br s, 2802 br, 1648 w, 1439 w, 957 m; ¹H NMR (400 MHz, *d*₄ - MeOD) δ _H 4.87 (app. s, 1H, H-10_a), 4.42 (app. s, 1H, H-10_b), 3.30 – 3.28 (m, 1H, H-1_a), 3.27 – 3.19 (stack, 3H, H-1_b and H-9), 2.40 – 2.33 (stack, 2H, H-6_a and H-8), 2.15 – 2.04 (m, 1H, H-6_b), 1.89 – 1.56 (stack, 6H, H-2, H-4 and H-5), exchangeable protons not observed; ¹³C NMR (101 MHz, *d*₄ - MeOD) δ _C 146.2 (C, C-7), 108.5 (CH₂, C-10), 69.4 (C, C-3), 46.0 (CH, C-8), 43.0 (CH₂, C-9), 41.2 (CH₂, C-1), 39.1 (CH₂, C-2), 36.8 (CH₂, C-6), 36.6 (CH₂, C-4), 23.4 (CH₂, C-5); LRMS (ASAP) *m/z* 150.1 [(M – H₂O + H)⁺, 100%], 168.1 (90); HRMS (ASAP) calc'd for C₁₀H₁₈NO (M + H)⁺ 168.1388, found 168.1389.

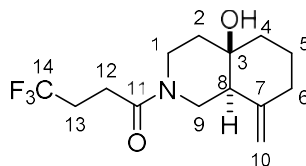
(4a*R, 8a*S**)-2-((1'-Methyl-1'*H*-indol-3'-yl)methyl)-8-methyleneoctahydroisoquinolin-4a(2*H*)-ol (200)**



A solution of amine **183** (42 mg, 0.25 mmol) and *N*-methylindole-3-carbaldehyde (40 mg, 0.25 mmol) in dichloroethane (2.5 mL) and the resultant mixture was stirred. After 5 min, glacial AcOH (29 μ L, 0.50 mmol) was added and the resultant solution was stirred for a further 15 min, after which time, NaBH(OAc)₃ (110 mg, 0.50 mmol) was added in one portion. After 17 h, the solution was diluted with CH₂Cl₂ (7.5 mL) and NaHCO₃ (aq) (5 mL) was added. The layers were separated and the organic layer was washed with brine (10 mL). The combined organic phases were dried (MgSO₄), filtered and the solvent was then removed under reduced

pressure to give an orange oil, which was purified by flash column chromatography (eluent: 10% MeOH in CH₂Cl₂) to yield amine **200** as a yellow oil (48 mg, 62%). *R*_f (10% MeOH in CH₂Cl₂) = 0.3; IR (neat / cm⁻¹) 3332 br (O-H), 2933 m, 2577 br, 1476 w, 1133 w, 964 w, 742 s; ¹H NMR (400 MHz, CDCl₃) δ_H 7.63 – 7.56 (m, 1H, H-15), 7.53 – 7.49 (m, 1H, H-12), 7.35 – 7.31 (m, 1H, H-18), 7.28 – 7.22 (m, 1H, H-17), 7.20 – 7.13 (m, 1H, H-16), 4.86 (app. s, 1H, H-10_a), 4.33 (app. s, 1H, H-10_b), 4.19 – 4.15 (stack, 2H, H-11), 3.79 (s, 3H, H-20), 3.21 – 3.10 (stack, 2H, H-1_a and H-9_a), 2.98 – 2.87 (m, 1H, H-1_b), 2.83 – 2.73 (stack, 2H, H-8 and H-9_b), 2.30 – 2.23 (m, 1H, H-6_a), 2.21 – 2.08 (m, 1H, H-2_a), 2.07 – 1.95 (m, 1H, H-2_b), 1.77 – 1.49 (stack, 5H, H-4, H-5 and H-6_b), *O**H* not observed; ¹³C NMR (101 MHz, CDCl₃) δ_C 146.0 (C, C-7), 136.9 (C, C-19), 132.0 (CH, C-12), 128.5 (C, C-14), 122.2 (CH, C-17), 120.2 (CH, C-16), 118.2 (CH, C-15), 109.9 (CH, C-18), 109.2 (CH₂, C-10), 69.4 (C, C-3), 52.3 (CH₂, C-11), 49.6 (CH₂, C-9), 47.7 (CH₂, C-1), 45.9 (CH, C-8), 37.7 (CH₂, C-4), 35.7 (2 × CH₂, C-2 and C-6), 33.1 (CH₃, C-20), 23.2 (CH₂, C-5)^{xxvii}; LRMS (ASAP) *m/z* 311.2 [(M + H)⁺, 100%]; HRMS (ASAP) calc'd for C₂₀H₂₇N₂O (M + H)⁺ 311.2123, found 311.2121.

(4a*R, 8a*S**)-4,4,4-Trifluoro-1-(4a-hydroxy-8-methyleneoctahydroisoquinolin-2(1*H*)-yl)butan-1-one (201)**

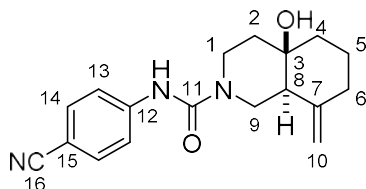


Amine **183** (42 mg, 0.25 mmol), 4,4,4-trifluorobutyric acid (39 mg, 0.28 mmol), EDC·HCl (53 mg, 0.28 mmol) and HOBt (37 mg, 0.28 mmol) were dissolved in CH₂Cl₂ (2.5 mL) and the resulting mixture was stirred. After 10 min, *N*-methylmorpholine (60 μL, 0.55 mmol) was added and the resultant solution. After 17 h, the solvent was removed under reduced pressure to give a brown residue, which was dissolved in EtOAc (10 mL) and sequentially washed with HCl_(aq) (1 M, 2 × 8 mL), NaHCO_{3(aq)} (2 × 8 mL) and brine (8 mL). The organic phase was dried (MgSO₄), filtered and the solvent was then removed under reduced pressure to give a yellow oil. Purification by flash column chromatography (eluent: 50% EtOAc in hexane) yielded amide **201** as a yellow oil (47 mg, 64%). *R*_f (50% EtOAc in hexane) = 0.2; IR (neat / cm⁻¹) 3449 br

^{xxvii} Within the HMBC spectrum a correlation between H-11 and a ¹³C resonance at 103.8 ppm can be seen, believed to be C-13; however, as the carbon resonance cannot be seen in the standard ¹³C NMR spectrum, the carbon resonance has not been explicitly assigned.

(O-H), 2932 m, 1630 s (C=O), 1442 m, 1256 m, 1134 s, 1102 s; ^1H NMR (400 MHz, CDCl_3) δ_{H} 5.00 – 4.95 (m, 1H, H-10_a), 4.62 – 4.46 (stack, 3H, H-2_a, H-4_b and H-10_b), 3.69 – 1.38 (stack, 15H, including [2.13 – 2.08 {m, 1H, H-8}], H-1, H-2_b, H-4_b, H-5, H-6, H-8, H-9, H-12, H-13), *OH* not observed^{xxviii}; ^{13}C NMR (101 MHz, CDCl_3) δ_{C} [168.1, 168.0 (C, C-11)], [146.8, 146.5 (C, C-7)], 127.3 (CF_3 , q, $J = 276$ Hz, C-14), [109.8, 109.4 (CH_2 , C-10)], [70.7, 70.5 (C, C-3)], [48.9, 48.1 (CH, C-8)], 43.4 (CH_2 , C-9), [41.7, 41.5 (CH_2 , C-1)], 39.9 (CH_2 , C-4), 38.1 (CH_2 , C-2), [36.2, 36.1 (CH_2 , C-6)], 29.8 (CH_2 , q, $J = 29$ Hz, C-13), [26.1, 26.0 (CH_2 , C-12)], 23.5 (CH_2 , C-5)^{xxix}; ^{19}F NMR (377 MHz, CDCl_3) δ_{F} –66.6 (CF_3); LRMS (ASAP) m/z 274.1 [(M – H₂O + H)⁺, 100%], 292.2 (80); HRMS (ASAP) calc'd for $\text{C}_{14}\text{H}_{21}\text{F}_3\text{NO}_2$ (M + H)⁺ 292.1524, found 292.1521.

(4a*R, 8a*S**)-*N*-(4'-Cyanophenyl)-4a-hydroxy-8-methyleneoctahydroisoquinoline-2(1*H*)-carboxamide (202)**



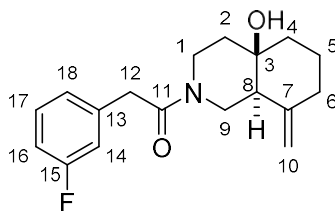
4-Cyanophenyl isocyanate (34 mg, 0.24 mmol) was added to a solution of amine **183** (42 mg, 0.25 mmol) in CH_2Cl_2 (2.5 mL) and the resulting solution was stirred at r.t. for 17 h. The solvent was then removed under reduced pressure to provide a brown oil, which was purified by flash column chromatography (eluent: 50% EtOAc in hexane) to yield urea **202** as a colourless oil (62 mg, 84%). R_f (70% EtOAc in hexane) = 0.2; IR (neat / cm^{-1}) 3340 br (O-H, N-H), 2935 m, 2222 s ($\text{C}\equiv\text{N}$), 1643 s (C=O), 1512 s, 1244 s, 1174 s, 751 s; ^1H NMR (400 MHz, CDCl_3) δ_{H} 7.56 – 7.48 (stack, 4H, H-13 and H-14), 4.97 (s, 1H, H-10_a), 4.58 (s, 1H, H-10_b), 4.02 – 3.94 (m, 1H, H-9_a), 3.92 – 3.84 (m, 1H, H-1_a), 3.30 (app. td, $J = 13.1, 3.0$ Hz, 1H, H-1_b), 3.13 (dd, $J = 13.0, 11.8$ Hz, 1H, H-9_b), 2.38 – 2.30 (m, 1H, H-6_a), 2.24 – 2.17 (m, 1H, H-8), 2.07 – 1.95 (m, 1H, H-6_b), 1.81 – 1.52 (stack, 5H, H-2, H-4_a and H-5), 1.45 (app. td, $J = 13.4, 4.7$ Hz, 1H, H-4_b), exchangeable protons not observed; ^{13}C NMR (101 MHz, CDCl_3) δ_{C} 154.1 (C, C-11), 146.6 (C, C-7), 143.9 (C, C-12), 133.2 (CH, C-13 or C-14), 119.4 (C, C-16), 119.3 (CH, C-13 or C-14), 109.6 (CH_2 , C-10), 105.2 (C, C-15), 70.5 (C, C-3), 48.2 (CH, C-8),

^{xxviii} The compound exists as a 1:1 mixture of rotamers on the NMR timescale, so only clearly assignable resonances are identified.

^{xxix} The compound exists as a 1:1 mixture of rotamers on the NMR timescale, so two carbon resonances appear in the ^{13}C NMR spectrum per carbon environment. Both resonances are given within each set of square brackets. If only one resonance is given then the resonances for each rotamer are co-incident.

42.4 (CH₂, C-9), 40.9 (CH₂, C-1), 38.7 (CH₂, C-4), 37.6 (CH₂, C-2), 36.2 (CH₂, C-6), 23.4 (CH₂, C-5); LRMS (ASAP) *m/z* 312.2 [(M + H)⁺, 100%]; HRMS (ASAP) calc'd for C₁₈H₂₂N₃O₂ (M + H)⁺ 312.1712, found 312.1718.

(4a*R, 8a*S**)-2-(3'-Fluorophenyl)-1-(4a-hydroxyhydroxy-8-methyleneoctahydroisoquinolin-2(1*H*)-yl)ethan-1'-one (203)**

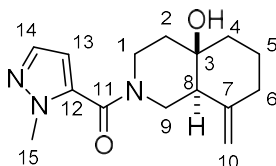


Amine **183** (42 mg, 0.25 mmol), 3-fluorophenylacetic acid (39 mg, 0.28 mmol), EDC·HCl (53 mg, 0.28 mmol) and HOBt (37 mg, 0.28 mmol) were dissolved in CH₂Cl₂ (2.5 mL) and the resulting mixture was stirred. After 10 min, *N*-methylmorpholine (60 μL, 0.55 mmol) was added and the resultant solution stirred for 17 h. The solvent was then removed to give a brown residue, which was dissolved in EtOAc (10 mL) and sequentially washed with HCl_(aq) (1 M, 2 × 8 mL), NaHCO_{3(aq)} (2 × 8 mL) and brine (8 mL). The organic phase was dried (MgSO₄), filtered and the solvent was then removed under reduced pressure to give a yellow oil. Purification by flash column chromatography (eluent: 50% EtOAc in hexane) yielded amide **203** as a clear, colourless oil (63 mg, 83%). *R_f* (50% EtOAc in hexane) = 0.1; IR (neat / cm⁻¹) 3417 br (O-H), 2932 m, 1623 s (C=O), 1447 br m, 1246 m, 1138 m, 773 s; ¹H NMR (400 MHz, CDCl₃) δ_H 7.32 – 7.23 (m, 1H, H-17), 7.07-6.90 (stack, 3H, H-14, H-16 and H-18), 4.98 – 4.45 (stack, 3H, H-9_a and H-10), 3.79 – 2.63 (stack, 5H, H-1, H-9_b and H-12), 2.34 – 2.26 (m, 1H, H-6_a), 2.12 – 2.05 (m, 1H, H-8), 2.04 – 1.20 (stack, 7H, H-2, H-4, H-5 and H-6_b), *OH* not observed^{xxx}; ¹³C NMR (101 MHz, CDCl₃) δ_C [168.9, 168.8 (C, C-11)], 163.1 (CF, d, *J* = 245 Hz, C-15), [146.8, 146.5 (C, C-7)], [137.9, 137.8 (C, C-13)], 130.2 (CH, d, *J* = 8 Hz, C-17), [124.6, 124.5 (CH, d, *J* = 3 Hz, C-18)], [115.9, 115.8 (CH₂, d, *J* = 22 Hz, C-14)], 113.9 (CH₂, d, *J* = 22 Hz, C-16), [109.9, 109.0 (CH₂, C-10)], [70.7, 70.5 (C, C-3)], [48.8, 48.0 (CH, C-8)], [44.3, 42.5 (CH₂, C-1)], 40.9 (CH₂, C-12), [39.8, 38.7 (CH₂, C-9)], [38.7, 38.2 (CH₂, C-4)], [38.0, 37.4 (CH₂, C-2)],

^{xxx} The compound exists as a 1:1 mixture of rotamers on the NMR timescale, so only clearly assignable resonances are identified.

36.1 (CH₂, C-6), 23.4 (CH₂, C-5)^{xxxi}; ¹⁹F NMR (377 MHz, CDCl₃) δ_F -112.9 (C/F); LRMS (ASAP) *m/z* 208.1 [(M - Ar)⁺, 100%], 304.2 (30); HRMS (ASAP) calc'd for C₁₈H₂₃FNO₂ (M + H)⁺ 304.1713, found 304.1717.

((4a*R,8a*S**)-4a-Hydroxy-8-methyleneoctahydroisoquinolin-2(1*H*)-yl)(1'-methyl-1*H*-pyrazol-5'-yl)methanone (204)**



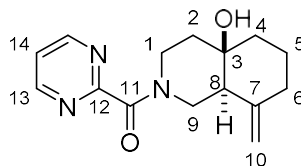
Amine **183** (37 mg, 0.22 mmol), 1-methyl-1*H*-pyrazole-5-carboxylic acid (30 mg, 0.24 mmol), EDC·HCl (46 mg, 0.24 mmol) and HOBT (38 mg, 0.24 mmol) were dissolved in CH₂Cl₂ (2.5 mL) and the resulting mixture was stirred. After 10 min, *N*-methylmorpholine (52 μL, 0.48 mmol) was added and the resultant solution stirred for 17 h. The solvent was then removed to give a brown residue, which was dissolved in EtOAc (10 mL) and sequentially washed with HCl_(aq) (0.33 M, 2 × 8 mL), NaHCO_{3(aq)} (2 × 8 mL) and brine (8 mL). The organic phase was dried (MgSO₄), filtered and the solvent was then removed under reduced pressure to yield amide **204** as a clear oil (33 mg, 55%). *R_f* (70% EtOAc in hexane) = 0.1; IR (neat / cm⁻¹) 3440 br (O-H), 2934 m, 1626 s (C=O), 1438 m, 1253 m, 960 m; ¹H NMR (400 MHz, CDCl₃) δ_H 7.42 – 7.38 (m, 1H, H-14), 6.27 – 6.19 (m, 1H, H-13), 4.96 – 4.32 (stack, 4H, H-1_a, H-9_a, H-10), 3.91 (s, 3H, H-15), 3.87 – 1.30 (stack, 11H, including [2.36 – 2.13 {stack, 2H, H-6_a and H-8}], H-1_b, H-2, H-4, H-5, H-6_a, H-6_b, H-8 and H-9_b), *OH* not observed^{xxxii}; ¹³C NMR (101 MHz, CDCl₃) δ_C [161.2, 161.1 (C, C-11)], [146.2, 146.1 (C, C-7)], 137.7 (CH, C-14), 135.4 (C, C-12), [109.8, 109.1 (CH₂, C-10)], [106.4, 106.2 (CH, C-13)], 70.6 (C, C-3), [48.1, 47.5 (CH, C-8)], [45.6, 45.2 (CH₂, C-1)], [41.1, 40.4 (CH₂, C-9)], [38.6, 38.5 (CH₂, C-4)], 37.4 (CH₃, C-15), 36.9 (CH₂, C-2), 36.0 (CH₂, C-6), 23.2 (CH₂, C-5)^{xxxiii}; LRMS (ASAP) *m/z* 276.2 [(M + H)⁺, 100%], 224.1 (60), 184.0 (40); HRMS (ASAP) calc'd for C₁₅H₂₂N₃O₂ (M + H)⁺ 276.1712, found 276.1715.

^{xxxi} The compound exists as a 1:1 mixture of rotamers on the NMR timescale, so two carbon resonances appear in the ¹³C NMR spectrum per carbon environment. Both resonances are given within each set of square brackets. If only one resonance is given then the resonances are co-incident.

^{xxxii} The compound exists as a 1:1 mixture of rotamers on the NMR timescale, so only clearly assignable resonances are identified.

^{xxxiii} The compound exists as a 1:1 mixture of rotamers on the NMR timescale, so two carbon resonances appear in the ¹³C NMR spectrum per carbon environment. Both resonances are given within each set of square brackets. If only one resonance is given then the resonances are co-incident.

((4a*R, 8a*S**)-4a-Hydroxy-8-methyleneoctahydroisoquinolin-2(1*H*)-yl)(pyrimidin-2'-yl)methanone (205)**

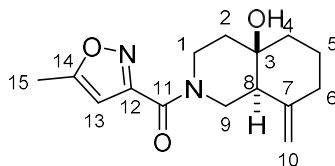


Amine **183** (37 mg, 0.22 mmol), pyrimidine-2-carboxylic acid (30 mg, 0.24 mmol), EDC·HCl (46 mg, 0.24 mmol) and HOBT (38 mg, 0.24 mmol) were dissolved in CH₂Cl₂ (2.5 mL) and the resulting mixture was stirred. After 10 min, *N*-methylmorpholine (52 μL, 0.48 mmol) was added and the resultant solution stirred for 17 h. The solvent was then removed to give a brown residue, which was dissolved in EtOAc (10 mL) and sequentially washed with HCl_(aq) (0.5 M, 2 × 8 mL), NaHCO_{3(aq)} (2 × 8 mL) and brine (8 mL). The organic phase was dried (MgSO₄), filtered and the solvent was then removed under reduced pressure to yield amide **205** as a clear oil (35 mg, 59%). *R*_f (100% EtOAc) = 0.1; IR (neat / cm⁻¹) 3436 br (O-H), 2932 m, 1634 s (C=O), 1561 s, 1405 s, 1205 w, 1134 w, 962 w; ¹H NMR (400 MHz, CDCl₃) δ_H 8.84 – 8.78 (m, 2H, H-13), 7.37 – 7.32 (m, 1H, H-14), 5.03 – 4.28 (stack, 3H, H-9_a and H-10), 3.52 – 2.88 (stack, 3H, H-1 and H-9_b), 2.39 – 1.44 (stack, 9H, including [2.39 – 2.31 {m, 1H, H-8}], H-2, H-4, H-5, H-6, H-8), *OH* not observed^{xxxiv}; ¹³C NMR (101 MHz, CDCl₃) δ_C [165.3, 165.2 (C, C-11)], [162.8, 162.7 (C, C-12)], 157.5 (CH, C-13), [146.8, 146.4 (C, C-7)], 121.2 (CH, C-14), [110.0, 109.0 (CH₂, C-10)], [71.0, 70.8 (C, C-3)], [48.8, 48.0 (CH, C-8)], [43.2, 43.1 (CH₂, C-1)], 39.8 (CH₂, C-9), 38.7 (CH₂, C-2 or C-4), [38.1, 38.0 (CH₂, C-2 or C-4)], 36.1 (CH₂, C-6), 23.4 (CH₂, C-5)^{xxxv}; LRMS (ASAP) *m/z* 274.2 [(M + H)⁺, 100%], 256.2 (90), 228.1 (50); HRMS (ASAP) calc'd for C₁₅H₂₀N₃O₂ (M + H)⁺ 274.1556, found 274.1566.

^{xxxiv} The compound exists as a 1:1 mixture of rotamers on the NMR timescale, so only clearly assignable resonances are identified.

^{xxxv} The compound exists as a 1:1 mixture of rotamers on the NMR timescale, so two carbon resonances appear in the ¹³C NMR spectrum per carbon environment. Both resonances are given within each set of square brackets. If only one resonance is given then the resonances are co-incident.

((4a*R, 8a*S**)-4a-Hydroxy-8-methyleneoctahydroisoquinolin-2(1*H*)-yl)(5'-methylisoxazol-3'-yl)methanone (206)**

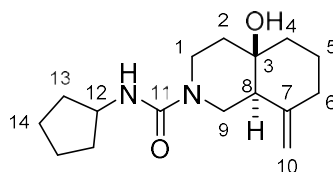


Amine **183** (37 mg, 0.22 mmol), 5-methylisoxazole-3-carboxylic acid (31 mg, 0.24 mmol), EDC·HCl (46 mg, 0.24 mmol) and HOBt (38 mg, 0.24 mmol) were dissolved in CH₂Cl₂ (2.5 mL) and the resulting mixture was stirred. After 10 min, *N*-methylmorpholine (52 μL, 0.48 mmol) was added and the resultant solution was stirred for 17 h. The solvent was then removed to give a brown residue, which was dissolved in EtOAc (10 mL) and sequentially washed with HCl_(aq) (1 M, 2 × 8 mL), NaHCO_{3(aq)} (2 × 8 mL) and brine (8 mL). The organic phase was dried (MgSO₄), filtered and the solvent was then removed under reduced pressure to yield amide **206** as a yellow oil (46 mg, 77%). *R*_f (70% EtOAc in hexane) = 0.3; IR (neat / cm⁻¹) 3448 br (O-H), 2931 m, 1630 s (C=O), 1452 m, 1394 m, 1273 m; ¹H NMR (400 MHz, CDCl₃) δ_H 6.23 (br s, 1H, H-13), 5.00 – 4.44 (stack, 3H, H-1_a and H-10), 4.23 – 4.14 (m, 1H, H-9_a), 3.49 – 2.93 (stack, 2H, H-1_b and H-9_b), 2.46 – 2.43 (m, 3H, H-15), 2.37 – 2.21 (stack, 2H, H-6_a and H-8), 2.07 – 1.97 (m, 1H, H-6_b), 1.82 – 1.41 (stack, 6H, H-2, H-4 and H-5), *OH* not observed^{xxxvi}; ¹³C NMR (101 MHz, CDCl₃) δ_C 170.0 (C, C-14), [160.0, 159.9 (C, C-11)], 158.8 (C, C-12), 146.5 (C, C-7), [109.8, 109.4 (CH₂, C-10)], [102.7, 102.6 (CH, C-13)], 70.7 (C, C-3), [49.2, 48.2 (CH, C-8)], [44.9, 43.3 (CH₂, C-1)], [40.4, 38.7 (CH₂, C-9)], [38.6, 38.5 (CH₂, C-4)], 37.4 (CH₂, C-2), 36.1 (CH₂, C-6), 23.4 (CH₂, C-5), 12.3 (CH₃, C-15)^{xxxvii}; LRMS (ASAP) *m/z* 259.1 [(M – H₂O + H)⁺, 100%], 277.2 (45); HRMS (ASAP) calc'd for C₁₅H₂₁N₂O₃ (M + H)⁺ 277.1552, found 277.1557.

^{xxxvi} The compound exists as a 1:1 mixture of rotamers on the NMR timescale, so only clearly assignable resonances are identified.

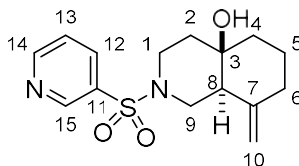
^{xxxvii} The compound exists as a 1:1 mixture of rotamers on the NMR timescale, so two carbon resonances appear in the ¹³C NMR spectrum per carbon environment. Both resonances are given within each set of square brackets. If only one resonance is given then the resonances are co-incident.

(4a*R, 8a*S**)-*N*-Cyclopentyl-4a-hydroxy-8-methyleneoctahydroisoquinoline-2(1*H*)-carboxamide (207)**



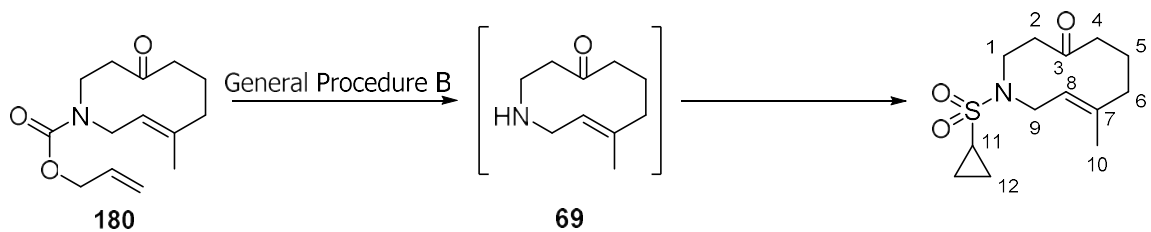
Cyclopentyl isocyanate (27 μ L, 0.24 mmol) was added to a solution of amine **183** (42 mg, 0.25 mmol) in CH_2Cl_2 (2.5 mL) and the resulting solution was stirred at r.t. for 17 h. The solvent was then removed under reduced pressure to provide a yellow oil, which was purified by flash column chromatography (eluent: 50% EtOAc in hexane) to yield urea **207** as a colourless oil (61 mg, 92%). R_f (70% EtOAc in hexane) = 0.1; IR (neat / cm^{-1}) 3348 br (O-H, N-H), 2937 m, 1616 s (C=O), 1526 s, 1260 m, 753 s; ^1H NMR (400 MHz, CDCl_3) δ_{H} 4.93 (d, J = 1.5 Hz, 1H, H-10_a), 4.57 (d, J = 1.5 Hz, 1H, H-10_b), 4.39 (br. d, J = 6.9 Hz, 1H, *NH*), 4.08 (app. q, J = 6.9 Hz, 1H, H-12), 3.83 (ddd, J = 12.9, 4.0, 2.0 Hz, 1H, H-9_a), 3.66 (app. ddt, J = 13.1, 4.4, 2.0 Hz, 1H, H-1_a), 3.14 (app. td, J = 13.1, 3.1 Hz, 1H, H-1_b), 3.13 (dd, J = 12.9, 11.7 Hz, 1H, H-9_b), 2.34 – 2.27 (m, 1H, H-6_a), 2.17 – 2.11 (m, 1H, H-8), 2.05 – 1.94 (stack, 3H, H-6_b and H-13_a), 1.77 -1.71 (m, 1H, H-5_a), 1.69 – 1.50 (stack, 9H, H-2, H-4_a, H-5_b, H-14 and *OH*), 1.47 – 1.39 (m, 1H, H-4_b), 1.37 – 1.29 (m, 2H, H-13_b); ^{13}C NMR (101 MHz, CDCl_3) δ_{C} 157.5 (C, C-11), 147.1 (C, C-7), 109.3 (CH_2 , C-10), 70.6 (C, C-3), 52.7 (CH, C-12), 47.9 (CH, C-8), 41.8 (CH_2 , C-9), 40.3 (CH_2 , C-1), 38.9 (CH_2 , C-4), 37.5 (CH_2 , C-2), 36.3 (CH_2 , C-6), 33.7 (CH_2 , C-13), 23.8 (CH_2 , C-14), 23.5 (CH_2 , C-5); LRMS (ASAP) m/z 279.2 [(M + H)⁺, 100%]; HRMS (ASAP) calc'd for $\text{C}_{16}\text{H}_{27}\text{N}_2\text{O}_2$ (M + H)⁺ 279.2073, found 279.2070.

(4a*R, 8a*S**)-8-Methylene-2-(pyridin-3'-ylsulfonyl)octahydroisoquinolin-4a(2*H*)-ol (208)**



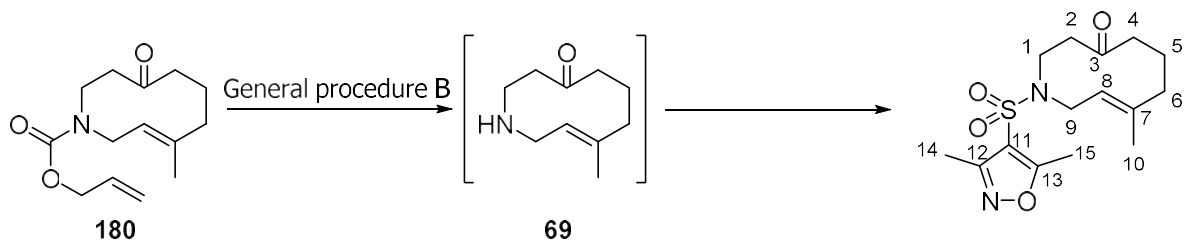
NEt₃ (44 μ L, 0.31 mmol) was added to a solution of amine **183** (42 mg, 0.25 mmol) in CH₂Cl₂ (2.5 mL) and the resulting solution was cooled to 0 °C. Pyridine-3-sulfonyl chloride (38 μ L, 0.31 mmol) was added dropwise over 1 min and the resulting solution was stirred at r.t. for 17 h. The reaction mixture was then washed sequentially with HCl_(aq) (1 M, 2 mL), H₂O (2 mL) and brine (2 mL). The organic layer was dried (MgSO₄), filtered and the solvent was then removed under reduced pressure to provide a yellow oil, which was purified by flash column chromatography (eluent: 60% EtOAc in hexane) to yield sulfonamide **208** as a clear, colourless oil (54 mg, 70%). *R*_f (50% EtOAc in hexane) = 0.1; IR (neat / cm⁻¹) 3533 br w (O-H), 2931 m, 1573 m, 1415 m, 1345 m, 1170 s, 923 m, 760 s; ¹H NMR (400 MHz, CDCl₃) δ _H 9.03 – 8.99 (m, 1H, H-15), 8.84 – 8.79 (m, 1H, H-14), 8.09 – 8.04 (m, 1H, H-12), 7.52 – 7.47 (m, 1H, H-13), 4.92 (d, *J* = 1.3 Hz, 1H, H-10_a), 4.45 (d, *J* = 1.3 Hz, 1H, H-10_b), 3.74 – 3.65 (stack, 2H, H-1_a and H-9_a), 2.76 – 2.67 (m, 1H, H-1_b), 2.58 (app. t, *J* = 11.3 Hz, 1H, H-9_b), 2.39 – 2.28 (stack, 2H, H-6_a and H-8), 2.08 – 1.97 (m, 1H, H-6_b), 1.81 – 1.39 (stack, 7H, H-2, H-4, H-5 and OH); ¹³C NMR (101 MHz, CDCl₃) δ _C 153.4 (CH, C-14), 148.5 (CH, C-15), 146.1 (C, C-7), 135.3 (CH, C-12), 133.6 (C, C-11), 123.9 (CH, C-13), 109.5 (CH₂, C-10), 69.7 (C, C-3), 47.8 (CH, C-8), 43.7 (CH₂, C-9), 42.1 (CH₂, C-1), 38.5 (CH₂, C-4), 37.2 (CH₂, C-2), 36.0 (CH₂, C-6), 23.3 (CH₂, C-5); LRMS (ASAP) *m/z* 309.1 [(M + H)⁺, 100%]; HRMS (ASAP) calc'd for C₁₅H₂₁N₂O₃S (M + H)⁺ 309.1273, found 309.1268.

**(E)-1-Cyclopropylsulfonyl-8-methyl-2,3,5,6,7,10-hexahydroazecin-4(1H)-one
(211)**



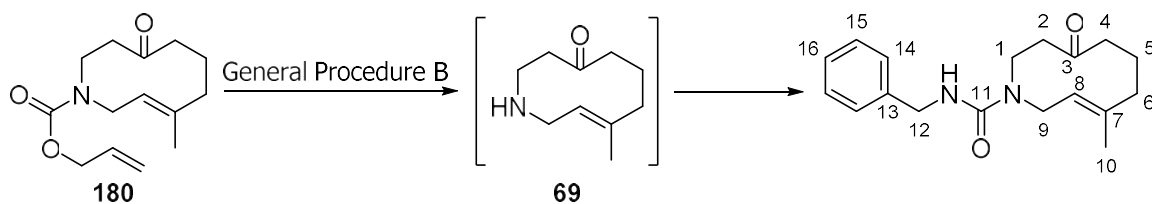
Carbamate **180** was deprotected according to general procedure **B** and the amine product **69** used without purification. NEt_3 (34 μL , 0.24 mmol) was added to a solution of amine **69** (32 mg, 0.19 mmol) in CH_2Cl_2 (2 mL). The resulting solution was cooled to 0 $^\circ\text{C}$. Cyclopropanesulfonyl chloride (25 μL , 0.24 mmol) was added dropwise over 1 min and the resulting solution was stirred at r.t. for 17 h. The reaction mixture was then washed sequentially with $\text{HCl}_{(\text{aq})}$ (1 M, 2 mL), H_2O (2 mL) and brine (2 mL). The organic layer was dried (MgSO_4), filtered and the solvent was then removed under reduced pressure to provide a clear oil, which was purified by flash column chromatography (eluent: 30% EtOAc in hexane) to yield sulfonamide **211** as a white, crystalline solid (30 mg, 58% over two steps from carbamate **180**). R_f (50% EtOAc in hexane) = 0.3; mp 131 – 133 $^\circ\text{C}$; IR (neat / cm^{-1}) 2926 br, 1699 s (C=O), 1333 s, 1143 s, 883 s; ^1H NMR (400 MHz, CDCl_3) δ_{H} 5.24 (app. t, J = 6.8 Hz, 1H, H-8), 4.20 – 4.06 (m, 1H H-9_a), 3.90 – 3.75 (m, 1H, H-1_a), 3.58 – 3.44 (m, 1H, H-9_b), 3.31 – 3.19 (m, 1H, H-1_b), 2.99 – 2.90 (m, 1H, H-2_a), 2.49 – 2.28 (stack, 4H, H-2_b, H-4_a, H-5_a and H-11), 2.27 – 2.19 (m, 1H, H-4_b), 2.14 – 2.05 (m, 1H, H-6_a), 1.94 – 1.84 (m, 1H, H-6_b), 1.81 – 1.70 (m, 1H, H-5_b), 1.49 (s, 3H, H-10), 1.17 – 1.14 (m, 2H, H-12_a), 0.99 – 0.96 (m, 2H, H-12_b); ^{13}C NMR (101 MHz, CDCl_3) δ_{C} 208.5 (C, C-3), 143.0 (C, C-7), 121.9 (CH, C-8), 48.1 (CH_2 , C-9), 46.2 (CH_2 , C-2), 44.5 (CH_2 , C-1), 43.3 (CH_2 , C-4), 40.9 (CH_2 , C-6), 29.1 (CH, C-11), 25.6 (CH_2 , C-5), 16.4 (CH_3 , C-10), 4.9 (CH_2 , C-12); LRMS (ASAP) m/z 272.1 [(M + H)⁺, 100%], 254.1 (85); HRMS (ASAP) calc'd for $\text{C}_{13}\text{H}_{22}\text{NO}_3\text{S}$ (M + H)⁺ 272.1320, found 272.1320.

(E)-1-((3',5'-Dimethylisoxazol-4'-yl)sulfonyl)-8-methyl-2,3,5,6,7,10-hexahydroazecin-4(1H)-one (212)



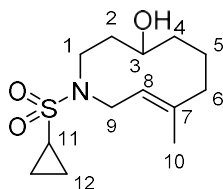
Carbamate **180** was deprotected according to general procedure **B** and the amine product **69** used without purification. NEt_3 (35 μL , 0.25 mmol) was added to a solution of amine **69** (33 mg, 0.20 mmol) in CH_2Cl_2 (2 mL) and the resulting solution was cooled to 0 $^\circ\text{C}$. 3,5-Dimethylisoxazole-4-sulfonyl chloride (48 mg, 0.25 mmol) was added in one portion and the resulting solution was stirred at r.t. for 17 h. The reaction mixture was then washed sequentially with $\text{HCl}_{(\text{aq})}$ (1 M, 2 mL), H_2O (2 mL) and brine (2 mL). The organic layer was dried (MgSO_4), filtered and the solvent was then removed under reduced pressure to provide a clear oil, which was purified by flash column chromatography (eluent: 30% EtOAc in hexane) to yield sulfonamide **210** as a white, crystalline solid (20 mg, 32% over two steps from carbamate **180**). R_f (50% EtOAc in hexane) = 0.4; mp 136 – 138 $^\circ\text{C}$; IR (neat / cm^{-1}) 2935 br, 1701 s (C=O), 1596 m, 1339 s, 1175 s, 1122 s; ^1H NMR (400 MHz, CDCl_3) δ_{H} 5.31 – 5.23 (m, 1H, H-8), 4.08 – 4.00 (m, 1H, H-9_a), 3.84 – 3.75 (m, 1H, H-1_a), 3.43 – 3.33 (m, 1H, H-9_b), 3.26 – 3.18 (m, 1H, H-1_b), 3.05 – 2.94 (m, 1H, H-2_a), 2.63 (s, 3H, H-15), 2.43 – 2.37 (stack, 5H, H-2_b, H-4_a and H-14), 2.30 – 2.20 (m, 1H, H-4_b), 2.15 – 2.07 (m, 1H, H-6_a), 1.97 – 1.88 (stack, 2H, H-5_a and H-6_b), 1.82 – 1.73 (m, 1H, H-5_b), 1.47 (s, 3H, H-10); ^{13}C NMR (101 MHz, CDCl_3) δ_{C} 208.1 (C, C-3), 173.2 (C, C-13), 157.6 (C, C-12), 144.0 (C, C-7), 121.0 (CH, C-8), 116.4 (C, C-11), 47.5 (CH_2 , C-9), 45.9 (CH_2 , C-2), 44.1 (CH_2 , C-1), 43.3 (CH_2 , C-4), 41.0 (CH_2 , C-6), 25.7 (CH_2 , C-5), 16.0 (CH_3 , C-10), 12.9 (CH_3 , C-15), 11.2 (CH_3 , C-14); LRMS (ASAP) m/z 327.1 [(M + H)⁺, 100%], 309.1 (60); HRMS (ASAP) calc'd for $\text{C}_{15}\text{H}_{23}\text{N}_2\text{O}_4\text{S}$ (M + H)⁺ 327.1379, found 327.1376.

(E)-N-Benzyl-8-methyl-4-oxo-3,4,5,6,7,10-hexahydroazecine-1(2H)-carboxamide (213)



Carbamate **180** was deprotected according to general procedure **B** and the amine product used without purification. Benzyl isocyanate (44 μL , 0.36 mmol) was added to a solution of amine **69** (35 mg, 0.21 mmol) in CH_2Cl_2 (2 mL) and the resulting solution was stirred at r.t. for 3 h. The solvent was then removed under reduced pressure to provide a clear oil, which was purified by flash column chromatography (eluent: 70% EtOAc in hexane) to yield urea **213** as a white, crystalline solid (53 mg, 86% over two steps from carbamate **180**). R_f (50% EtOAc in hexane) = 0.1; IR (neat / cm^{-1}) 3335 (N-H), 2924 br, 1698 s (C=O), 1617 s (C=O), 1533 m, 1252 m, 724 s, 695 s; ^1H NMR (400 MHz, CDCl_3) δ_{H} 7.31 – 7.19 (stack, 5H, H-14, H-15 and H-16), 5.08 – 5.02 (m, 1H, H-8), 4.93 – 4.84 (m, 1H, *NH*), 4.41 (d, J = 5.5 Hz, 2H, H-12), 4.26 – 4.13 (m, 1H, H-9_a), 3.89 – 3.76 (m, 1H, H-1_a), 3.43 – 3.31 (m, 1H, H-9_b), 3.24 – 3.09 (m, 1H, H-1_b), 2.79 – 2.66 (m, 1H, H-2_a), 2.40 – 2.28 (stack, 4H, H-2_b, H-4 and H-5_a), 2.15 – 2.03 (m, 1H, H-6_a), 1.93 – 1.66 (stack, 2H, H-5_b and H-6_b), 1.41 (s, 3H, H-10); ^{13}C NMR (101 MHz, CDCl_3) δ_{C} 207.5 (C, C-3), 167.1 (C, C-11), 143.2 (C, C-7), 132.4 (CH, ArC), 125.2 (C, C-13), 122.0 (CH, C-8), 121.4 (CH, ArC), 116.1 (CH, ArC), 52.5 (CH_2 , C-12), 48.2 (CH_2 , C-9), 46.4 (CH_2 , C-2), 44.8 (CH_2 , C-1), 43.1 (CH_2 , C-4), 41.4 (CH_2 , C-6), 25.6 (CH_2 , C-5), 15.8 (CH_3 , C-10); LRMS (ASAP) m/z 301.2 [(M + H)⁺, 100%], 279.1 (80), 241.1 (75); HRMS (ASAP) calc'd for $\text{C}_{18}\text{H}_{25}\text{N}_2\text{O}_2$ (M + H)⁺ 301.1916, found 301.1920.

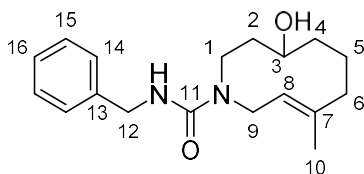
(E)-1-Cyclopropylsulfonyl-8-methyl-1,2,3,4,5,6,7,10-octahydroazecin-4-ol (214)



LiBH₄ (2.0 M in THF, 83 μ L, 0.17 mmol) was added to a cooled (0 $^{\circ}$ C) solution of ketone **211** (30 mg, 0.11 mmol) in THF (2 mL) and the resulting mixture was stirred at 0 $^{\circ}$ C. The cooling bath was then removed and the solution allowed to warm to r.t. After 17 h, H₂O (3 mL) was added. The two phases were separated and the aqueous layer was washed with Et₂O (3 \times 5 mL). The combined organic phases were dried (MgSO₄), filtered and the solvent was then removed under reduced pressure to give a colourless oil, which was purified by flash column chromatography (eluent: 55% EtOAc in hexane) to yield alcohol **214** as a clear oil (9 mg, 33%). R_f (50% EtOAc in hexane) = 0.2; IR (neat / cm⁻¹) 3501 br w (O-H), 2928 w, 1452 w, 1329 m, 1144 s; ¹H NMR (400 MHz, CDCl₃) δ_H 5.28 – 5.18 (m, 1H, H-8), 4.15 – 3.97 (m, 1H, H-9_a), 3.84 – 3.70 (m, 1H, H-3), 3.47 – 3.35 (m, 1H, H-1_a), 3.35 – 3.19 (m, 1H, H-9_b), 2.97 – 2.81 (m, 1H, H-1_b), 2.23 – 2.16 (m, 1H, H-6_a), 2.03 – 1.86 (stack, 2H, H-2_a and H-6_b), 1.72 (s, 3H, H-10), 1.62 – 1.54 (stack, 2H, H-5), 1.45 – 1.29 (stack, 3H, H-2_b and H-4), 1.15 – 1.09 (m, 2H, H-12_a), 0.97 -0.84 (stack, 3H, H-11 and H-12_b), *OH* not observed; ¹³C NMR (101 MHz, CDCl₃) δ_C 118.4 (CH, C-8), 70.7 (CH, C-3), 45.7 (CH₂, C-9), 44.0 (CH₂, C-1), 40.5 (CH₂, C-6), 39.1 (CH₂, C-2), 34.1 (CH₂, C-4), 22.6 (CH, C-11), 21.9 (CH₂, C-5), 16.8 (CH₃, C-10), 4.7 (CH₂, C-12)^{xxxviii}; LRMS (ASAP) m/z 274.1 [(M + H)⁺, 100%]; HRMS (ASAP) calc'd for C₁₃H₂₄NO₃S (M + H)⁺ 274.1477, found 274.1475.

^{xxxviii} Within the HMBC spectrum a correlation between H-10 and a ¹³C resonance at 144.8 ppm can be seen, believed to be C-17; however, as the carbon resonance cannot be seen in the standard ¹³C NMR spectrum, the carbon resonance has not been explicitly assigned.

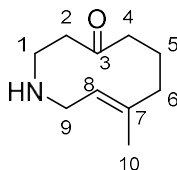
(*E*)-*N*-Benzyl-4-hydroxy-8-methyl-3,4,5,6,7,10-hexahydroazecine-1(2*H*)-carboxamide (216**)**



LiBH₄ (2.0 M in THF, 0.15 mL, 0.31 mmol) was added to a cooled (0 °C) solution of ketone **213** (61 mg, 0.20 mmol) in THF (2 mL) and the resulting mixture was stirred at 0 °C. The cooling bath was then removed and the solution allowed to warm to r.t. After 17 h, H₂O (3 mL) was added. The two phases were separated and the aqueous layer was washed with Et₂O (3 × 5 mL). The combined organic phases were dried (MgSO₄), filtered and the solvent was then removed under reduced pressure to give a colourless oil, which was purified by flash column chromatography (eluent: 70% EtOAc in hexane) to yield alcohol **216** as a clear oil (31 mg, 50%). *R_f* (50% EtOAc in hexane) = 0.1; IR (neat / cm⁻¹) 3341 br w (O-H and N-H), 2923 w, 1624 s (C=O), 1529 s; ¹H NMR (400 MHz, CDCl₃) δ_H 7.33 – 7.30 (stack, 5H, H-14, H-15 and H-16), 5.38 – 5.29 (m, 1H, *NH*), 4.92 – 4.86 (m, 1H, H-8), 4.45 – 4.43 (m, 2H, H-12), 4.05 – 3.98 (m, 1H, H-3), 3.76 – 3.67 (m, 1H, H-9_a), 3.66 – 3.56 (m, 1H, H-1_a), 3.24 – 3.09 (stack, 2H, H-1_b and H-9_b), 2.25 – 2.16 (m, 1H, H-6_a), 2.06 – 2.00 (m, 1H, H-6_b), 1.70 (s, 3H, H-10), 1.68 – 1.62 (stack, 3H, H-2_a, H-4_a and H-5_a), 1.50 – 1.39 (stack, 2H, H-2_b and H-5_b), 1.36 – 1.30 (m, 1H, H-4_b); ¹³C NMR (101 MHz, CDCl₃) δ_C 159.4 (C, C-11), 139.8 (C, C-8), 132.2 (C, C-13), 128.7 (CH, ArC), 127.9 (CH, ArC), 127.4 (CH, ArC), 68.9 (CH, C-3), 47.0 (CH₂, C-9), 46.3 (CH₂, C-1), 45.2 (CH₂, C-12), 35.4 (CH₂, C-2), 34.4 (CH₂, C-4), 21.0 (CH₂, C-5), 16.9 (CH₃, C-10)^{xxxix}; LRMS (ASAP) *m/z* 305.2 [(M + H)⁺, 100%]; HRMS (ASAP) calc'd for C₁₈H₂₇N₂O₂ (M + H)⁺ 303.2073, found 303.2076.

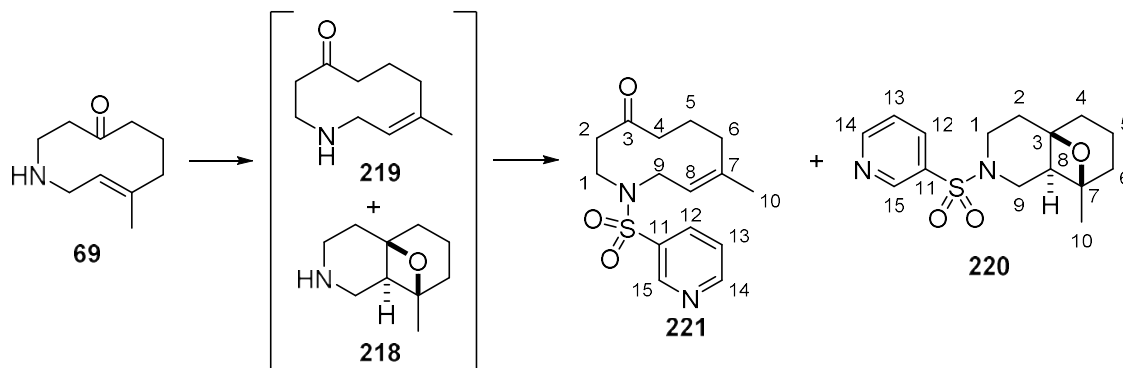
^{xxxix} Within the HMBC spectrum a correlation between H-8 and a ¹³C resonance at 120.8 ppm can be seen, believed to be C-8. A correlation between H-10 and a ¹³C resonance at 40.1 ppm can also be seen, believed to be C-6; however, as these carbon resonances cannot be seen in the standard ¹³C NMR spectrum, the carbon resonances have not been explicitly assigned.

(E)-8-methyl-2,3,5,6,7,10-hexahydroazecin-4(1H)-one (69)



Pd(PPh₃)₄ (271 mg, 0.235 mmol) was added in one portion to a solution of carbamate **180** (1.18 g, 4.69 mmol) in degassed CH₂Cl₂ (50 mL) and the resulting mixture was stirred. After 5 min, pyrrolidine (1.93 mL, 23.5 mmol) was added rapidly and the resulting solution stirred. After 30 min, the solvent was removed under reduced pressure to give a brown oil, which was purified by flash column chromatography (eluent: 5 to 20% MeOH (with 1% NH₃) in CH₂Cl₂) to yield amine **69** as a light yellow oil (690 mg, 88%). *R_f* (20% MeOH in CH₂Cl₂) = 0.1; IR (neat / cm⁻¹) 3339 br (N-H), 2924 s, 1698 s (C=O), 1452 m, 1281 m, 1105 m; ¹H NMR (400 MHz, CDCl₃) δ_H 5.24 – 5.19 (m, 1H, H-8), 3.28 – 3.12 (stack, 2H, H-1), 3.03 – 2.85 (stack, 2H, H-2), 2.85 – 2.72 (m, 1H, H-9_a), 2.39 – 2.25 (stack, 3H, H-4_a, H-5_a and H-9_b), 2.18 – 2.08 (m, 1H, H-4_b), 2.05 – 1.94 (m, 1H, H-6_a), 1.90 – 1.76 (m, 1H, H-6_b), 1.75 – 1.61 (m, 1H, H-5_b), 1.44 (s, 3H, H-10), exchangeable protons not observed; ¹³C NMR (101 MHz, CDCl₃) δ_C 208.8 (C, C-3), 141.0 (C, C-7), 125.5 (CH, C-8), 47.5 (CH₂, C-9), 47.3 (CH₂, C-1), 44.1 (CH₂, C-2), 43.5 (CH₂, C-4), 41.2 (CH₂, C-6), 26.4 (CH₂, C-5), 16.1 (CH₃, C-10); LRMS (ASAP) *m/z* 168.2 [(M + H)⁺, 100%]; HRMS (ASAP) calc'd for C₁₀H₁₈NO (M + H)⁺ 168.1388, found 168.1383.

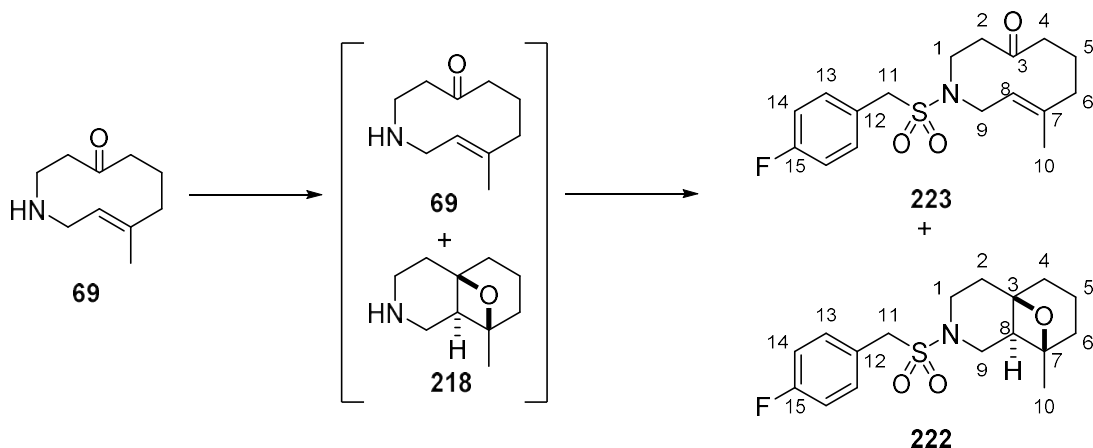
(Z)-8-Methyl-1-(pyridin-3'-ylsulfonyl)-2,3,5,6,7,10-hexahydroazecin-4(1H)-one (221) and (4a*R, 8*R**, 8a*R**)-8-methyl-2-(pyridin-3'-ylsulfonyl)octahydro-2*H*-4a,8-epoxyisoquinoline (220)**



Amine **69** (0.110 g, 0.63 mmol) was dissolved in degassed MeCN (75 mL) within a vessel of quartz glass. The resulting solution was stirred and irradiated with a 125 W medium pressure lamp that was suspended in the middle of the reactor vessel (path length ~2 cm) for 2 h. The solvent was then removed under reduced pressure to give an orange oil, which was used directly in the next step. NEt₃ (110 μL, 0.78 mmol) was added to a solution of the product mixture (0.110 g) in CH₂Cl₂ (7 mL) and the resulting solution was cooled to 0 °C. Pyridine-3-sulfonyl chloride (95 μL, 0.79 mmol) was added dropwise over 1 min and the resulting solution was stirred at r.t. for 17 h. The reaction mixture was then washed sequentially with HCl_(aq) (1 M, 2 mL), H₂O (2 mL) and brine (2 mL). The organic layer was dried (MgSO₄), filtered and the solvent was then removed under reduced pressure to provide a yellow oil, which was purified by flash column chromatography (eluent: 40% Et₂O in CH₂Cl₂) to yield, in order of elution, sulfonamide **221** as a colourless oil (17 mg, 7% over two steps from amine **69**). *R*_f (50% EtOAc in hexane) = 0.3; IR (neat / cm⁻¹) 2930 br m, 1700 s (C=O), 1345 s, 1324 s, 1164 s, 1105 m; ¹H NMR (400 MHz, CDCl₃) δ_H 9.01 – 8.98 (m, 1H, H-15), 8.81 (dd, *J* = 4.9, 1.6 Hz, 1H, H-14), 8.06 (ddd, *J* = 8.0, 2.4, 1.6 Hz, 1H, H-13), 7.47 (ddd, *J* = 8.0, 4.9, 0.9 Hz, 1H, H-12), 5.27 – 5.21 (m, 1H, H-8), 4.23 – 4.14 (m, 1H, H-9_a), 3.86 – 3.76 (m, 1H, H-1_a), 3.33 – 3.23 (m, 1H, H-9_b), 3.14 – 2.93 (stack, 2H, H-1_b and H-2_a), 2.56 – 2.30 (stack, 3H, H-2_b, H-4_a and H-5_a), 2.29 – 2.19 (m, 1H, H-4_b), 2.16 – 2.04 (m, 1H, H-6_a), 1.97 – 1.83 (m, 1H, H-6_b), 1.79 – 1.71 (m, 1H, H-5_b), 1.42 (s, 3H, H-10); ¹³C NMR (101 MHz, CDCl₃) δ_C 208.2 (C, C-3), 153.3 (CH, C-14), 147.8 (CH, C-15), 143.9 (C, C-7), 136.5 (CH, C-13), 134.6 (C, C-11), 124.0 (CH, C-12), 121.0 (CH, C-8), 48.1 (CH₂, C-9), 45.8 (CH₂, C-2), 44.5 (CH₂, C-1), 43.3 (CH₂, C-4), 40.9 (CH₂, C-6), 25.5 (CH₂, C-5), 16.0 (CH₃, C-10); LRMS (ASAP) *m/z* 309.1 [(M + H)⁺,

100%]; HRMS (ASAP) calc'd for $C_{15}H_{21}N_2O_3S$ ($M + H$)⁺ 309.1273, found 309.1268, and then oxetane **220** as a colourless oil (7 mg, 4% over two steps from amine **69**). R_f (50% EtOAc in hexane) = 0.2; IR (neat / cm^{-1}) 2929 br m, 1572 m, 1348 m, 1169 s, 755 s; 1H NMR (400 MHz, $CDCl_3$) δ_H 8.98 – 8.96 (m, 1H, H-15), 8.78 (dd, $J = 4.8, 1.6$ Hz, 1H, H-14), 8.03 (ddd, $J = 8.0, 2.4, 1.6$ Hz, 1H, H-13), 7.45 (ddd, $J = 8.0, 4.8, 0.9$ Hz, 1H, H-12), 3.90 (ddd, $J = 12.2, 8.6, 2.3$ Hz, 1H, H-9_a), 3.68 – 3.61 (m, 1H, H-1_a), 2.92 (dd, $J = 12.2, 9.8$ Hz, 1H, H-9_b), 2.68 – 2.60 (m, 1H, H-1_b), 2.53 – 2.47 (m, 1H, H-8), 2.00 – 1.89 (m, 1H, H-5_a), 1.87 – 1.73 (stack, 3H, H-2_a, H-5_b and H-6_a), 1.71 – 1.55 (stack, 3H, H-2_b, H-4_a and H-6_b), 1.54 – 1.45 (m, 1H, H-4_b), 1.02 (s, 3H, H-10); ^{13}C NMR (101 MHz, $CDCl_3$) δ_C 153.5 (CH, C-14), 148.5 (CH, C-15), 135.2 (CH, C-13), 134.0 (C, C-11), 124.0 (CH, C-12), 83.7 (C, C-7), 79.0 (C, C-3), 44.2 (CH_2 , C-9), 42.9 (CH_2 , C-1), 40.4 (CH, C-8), 33.9 (CH_2 , C-6), 33.1 (CH_2 , C-4), 32.6 (CH_2 , C-2), 22.1 (CH_3 , C-10), 16.2 (CH_2 , C-5); LRMS (ASAP) m/z 309.1 [$(M + H)^+$, 100%]; HRMS (ASAP) calc'd for $C_{15}H_{21}N_2O_3S$ ($M + H$)⁺ 309.1273, found 309.1288.

(*E*)-1-((4'-Fluorobenzyl)sulfonyl)-8-methyl-2,3,5,6,7,10-hexahydroazecin-4(1*H*)-one (223) and (4*aR, 8*R**, 8*aR**)-2-((4'-fluorobenzyl)sulfonyl)-8-methyloctahydro-2*H*-4*a*,8-epoxyisoquinoline (222)**

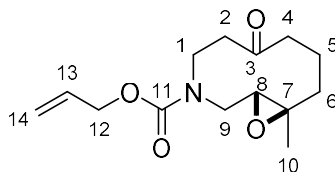


Amine **69** (0.110 g, 0.63 mmol) was dissolved in degassed MeCN (75 mL) within a vessel of quartz glass. The resulting solution was stirred and irradiated with a 125 W medium pressure lamp that was suspended in the middle of the reactor vessel (path length \sim 2 cm) for 1 h. The solvent was then removed under reduced pressure to give an orange oil, which was used directly in the next step. NEt₃ (110 μ L, 0.78 mmol) was added to a solution of the product mixture (0.110 g) in CH₂Cl₂ (7 mL) and the resulting solution was cooled to 0 °C. (4-Fluorophenyl)methanesulfonyl chloride (165 mg, 0.79 mmol) was added in one portion and the resulting solution was stirred at r.t. for 17 h. The reaction mixture was then washed sequentially with HCl_(aq) (1 M, 2 mL), H₂O (2 mL) and brine (2 mL). The organic layer was dried (MgSO₄), filtered and the solvent was then removed under reduced pressure to provide a yellow oil, which was purified by flash column chromatography (eluent: 2.5% Et₂O in CH₂Cl₂) to yield, in order of elution, sulfonamide **223** as a colourless oil (21 mg, 10% over two steps from amine **69**). *R*_f (5% Et₂O in CH₂Cl₂) = 0.4; IR (neat / cm⁻¹) 2933 br m, 1700 s (C=O), 1509 s, 1335 s, 1126 s, 888 s; ¹H NMR (400 MHz, CDCl₃) δ _H 7.36 – 7.30 (AA' of AA'BB', 2H, H-13), 7.12 – 7.06 (BB' of AA'BB', 2H, H-14), 5.15 – 5.09 (m, 1H, H-8), 4.18 (d, *J* = 2.4 Hz, 2H, H-11), 3.87 – 3.77 (m, 1H, H-9_a), 3.45 – 3.35 (m, 1H, H-1_a), 3.24 – 3.12 (m, 1H, H-9_b), 3.09 – 2.95 (m, 1H, H-1_b), 2.91 – 2.79 (m, 1H, H-2_a), 2.40 – 2.28 (stack, 3H, H-2_b, H-4_a and H-5_a) 2.26 – 2.14 (m, 1H, H-4_b), 2.10 – 2.01 (m, 1H, H-6_a), 1.91 – 1.80 (m, 1H, H-6_b), 1.78 – 1.66 (m, 1H, H-5_b), 1.41 (s, 3H, H-10); ¹³C NMR (101 MHz, CDCl₃) δ _C 208.5 (C, C-3), 163.1 (CF, d, *J* = 249 Hz, C-15), 143.0 (C, C-7), 132.4 (CH, d, *J* = 9 Hz, C-13), 125.2

(C, d, $J = 3$ Hz, C-12), 122.0 (CH, C-8), 116.1 (CH, d, $J = 22$ Hz, C-14), 57.2 (CH₂, C-11), 48.5 (CH₂, C-9), 46.6 (CH₂, C-2), 45.1 (CH₂, C-1), 43.4 (CH₂, C-4), 40.9 (CH₂, C-6), 25.6 (CH₂, C-5), 15.9 (CH₃, C-10); ¹⁹F NMR (377 MHz, CDCl₃) δ_F -112.4 (CF, C-15); LRMS (ASAP) m/z 322.1 [(M - H₂O + H)⁺, 100%], 340.1 (90); HRMS (ASAP) calc'd for C₁₇H₂₃FNO₃S (M + H)⁺ 340.1383, found 340.1383, and then oxetane **222** as a colourless oil (8 mg, 4% over two steps from amine **69**). R_f (5% Et₂O in CH₂Cl₂) = 0.2; IR (neat / cm⁻¹) 2927 br m, 1509 s, 1330 m, 1225 s, 1160 s, 842 m; ¹H NMR (400 MHz, CDCl₃) δ_H 7.42 – 7.37 (AA' of AA'BB', 2H, H-13), 7.13 – 7.06 (BB' of AA'BB', 2H, H-14), 4.21 (d, $J = 2.0$ Hz, 2H, H-11), 3.72 (ddd, $J = 13.0, 8.7, 2.2$ Hz, 1H, H-9_a), 3.53 – 3.46 (m, 1H, H-1_a), 3.19 (dd, $J = 13.0, 10.0$ Hz, 1H, H-9_b), 2.96 (ddd, $J = 12.6, 10.5, 5.4$ Hz, 1H, H-1_b), 2.42 – 2.36 (m, 1H, H-8), 2.05 – 1.94 (m, 1H, H-5_a), 1.90 – 1.78 (stack, 3H, H-2_a, H-5_b and H-6_a), 1.70 – 1.61 (m, 1H, H-6_b), 1.58 – 1.54 (stack, 3H, H-2_b and H-4), 1.02 (s, 3H, H-10); ¹³C NMR (101 MHz, CDCl₃) δ_C 132.6 (CH, d, $J = 8$ Hz, C-13), 116.0 (CH, d, $J = 22$ Hz, C-14), 83.8 (C, C-7), 79.3 (C, C-3), 56.6 (CH₂, C-11), 44.3 (CH₂, C-9), 42.9 (CH₂, C-1), 40.6 (CH, C-8), 34.0 (CH₂, C-6), 33.3 (CH₂, C-4), 33.2 (CH₂, C-2), 22.0 (CH₃, C-10), 16.2 (CH₂, C-5)^{xi}; LRMS (ASAP) m/z 340.1 [(M + H)⁺, 100%]; HRMS (ASAP) calc'd for C₁₇H₂₃FNO₃S (M + H)⁺ 340.1383, found 340.1375.

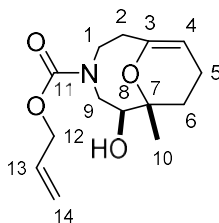
^{xi} C-12 and C-15 were not observed.

Allyl (1*R, 10*R**)-10-methyl-6-oxo-11-oxa-3-azabicyclo[8.1.0]undecane-3-carboxylate (**224**)**



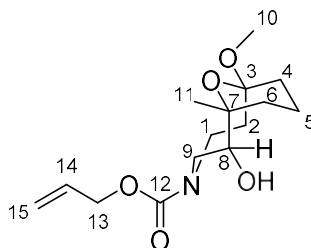
*m*CPBA (85%, 0.514 g, 2.53 mmol) was added to a cooled (0 °C) solution of ketone **180** (0.606 g, 2.41 mmol) in CH₂Cl₂ (14 mL). The resultant solution was stirred for 6 h at 0 °C, after which time, Na₂S₂O₃ (aq) (10 mL) was added and the mixture was stirred for 10 min. The two phases were then separated and the organic phase was washed sequentially with NaHCO₃ (aq) (10 mL), H₂O (10 mL) and brine (10 mL). The organic phase was dried (MgSO₄), filtered and the solvent was then removed under reduced pressure to give a yellow oil, which was purified by flash column chromatography (eluent: 35% EtOAc in hexane) to yield epoxide **224** as a light yellow oil (0.576 g, 89%). *R*_f (50% EtOAc in hexane) = 0.4; IR (neat / cm⁻¹) 2946 w, 1697 s (C=O), 1411 m, 1237 m, 1136 m; ¹H NMR (400 MHz, CDCl₃) δ_H 6.01 – 5.87 (m, 1H, H-13), 5.35 – 5.17 (stack, 2H, H-14), 4.70 – 4.56 (stack, 2H, H-12), 4.14 – 4.04 (m, 1H, H-1_a), 4.00 (app. d, *J* = 15.1 Hz, H-9_a), 3.48 – 3.32 (m, 1H, H-9_b), 2.89 – 2.36 (stack, 6H, H-1_b, H-2, H-4 and H-8), 2.29 – 2.12 (stack, 2H, H-5_a and H-6_a), 1.67 – 1.58 (m, 1H, H-5_b), 1.21 (s, 3H, H-10), 0.98 – 0.88 (m, 1H, H-6_b); ¹³C NMR (101 MHz, CDCl₃) δ_C 210.9 (C, C-3), 155.6 (C, C-11), 132.7 (CH, C-13), 117.8 (CH₂, C-14), 66.5 (CH₂, C-12), 62.4 (CH, C-8), 61.1 (C, C-7), 46.1 (CH₂, C-1), 45.7 (CH₂, C-9), 43.8 (CH₂, C-2 or C-4), 43.6 (CH₂, C-2 or C-4), 39.2 (CH₂, C-6), 18.8 (CH₂, C-5), 16.1 (CH₃, C-10); LRMS (ASAP) *m/z* 268.2 [(M + H)⁺, 100%], 250.1 (50); HRMS (ASAP) calc'd for C₁₄H₂₂NO₄ (M + H)⁺ 268.1549, found 268.1550.

Allyl (1*R, 2*S**)-2-hydroxy-1-methyl-11-oxa-4-azabicyclo[5.3.1]undec-7-ene-4-carboxylate (**225**)**



TsOH·H₂O (20.0 mg, 0.108 mmol) was added to a solution of epoxide **224** (576 mg, 2.15 mmol) in CH₂Cl₂ (22 mL). After 3 h, NaHCO₃ (aq) (15 mL) was added. The layers were separated and the aqueous layer was washed with EtOAc (3 × 10 mL). The combined organic phases were dried (MgSO₄), filtered and the solvent was then removed under reduced pressure to give a colourless oil, which was purified by flash column chromatography (eluent: 25% EtOAc in hexane) to yield enol ether **225** as a colourless oil (525 mg, 91%). *R*_f (50% EtOAc in hexane) = 0.4; IR (neat / cm⁻¹) 3345 br (O-H), 2974 m, 1698 s (C=O), 1331 s, 1147 s; ¹H NMR (400 MHz, CDCl₃) δ_H 5.98 – 5.86 (m, 1H, H-13), 5.33 – 5.18 (stack, 2H, H-14), 4.69 – 4.51 (stack, 3H, H-4 and H-12), 4.23 – 4.15 (m, 1H, H-8), 3.94 – 3.75 (m, 1H, H-1_a), 3.72 – 3.61 (m, 1H, H-9_a), 3.21 – 3.01 (stack, 2H, H-1_b and H-9_b), 2.30 – 2.17 (stack, 2H, H-2), 2.15 – 1.96 (stack, 3H, H-5 and H-6_a), 1.86 – 1.65 (m, 1H, H-6_b), 1.22 (s, 3H, H-10), *OH* not observed; ¹³C NMR (101 MHz, CDCl₃) δ_C 156.5 (C, C-11), 149.6 (C, C-3), 133.1 (CH, C-13), 117.5 (CH₂, C-14), 103.1 (CH, C-4), 76.1 (C, C-7), 69.3 (CH, C-8), 66.1 (CH₂, C-12), 54.9 (CH₂, C-9), 47.9 (CH₂, C-1), 32.3 (CH₂, C-2), 29.6 (CH₂, C-6), 20.7 (CH₃, C-10), 18.7 (CH₂, C-5); LRMS (EI) *m/z* 267.2 [(M)⁺, 100%], 208.1 (45), 123.1 (70); HRMS (EI) calc'd for C₁₄H₂₁NO₄ (M)⁺ 267.1471, found 267.1478.

Allyl (1*R, 2*S**, 7*S**)-2-hydroxy-7-methoxy-1-methyl-11-oxa-4-azabicyclo[5.3.1]undecane-4-carboxylate (**226**)**



Method A: TsOH·H₂O (18 mg, 0.096 mmol) was added to a solution of enol ether **225** (0.515 g, 1.93 mmol) in MeOH (10 mL). The resultant solution was stirred for 2 h at r.t., after which time, NaHCO_{3(aq)} (10 mL) was added. The solution was diluted with EtOAc (10 mL) and the layers were separated. The aqueous layer was washed with EtOAc (3 × 10 mL). The combined organic phases were dried (MgSO₄), filtered and the solvent was then removed under reduced pressure to give a yellow oil, which was purified by flash column chromatography (eluent: 35% EtOAc in hexane) to yield acetal **226** as a bright yellow oil (0.504 g, 91%). *R*_f (50% EtOAc in hexane) = 0.4; IR (neat / cm⁻¹) 3425 br w (O-H), 2940 w, 1675 s (C=O), 1529 s, 1413 m, 1244 m; ¹H NMR (400 MHz, CDCl₃) δ_H 6.01 – 5.86 (m, 1H, H-14), 5.36 – 5.16 (stack, 2H, H-15), 4.69 – 4.50 (stack, 2H, H-13), 4.21 – 4.14 (m, 1H, H-8), 4.03 – 3.61 (stack, 3H, H-1 and H-9_a), 3.51 – 3.37 (m, 1H, H-9_b), 3.23 (s, 3H, H-10), 3.20 – 2.99 (stack, 2H, H-2), 2.48 – 1.59 (stack, 6H, H-4, H-5 and H-6), 1.22 – 1.17 (m, 3H, H-11), *OH* not observed^{xli}; ¹³C NMR (101 MHz, CDCl₃) δ_C [149.9, 149.7 (C, C-12)], [133.4, 133.2 (CH, C-14)], [117.4, 117.3 (CH₂, C-15)], [103.1, 102.8 (C, C-3)], [76.2, 76.1 (C, C-7)], [75.8, 75.3 (CH, C-8)], [54.9, 53.9 (CH₂, C-9)], [53.1, 52.3 (CH₃, C-10)], [48.2, 47.9 (CH₂, C-13)], [43.2, 42.8 (CH₂, C-1)], [41.3, 40.9 (CH₂, C-2)], [32.4, 31.9 (CH₂, C-6)], [29.0, 28.9 (CH₂, C-4)], [23.3, 23.2 (CH₃, C-11)], 17.3 (CH₂, C-5)^{xlii}; LRMS (ASAP) *m/z* 268.2 [(M + H)⁺, 100%]; HRMS (ASAP) calc'd for C₁₅H₂₆NO₅ (M + H)⁺ 300.1811, found 300.1804.

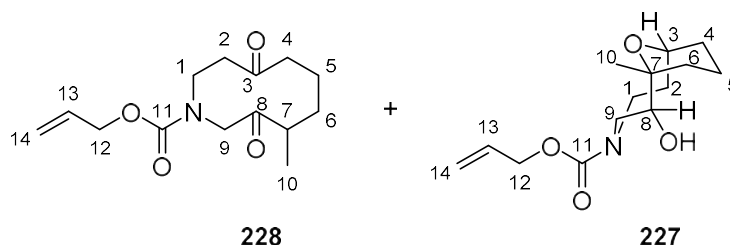
Method B: TsOH·H₂O (32 mg, 0.17 mmol) was added to a solution of epoxide **224** (890 mg, 3.33 mmol) in MeOH (33 mL). The resultant solution was stirred for 6 h at r.t., after which

^{xli} The compound exists as a 1:1 mixture of rotamers on the NMR timescale, so only clearly assignable resonances are identified.

^{xlii} The compound exists as a 1:1 mixture of rotamers on the NMR timescale, so two carbon resonances typically appear in the ¹³C NMR spectrum per carbon environment. Both resonances are given within each set of square brackets. If only one resonance is given, then the resonances from each rotamer are co-incident.

time, $\text{NaHCO}_3(\text{aq})$ (20 mL) was added. The solution was diluted with EtOAc (20 mL) and the layers were separated. The aqueous layer was washed with EtOAc (3 × 20 mL). The combined organic phases were dried (MgSO_4), filtered and the solvent was then removed under reduced pressure to give a white crystalline solid. Purification by flash column chromatography (eluent: 35% EtOAc in hexane) yielded acetal **226** as a yellow oil (947 mg, 95%).

Allyl 4-methyl-3,8-dioxoazecane-1-carboxylate (228) and allyl (1*R, 2*S**, 7*S**)-2-hydroxy-1-methyl-11-oxa-4-azabicyclo[5.3.1]undecane-4-carboxylate (227)**

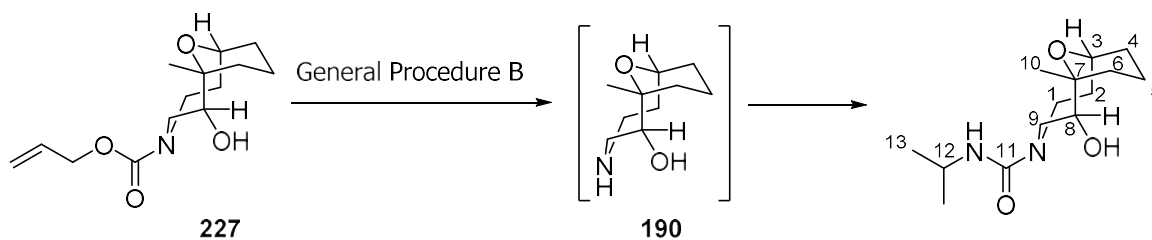


Method A: $\text{BF}_3 \cdot \text{Et}_2\text{O}$ (0.18 mL, 1.48 mmol) was added to a cooled solution (0 °C) of acetal **226** (0.422 g, 1.48 mmol) in CH_2Cl_2 (15 mL). Et_3SiH (1.18 mL, 7.38 mmol) was then added dropwise over 1 min. The resultant solution was stirred for 3 h at 0 °C, after which time, $\text{NaHCO}_3(\text{aq})$ (10 mL) was added. The aqueous layer was washed with CH_2Cl_2 (3 × 8 mL). The combined organic phases were dried (MgSO_4), filtered and the solvent was then removed under reduced pressure to give a yellow oil. Purification by flash column chromatography (eluent: 12.5% Et_2O in CH_2Cl_2) afforded, in order of elution, diketone **228** as a colourless oil (0.104 g, 27%). R_f (50% EtOAc in hexane) = 0.5; IR (neat / cm^{-1}) 2934 br m, 1693 br s (C=O), 1246 s, 912 s, 726 s; ^1H NMR (400 MHz, CDCl_3) δ_{H} 6.01 – 5.78 (m, 1H, H-13), 5.38 – 5.10 (stack, 2H, H-14), 4.65 – 4.48 (stack, 2H, H-12), 4.12 – 3.56 (stack, 4H, H-1 and H-9), 2.79 – 2.67 (m, 1H, H-2_a), 2.67 – 2.56 (m, 1H, H-7), 2.51 – 2.40 (m, 1H, H-4_a), 2.35 – 2.18 (stack, 2H, H-2_b and H-4_b), 2.00 – 1.83 (stack, 2H, H-5_a and H-6_a), 1.75 – 1.62 (m, 1H, H-5_b), 1.47 – 1.35 (m, 1H, H-6_b), 0.96 (d, J = 7.0 Hz, 3H, H-10); ^{13}C NMR (101 MHz, CDCl_3) δ_{C} 212.9 (C × 2, C-3 and C-8), 156.2 (C, C-11), 132.8 (CH, C-13), 117.5 (CH_2 , C-14), 66.4 (CH_2 , C-12), 56.6 (CH_2 , C-9), 44.2 (CH_2 , C-1), 43.3 (CH_2 , C-4), 42.2 (CH, C-7), 41.8 (CH_2 , C-2), 32.9 (CH_2 , C-6), 22.6 (CH_2 , C-5), 18.9 (CH_3 , C-10); LRMS (ASAP) m/z 268.2 [(M + H)⁺, 100%], 250.1 (70), 206 (95); HRMS (ASAP) calc'd for $\text{C}_{14}\text{H}_{22}\text{NO}_4$ (M + H)⁺ 268.1549, found 268.1550 and then alcohol **227** as a colourless oil (0.212 g, 53%). R_f (50% EtOAc in hexane) = 0.5; IR (neat / cm^{-1}) 3417 br (O-H), 2939 br m, 1674 s (C=O), 1416 w, 1246 s, 1049 s, 727 s; ^1H NMR (400

MHz, CDCl₃) δ _H 5.96 – 5.82 (m, 1H, H-13), 5.31 – 5.11 (stack, 2H, H-14), 4.63 – 4.50 (stack, 2H, H-12), 4.18 – 3.73 (stack, 4H, H-1_a, H-3, H-8 and H-9_a), 3.64 – 3.58 (m, 1H, OH), 3.44 – 3.26 (m, 1H, H-9_b), 2.96 – 2.80 (m, 1H, H-1_b), 1.92 – 1.40 (stack, 6H, H-2, H-4_a, H-5 and H-6_a), 1.34 – 1.21 (stack, 2H, H-4_b and H-6_b), 1.04 (s, 3H, H-10); ¹³C NMR (101 MHz, CDCl₃) δ _C 156.8 (C, C-11), 133.1 (CH, C-13), 117.2 (CH₂, C-14), 75.4 (CH, C-8), 73.4 (C, C-7), 70.2 (CH, C-3), 66.2 (CH₂, C-12), 52.7 (CH₂, C-9), 44.2 (CH₂, C-1), 36.7 (CH₂, C-2), 32.6 (CH₂, C-6), 27.6 (CH₂, C-4), 23.7 (CH₃, C-10), 14.2 (CH₂, C-5); LRMS (ASAP) *m/z* 270.1 [(M + H)⁺, 100%]; HRMS (ASAP) calc'd for C₁₄H₂₄NO₄ (M + H)⁺ 270.1705, found 270.1708.

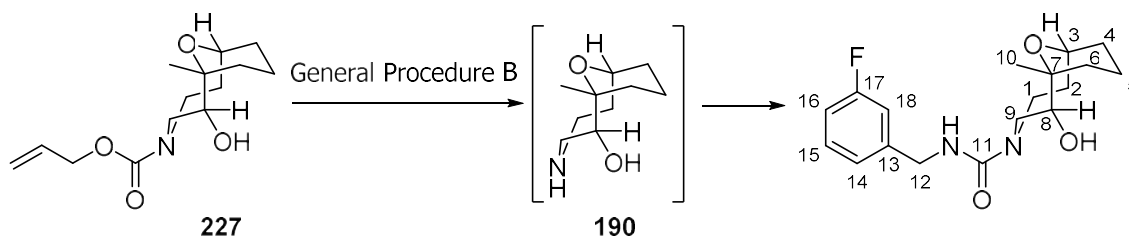
Method B: Et₃SiH (2.70 mL, 16.9 mmol) was added to a cooled solution (0 °C) of acetal **226** (1.01 g, 3.39 mmol) in CH₂Cl₂ (22 mL). BF₃·Et₂O (0.42 mL, 3.39 mmol) was then added dropwise over 10 min. The resultant solution was stirred for 3 h at 0 °C, after which time, NaHCO₃ (aq) (10 mL) was added. The aqueous layer was washed with CH₂Cl₂ (3 × 8 mL). The combined organic phases were dried (MgSO₄), filtered and the solvent was then removed under reduced pressure to give a yellow oil. Purification by flash column chromatography (eluent: 35% EtOAc in hexane) yielded alcohol **227** as a colourless oil (0.808 g, 89%). Data were in agreement with those obtained for alcohol **227** that was prepared using method A.

(1*R, 2*S**, 7*S**)-2-Hydroxy-*N*-isopropyl-1-methyl-11-oxa-4-azabicyclo[5.3.1]undecane-4-carboxamide (**230**)**



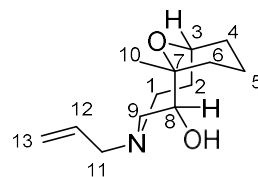
Carbamate **227** was deprotected according to general procedure **B** and the amine product **190** used without purification. Isopropyl isocyanate (42 μ L, 0.42 mmol) was added to a solution of amine **190** (63 mg, 0.34 mmol) in CH_2Cl_2 (3.5 mL) and the resulting solution was stirred at r.t. for 3 h. The solvent was then removed under reduced pressure to afford a brown oil, which was purified by flash column chromatography (eluent: 100% EtOAc) to yield urea **230** as a yellow oil (35 mg, 38% over two steps from carbamate **227**). R_f (100% EtOAc) = 0.3; IR (neat / cm^{-1}) 3331 br (O-H, N-H), 2935 m, 1614 m (C=O), 1524 m, 1049 s, 721 s; ^1H NMR (400 MHz, CDCl_3) δ_{H} 4.60 – 4.53 (m, 1H, *N*H), 4.03 – 3.93 (stack, 2H, H-3 and H-12), 3.86 – 3.76 (stack, 2H, H-1_a and H-8), 3.64 (app. d, $J = 15.0$ Hz, 1H, H-9_a), 3.44 (dd, $J = 15.0, 6.2$ Hz, 1H, H-9_b), 3.23 – 3.17 (m, 1H, *O*H), 3.05 (app. dd, $J = 15.2, 8.2$ Hz, 1H, H-1_b), 1.93 – 1.85 (m, 1H, H-6_a), 1.83 – 1.69 (stack, 2H, H-2_a and H-4_a), 1.69 – 1.62 (m, 1H, H-5_a), 1.60 – 1.47 (stack, 2H, H-2_b and H-5_b), 1.38 – 1.30 (stack, 2H, H-4_b and H-6_b), 1.16 (app. d, $J = 6.6$ Hz, 6H, H-13), 1.11 (s, 3H, H-10); ^{13}C NMR (101 MHz, CDCl_3) δ_{C} 157.9 (C, C-11), 75.7 (CH, C-8), 73.5 (C, C-7), 70.3 (CH, C-3), 52.2 (CH_2 , C-9), 44.4 (CH_2 , C-1), 42.8 (CH, C-12), 36.1 (CH_2 , C-2), 32.5 (CH_2 , C-6), 27.6 (CH_2 , C-4), 23.6 (CH_3 , C-13), 23.5 (CH_3 , C-10), 14.2 (CH_2 , C-5); LRMS (ASAP) m/z 271.2 [(M + H)⁺, 20%], 57.1 (100); HRMS (ASAP) calc'd for $\text{C}_{14}\text{H}_{27}\text{N}_2\text{O}_3$ (M + H)⁺ 271.2022, found 271.2029.

(1*R, 2*S**, 7*S**)-*N*-(3'-fluorobenzyl)-2-hydroxy-1-methyl-11-oxa-4-azabicyclo[5.3.1]undecane-4-carboxamide (**231**)**



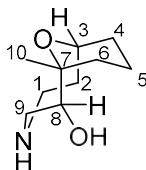
Carbamate **227** was deprotected according to general procedure **B** and the amine product **190** was used without purification. 3-Fluorobenzyl isocyanate (54 μL , 0.42 mmol) was added to a solution of amine **190** (63 mg, 0.34 mmol) in CH_2Cl_2 (4 mL) and the resulting solution was stirred at r.t. for 3 h. The solvent was then removed under reduced pressure to provide a brown oil, which was purified by flash column chromatography (eluent: 60% EtOAc in hexane) to yield urea **231** as a colourless oil (35 mg, 23% over two steps from carbamate **227**). R_f (70% EtOAc in hexane) = 0.3; IR (neat / cm^{-1}) 3370 br (O-H), 2938 br w, 1616 s, 1527 s, 1252 m, 1050 s; ^1H NMR (400 MHz, CDCl_3) δ_{H} 7.28 – 7.21 (m, 1H, H-15), 7.05 – 6.99 (m, 1H, H-14), 6.97 – 6.87 (stack, 2H, H-16 and H-18), 5.51 (br. s, 1H, NH), 4.41 (dd, J = 15.3, 5.7 Hz, 1H, H-12_a), 4.30 (dd, J = 15.3, 5.5 Hz, 1H, H-12_b), 4.00 – 3.79 (stack, 4H, H-1_a, H-3, H-8 and OH), 3.65 – 3.55 (m, 1H, H-9_a), 3.46 (dd, J = 15.1, 6.1 Hz, 1H, H-9_b), 3.01 (app. dd, J = 14.9, 8.1 Hz, 1H, H-1_b), 1.91 – 1.83 (m, 1H, H-6_a), 1.83 – 1.69 (stack, 2H, H-2_a and H-4_a), 1.69 – 1.58 (m, 1H, H-5_a), 1.57 – 1.45 (stack, 2H, H-2_b and H-5_b), 1.37 – 1.28 (stack, 2H, H-4_b and H-6_b), 1.09 (s, 3H, H-10); ^{13}C NMR (101 MHz, CDCl_3) δ_{C} 163.1 (CF, d, J = 246 Hz, C-17), 158.5 (C, C-11), 142.6 (C, d, J = 7 Hz, C-13), 130.1 (CH, d, J = 8 Hz, C-15), 122.9 (CH, d, J = 3 Hz, C-14), 114.1 (CH, d, J = 22 Hz, C-16 or C-18), 114.0 (CH, d, J = 22 Hz, C-16 or C-18), 75.7 (CH, C-8), 73.6 (C, C-7), 70.3 (CH, C-3), 52.3 (CH_2 , C-9), 44.5 (2 \times CH_2 , C-1 and C-12), 36.4 (CH_2 , C-2), 32.6 (CH_2 , C-6), 27.6 (CH_2 , C-4), 23.4 (CH_3 , C-10), 14.2 (CH_2 , C-5); ^{19}F NMR (377 MHz, CDCl_3) δ_{F} -113.0 (CF, C-17); LRMS (ASAP) m/z 337.2 [(M + H)⁺, 60%], 279.1 (100); HRMS (ASAP) calc'd for $\text{C}_{18}\text{H}_{26}\text{FN}_2\text{O}_3$ (M + H)⁺ 337.1927, found 337.1937.

(1*R, 2*S**, 7*S**)-4-Allyl-1-methyl-11-oxa-4-azabicyclo[5.3.1]undecan-2-ol (229)**



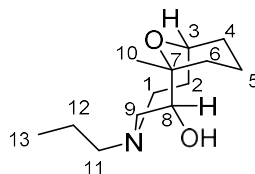
Pd(dba)₂ (85 mg, 150 μmol) and 1,4-bis(diphenylphosphino)butane (63 mg, 150 μmol) were added sequentially to a solution of carbamate **227** (0.80 g, 3.0 mmol) in degassed CH₂Cl₂ (20 mL) and the resulting mixture was stirred until a yellow colour persisted (typically 5 min). At that time, pyrrolidine (1.2 mL, 15 mmol) was added rapidly and the resulting solution stirred. After 30 min, the solvent was removed under reduced pressure to give a brown oil, which was purified by flash column chromatography (eluent: 10% MeOH in CH₂Cl₂) to yield allyl amine **229** as a yellow oil (480 mg, 72%). *R*_f (20% MeOH in CH₂Cl₂) = 0.2; IR (neat / cm⁻¹) 3290 br w (O-H), 2930 br m, 2890 br w, 1454 m, 1074 s, 1044 s; ¹H NMR (400 MHz, CDCl₃) δ_H 6.34 (br. s, 1H, OH), 5.99 – 5.87 (m, 1H, H-12), 5.22 – 5.13 (m, 2H, H-13), 4.36 (app. d, *J* = 6.2 Hz, 1H, H-8), 3.84 (app. dt, *J* = 12.0, 5.6 Hz, 1H, H-3), 3.26 – 3.19 (m, 1H, H-9_a), 3.13 (dd, *J* = 13.2, 6.4 Hz, 2H, H-11), 3.03 – 2.95 (m, 1H, H-1_a), 2.78 (dd, *J* = 13.0, 1.7 Hz, 1H, H-9_b), 2.45 (app. dd, *J* = 12.8, 8.4 Hz, 1H, H-1_b), 2.07 – 1.98 (m, 1H, H-2_a), 1.98 – 1.91 (m, 1H, H-6_a), 1.76 – 1.69 (stack, 2H, H-4_a and H-5_a), 1.67 – 1.58 (m, 1H, H-2_b), 1.56 – 1.49 (m, 1H, H-5_b), 1.36 – 1.25 (stack, 2H, H-4_b and H-6_b), 1.08 (s, 3H, H-10); ¹³C NMR (101 MHz, CDCl₃) δ_C 133.8 (CH, C-12), 119.6 (CH₂, C-13), 74.1 (C, C-7), 71.0 (CH, C-3), 70.2 (CH, C-8), 63.1 (CH₂, C-9 or C-11), 62.9 (CH₂, C-9 or C-11), 52.5 (CH₂, C-1), 33.4 (CH₂, C-2), 32.6 (CH₂, C-6), 27.6 (CH₂, C-4), 23.4 (CH₃, C-10), 14.6 (CH₂, C-5); LRMS (ASAP) *m/z* 226.2 [(M + H)⁺, 100%]; HRMS (ASAP) calc'd for C₁₃H₂₄NO₂ (M + H)⁺ 226.1807, found 226.1807.

(1*R, 2*S**, 7*S**)-1-Methyl-11-oxa-4-azabicyclo[5.3.1]undecan-2-ol (190)**



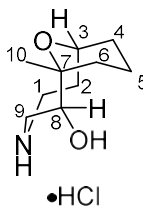
Pd(PPh₃)₄ (146 mg, 0.126 mmol) was added in one portion to a solution of carbamate **227** (680 mg, 2.52 mmol) in degassed CH₂Cl₂ (25 mL) and the resulting mixture was stirred. After 5 min, pyrrolidine (1.03 mL, 12.6 mmol) was added rapidly and the resulting solution stirred. After 30 min, the solvent was removed under reduced pressure to give a brown oil, which was purified by flash column chromatography (eluent: 5 to 20% MeOH (with 1% NH₃) in CH₂Cl₂) to yield amine **190** as a light yellow oil (124 mg, 27%). *R*_f (20% MeOH in CH₂Cl₂) = 0.1; IR (neat / cm⁻¹) 3283 br (N-H and O-H), 2936 s, 1452 m, 1083 m, 726 s; ¹H NMR (400 MHz, CDCl₃) δ_H 4.13 (app. d, *J* = 6.7 Hz, 1H, H-8), 3.95 – 3.88 (m, 1H, H-3), 3.33 (dd, *J* = 13.4, 6.7 Hz, 1H, H-9_a), 3.13 – 3.05 (m, 1H, H-1_a), 2.90 – 2.81 (stack, 2H, H-1_b and H-9_b), 1.98 – 1.91 (m, 1H, H-6_a), 1.82 – 1.67 (stack, 3H, H-2_a, H-4_a and H-5_a), 1.57 – 1.40 (stack, 2H, H-2_b and H-5_b), 1.39 – 1.28 (stack, 2H, H-4_b and H-6_b), 1.11 (s, 3H, H-10), exchangeable protons not observed; ¹³C NMR (101 MHz, CDCl₃) δ_C 75.7 (C, C-7), 74.3 (CH, C-8), 71.1 (CH, C-3), 54.9 (CH₂, C-9), 46.1 (CH₂, C-1), 36.6 (CH₂, C-2), 32.8 (CH₂, C-6), 27.8 (CH₂, C-4), 23.7 (CH₃, C-10), 14.6 (CH₂, C-5); LRMS (ASAP) *m/z* 186.1 [(M + H)⁺, 100%]; HRMS (ASAP) calc'd for C₁₀H₂₀NO₂ (M + H)⁺ 186.1494, found 186.1492.

(1*R, 2*S**, 7*S**)-1-Methyl-4-propyl-11-oxa-4-azabicyclo[5.3.1]undecan-2-ol
(232)**



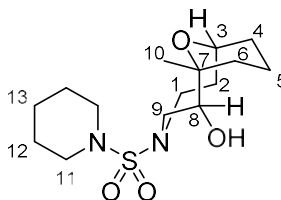
Pd/C (10%, 155 mg) was added to a solution of amine **190** (131 mg, 0.581 mmol) in MeOH (6 mL) and the resulting mixture was stirred. Hydrogen was directly bubbled through the solution for 5 min, after which time the reaction mixture was maintained under an atmosphere of H₂. After 24 h, the solution was filtered through a pad of Celite, dried (MgSO₄), filtered and the solvent was then removed under reduced pressure to give a colourless oil, which was purified by flash column chromatography (eluent: 10% MeOH in CH₂Cl₂) to yield amine **232** as a colourless oil (22 mg, 17%). *R*_f (20% MeOH in CH₂Cl₂) = 0.2; IR (neat / cm⁻¹) 3307 br w (O-H), 2938 br m, 1452 m, 1093 s, 1045 s, 725 s; ¹H NMR (400 MHz, CDCl₃) δ_H 5.92 (br. s, 1H, OH), 4.34 (app. d, *J* = 6.3 Hz, 1H, H-8), 3.89 (app. dt, *J* = 11.8, 5.5 Hz, 1H, H-3), 3.19 (dd, *J* = 13.1, 6.3 Hz, 1H, H-9_a), 3.01 – 2.93 (m, 1H, H-1_a), 2.72 (dd, *J* = 13.1, 1.7 Hz, 1H, H-9_b), 2.55 – 2.45 (stack, 3H, H-1_a and H-11), 2.05 – 1.92 (stack, 2H, H-2_a and H-6_a), 1.80 – 1.73 (stack, 2H, H-4_a and H-5_a), 1.71 – 1.52 (stack, 4H, H-2_b, H-5_b and H-12), 1.38 – 1.30 (stack, 2H, H-4_b and H-6_b), 1.12 (s, 3H, H-10), 0.88 (t, *J* = 7.4 Hz, 3H, H-13); ¹³C NMR (101 MHz, CDCl₃) δ_C 74.1 (C, C-7), 71.0 (CH, C-3), 70.5 (CH, C-8), 63.2 (CH₂, C-9), 61.9 (CH₂, C-11), 52.1 (CH₂, C-1), 33.7 (CH₂, C-2), 32.7 (CH₂, C-6), 27.7 (CH₂, C-4), 23.5 (CH₃, C-10), 19.5 (CH₂, C-12) 14.6 (CH₂, C-5), 11.9 (CH₂, C-13); LRMS (ESI) *m/z* 228.2 [(M + H)⁺, 100%]; HRMS (ESI) calc'd for C₁₃H₂₆NO₂ (M + H)⁺ 228.1964, found 228.1959.

(1*R, 2*S**, 7*S**)-1-Methyl-11-oxa-4-azabicyclo[5.3.1]undecan-2-ol hydrochloride
(234)**



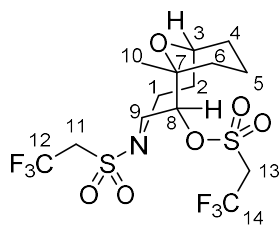
Amine **190** (24 mg, 0.13 mmol) was dissolved in Et₂O (1.0 mL) and HCl (2.0 M in Et₂O, 1 mL) was added dropwise over 1 min. The solvent was immediately removed under reduced pressure to yield hydrochloride salt **234** as a white crystalline solid (27 mg, 100%); mp 165 – 167 °C dec.; IR (neat / cm⁻¹) 3324 br (N-H and O-H), 2942 br s, 2821 br, 1456 m, 1083 s, 1059 s; ¹H NMR (400 MHz, *d*₄ - MeOD) δ _H 4.41 (dd, *J* = 8.1, 2.1 Hz, 1H, H-8), 4.02 (app. dt, *J* = 11.8, 5.4, Hz, 1H, H-3), 3.48 – 3.38 (stack, 2H, H-1_a and H-9_a), 3.24 – 3.12 (stack, 2H, H-1_b and H-9_b), 2.20 – 2.07 (m, 1H, H-2_a), 2.01 – 1.94 (m, 1H, H-6_a), 1.90 – 1.69 (stack, 3H, H-2_b, H-4_a and H-5_a), 1.61 – 1.55 (m, 1H, H-5_b), 1.51 – 1.43 (m, 1H, H-4_b), 1.39 – 1.29 (m, 1H, H-6_b), 1.09 (s, 3H, H-10), exchangeable protons not observed; ¹³C NMR (101 MHz, *d*₄ - MeOD) δ _C 75.8 (C, C-7), 71.7 (CH, C-3), 68.7 (CH, C-8), 51.7 (CH₂, C-9), 46.2 (CH₂, C-1), 33.2 (CH₂, C-6), 31.6 (CH₂, C-2), 28.1 (CH₂, C-4), 23.5 (CH₃, C-10), 15.0 (CH₂, C-5); LRMS (ESI) *m/z* 186.2 [(M + H)⁺, 100%]; HRMS (ESI) calc'd for C₁₀H₂₀NO₂ (M + H)⁺ 186.1494, found 186.1495.

(1*R, 2*S**, 7*S**)-1-Methyl-4-(piperidin-1'-ylsulfonyl)-11-oxa-4-azabicyclo[5.3.1]undecan-2-ol (235)**



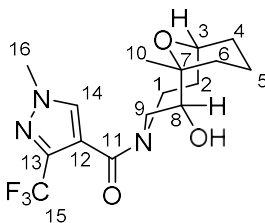
NEt₃ (23 μ L, 0.16 mmol) was added to a stirred solution of amine **190** (24 mg, 0.13 mmol) in CH₂Cl₂ (1.5 mL). The solution was cooled to 0 $^{\circ}$ C. Piperidine-1-sulfonyl chloride (23 μ L, 0.16 mmol) was added and the reaction mixture was warmed to r.t. After 2 h, the reaction mixture was diluted with CH₂Cl₂ (5 mL) and washed sequentially with HCl_(aq) (1 M, 5 mL), H₂O (5 mL) and brine (5 mL). The organic layer was dried (MgSO₄), filtered and the solvent was then removed under reduced pressure to yield sulfamide **235** as a clear oil (35 mg, 81%). *R*_f (50% EtOAc in hexane) = 0.3; IR (neat / cm⁻¹) 3489 br m (O-H), 2938 br m, 1446 m, 1392 m, 1187 s, 1141 s, 1048 s; ¹H NMR (400 MHz, CDCl₃) δ _H 4.26 – 4.19 (m, 1H, H-8), 3.96 – 3.82 (stack, 2H, H-1_a and H-3), 3.59 – 3.45 (stack, 2H, H-9), 3.22 – 3.17 (m, 1H, H-1_b), 3.14 – 3.04 (stack, 4H, H-11), 2.37 (d, *J* = 4.6 Hz, 1H, OH), 1.96 – 1.86 (stack, 2H, H-2_a and H-6_a), 1.83 – 1.70 (stack, 5H, H-2_b, H-4_a, H-5_a and H-13), 1.64 – 1.56 (stack, 4H, H-12), 1.55 – 1.48 (m, 1H, H-5_b), 1.40 – 1.28 (stack, 2H, H-4_b and H-6_b), 1.07 (s, 3H, H-10); ¹³C NMR (101 MHz, CDCl₃) δ _C 75.2 (CH, C-8), 73.3 (C, C-7), 70.7 (CH, C-3), 54.5 (CH₂, C-9), 47.2 (CH₂, C-1), 47.0 (CH₂, C-11), 36.6 (CH₂, C-2), 32.6 (CH₂, C-6), 27.6 (CH₂, C-4), 25.5 (CH₂, C-12), 23.9 (CH₂, C-13) 23.1 (CH₃, C-10), 14.3 (CH₂, C-5); LRMS (ASAP) *m/z* 333.2 [(M + H)⁺, 100%], 219.1 (60); HRMS (ASAP) calc'd for C₁₅H₂₉N₂O₄S (M + H)⁺ 333.1848, found 333.1856.

(1'R*, 2'S*, 7'S*)-1'-Methyl-4'-((2'',2'',2''-trifluoroethyl)sulfonyl)-11'-oxa-4'-azabicyclo[5.3.1]undecan-2'-yl 2,2,2-trifluoroethane-1-sulfonate (236)



NEt₃ (23 μL, 0.16 mmol) was added to a stirred solution of amine **190** (24 mg, 0.13 mmol) in CH₂Cl₂ (1.5 mL). The solution was cooled to 0 °C. 2,2,2-Trifluoroethanesulfonyl chloride (23 μL, 0.16 mmol) was added in one portion and the reaction mixture was warmed to r.t. After 14 h, the reaction mixture was diluted with CH₂Cl₂ (5 mL) and washed sequentially with HCl_(aq) (1 M, 5 mL), H₂O (5 mL) and brine (5 mL). The organic layer was dried (MgSO₄), filtered and the solvent was then removed under reduced pressure to give a yellow oil, which was purified by flash column chromatography (eluent: 40% EtOAc in hexane) to yield sulfonamide **236** as a pale yellow oil (20 mg, 32%). *R*_f (50% EtOAc in hexane) = 0.4; IR (neat / cm⁻¹) 2948 br w, 1355 m, 1252 s, 1133 s, 951 s; ¹H NMR (400 MHz, CDCl₃) δ_H 5.10 (app. d, *J* = 6.3 Hz, 1H, H-8), 4.44 – 4.30 (m, 1H, H-11 or H-13), 4.07 – 3.90 (stack, 3H, H-1_a, H-3 and H-11 or H-13), 3.83 – 3.67 (stack, 4H, H-9 and H-11 or H-13), 3.18 – 3.10 (m, 1H, H-1_b), 2.01 – 1.85 (stack, 3H, H-2 and H-6_a), 1.82 – 1.72 (stack, 2H, H-4_a and H-5_a), 1.66 – 1.59 (m, 1H, H-5_b), 1.47 – 1.36 (stack, 2H, H-4_b and H-6_b), 1.14 (s, 3H, H-10); ¹³C NMR (101 MHz, CDCl₃) δ_C 121.7 (CF₃, q, *J* = 277 Hz, C-12 or C-14), 121.2 (CF₃, q, *J* = 277 Hz, C-12 or C-14), 86.5 (CH, C-8), 72.4 (C, C-7), 70.9 (CH, C-3), 54.0 (CH₂, q, *J* = 32 Hz, C-11 or C-13), 53.8 (CH₂, q, *J* = 32 Hz, C-11 or C-13), 50.2 (CH₂, C-9), 46.4 (CH₂, C-1), 36.9 (CH₂, C-2), 31.6 (CH₂, C-6), 27.0 (CH₂, C-4), 23.8 (CH₃, C-10), 13.6 (CH₂, C-5); ¹⁹F NMR (377 MHz, CDCl₃) δ_F -62.2 (CF₃, C-12 or C-14), -62.5 (CF₃, C-12 or C-14); LRMS (ESI) *m/z* 336.1 [(M -OSO₂CH₂CF₃ + Na)⁺, 100%], 500.1 (30); HRMS (ESI) calc'd for C₁₄H₂₁F₆NO₆S₂Na (M + Na)⁺ 500.0612, found 500.0619.

((1*R, 2*S**, 7*S**)-2-hydroxy-1-methyl-11-oxa-4-azabicyclo[5.3.1]undecan-4-yl)(1'-methyl-3'-trifluoromethyl-1*H*-pyrazol-4'-yl)methanone (**237**)**



Amine **190** (24 mg, 0.13 mmol), 1-methyl-3-(trifluoromethyl)-1*H*-pyrazole-4-carboxylic acid (28 mg, 0.14 mmol), EDC·HCl (27 mg, 0.14 mmol) and HOBT (22 mg, 0.14 mmol) were dissolved in CH₂Cl₂ (2.5 mL) and the resulting mixture. After 10 min, *N*-methylmorpholine (31 μL, 0.29 mmol) was added and the resultant solution was stirred for 17 h. The solvent was then removed to give a brown residue, which was dissolved in EtOAc (10 mL) and washed sequentially with HCl_(aq) (1 M, 2 × 8 mL), NaHCO_{3(aq)} (2 × 8 mL) and brine (8 mL). The organic phase was dried (MgSO₄), filtered and the solvent was then removed under reduced pressure to give a yellow oil. Purification by flash column chromatography (eluent: 50% EtOAc in hexane, followed by a MeOH flush) yielded amide **237** as a colourless oil (25 mg, 53%). *R*_f (50% EtOAc in hexane) = 0.1; IR (neat / cm⁻¹) 3404 br (O-H), 2945 m, 1618 s (C=O), 1447 br m, 1219 m, 1131 s; ¹H NMR (400 MHz, CDCl₃) δ_H 7.52 (s, 1H, H-14), 4.21 (app. d, *J* = 13.6 Hz, 1H, H-9_a), 4.24 – 4.17 (stack, 5H, H-3, H-8 and H-16), 3.84 – 3.75 (m, 1H, H-1_a), 3.50 – 3.41 (stack, 2H, H-9_b and OH), 3.31 – 3.21 (m, 1H, H-1_b), 2.01 – 1.93 (m, 1H, H-6_a), 1.78 – 1.46 (stack, 5H, H-2, H-4_a and H-5), 1.43 – 1.22 (stack, 2H, H-4_b and H-6_b), 1.13 (s, 3H, H-10); ¹³C NMR (101 MHz, CDCl₃) δ_C 164.1 (C, C-11), 139.2 (C, C-13), 130.4 (CH, C-14), 123.5 (CF₃, q, *J* = 269 Hz, C-15), 116.6 (C, C-12), 74.8 (CH, C-8), 73.8 (C, C-7), 70.0 (CH, C-3), 51.5 (CH₂, C-9), 47.7 (CH₂, C-1), 39.8 (CH₃, C-16), 36.9 (CH₂, C-2), 32.5 (CH₂, C-6), 27.5 (CH₂, C-4), 23.5 (CH₃, C-10), 14.2 (CH₂, C-5); ¹⁹F NMR (377 MHz, CDCl₃) δ_F -60.7 (CF₃); LRMS (ASAP) *m/z* 362.2 [(M + H)⁺, 35%], 248.1 (100); HRMS (ASAP) calc'd for C₁₆H₂₃F₃N₃O₃ (M + H)⁺ 362.1692, found 362.1700.

Chapter Six: Appendix

6.1 Crystallographic Data

Crystallographic data for compound **96**

Single crystals of compound **96**, suitable for X-ray diffraction, were grown from the diffusion of hexane and CH₂Cl₂ at room temperature. A suitable crystal was selected and X-ray intensity data were collected on a SuperNova, Dual, Cu at zero, Atlas diffractometer. The crystal was kept at 100.01(10) K during data collection. Using Olex2,²³⁴ the structure was solved with the ShelXS²³⁵ structure solution program using Direct Methods and refined with the ShelXL²³⁶ refinement package using Least Squares minimisation. The structure occupies a chiral space group and has been confirmed as a single enantiomer, with a Flack parameter of $-0.003(7)$. Non-hydrogen atoms were anisotropically refined and the hydrogen atoms in the riding mode with isotropic temperature factors were fixed at 1.2 times U_{eq} of the parent atoms (1.5 for methyl groups).

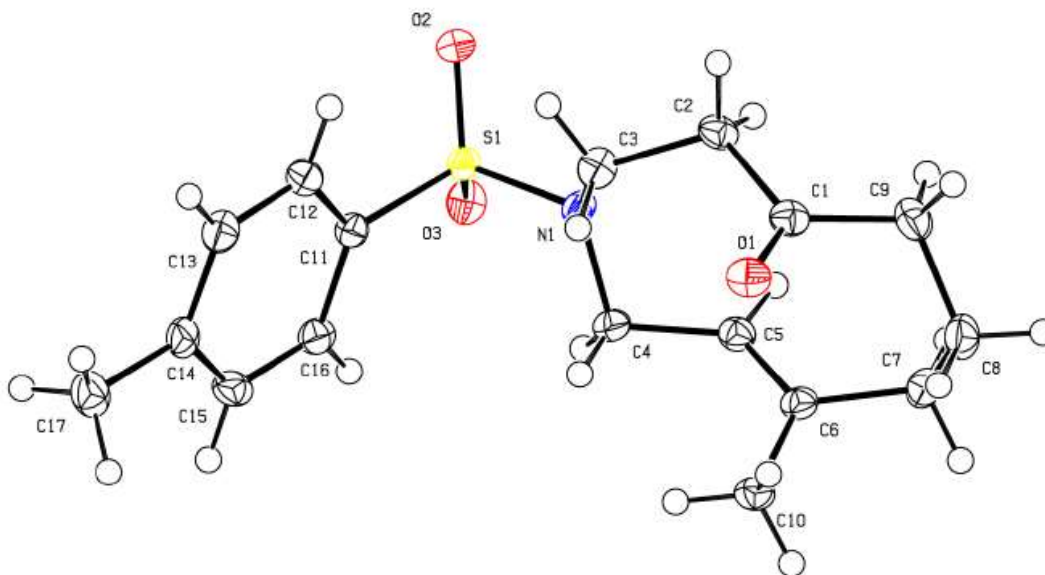


Figure 56- Crystal structure of compound **96**. Thermal ellipsoids are drawn at the 50% probability level.

Details of Crystallographic Data

Identification code	96
Empirical formula	C ₁₇ H ₂₃ NO ₃ S
Formula weight	321.42
Temperature/K	100.01(10)
Crystal system	orthorhombic
Space group	P2 ₁ 2 ₁ 2 ₁
a/Å	7.92584(14)
b/Å	11.89642(19)
c/Å	17.3548(3)
α/°	90
β/°	90
γ/°	90
Volume/Å ³	1636.37(5)
Z	4
ρ _{calc} /cm ³	1.305
μ/mm ⁻¹	1.857
F(000)	688
Crystal size/mm ³	0.271 × 0.18 × 0.092
Radiation	CuKα (λ = 1.54184)
2θ range for data collection/°	9.012 to 144.258
Index ranges	-9 ≤ h ≤ 9, -14 ≤ k ≤ 14, -21 ≤ l ≤ 20
Reflections collected	15158
Independent reflections	3218 [R _{int} = 0.0373, R _{sigma} = 0.0232]
Data/restraints/parameters	3218/0/201
Goodness-of-fit on F ²	1.035
Final R indexes [I ≥ 2σ (I)]	R ₁ = 0.0263, wR ₂ = 0.0682
Final R indexes [all data]	R ₁ = 0.0270, wR ₂ = 0.0690
Largest diff. peak/hole / e Å ⁻³	0.20/-0.22
Flack parameter	-0.003(7)

Crystallographic data for compound **107**

Single crystals of compound **107**, suitable for X-ray diffraction, were grown from the diffusion of hexane and CH₂Cl₂ at room temperature. A suitable crystal was selected and X-ray intensity data were collected on a SuperNova, Dual, Cu at home/ near, Atlas diffractometer. The crystal was kept at 100.01(10) K during data collection. Using Olex2,²³⁴ the structure was solved with the ShelXS²³⁵ structure solution program using Direct Methods and refined with the ShelXL²³⁶ refinement package using Least Squares minimisation. The structure contains two crystallographically-independent molecules. The hydrogen atoms bonded to O(1) and O(101) were located in the electron density and refined freely while all remaining hydrogen atoms were fixed as riding models and the isotropic thermal parameters (U_{iso}) were based on the U_{eq} of the parent atom.

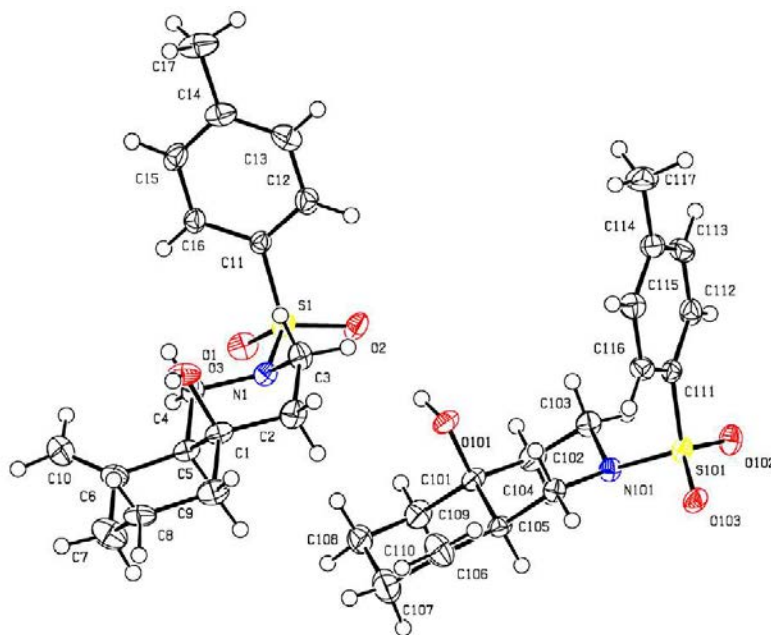


Figure 57 - Crystal structure of compound **107** with ellipsoids drawn at the 50% probability level. The structure contains two crystallographically-independent molecules.

Details of crystallographic data

Identification code	107
Empirical formula	C ₁₇ H ₂₃ NO ₃ S
Formula weight	321.42
Temperature/K	100.01(10)
Crystal system	monoclinic
Space group	P2 ₁ /c
a/Å	17.2338(3)
b/Å	7.87320(10)
c/Å	24.0830(4)
α/°	90
β/°	95.946(2)
γ/°	90
Volume/Å ³	3250.13(9)
Z	8
ρ _{calc} /cm ³	1.314
μ/mm ⁻¹	1.87
F(000)	1376
Crystal size/mm ³	0.226 × 0.159 × 0.073
Radiation	CuKα (λ = 1.54184)
2θ range for data collection/°	7.382 to 148.946
Index ranges	-20 ≤ h ≤ 21, -8 ≤ k ≤ 9, -29 ≤ l ≤ 24
Reflections collected	12989
Independent reflections	6431 [R _{int} = 0.0224, R _{sigma} = 0.0270]
Data/restraints/parameters	6431/0/407
Goodness-of-fit on F ²	1.042
Final R indexes [I >= 2σ (I)]	R ₁ = 0.0395, wR ₂ = 0.1050
Final R indexes [all data]	R ₁ = 0.0451, wR ₂ = 0.1104
Largest diff. peak/hole / e Å ⁻³	0.85/-0.40

Details of crystallographic data

Identification code	119
Empirical formula	C ₁₇ H ₂₅ NO ₃ S
Formula weight	323.44
Temperature/K	100.00(10)
Crystal system	monoclinic
Space group	P2 ₁ /n
a/Å	12.2892(3)
b/Å	11.1531(3)
c/Å	12.3023(3)
α/°	90
β/°	99.690(2)
γ/°	90
Volume/Å ³	1662.13(7)
Z	4
ρ _{calc} /cm ³	1.293
μ/mm ⁻¹	1.829
F(000)	696
Crystal size/mm ³	0.245 × 0.177 × 0.062
Radiation	CuKα (λ = 1.54184)
2θ range for data collection/°	9.41 to 148.902
Index ranges	-15 ≤ h ≤ 14, -13 ≤ k ≤ 13, -13 ≤ l ≤ 15
Reflections collected	6984
Independent reflections	3280 [R _{int} = 0.0164, R _{sigma} = 0.0197]
Data/restraints/parameters	3280/0/205
Goodness-of-fit on F ²	1.058
Final R indexes [I >= 2σ (I)]	R ₁ = 0.0315, wR ₂ = 0.0828
Final R indexes [all data]	R ₁ = 0.0339, wR ₂ = 0.0851
Largest diff. peak/hole / e Å ⁻³	0.35/-0.35

Details of crystallographic data

Identification code	122
Empirical formula	C ₁₇ H ₂₃ NO ₄ S
Formula weight	337.42
Temperature/K	100.00(10)
Crystal system	monoclinic
Space group	P2 ₁ /c
a/Å	21.2954(8)
b/Å	5.6556(2)
c/Å	13.6085(5)
α/°	90
β/°	95.558(4)
γ/°	90
Volume/Å ³	1631.28(10)
Z	4
ρ _{calc} /cm ³	1.374
μ/mm ⁻¹	1.938
F(000)	720
Crystal size/mm ³	0.27 × 0.053 × 0.024
Radiation	CuKα (λ = 1.54184)
2θ range for data collection/°	8.344 to 140.14
Index ranges	-20 ≤ h ≤ 25, -6 ≤ k ≤ 6, -16 ≤ l ≤ 13
Reflections collected	5883
Independent reflections	3086 [R _{int} = 0.0256, R _{sigma} = 0.0342]
Data/restraints/parameters	3086/0/210
Goodness-of-fit on F ²	1.045
Final R indexes [I >= 2σ (I)]	R ₁ = 0.0489, wR ₂ = 0.1241
Final R indexes [all data]	R ₁ = 0.0553, wR ₂ = 0.1303
Largest diff. peak/hole / e Å ⁻³	0.92/-0.49

Crystallographic data for compound **124**

Single crystals of compound **124**, suitable for X-ray diffraction, were grown from the diffusion of hexane and CH₂Cl₂ at room temperature. A suitable crystal was selected and X-ray intensity data were collected on a SuperNova, Dual, Cu at home/ near, Atlas diffractometer. The crystal was kept at 100.01(10) K during data collection. Using Olex2,²³⁴ the structure was solved with the ShelXT²³⁷ structure solution program using Intrinsic Phasing and refined with the ShelXL²³⁶ refinement package using Least Squares minimisation. The structure occupies a centrosymmetric space group such that in half of cases C(1) is *R* and C(2) is *S*, while in the other half C(1) is *S* and C(2) is *R*. In all molecules, the relative stereochemistry of C(1) and C(2) is the same. The hydrogen atom bonded to O(2) was located in the electron density and refined freely. All remaining hydrogen atoms were fixed as riding models and the isotropic thermal parameters (U_{iso}) were based on the U_{eq} of the parent atom.

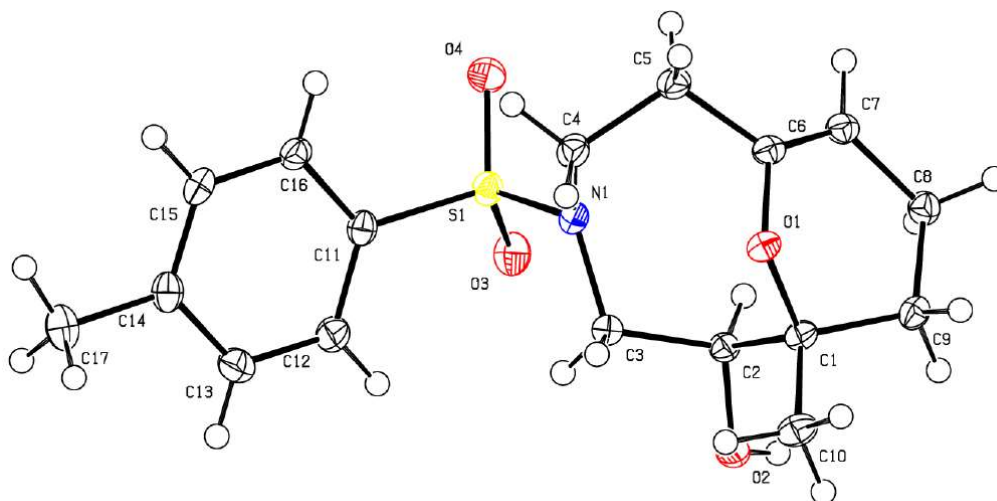


Figure 60 - Crystal structure of compound **124** with ellipsoids drawn at the 50% probability level.

Details of crystallographic data

Identification code	124
Empirical formula	C ₁₇ H ₂₃ NO ₄ S
Formula weight	337.42
Temperature/K	100.01(10)
Crystal system	orthorhombic
Space group	Pccn
a/Å	10.7936(3)
b/Å	21.6827(5)
c/Å	14.0589(4)
α/°	90
β/°	90
γ/°	90
Volume/Å ³	3290.27(15)
Z	8
ρ _{calc} /cm ³	1.362
μ/mm ⁻¹	1.921
F(000)	1440
Crystal size/mm ³	0.248 × 0.139 × 0.074
Radiation	CuKα (λ = 1.54184)
2θ range for data collection/°	8.156 to 148.83
Index ranges	-13 ≤ h ≤ 9, -24 ≤ k ≤ 26, -17 ≤ l ≤ 16
Reflections collected	8311
Independent reflections	3276 [R _{int} = 0.0291, R _{sigma} = 0.0302]
Data/restraints/parameters	3276/0/214
Goodness-of-fit on F ²	1.032
Final R indexes [I ≥ 2σ (I)]	R ₁ = 0.0321, wR ₂ = 0.0822
Final R indexes [all data]	R ₁ = 0.0376, wR ₂ = 0.0869
Largest diff. peak/hole / e Å ⁻³	0.35/-0.35

Details of crystallographic data

Identification code	134
Empirical formula	C ₁₇ H ₂₃ NO ₄ S
Formula weight	337.42
Temperature/K	100.00(10)
Crystal system	orthorhombic
Space group	Pbca
a/Å	10.2493(3)
b/Å	14.8219(5)
c/Å	21.6731(8)
α/°	90
β/°	90
γ/°	90
Volume/Å ³	3292.45(19)
Z	8
ρ _{calc} /cm ³	1.361
μ/mm ⁻¹	1.92
F(000)	1440
Crystal size/mm ³	0.252 × 0.188 × 0.134
Radiation	CuKα (λ = 1.54184)
2θ range for data collection/°	8.16 to 149.094
Index ranges	-11 ≤ h ≤ 12, -15 ≤ k ≤ 18, -26 ≤ l ≤ 23
Reflections collected	8256
Independent reflections	3282 [R _{int} = 0.0233, R _{sigma} = 0.0237]
Data/restraints/parameters	3282/0/210
Goodness-of-fit on F ²	1.049
Final R indexes [I >= 2σ (I)]	R ₁ = 0.0336, wR ₂ = 0.0874
Final R indexes [all data]	R ₁ = 0.0378, wR ₂ = 0.0913
Largest diff. peak/hole / e Å ⁻³	0.30/-0.38

Crystallographic data for compound **154**

Single crystals of compound **154**, suitable for X-ray diffraction, were grown from the diffusion of hexane and CH₂Cl₂ at room temperature. A suitable crystal was selected and X-ray intensity data were collected on a SuperNova, Dual, Cu at home/ near, Atlas diffractometer. The crystal was kept at 100.01(10) K during data collection. Using Olex2,²³⁴ the structure was solved with the ShelXT²³⁷ structure solution program using Intrinsic Phasing and refined with the ShelXL²³⁶ refinement package using Least Squares minimisation. The structure occupies a centrosymmetric space group such that in half of cases C(1) is *R*, C(5) is *R* and C(6) is *S*, while in the other half C(1) is *S*, C(5) is *S* and C(6) is *R*. In all molecules, the relative stereochemistry of C(1), C(5) and C(6) is the same. The hydrogen atom bonded to O(3) was located in the electron density and refined freely. All remaining hydrogen atoms were fixed as riding models and the isotropic thermal parameters (U_{iso}) were based on the U_{eq} of the parent atom.

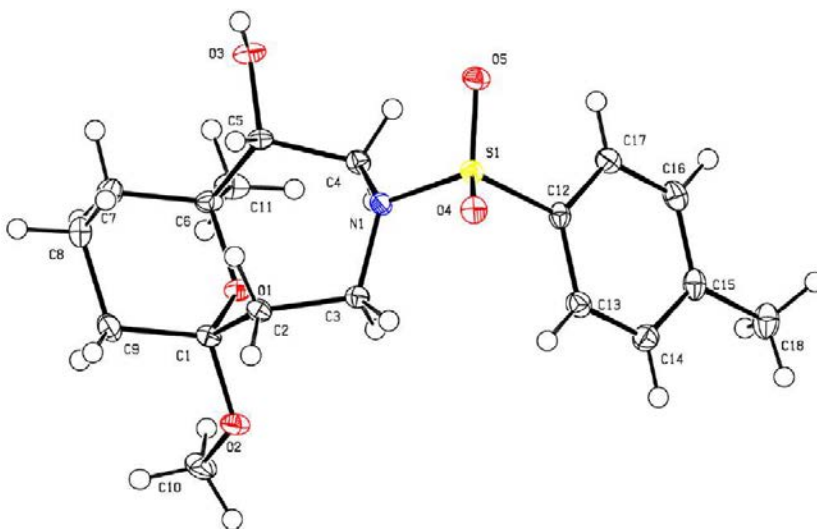


Figure 62 - Crystal structure of compound **154** with ellipsoids drawn at the 50% probability level.

Details of crystallographic data

Identification code	154
Empirical formula	C ₁₈ H ₂₇ NO ₅ S
Formula weight	369.46
Temperature/K	100.01(10)
Crystal system	monoclinic
Space group	P2 ₁ /c
a/Å	7.94900(10)
b/Å	10.7743(2)
c/Å	20.8406(4)
α/°	90
β/°	94.2110(10)
γ/°	90
Volume/Å ³	1780.07(5)
Z	4
ρ _{calc} /cm ³	1.379
μ/mm ⁻¹	1.865
F(000)	792
Crystal size/mm ³	0.261 × 0.163 × 0.141
Radiation	CuKα (λ = 1.54184)
2θ range for data collection/°	8.508 to 149.608
Index ranges	-9 ≤ h ≤ 9, -13 ≤ k ≤ 13, -25 ≤ l ≤ 25
Reflections collected	32920
Independent reflections	3618 [R _{int} = 0.0255, R _{sigma} = 0.0117]
Data/restraints/parameters	3618/0/233
Goodness-of-fit on F ²	1.071
Final R indexes [I >= 2σ (I)]	R ₁ = 0.0299, wR ₂ = 0.0768
Final R indexes [all data]	R ₁ = 0.0314, wR ₂ = 0.0782
Largest diff. peak/hole / e Å ⁻³	0.34/-0.43

Crystallographic data for compound **156**

Single crystals of compound **156**, suitable for X-ray diffraction, were grown from the diffusion of hexane and CH₂Cl₂ at room temperature. A suitable crystal was selected and X-ray intensity data were collected on a SuperNova, Dual, Cu at home/ near, Atlas diffractometer. The crystal was kept at 100.01(10) K during data collection. Using Olex2,²³⁴ the structure was solved with the ShelXT²³⁷ structure solution program using Intrinsic Phasing and refined with the ShelXL²³⁶ refinement package using Least Squares minimisation. The structure occupies a centrosymmetric space group such that in half of cases C(1) and C(5) are *S* and C(9) is *R*, while in the other half C(1) and C(5) are *R* and C(9) is *S*. The hydroxyl hydrogen atoms bonded to O(1), O(3) and O(4) were located in the electron density and freely refined. All remaining hydrogen atoms were fixed as riding models and the isotropic thermal parameters (U_{iso}) were based on the U_{eq} of the parent atom.

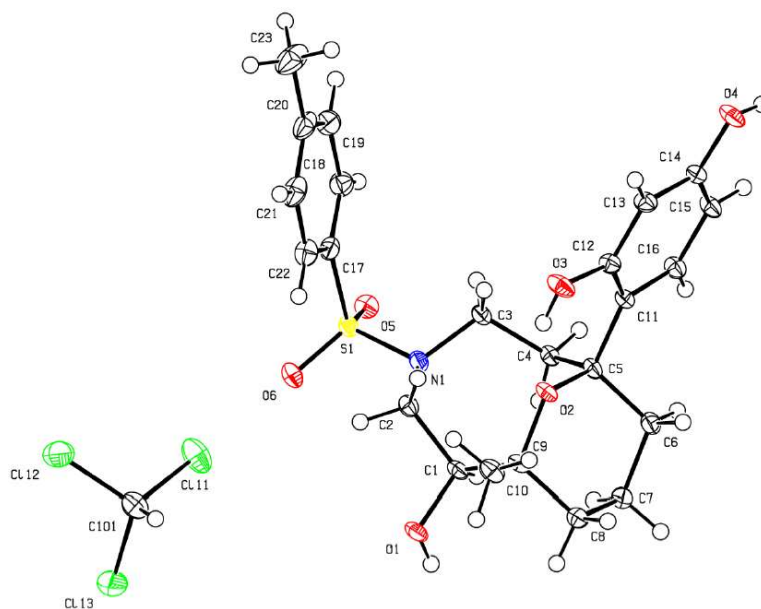


Figure 63 - Crystal structure of compound **156** with ellipsoids drawn at the 50% probability level.

Details of crystallographic data

Identification code	156
Empirical formula	C ₂₄ H ₃₀ Cl ₃ NO ₆ S
Formula weight	566.9
Temperature/K	100.01(10)
Crystal system	triclinic
Space group	P-1
a/Å	10.8161(7)
b/Å	11.6848(7)
c/Å	12.1893(8)
α/°	61.444(6)
β/°	87.599(5)
γ/°	73.430(5)
Volume/Å ³	1288.75(16)
Z	2
ρ _{calc} /cm ³	1.461
μ/mm ⁻¹	4.324
F(000)	592
Crystal size/mm ³	0.154 × 0.137 × 0.101
Radiation	CuKα (λ = 1.54184)
2θ range for data collection/°	8.31 to 148.744
Index ranges	-12 ≤ h ≤ 13, -12 ≤ k ≤ 14, -14 ≤ l ≤ 14
Reflections collected	8838
Independent reflections	5004 [R _{int} = 0.0249, R _{sigma} = 0.0325]
Data/restraints/parameters	5004/0/330
Goodness-of-fit on F ²	1.066
Final R indexes [I ≥ 2σ (I)]	R ₁ = 0.0345, wR ₂ = 0.0841
Final R indexes [all data]	R ₁ = 0.0431, wR ₂ = 0.0898
Largest diff. peak/hole / e Å ⁻³	0.40/-0.34

6.2 Conformational analysis settings

Conformational analysis was conducted in Forge 10.5. Each molecule for which conformational analysis was run was placed in the prediction set. A conformation hunt was undertaken using the settings:

Maximum number of conformations: 250

No. of high-T dynamics runs for flexible rings: 50

Gradient cutoff for conformer minimization: $0.25 \text{ kcal mol}^{-1} \text{ \AA}^{-1}$

Filter duplicate conformers at RMS: 1.0 \AA

Energy window: 6 kcal mol^{-1}

Coulombic and attractive vdW forces were turned on.

Chapter Seven: References

7.1 Bibliography

- 1 A. W. Jones, *Drug Test. Anal.*, 2011, **3**, 337–344.
- 2 G. R. Hamilton and T. F. Baskett, *Can. J. Anesth.*, 2000, **47**, 367–374.
- 3 W. Sneader, *Drug Discovery: A History*, Wiley, New York, 2005.
- 4 W. H. Brock, *Justus von Liebig: The Chemical Gatekeeper*, Cambridge University Press, Cambridge, 1997.
- 5 A. Baeyer, *Ann. Chem. Pharm*, 1864, **130**, 129.
- 6 H. Kunz, *Angew. Chem. Int. Ed.*, 2002, **41**, 4439–4451.
- 7 F. López-Muñoz, R. Ucha-Udabe and C. Alamo, *Neuropsychiatr. Dis. Treat.*, 2005, **1**, 329–343.
- 8 W. Sneader, *B. M. J.*, 2000, **321**, 1591.
- 9 K. C. Nicolaou, *Angew. Chem. Int. Ed.*, 2013, **52**, 131–146.
- 10 A. Fleming, *Br. J. Exp. Pathol.*, 1929, **10**, 226–236.
- 11 M. S. Butler, *J. Nat. Prod.*, 2004, **67**, 2141–2153.
- 12 J. M. Conly and B. L. Johnston, *Can. J. Infect. Dis. Med. Microbiol.*, 2005, **16**, 159–160.
- 13 M. Wainwright, *Miracle Cure: The Story of Penicillin and the Golden Age of Antibiotics*, Wiley, New York, 1990.
- 14 K. C. Nicolaou, D. Vourloumis, N. Winssinger and P. S. Baran, *Angew. Chem. Int. Ed.*, 2000, **39**, 44–122.
- 15 O. O. Grygorenko, D. M. Volochnyuk, S. V. Ryabukhin and D. B. Judd, *Chem. Eur. J.*, 2020, **26**, 1196–1237.
- 16 E. J. Corey and X.-M. Cheng, *The Logic of Chemical Synthesis*, Wiley, New York, 1989.
- 17 J. W.-H. Li and J. C. Vederas, *Science*, 2009, **325**, 161–165.
- 18 J. A. Tobert, *Nat. Rev. Drug Discov.*, 2003, **2**, 517–526.
- 19 A. Endo, M. Kuroda and Y. Tsujita, *J. Antibiot.*, 1976, **29**, 1346–1348.
- 20 A. G. Brown, T. C. Srnale, T. J. King, R. Hasenkamp and R. H. Thompson, *J. Chem. Soc. Perkin Trans. 1*, 1976, 1165–1170.
- 21 R. M. Wilson and S. J. Danishefsky, *J. Org. Chem.*, 2006, **71**, 8329–8351.
- 22 A. D. Steele, G. Ernouf, Y. E. Lee and W. M. Wuest, *Org. Lett.*, 2018, **20**, 1126–1129.

- 23 F. E. Koehn and G. T. Carter, *Nat. Rev. Drug Discov.*, 2005, **4**, 206–220.
- 24 K. C. Nicolaou, *Angew. Chem. Int. Ed.*, 2014, **53**, 9128–9140.
- 25 J. Drews, *Science*, 2000, **287**, 1960–1964.
- 26 D. A. Pereira and J. A. Williams, *Br. J. Pharmacol.*, 2007, **152**, 53–61.
- 27 M. S. Butler, *Nat. Prod. Rep.*, 2002, **22**, 162–195.
- 28 M. R. Spaller, M. T. Burger, M. Fardis and P. A. Bartlett, *Curr. Opin. Chem. Biol.*, 1997, **1**, 47–53.
- 29 R. B. Merrifield, *J. Am. Chem. Soc.*, 1963, **85**, 2149–2154.
- 30 B. A. Bunin and J. A. Ellman, *J. Am. Chem. Soc.*, 1992, **114**, 10997–10998.
- 31 K. S. Lam, S. E. Salmon, E. M. Hersh, V. J. Hruby, W. M. Kazmierski and R. J. Knapp, *Nature*, 1991, **354**, 82–84.
- 32 R. A. Houghten, C. Pinilla, S. E. Blondelle, J. R. Appel, C. T. Dooley and J. H. Cuervo, *Nature*, 1991, **354**, 84–86.
- 33 D. S. Tan, M. A. Foley, M. D. Shair and S. L. Schreiber, *J. Am. Chem. Soc.*, 1998, **120**, 8565–8566.
- 34 C. Barnes and S. Balasubramanian, *Curr. Opin. Chem. Biol.*, 2000, **4**, 346–350.
- 35 A. Vasudevan, A. R. Bogdan, H. F. Koolman, Y. Wang and S. W. Djuric, in *Progress in Medicinal Chemistry*, Elsevier, Heidelberg, 2017, vol. 56, pp. 1–35.
- 36 F. Lovering, J. Bikker and C. Humblet, *J. Med. Chem.*, 2009, **52**, 6752–6756.
- 37 S. L. Dixon and H. O. Villar, *J. Chem. Inf. Comput. Sci.*, 1998, **38**, 1192–1203.
- 38 D. J. Newman and G. M. Cragg, *J. Nat. Prod.*, 2020, **83**, 770–803.
- 39 L. Laraia and H. Waldmann, *Drug Discov. Today Technol.*, 2017, **23**, 75–82.
- 40 L. Laraia, L. Robke and H. Waldmann, *Chem*, 2018, **4**, 705–730.
- 41 S. L. Schreiber, *Science*, 2000, **287**, 1964–1969.
- 42 S. Wilhelm, C. Carter, M. Lynch, T. Lowinger, J. Dumas, R. A. Smith, B. Schwartz, R. Simantov and R. Kelley, *Nat. Rev. Drug Discov.*, 2006, **5**, 835–844.
- 43 N. J. Ryan, *Drugs*, 2014, **74**, 1709–1714.
- 44 G. Bollag, P. Hirth, J. Tsai, J. Zhang, P. N. Ibrahim, H. Cho, W. Spevak, C. Zhang, Y. Zhang, G. Habets, E. A. Burton, B. Wong, G. Tsang, B. L. West, B. Powell, R. Shellooe, A. Marimuthu, H. Nguyen, K. Y. J. Zhang, D. R. Artis, J. Schlessinger, F. Su, B. Higgins, R. Iyer, K. Dandrea, A. Koehler, M. Stumm, P. S. Lin, R. J. Lee, J. Grippo, I. Puzanov,

- K. B. Kim, A. Ribas, G. A. McArthur, J. A. Sosman, P. B. Chapman, K. T. Flaherty, X. Xu, K. L. Nathanson and K. Nolop, *Nature*, 2010, **467**, 596–599.
- 45 D. R. Spring, *Org. Biomol. Chem.*, 2003, **1**, 3867–3870.
- 46 C. M. Dobson, *Nature*, 2004, **432**, 824–828.
- 47 M. D. Burke and S. L. Schreiber, *Angew. Chem. Int. Ed.*, 2004, **43**, 46–58.
- 48 T. I. Oprea and J. Gottfries, *J. Comb. Chem.*, 2001, **3**, 157–166.
- 49 T. I. Oprea, *Curr. Opin. Chem. Biol.*, 2002, **6**, 384–389.
- 50 W. H. B. Sauer and M. K. Schwarz, *J. Chem. Inf. Model.*, 2003, **43**, 987–1003.
- 51 P. G. Polishchuk, T. I. Madzhidov and A. Varnek, *J. Comput. Aided. Mol. Des.*, 2013, **27**, 675–679.
- 52 A. H. Lipkus, S. P. Watkins, K. Gengras, M. J. McBride and T. J. Wills, *J. Org. Chem.*, 2019, **84**, 13948–13956.
- 53 J. L. Reymond and M. Awale, *ACS Chem. Neurosci.*, 2012, **3**, 649–657.
- 54 M. Congreve, R. Carr, C. Murray and H. Jhoti, *Drug Discov. Today*, 2003, **8**, 876–877.
- 55 W. P. Walters, *Expert Opin. Drug Discov.*, 2012, **7**, 99–107.
- 56 M. P. Gleeson, *J. Med. Chem.*, 2008, **51**, 817–834.
- 57 T. W. Johnson, K. R. Dress and M. Edwards, *Bioorganic Med. Chem. Lett.*, 2009, **19**, 5560–5564.
- 58 C. A. Lipinski, F. Lombardo, B. W. Dominy and P. J. Feeney, *Adv. Drug Deliv. Rev.*, 1997, **23**, 3–25.
- 59 W. P. Walters, M. T. Stahl and M. A. Murcko, *Drug Discov. Today*, 1998, **3**, 160–178.
- 60 J. B. Baell and G. A. Holloway, *J. Med. Chem.*, 2010, **53**, 2719–2740.
- 61 K.-H. Altmann, J. Buchner, H. Kessler, F. Diederich, B. Kräutler, S. Lippard, R. Liskamp, K. Müller, E. M. Nolan, B. Samori, G. Schneider, S. L. Schreiber, H. Schwalbe, C. Toniolo, C. A. A. van Boeckel, H. Waldmann and C. T. Walsh, *ChemBioChem*, 2009, **10**, 16–29.
- 62 K. M. G. O. Connell, W. R. J. D. Galloway and D. R. Spring, in *Diversity-Oriented Synthesis: Basics and Applications in Organic Synthesis, Drug Discovery, and Chemical Biology*, 1st edn., 2013, pp. 1–26.
- 63 T. Böttcher, *J. Mol. Evol.*, 2018, **86**, 1–10.
- 64 E. Lenci and A. Trabocchi, *ChemBioChem*, 2019, **20**, 1115–1123.
- 65 I. Pavlinov, E. M. Gerlach and L. N. Aldrich, *Org. Biomol. Chem.*, 2018, 1608–1623.

- 66 S. Wetzel, R. S. Bon, K. Kumar and H. Waldmann, *Angew. Chem. Int. Ed.*, 2011, **50**, 10800–10826.
- 67 T. I. Oprea, A. M. Davis, S. J. Teague and P. D. Leeson, *J. Chem. Inf. Comput. Sci.*, 2001, **41**, 1308–1315.
- 68 M. M. Hann and T. I. Oprea, *Curr. Opin. Chem. Biol.*, 2004, **8**, 255–263.
- 69 A. Nadin, C. Hattotuwigama and I. Churcher, *Angew. Chem. Int. Ed.*, 2012, **51**, 1114–1122.
- 70 P. Willett, *Wiley Interdiscip. Rev. Comput. Mol. Sci.*, 2011, **1**, 46–56.
- 71 S. Wetzel, K. Klein, S. Renner, D. Rauh, T. I. Oprea, P. Mutzel and H. Waldmann, *Nat. Chem. Biol.*, 2009, **5**, 581–583.
- 72 D. J. Foley, P. G. E. Craven, P. M. Collins, R. G. Doveston, A. Aimon, R. Talon, I. Churcher, F. von Delft, S. P. Marsden and A. Nelson, *Chem. Eur. J.*, 2017, **23**, 15227–15232.
- 73 I. Colomer, C. J. Empson, P. Craven, Z. Owen, R. G. Doveston, I. Churcher, S. P. Marsden and A. Nelson, *Chem. Commun.*, 2016, **52**, 7209–7212.
- 74 M. D. Burke, E. M. Berger and S. L. Schreiber, *Science*, 2003, **302**, 613–618.
- 75 D. Tejedor, A. Santos-Expósito and F. García-Tellado, *Chem. Eur. J.*, 2007, **13**, 1201–1209.
- 76 D. Tejedor, A. Santos-Expósito and F. García-Tellado, *Chem. Commun.*, 2006, 2667–2669.
- 77 R. V. Hoffman and D. J. Huizenga, *J. Org. Chem.*, 1991, **56**, 6435–6439.
- 78 D. Morton, S. Leach, C. Cordier, S. Warriner and A. Nelson, *Angew. Chem. Int. Ed.*, 2009, **121**, 110–115.
- 79 W. R. J. D. Galloway, M. Díaz-Gavilán, A. Isidro-Llobet and D. R. Spring, *Angew. Chem. Int. Ed.*, 2009, **48**, 1194–1196.
- 80 M. Ulman and R. H. Grubbs, *Organometallics*, 1998, **17**, 2484–2489.
- 81 E. E. Wyatt, S. Fergus, W. R. J. D. Galloway, A. Bender, D. J. Fox, A. T. Plowright, A. S. Jessiman, M. Welch and D. R. Spring, *Chem. Commun.*, 2006, 3296–3298.
- 82 E. Borsini, G. Broggin, F. Colombo, M. Khansaa, A. Fasana, S. Galli, D. Passarella, E. Riva and S. Riva, *Tetrahedron Asymmetry*, 2011, **22**, 264–269.
- 83 E. Bonandi, P. Marzullo, F. Foschi, D. Perdicchia, L. Lo Presti, M. Sironi, S. Pieraccini, G. Gambacorta, J. Saupe, L. Dalla Via and D. Passarella, *European J. Org. Chem.*, 2019, **2019**, 4013–4019.
- 84 C. Marucci, M. S. Christodoulou, S. Pieraccini, M. Sironi, F. Dapiaggi, D. Cartelli, A. M.

- Calogero, G. Cappelletti, C. Vilanova, S. Gazzola, G. Brogginini and D. Passarella, *European J. Org. Chem.*, 2016, 2029–2036.
- 85 D. Passarella, A. Barilli, F. Belinghieri, P. Fassi, S. Riva, A. Sacchetti, A. Silvani and B. Danieli, *Tetrahedron Asymmetry*, 2005, **16**, 2225–2229.
- 86 A. R. Hanby, N. S. Troelsen, T. Osberger, S. L. Kidd, K. T. Mortensen and D. R. Spring, *Chem. Commun.*, 2020, **3**, 2280–2283.
- 87 N. S. Troelsen, E. Shanina, D. Gonzalez-romero, D. Dankovµ, F. Nami, H. Zhang, I. S. A. Jensen, J. S. Katarzyna, C. Rademacher, A. Cuenda and C. H. Gotfredsen, *Angew. Chem. Int. Ed.*, 2020, **59**, 2204–2210.
- 88 R. J. Spandl, A. Bender and D. R. Spring, *Org. Biomol. Chem.*, 2008, **6**, 1149–1158.
- 89 T. E. Nielsen and S. L. Schreiber, *Angew. Chem. Int. Ed.*, 2008, **47**, 48–56.
- 90 A. Zhou, D. Rayabarapu and P. R. Hanson, *Org. Lett.*, 2009, **11**, 531–534.
- 91 T. Luo and S. L. Schreiber, *J. Am. Chem. Soc.*, 2009, **131**, 5667–5674.
- 92 S. Collins, S. Bartlett, F. Nie, H. F. Sore and D. R. Spring, *Synthesis*, 2016, **48**, 1457–1473.
- 93 A. Isidro-Llobet, T. Murillo, P. Bello, A. Cilibrizzi, J. T. Hodgkinson, W. R. Galloway, A. Bender, M. Welch and D. R. Spring, *Proc. Natl. Acad. Sci. U. S. A.*, 2011, **108**, 6793–6798.
- 94 M. E. Fitzgerald, C. A. Mulrooney, J. R. Duvall, J. Wei, B. C. Suh, L. B. Akella, A. Vrcic and L. A. Marcaurelle, *ACS Comb. Sci.*, 2012, **14**, 89–96.
- 95 S. Yi, B. V. Varun, Y. Choi and S. B. Park, *Front. Chem.*, 2018, **6**, 1–8.
- 96 S. L. Kidd, T. J. Osberger, N. Mateu, H. F. Sore and D. R. Spring, *Front. Chem.*, 2018, **6**, 460.
- 97 D. J. Foley, A. Nelson and S. P. Marsden, *Angew. Chem. Int. Ed.*, 2016, **55**, 13650–13657.
- 98 M. Garcia-Castro, S. Zimmermann, M. G. Sankar and K. Kumar, *Angew. Chem. Int. Ed.*, 2016, **55**, 7586–7605.
- 99 R. Innocenti, E. Lenci, L. Baldini, C. Faggi, G. Menchi and A. Trabocchi, *European J. Org. Chem.*, 2019, 6203–6210.
- 100 R. Zhang, P. J. McIntyre, P. M. Collins, D. J. Foley, C. Arter, F. von Delft, R. Bayliss, S. Warriner and A. Nelson, *Chem. Eur. J.*, 2019, **25**, 6831–6839.
- 101 J. A. Haigh, B. T. Pickup, J. A. Grant and A. Nicholls, *J. Chem. Inf. Model.*, 2005, **45**, 673–684.
- 102 D. J. Foley, R. G. Doveston, I. Churcher, A. Nelson and S. P. Marsden, *Chem. Commun.*,

- 2015, **51**, 11174–11177.
- 103 R. G. Doveston, P. Tosatti, M. Dow, D. J. Foley, H. Y. Li, A. J. Campbell, D. House, I. Churcher, S. P. Marsden and A. Nelson, *Org. Biomol. Chem.*, 2015, **13**, 859–865.
- 104 T. James, P. Maclellan, G. M. Burslem, I. Simpson, J. A. Grant, S. Warriner, V. Sridharan and A. Nelson, *Org. Biomol. Chem.*, 2014, **12**, 2584–2591.
- 105 T. James, I. Simpson, J. A. Grant, V. Sridharan and A. Nelson, *Org. Lett.*, 2013, **15**, 6094–6097.
- 106 K. T. Mortensen, T. J. Osberger, T. A. King, H. F. Sore and D. R. Spring, *Chem. Rev.*, 2019, **119**, 10288–10317.
- 107 A. Isidro-Llobet, K. Hadje Georgiou, W. Galloway, E. Giacomini, M. R. Hansen, G. Méndez-Abt, Y. S. Tan, L. Carro, H. Sore and D. R. Spring, *Org. Biomol. Chem.*, 2015, **13**, 4570–4580.
- 108 F. Nie, D. L. Kunciw, D. Wilcke, J. E. Stokes, W. R. J. D. Galloway, S. Bartlett, H. F. Sore and D. R. Spring, *Angew. Chem. Int. Ed.*, 2016, **55**, 11139–11143.
- 109 J. J. Ciardiello, W. R. J. D. Galloway, C. J. O'Connor, H. F. Sore, J. E. Stokes, Y. Wu and D. R. Spring, *Tetrahedron*, 2016, **72**, 3567–3578.
- 110 D. Lee, J. K. Sello and S. L. Schreiber, *J. Am. Chem. Soc.*, 1999, **121**, 10648–10649.
- 111 L. F. Peng, B. Z. Stanton, N. Maloof, X. Wang and S. L. Schreiber, *Bioorganic Med. Chem. Lett.*, 2009, **19**, 6319–6325.
- 112 L. L. Rubin and F. J. de Sauvage, *Nat. Rev. Drug Discov.*, 2006, **5**, 1026–1033.
- 113 B. Z. Stanton, L. F. Peng, N. Maloof, K. Nakai, X. Wang, J. L. Duffner, K. M. Taveras, J. M. Hyman, S. W. Lee, A. N. Koehler, J. K. Chen, J. L. Fox, A. Mandinova and S. L. Schreiber, *Nat. Chem. Biol.*, 2009, **5**, 154–156.
- 114 B. M. Ibbeson, L. Laraia, E. Alza, C. J. O'Connor, Y. S. Tan, H. M. L. Davies, G. Mckenzie, A. R. Venkitaraman and D. R. Spring, *Nat. Commun.*, 2014, **5**, 3155.
- 115 S. Dandapani, A. R. Germain, I. Jewett, S. Le Quement, J. C. Marie, G. Muncipinto, J. R. Duvall, L. C. Carmody, J. R. Perez, J. C. Engel, J. Gut, D. Kellar, J. L. Siqueira-Neto, J. H. McKerrow, M. Kaiser, A. Rodriguez, M. A. Palmer, M. Foley, S. L. Schreiber and B. Munoz, *ACS Med. Chem. Lett.*, 2014, **5**, 149–153.
- 116 D. C. Blakemore, L. Castro, I. Churcher, D. C. Rees, A. W. Thomas, D. M. Wilson and A. Wood, *Nat. Chem.*, 2018, **10**, 383–394.
- 117 E. A. Villar, D. Beglov and A. Whitty, *Nat. Chem. Biol.*, 2014, **10**, 723–731.
- 118 C. H. Arrowsmith, J. E. Audia, C. Austin, J. Baell, J. Bennett, J. Blagg, C. Bountra, P. E. Brennan, P. J. Brown, M. E. Bunnage, C. Buser-Doepner, R. M. Campbell, A. J. Carter, P. Cohen, R. A. Copeland, B. Cravatt, J. L. Dahlin, D. Dhanak, A. M. Edwards, S. V. Frye, N. Gray, C. E. Grimshaw, D. Hepworth, T. Howe, K. V. M. Huber, J. Jin, S. Knapp, J. D.

- Kotz, R. G. Kruger, D. Lowe, M. M. Mader, B. Marsden, A. Mueller-Fahnow, S. Müller, R. C. O'Hagan, J. P. Overington, D. R. Owen, S. H. Rosenberg, B. Roth, R. Ross, M. Schapira, S. L. Schreiber, B. Shoichet, M. Sundström, G. Superti-Furga, J. Taunton, L. Toledo-Sherman, C. Walpole, M. A. Walters, T. M. Willson, P. Workman, R. N. Young and W. J. Zuercher, *Nat. Chem. Biol.*, 2015, **11**, 536–541.
- 119 M. F. Qiao, N. Y. Ji, X. H. Liu, K. Li, Q. M. Zhu and Q. Z. Xue, *Bioorganic Med. Chem. Lett.*, 2010, **20**, 5677–5680.
- 120 J. A. Laakso, J. B. Gloer, D. T. Wicklow and P. F. Dowd, *J. Org. Chem.*, 1992, **57**, 138–141.
- 121 P. Sahakitpichan and S. Ruchirawat, *Tetrahedron Lett.*, 2003, **44**, 5239–5241.
- 122 H. Kishuku, M. Shindo and K. Shishido, *Chem. Commun.*, 2003, 350–351.
- 123 B. David, T. Sévenet, O. Thoison, K. Awang, M. Païs, M. Wright and D. Guénard, *Bioorganic Med. Chem. Lett.*, 1997, **7**, 2155–2158.
- 124 D. Brückner, F. T. Hafner, V. Li, C. Schmeck, J. Telser, A. Vakalopoulos and G. Wirtz, *Bioorganic Med. Chem. Lett.*, 2005, **15**, 3611–3614.
- 125 A. Hussain, S. K. Yousuf and D. Mukherjee, *RSC Adv.*, 2014, **4**, 43241–43257.
- 126 E. Vitaku, D. T. Smith and J. T. Njardarson, *J. Med. Chem.*, 2014, **57**, 10257–10274.
- 127 C. Zhao, Z. Ye, Z. xiong Ma, S. A. Wildman, S. A. Blaszczyk, L. Hu, I. A. Guizei and W. Tang, *Nat. Commun.*, 2019, **10**, 4015.
- 128 P. S. Wharton and M. D. Baibd, *J. Org. Chem.*, 1971, **36**, 2932–2937.
- 129 H. Suginome, T. Kondoh, C. Gogonea, V. Singh, H. Goto and E. Osawa, *J. Chem. Soc. Perkin Trans. 1*, 1995, 69–81.
- 130 P. Dowd and S. chang Choi, *J. Am. Chem. Soc.*, 1987, **109**, 6548–6549.
- 131 Y. Choi, H. Kim and S. B. Park, *Chem. Sci.*, 2019, **10**, 569–575.
- 132 M. Morales-Chamorro and A. Vázquez, *Synthesis*, 2019, **51**, 842–847.
- 133 J. E. Hall, J. V. Matlock, J. W. Ward, K. V. Gray and J. Clayden, *Angew. Chem. Int. Ed.*, 2016, **55**, 11153–11157.
- 134 A. K. Clarke and W. P. Unsworth, *Chem. Sci.*, 2020, **11**, 2876–2881.
- 135 D. Foley, R. Doveston, I. Churcher, A. Nelson and S. P. Marsden, *Chem. Commun.*, 2015, **51**, 11174–11177.
- 136 N. S. Rajapaksa and E. N. Jacobsen, *Org. Lett.*, 2013, **15**, 4238–4241.
- 137 I. Chataigner, C. Panel, H. Gérard and S. R. Piettre, *Chem. Commun.*, 2007, 3288.

- 138 P. G. M. Wuts, *Greene's Protective Groups in Organic Synthesis*, Wiley, New York, 5th edn., 2014.
- 139 J. T. Williams, P. S. Bahia, B. M. Kariuki, N. Spencer, D. Philp and J. S. Snaith, *J. Org. Chem.*, 2006, **71**, 2460–2471.
- 140 J. K. Vandavasi, W. P. Hu, H. Y. Chen, G. C. Senadi, C. Y. Chen and J. J. Wang, *Org. Lett.*, 2012, **14**, 3134–3137.
- 141 A. G. Capacci, J. T. Malinowski, N. J. McAlpine, J. Kuhne and D. W. C. Macmillan, *Nat. Chem.*, 2017, **9**, 1073–1077.
- 142 S. J. Gharpure and J. V. K. Prasad, *European J. Org. Chem.*, 2013, 2076–2079.
- 143 I. Hayakawa, T. Nakamura, O. Ohno, K. Suenaga and H. Kigoshi, *Org. Biomol. Chem.*, 2015, **13**, 9969–9976.
- 144 P. S. Bahia and J. S. Snaith, *J. Org. Chem.*, 2004, **69**, 3226–3229.
- 145 E. Arundale and L. A. Mikeska, *Chem. Rev.*, 1952, **51**, 505–555.
- 146 K. Mikami and M. Shimizu, *Chem. Rev.*, 1992, **92**, 1021–1050.
- 147 C. E. Davis and R. M. Coates, *Angew. Chem. Int. Ed.*, 2002, **41**, 491–493.
- 148 J. J. Jaber, K. Mitsui and S. D. Rychnovsky, *J. Org. Chem.*, 2001, **66**, 4679–4686.
- 149 D. X. Hu, M. D. Clift, K. E. Lazarski and R. J. Thomson, *J. Am. Chem. Soc.*, 2011, **133**, 1799–1804.
- 150 G. D. Meakins, R. K. Percy, E. E. Richards and R. N. Young, *J. Chem. Soc. C*, 1968, 1106–1109.
- 151 S. E. Chillous, D. J. Hart and D. K. Hutchinson, *J. Org. Chem.*, 1982, **47**, 5418–5420.
- 152 S. Panev, A. Linden and V. Dimitrov, *Tetrahedron Asymmetry*, 2001, **12**, 1313–1321.
- 153 D. B. Ushakov, V. Navickas, M. Strobele, C. Maichle-Mossmer, F. Sasse and M. E. Maier, *Org. Lett.*, 2011, **13**, 2090–2093.
- 154 A. S. Cieplak, *J. Am. Chem. Soc.*, 1981, **103**, 4540–4552.
- 155 T. Imamoto, T. Kusumoto, Y. Tawarayama, Y. Sugiura, T. Mita, Y. Hatanaka and M. Yokoyama, *J. Org. Chem.*, 1984, **49**, 3904–3912.
- 156 T. Imamoto, Y. Sugiura and N. Takiyama, *Tetrahedron Lett.*, 1984, **25**, 4233–4236.
- 157 H. J. Liu, K. S. Shia, X. Shang and B. Y. Zhu, *Tetrahedron*, 1999, **55**, 3803–3830.
- 158 A. C. Cope and E. M. Hardy, *J. Am. Chem. Soc.*, 1940, **62**, 441–444.
- 159 W. von E. Doering and W. R. Roth, *Tetrahedron*, 1962, **18**, 67–74.

- 160 J. A. Berson and M. Jones, *J. Am. Chem. Soc.*, 1964, **86**, 5019–5020.
- 161 D. A. Evans and A. M. Golob, *J. Am. Chem. Soc.*, 1975, **97**, 4765–4766.
- 162 L. A. Paquette, *Tetrahedron*, 1997, **53**, 13971–14020.
- 163 L. E. Overman and F. M. Knoll, *J. Am. Chem. Soc.*, 1980, **102**, 865–867.
- 164 N. Bluthe, M. Malacria and J. Gore, *Tetrahedron Lett.*, 1983, **24**, 1157–1160.
- 165 L. E. Overman and E. J. Jacobsen, *J. Am. Chem. Soc.*, 1982, **104**, 7225–7231.
- 166 L. E. Overman and A. F. Renaldo, *J. Am. Chem. Soc.*, 1990, **112**, 3945–3949.
- 167 A. C. Cope, K. Banholzer, H. Keller, B. A. Pawson, J. J. Whang and H. J. S. Winkler, *J. Am. Chem. Soc.*, 1965, **87**, 3644–3649.
- 168 G. Binsch and J. D. Roberts, *J. Am. Chem. Soc.*, 1965, **87**, 5157–5162.
- 169 J. A. Marshall, T. R. Konicek and K. E. Flynn, *J. Am. Chem. Soc.*, 1980, **102**, 3287–3288.
- 170 H. H. Westen, *Helv. Chim. Acta*, 1964, **47**, 575–590.
- 171 R. L. Hilderbrandt, J. D. Wieser and L. K. Montgomery, *J. Am. Chem. Soc.*, 1973, **95**, 8598–8605.
- 172 D. M. Pawar, S. V. Smith, H. L. Mark, R. M. Odom and E. A. Noe, *J. Am. Chem. Soc.*, 1998, **120**, 10715–10720.
- 173 T. Ohwada, I. Okamoto, K. Shudo and K. Yamaguchi, *Tetrahedron Lett.*, 1998, **39**, 7877–7880.
- 174 I. R. Kleckner and M. P. Foster, *Biochim. Biophys. Acta - Proteins Proteomics*, 2011, **1814**, 942–968.
- 175 A. D. Bain, G. J. Duns, F. Rathgeb and J. Vanderkloet, *J. Phys. Chem.*, 1995, **99**, 17338–17343.
- 176 D. O. Cicero, G. Barbato and R. Bazzo, *J. Am. Chem. Soc.*, 1995, **117**, 1027–1033.
- 177 *Forge*, Cresset, Litlington, Cambridgeshire, 10.5.0.
- 178 M. L. Peach, R. E. Cachau and M. C. Nicklaus, *J. Mol. Recognit.*, , DOI:10.1002/jmr.2618.
- 179 N. Foloppe and I. J. Chen, *Bioorg. Med. Chem.*, 2016, **24**, 2159–2189.
- 180 A. M. Belostotskii, *Conformational Concept For Synthetic Chemist's Use: Principles And In Lab Exploitation*, World Scientific, 1st edn., 2015.
- 181 Y. Hu, D. Stumpfe and J. Bajorath, *J. Med. Chem.*, 2016, **59**, 4062–4076.

- 182 G. W. Bemis and M. A. Murcko, *J. Med. Chem.*, 1996, **39**, 2887–2893.
- 183 G. L. Lange and M. Bosch, *Tetrahedron Lett.*, 1971, **4**, 315–316.
- 184 S. Ruengsri, J. Kaewkhao and P. Limsuwan, *Procedia Eng.*, 2012, **32**, 772–779.
- 185 R. Kitamura, L. Pilon and M. Jonasz, *Appl. Opt.*, 2007, **46**, 8118–8133.
- 186 R. F. Nystrom, S. W. Chaikin and W. G. Brown, *J. Am. Chem. Soc.*, 1949, **71**, 3245–3246.
- 187 V. Poongavanam, E. Danelius, S. Peintner, L. Alcaraz, G. Caron, M. D. Cummings, S. Wlodek, M. Erdelyi, P. C. D. Hawkins, G. Ermondi and J. Kihlberg, *ACS Omega*, 2018, **3**, 11742–11757.
- 188 L. H. M. Janssen, *Bioorg. Med. Chem.*, 1998, **6**, 785–788.
- 189 E. Perola and P. S. Charifson, *J. Med. Chem.*, 2004, **47**, 2499–2510.
- 190 D. A. Singleton, S. R. Merrigan, J. Liu and K. N. Houk, *J. Am. Chem. Soc.*, 1997, **119**, 3385–3386.
- 191 F. C. Lightstone and T. C. Bruice, *Bioorg. Chem.*, 1998, **26**, 193–199.
- 192 W. Clark Still and I. Galynter, *Tetrahedron*, 1981, **37**, 3981–3996.
- 193 S. J. Pastine and D. Sames, *Org. Lett.*, 2005, **7**, 5429–5431.
- 194 J. Barluenga, A. Fernández, F. Rodríguez and F. J. Fañanás, *Chem. Eur. J.*, 2009, **15**, 8121–8123.
- 195 D. S. Hamilton and D. A. Nicewicz, *J. Am. Chem. Soc.*, 2012, **134**, 18577–18580.
- 196 N. A. Romero and D. A. Nicewicz, *J. Am. Chem. Soc.*, 2014, **136**, 17024–17035.
- 197 J. Panten, H. Surburg and B. Holscher, *Chem. Biodivers.*, 2008, **5**, 1011–1022.
- 198 B. N. Blackett, J. M. Coxon, M. P. Hartshorn and K. E. Richards, *Aust. J. Chem.*, 1970, **23**, 2077–2084.
- 199 J. Meinwald, S. S. Labana and M. S. Chadha, *J. Am. Chem. Soc.*, 1963, **85**, 582–585.
- 200 F. A. L. Anet, M. St. Jacques, P. M. Henrichs, A. K. Cheng, J. Krane and L. Wong, *Tetrahedron*, 1974, **30**, 1629–1637.
- 201 D. B. G. Williams and M. Lawton, *J. Org. Chem.*, 2010, **75**, 8351–8354.
- 202 I. Karamé, M. L. Tommasino and M. Lemaire, *Tetrahedron Lett.*, 2003, **44**, 7687–7689.
- 203 T. A. Blumenkopf, M. Bratz, A. Castañeda, G. C. Look, L. E. Overman, D. Rodriguez and A. S. Thompson, *J. Am. Chem. Soc.*, 1990, **112**, 4386–4399.

- 204 M. R. Sarkar, S. Dasgupta, S. M. Pyke and S. G. Bell, *Chem. Commun.*, 2019, **55**, 5029–5032.
- 205 M. De Castro and C. H. Marzabadi, *Tetrahedron Lett.*, 2004, **45**, 6501–6504.
- 206 I. P. Beletskaya and A. V. Cheprakov, *Chem. Rev.*, 2000, **100**, 3009–3066.
- 207 T. Ankner and G. Hilmersson, *Org. Lett.*, 2009, **11**, 503–506.
- 208 B. Nyasse, L. Grehn and U. Ragnarsson, *Chem. Commun.*, 1997, 1017–1018.
- 209 W. D. Closson, P. Wriede and S. Bank, *J. Am. Chem. Soc.*, 1966, **88**, 1581–1583.
- 210 T. Kan and T. Fukuyama, *Chem. Commun.*, 2004, 353.
- 211 E. Emer, L. Pfeifer, J. M. Brown and V. Gouverneur, *Angew. Chem. Int. Ed.*, 2014, **53**, 4181–4185.
- 212 G. Bartoli, E. Marcantoni, M. Marcolini and L. Sambri, *Chem. Rev.*, 2010, **110**, 6104–6143.
- 213 J. E. Kim, A. V. Zabula, P. J. Carroll and E. J. Schelter, *Organometallics*, 2016, **35**, 2086–2091.
- 214 J. Kujawski, H. Popielarska, A. Myka, B. Drabińska and M. Bernard, *Comput. Methods Sci. Technol.*, 2012, **18**, 81–88.
- 215 C. M. Grisé, E. M. Rodrigue and L. Barriault, *Tetrahedron*, 2008, **64**, 797–808.
- 216 J. P. Genet, E. Blart, M. Savignac, S. Lemeurie, S. Lemaire-Audoire and J. M. Bernard, *Synlett*, 1993, 680–682.
- 217 O. Dangles, F. Guibé, G. Balavoine, S. Lavielle and A. Marquet, *J. Org. Chem.*, 1987, **52**, 4984–4993.
- 218 M. Sakaitani and Y. Ohfuné, *J. Org. Chem.*, 1990, **55**, 870–876.
- 219 R. Beugelmans, L. Neuville, M. Bois-Choussy, J. Chastanet and J. Zhu, *Tetrahedron Lett.*, 1995, **36**, 3129–3132.
- 220 I. Minami, Y. Ohashi, I. Shimizu and J. Tsuji, *Tetrahedron Lett.*, 1985, **26**, 2449–2452.
- 221 H. Kunz and C. Unverzagt, *Angew. Chem. Int. Ed.*, 1984, **23**, 436–437.
- 222 J. D. Weaver, A. Recio, A. J. Grenning and J. A. Tunge, *Chem. Rev.*, 2011, **111**, 1846–1913.
- 223 L. R. Vidler, I. A. Watson, B. J. Margolis, D. J. Cummins and M. Brunavs, *ACS Med. Chem. Lett.*, 2018, **9**, 792–796.
- 224 C. J. C. Whitehouse, S. G. Bell and L. L. Wong, *Chem. Soc. Rev.*, 2012, **41**, 1218–1260.

- 225 L. Paquette, in *Handbook of Reagents for Organic Synthesis: Oxidising and Reducing Reagents*, eds. S. D. Burke and R. L. Danheiser, Wiley, New York, 1999, pp. 199–204.
- 226 H. M. Bell and H. C. Brown, *J. Am. Chem. Soc.*, 1966, **88**, 1473–1477.
- 227 H. C. Brown, E. J. Mead and B. C. S. Rao, *J. Am. Chem. Soc.*, 1955, **77**, 6209–6213.
- 228 H. C. Brown and S. Narasimhan, *J. Org. Chem.*, 1982, **47**, 1604–1606.
- 229 K. C. Nicolaou, Y. Wang, M. Lu, D. Mandal, M. R. Pattanayak, R. Yu, A. A. Shah, J. S. Chen, H. Zhang, J. J. Crawford, L. Pasunoori, Y. B. Poudel, N. S. Chowdari, C. Pan, A. Nazeer, S. Gangwar, G. Vite and E. N. Pitsinos, *J. Am. Chem. Soc.*, 2016, **138**, 8235–8246.
- 230 B. M. Trost and X. Li, *Chem. Sci.*, 2017, **8**, 6815–6821.
- 231 K. R. Wilson, S. Sedberry, R. Pescatore, D. Vinton, B. Love, S. Ballard, B. C. Wham, S. K. Hutchison and E. J. Williamson, *J. Pept. Sci.*, 2016, **22**, 622–627.
- 232 H.-S. Lin and L. Paquette, *Synth. Commun.*, 1994, **24**, 2503–2506.
- 233 M. Szostak, M. Spain and D. J. Procter, *J. Org. Chem.*, 2012, **77**, 3049–3059.
- 234 O. V. Dolomanov, L. J. Bourhis, R. J. Gildea, J. A. K. Howard and H. Puschmann, *J. Appl. Crystallogr.*, 2009, **42**, 339–341.
- 235 G. M. Sheldrick, *Acta Crystallogr. Sect. A Found. Crystallogr.*, 2007, **64**, 112–122.
- 236 G. M. Sheldrick, *Acta Crystallogr. Sect. C Struct. Chem.*, 2015, **71**, 3–8.
- 237 G. M. Sheldrick, *Acta Crystallogr. Sect. A Found. Crystallogr.*, 2015, **71**, 3–8.